Investigations Beyond the Standard Model: Neutrino Oscillation, Left-Right Symmetry, and Grand Unification

Submitted in partial fulfillment of requirements

of degree of

(Doctor of Philosophy)

By

Bidyut Prava Nayak
(Registration No. 1271091001)

Supervisor

Prof. Mina Ketan Parida

Centre of Excellence in Theoretical and Mathematical Sciences

Siksha 'O' Anusandhan
(Deemed to be University)

Bhubaneswar, Odisha, India

Centre of Excellence in Theoretical and Mathematical Sciences

Siksha 'O' Anusandhan
(Deemed to be University)

Bhubaneswar, Odisha, India

2018

CERTIFICATE

This is to certify that the thesis entitled **"Investigations Beyond the Standard Model: Neutrino Oscillation, Left-Right Symmetry, and Grand Unification"** by **Bidyut Prava Nayak** which is submitted for award of Ph.D. degree of the University, embodies original work done by her under my supervision.

(Signature in full of the Supervisor)

Professor M. K. Parida

Centre of Excellence in Theoretical and Mathematical Sciences

Siksha 'O' Anusandhan (Deemed to be University), Bhubaneswar

Date : 20.06.2018

Place : Bhubaneswar

APPROVAL SHEET

This thesis/dissertation/report entitled **"Investigations Beyond the Standard Model: Neutrino Oscillation, Left-Right Symmetry, and Grand Unification"** by **Bidyut Prava Nayak** is approved for the degree of Doctor of Philosophy.

Examiners.

Supervisor.

Chairman.

Date : 20/06/2018

Place : SOA Deemed to be Univ.

DECLARATION

I declare that this written submission represents my ideas in my own words and where others ideas or words have been included, I have adequately cited and referenced the original sources. I also declare that I have adhered to all principles of academic honesty and integrity and have not misrepresented or fabricated or falsified any idea/ data/ fact/ source in my submission. I understand that any violation of the above will be cause for disciplinary action by the institute and can also evoke penal action from the sources which have thus not been properly cited or from whom proper permission has not been taken when needed.

Bidyut Prava Nayak.

(Signature)

Name of the Student: Bidyut Prava Nayak

Registration No: 1271091001

Date : 20.06.2018

Place : Bhubaneswar

ACKNOWLEDGEMENTS

At the outset I profusely thank my esteemed guide, Prof. Mina Ketan Parida for his sincere guidance, ungrudging support and encouragement to complete my Ph.D degree. It was his trust on my abilities and scientific attitude that provided me the necessary impetus to carry out this research work.

I would also like to thank our honourable Vice-Chancellor, Prof. Amit Banerjee, Prof. P. K. Nanda, Dean(Research), Prof. P. K. Sahoo, Dean(ITER) for rendering their valuable help and encouragement throughout this research work.

I am indebted to Dr. Tapas Ranjan Routray and Dr. Sudhanwa Patra, faculties of CETMS, Siksha 'O' Anusandhan (Deemed to be University) for their motivation and guidance. I would be thankful to Prof. Pradeep Kumar Sahu, Institute of Physics, Bhubaneswar, and Dr. Shesanshu Sekhar Pal, Dept. of Physics, Utkal University, Bhubaneswar for providing me the necessary support as and when required. I would like to mention the name of my senior, Dr. Ramlal Awasthi for his useful discussions on relevant topic during the research work.

Special thanks are due to Mr. Samiran bose, system operator and my friends Rinmayee, Biswonath, Rajesh, Prativa, Subhasmita, Satish, Deepan, Deepti for being a source of my strength to bring this research to its logical conclusion.

I would be failing in my duty if I don't mention the name of my father, Mr. Dhanurdhar Nayak, mother Mrs. Anita Nayak and brother Mr. Bijay Kumar Nayak whose moral support has helped me considerably to undertake this work. My husband Dr. Sushanta Kumar Sahu deserves a special mention without whom, it would not have been possible to complete this work. I am also equally thankful to my little son, Mr. Sai Subidit Sahu, who has suffered a lot during my Ph.D work and braved the absence of his MAMA like a matured boy.

Last but not the least, I bow down before Maa Tarini for Her invisible inspiration, encouragement and strength to give a facelift to this Ph.D work, without whom, I could not have completed this work.

ABSTRACT

Title of the thesis **"Investigations Beyond the Standard Model: Neutrino Oscillation, Left-Right Symmetry, and Grand Unification"**.

SUSY GUTS provide an attractive framework for representing particles and forces of nature as they solve the gauge hierarchy problem. They unify three forces of nature, and also explain the tiny neutrino masses through seesaw paradigm. The R-parity preserving SUSY models like SO(10) also provide stability to possible cold dark matter candidates of the universe. An evidence of SUSY at the LHC would be a land-mark discovery which would certainly change the future course of physics. But, in the absence of any evidence of SUSY so far, it is worthwhile to explore new physics prospects of non-SUSY GUTs.

In the context of a new non-SUSY SO(10) framework in the 1st publication of this thesis, we explored the complete dominance of type-II seesaw mechanism. The non-SUSY SO(10) breaks to left-right symmetry $SU(2)_L \otimes SU(2)_R \otimes U(1)_{B-L} \otimes SU(3)_C$ or (G_{2213D}) at intermediate scale. Then this breaks into $SU(2)_L \otimes U(1)_R \otimes U(1)_{B-L} \otimes SU(3)_C$ (G_{2113}) at TeV scale. The parity restoration scale is very high (10^8 GeV). In this model the Z' boson is present at low energy scale. So it can be verified experimentally. This model shows the precious gauge coupling unification at $10^{15.56}$ GeV and predicts proton lifetime close to the experimental bound. The basic feature of this model is that the type-I seesaw term is automatically cancelled out due to the addition of extra fermion singlets. The model predicts non-unitarity effect and lepton flavor violating decays accessible to ongoing experimental searches for $\tau \to e\gamma$, $\tau \to \mu\gamma$, $\mu \to e\gamma$. The corresponding branching ratios are only few order smaller than the current experimental limits. This model can be verified experimentally

through its predictions on observable non-unitarity effects and additional contributions to lepton flavor violations. In this case although the mass of the W_R boson is at high scale, the addition of one extra fermion singlet per generation gives a new contribution to neutrinoless double beta decay in the $W_L - W_L$ channel due to the exchange of first generation sterile neutrino. Resonant leptogenesis leads to baryon asymmetry of the universe which is achieved by the quasi degeneracy of second and third generation sterile neutrinos.

In the 2nd publication of this thesis, we have shown different types of seesaw mechanisms in the same breaking chains mentioned above. The basic feature of this work is that due to the addition of extra fermion singlets, the type-I seesaw term is automatically cancelled out. Under different conditions, alternate types of seesaw mechanisms are shown to be dominant. New contributions to neutrinoless double beta decay in the $W_L - W_L$ channel are discussed. Leptogenesis leading to baryon asymmetry of the universe is discussed through resonant leptogenesis both in quasi-degenerate (QD) case as well as in normal hierarchical (NH) case.

In the 3rd paper of this thesis, we have discussed the collider phenomenon of type-II seesaw dominance model. The symmetry breaking model is same as that of the 1st paper. Since in this model the RH neutrinos are present at TeV scale, their signatures can be verified experimentally at LHC. The heavy RH neutrinos can be detected at LHC and other high energy experiments in the channel $pp \rightarrow l^{\pm} l^{\pm} X$ where $l = e, \mu$. We have also discussed the DLSD events mediated by lightest sterile neutrino. Similarly since in our model, the Z' boson is present at TeV scale, its experimental signature can be verified in different collider experiments such as LHC and ILC by dilepton production due to the mediation of Z' boson .
Even though the grand unification SO(10) models we studied are non-SUSY, their LFV branching ratio predictions are of same order as of SUSY SO(10) model with

or without TeV scale LR symmetry. Almost all of these models predict LFV, LNV, proton life time which have a proper match with the current experimental data.

Contents

List of Figures

List of Tables

Abbreviations

The following abbreviations have been used in this thesis.

1. LFV = Lepton Flavour Violation or Lepton Flavour Violating
2. LNV = Lepton Number Violation or Lepton Number Violating
3. LRS = Left-Right Symmetric
4. LR = Left-Right
5. BAU = Baryon Asymmetry of the Universe
6. P = Parity
7. B-L = Baryon Number(B) minus Lepton Number(L)
8. CP = Charge Conjugation(C) and Parity(P)
9. Super K. = Super Kamiokande
10. Hyper K. = Hyper Kamiokande
11. reps. = Representations
12. SM = Standard Model
13. MSSM = Minimal Supersymmetric Standard Model
14. GUT = Grand Unified Theory
15. SUSY = Supersymmetry or Supersymmetric
16. non-SUSY = Non-Supersymmetric
17. LHC = Large Hadron Collider
18. ILC = International Linear Collider
19. LEP = Large Electron Positron Collider
20. $0\nu\beta\beta$ = Neutrinoless Double Beta Decay
21. BSM = Beyond Standard Model
22. DLSD = Dilepton Signals with Displaced Vertices
23. LSD = Like Sign Dilepton
24. NH = Normal Hierarchy
25. IH = Inverted Hierarchy

26. QD = Quasi Degenerate
27. QFT = Quantum Field Theory
28. RH = Right Handed
29. LH = Left Handed
30. SSB = Spontaneous Symmetry Breaking
31. CKM = Cabibbo- Kobayashi-Maskawa
32. PMNS = Pontecorvo-Maki-Nakagawa-Sakata
33. DM = Dark Matter
34. VEV = Vacuum Expectation Value
35. EM = Electro Magnetic
36. RGE = Renormalization Group Evolution
37. PDF = Parton Distribution Function

Chapter 1

Introduction

In the last hundred years of scientific development, our understanding about the behavior of nature has evolved from classical to a very neat and clear quantum picture. In the course of this evolution, starting from the discovery of electron, the fundamental constituents of matter (fermions) and the messengers (gauge bosons) of their interaction have been discovered. Like the unification of electricity and magnetism in to electromagnetic theory, the construction of a single mathematical form to explain various distinct phenomena is one of the virtuous paths has been followed by theoretical scientists. It is found that every action of nature can be explained in terms of four fundamental interactions namely gravitational, electromagnetic, weak and strong. The last three of these are nicely expressed in the mathematical formulation of quantum field theory (QFT) under the Poincare symmetry. The gravitational interaction is much weaker compared to other interactions at any reachable energy scale. Therefore, in all micro-scale studies the gravitational interaction is usually ignored. Also, a successful QFT of gravitation is not yet well established. On the other hand, an elegant cocktail of abelian and non-abelian local gauge symmetries (Weyl [1], Yang-Mills [2]) is found to explain nature at fundamental scales. A single, coherent theoretical framework which could explain all physical aspects of the universe, known till date, is yet to incarnate.

The attempts to cure the high energy behavior of Fermi theory of beta decay laid the foundation of today's theory of fundamental interactions. Glashow [3] added a $U(1)$ piece to Schwinger's [4] $SU(2)$ local gauge theory of weak and electromagnetic interaction. This addition was necessary to explain the experimental data for non-leptonic decay modes of strange particles, which indicated the existence of neutral, weakly interacting current. In summary, a theory with massive vector bosons is required to explain the short ranged weak interaction. With the implementation of

Higgs mechanism [5,6] in the $SU(2)_L \otimes U(1)_Y$ structure, Salam [7] and Weinberg [8] could successfully explain electro-weak behavior of the fundamental particles. This mathematical construct was further extended by Gross, Wilczek [9] and Politzer [10] to incorporate the explanation of interaction holding the quarks together, called strong interaction. This completes our cocktail of gauge structure of internal symmetries based upon $SU(2)_L \otimes U(1)_Y \otimes SU(3)_C$, known as the Standard Model (SM). A delightful description of 'The Rise of the Standard Model' [11] by its pioneers is a science history worth reading. The anomalies generated, due to charge quantization through $U(1)$ symmetry by quarks fortunately cancel with anomalies generated by leptons. Hence, though accidentally, it is an anomaly free theory. The renormalizability of the SM was shown by G. 'tHooft [12–15].

The SM is a remarkably successful theory of interactions of fundamental particles in low energy regime and near electroweak scale. The recent discovery of Higgs boson by *A Toroidal LHC Apparatus* (ATLAS) [16] and *Compact Muon Solenoid* (CMS) [17] detectors at Large Hadron Collider (LHC) completes the search of basic ingredients of SM. Despite the fact that the SM has unraveled the gauge origin of fundamental forces and the structure of universe while successfully confronting numerous experimental tests, it has various limitations. In the next chapter we will discuss about its success and failures in more detail. Reliable extensions of the SM to a simple groups are considered through differet models for Grand Unification. The aims of Grand Unified Theories (GUTs) include: (i) unification of SM gauge couplings g_{1Y}, g_{2L}, & g_{3C} at some high enough energy, (ii) quarks and leptons are treated under same Lie structure, i.e., the theory must also ensure the coalescence of quarks and leptons in one or at most two irreducible representations of the unifying group. This unification of quarks and leptons would explain the electric charge quantization. The energy scale of gauge coupling unification should be consistent with the current bounds on proton decay lifetime. In addition to the above requirements, the structure should also be anomaly free and should able to explain quark, charged lepton, and neutrino masses. The beyond standard model (BSM) predictions such as large flavor violation, baryonic asymmetry of universe, Dirac or Majorana nature of neutrinos, dark matter etc. are the premier goals of GUTs. If possible, they should also explain long standing problems like fine-tuning problem, Dirac monopoles, which have disappointed us till date. Models based on SU(5) and SO(10) gauge groups with their minimal and extended structures in supersymmetric (SUSY) as well as non-SUSY framework have been the most popular, and have partially accomplished the goal.

SUSY GUTs provide an attractive framework for representing particles and forces of nature as they solve the gauge hierarchy problem. They unify three forces of nature, and also explain the tiny neutrino masses through seesaw paradigm [18–27]. The R-parity preserving SUSY models like SO(10) also provide stability to possible cold dark matter candidates of the universe. An evidence of SUSY at the LHC would be a land-mark discovery, which would certainly change the future course of physics. But, in the absence of any evidence of SUSY so far, it is worthwhile to explore new physics prospects of non-SUSY GUTs [28–35]. GUTs based on SO(10) gauge group have particularly grown in popularity compared to SU(5). This is because SO(10) is the smallest, anomaly free group which unifies all fermions of one generation, including the right-handed (RH) neutrino, into a single spinorial representation. It provides spontaneous origins of P (= Parity) and CP (C= Charge conjugation) violations [30, 31, 36–38] Most interestingly, it predicts the right order of tiny neutrino masses through the canonical ($\equiv$ type-I) [39–43] and type-II [44–50] seesaw mechanism. In addition, it has high potentiality to explain all the fermion masses [51–54] including large neutrino mixings [55] with type-II seesaw dominance [44–50]. In fact, neither seesaw mechanism nor grand unification require SUSY per se. The gauge couplings g_{1Y}, g_{2L}, & g_{3C} automatically unify in the Minimal Supersymmetric Standard Model (MSSM) [56–58]. But, they fail to unify through the minimal particle content of the SM. Therefore, in one-step breaking of non-SUSY SU(5) or SO(10) gauge coupling can not predict the right *Weinberg angle*. However, once intermediate symmetries are included to populate the grand desert in case of non-SUSY $SO(10)$ [38, 59–61], gauge couplings may unify. The intermediate gauge symmetries may also occur near accelerator reachable energies.

Experimental evidences on tiny neutrino masses and their large mixings have attracted considerable attention as physics beyond the standard model (SM) leading to different mechanisms for neutrino mass generation. Most of these models are based upon the underlying assumption that neutrinos are Majorana fermions that may manifest in the detection of events in neutrino-less double beta ($0\nu\beta\beta$) decay experiments on which a number of investigations are in progress [62–75]. Theories of neutrino masses and mixings are placed on a much stronger footing if they originate from left-right symmetric (LRS) [28–31] grand unified theories such as SO(10) where, besides grand unification of three forces of nature, P (=Parity) and CP-viloations have spontaneous-breaking origins, the fermion masses of all the three generations are adequately fitted [51], all the 15 fermions plus the right-handed neutrino (N) are unified into a single spinorial representation **16** and the canonical ($\equiv$ type-I

) seesaw formula for neutrino masses is predicted by the theory. Although type-I seesaw formula was also proposed by using extensions of the SM [39–42, 76, 77], it is well known that this was advanced even much before the atmospheric neutrino oscillation data [78] and it is interesting to note that Gell-Mann, Ramond and Slansky had used the left-right symmetric SO(10) theory and its Higgs representations $10_H, 126_H$ to derive it. A special feature of left-right (LR) gauge theories and SO(10) grand unification is that the canonical seesaw formula for neutrino masses is always accompanied by type-II seesaw formula [79–82] for Majorana neutrino mass matrix

$$\mathcal{M}_\nu = m_\nu^{II} + m_\nu^{I}, \tag{1.1}$$

$$m_\nu^{I} = -M_D \frac{1}{M_N} M_D^T, \tag{1.2}$$

$$m_\nu^{II} = f v_L \tag{1.3}$$

where $M_D(M_N)$ is Dirac (RH-Majorana) neutrino mass, v_L is the induced vacuum expectation value (VEV) of the left-handed (LH) triplet Δ_L, and f is the Yukawa coupling of the triplet. Normally, because of the underlying quark-lepton symmetry in SO(10), M_D is of the same order as M_u, the up-quark mass matrix that drives the seesaw scale to be large, $M_N \geq 10^{11}$ GeV. Similarly the type-II seesaw scale is also large. With such high seesaw scales, these two mechanisms in SO(10) can not be directly verified at low energies or by the Large Hadron Collider (LHC) except for the indirect signature through the light active neutrino mediated $0\nu\beta\beta$ decay and possible leptogenesis.

It is well known that the theoretical predictions of branching ratios for LFV decays such as $\mu \to e\gamma$, $\tau \to \mu\gamma$, and $\tau \to e\gamma$ and $\mu \to e\bar{e}e$ closer to their experimental limits are generic features of SUSY GUTs even with high seesaw scales but, in non-SUSY models with such seesaw scales, they are far below the experimental limits. Recently they have been also predicted to be experimentally accessible along with low-mass W_R, Z_R bosons through TeV scale gauged inverse seesaw mechanism [83–85] in SUSY SO(10). In the absence of any evidence of supersymmetry so far, alternative non-SUSY SO(10) models have been found with predictions of substantial LFV decays and TeV scale Z' bosons with inverse seesaw dominance [86] or with the predictions of low-mass W_R, Z_R bosons, LFV decays, observable neutron oscillatios, and dominant LNV decay in the $W_L - W_L$ channel via extended seesaw mechanism [87].

Another feature of non-SUSY SO(10) is rare kaon decay and neutron-antineutron oscillation which is discussed in a recent work [88] with inverse seesaw mechanism of light neutrino masses. The viability of the model of ref. [83–85] depends on discovery of TeV scale SUSY, TeV scale W_R, Z_R bosons, and TeV scale pseudo-Dirac neutrinos which are almost degenerate in masses. The viability of the non-SUSY model of ref. [86] depends on the discovery of TeV scale low-mass Z_R boson and partially degenerate pseudo Dirac neutrinos in the range $100 - 1200$ GeV. Both types of model predict proton lifetime within the Super-K search limit. The falsifiability of the non-SUSY model of ref. [88] depends upon any one of the following predicted observables: TeV scale Z_R boson, dominant neutrino-less double beta decay, heavy Majorana type sterile and righ-handed neutrinos, neutron oscillation, and rare kaon decays. Whereas the neutrino mass generation mechanism in all these models is through gauged inverse seesaw mechanism, our main thrust in the present work is type-II seesaw. A key ansatz to resolve the issue of large mixing in the neutrino sector and small mixing in the quark sector has been suggested to be through type-II seesaw dominance [89–91] via renormalisation group evolution of quasi-degenerate neutrino masses that holds in supersymmetric quark-lepton unified theories [28, 29] or SO(10) and for large values of $\tan\beta$ which represents the ratio of vacuum expectation values (VEVs) of up-type and down type doublets. In an interesting approach to understand neutrino mixing in SUSY theories, it has been shown [55] that the maximality of atmospheric neutrino mixing is an automatic cosnsequence of type-II seesaw dominance and $b-\tau$ unification that does not require quasi-degeneracy of the associated neutrino masses. A number of consequences of this approach have been explored to explain all the fermion masses and mixings including type-II seesaw, or a combination of both type-I and type-II seesaw [49, 92–99] through SUSY SO(10). As a further interesting property of type-II seesaw dominance, it has been recently shown [47–50] without using any flavor symmetry that the well known tri-bimaximal mixing pattern for neutrino mixings is simply a consequence of rotation in the flavor space. Different SUSY SO(10) models requiring type-II seesaw or an admixure of type-I and type-II for fitting fermion masses is given in ref. [55] and a brief review of distortion occuring to precision gauge coupling unification is given in ref. [45]. All the charged fermion mass fittings in the conventional one-step breaking of SUSY GUTs including fits to the neutrino oscillation data require the left-handed triplet to be lighter than the type-I seesaw scale. The gauge coupling evolutions being sensitive to the quantum numbers of the LH triplet $\Delta_L(3, -2, 1)$ under SM gauge group, tend to misalign the precision unification in the minimal scenario achieved without the triplet being lighter.

Two kinds of SO(10) models have been suggested for ensuring precision gauge coupling unification in the presence of type-II seesaw dominance. In the first type of SUSY model [44], SO(10) breaks at a very high scale $M_U \geq 10^{17}$ GeV to SUSY SU(5) which further breaks to MSSM at the usual SUSY GUT scale $M_U \sim 2 \times 10^{16}$ GeV. Type-II seesaw dominance is achieved by fine tuning the mass of the full $SU(5)$ multiplet 15_H containing the $\Delta_L(3,-2,1)$ to remain at the desired type-II scale $M_{\Delta_L} = 10^{11} - 10^{13}$ GeV. Since the full multiplet 15_H is at the intermediate scale, although the paths of the three gauge couplings of the MSSM gauge group deflect from their original paths for $\mu > M_{\Delta_L}$, they converge exactly at the same scale M_U as the MSSM unification scale but with a slightly larger value of the GUT coupling leading to a marginal reduction of proton-lifetime prediction compared to SUSY SU(5). In the second class of models applicable to a non-SUSY or split-SUSY case [45], the grand unificatication group SO(10) breaks directly to the SM gauge symmetry at the GUT-scale $M_U \sim 2 \times 10^{16}$ GeV and by tuning the full SU(5) scalar multiplet 15_H to have degenerate masses at $M_{\Delta_L} = 10^{11} - 10^{13}$ GeV, type-II seesaw dominance is achieved. The question of precision unification is answered in this model by pulling out all the super-partner scalar components of the MSSM but by keeping all the fermionic superpartners and the two Higgs doublets near the TeV scale. In the non-SUSY case the TeV scale fermions can be equivalently replaced by complex scalars carrying the same quantum numbers. The proton lifetime prediction is around $\tau_P(p \to e^+\pi^0) \simeq 10^{35}$ Yrs. in this model.

In the context of LR gauge theory, type-II seesaw mechanism was originally proposed with manifest left right symmetric gauge group $SU(2)_L \times SU(2)_R \times U(1)_{B-L} \times SU(3)_C \times D$ $(g_{2L} = g_{2R})$ $(\equiv G_{2213D})$ where both the left- and the right-handed triplets are allowed to have the same mass scale as the LR symmetry breaking (or the Parity breaking) scale [43]. With the emergence of D-Parity and its breaking leading to decoupling of Parity and $SU(2)_R$ breakings [36, 37], a new class of asymmetric LR gauge group emerged: $SU(2)_L \times SU(2)_R \times U(1)_{B-L} \times SU(3)_C$ $(g_{2L} \neq g_{2R})$ $(\equiv G_{2213})$ where the left-handed triplet acquired larger mass than the RH triplet leading to the type-I seesaw dominance and suppression of type-II seesaw in SO(10) [100]. It is possible to accommodate both types of intermediate symmetries in non-SUSY SO(10) but these models make negligible predictions for branching ratios of charged LFV processes and they leave no other experimental signatures to be verifiable at low or LHC energies.

As a new development along this line we have suggested a new class of SO(10) models where type-II seesaw accounts for neutrino masses, but additional fermion singlets mediate LFV and LNV processes.

Compared to earlier existing SO(10) based type-II seesaw dominant [44,45] models whose RH neutrino masses are in the experimentally inaccessible range and new gauge bosons are in the mass range $10^{15} - 10^{17}$ GeV, the present model predictions on LHC scale Z', light and heavy Majorana type sterile neutrinos, RH Majorana neutrino masses in the range 1000 GeV accessible to LHC in the $W_L - W_L$ channel through dilepton production, the LFV branching ratios closer to experimental limits. The model also predicts dominant $0\nu\beta\beta$ decay amplitudes in the $W_L - W_L$ channel caused by sterile neutrino exchanges providing a rich testing ground for new physics signatures.

The proton lifetime in this model for $p \to e^+\pi^0$ is accessible to ongoing experiments [101–104]. We have also discussed related collider phenomenology in this dissertation. We have discussed the collider signature of RH neutrino through the production of dileptons in the $W_L - W_L$ channel. We have also discussed the collider signature of Z' boson [85, 105–120] at LHC and ILC. In addition we have also predicted the production of dilepton events through displaced vertex due to the sterile neutrino exchange. We have also discussed a special mechaism for the automatic cancellation canonical seesaw and dominance of other seesaw mechanisms without finetuning by the suitable choice of appropriate parameters by adding extra singlet fermions.

In chapter 2, we have discussed the SM and some of its consequences. We have discussed the extension of SM to grand unified theories like $SU(5)$ and $SO(10)$ in chapter 3. The general mechanism for the cancellation of cannonical seesaw and dominance of other seesaw is discussed in chapter 4. Two step breaking of $SO(10)$ GUT to SM is presented in chapter 5 along with the cardinal points of this study namely (i)matching the neutrino oscillation data by type-II seesaw and determination of M_{N_i}, (i=1,2,3) (ii) LHC reachable Z' boson, (iii) proton lifetime prediction, (iv) LFV and CP asymmetry. In chapter 6, we discuss the neutrinoless double beta decay predictions in the $W_L - W_L$ channel due to exchange of a singlet fermion predicted by the model. We then discuss resonant leptogenesis by two quasi-degenerate sterile neutrinos in chapter 6. Sterile neutrino assisted dilepton events with displaced vertices and its collider phenomenology are discussed in chapter 7. In chapter 8, we draw our conclusion. We have also discussed the relevat supplementary material in the appendix.

Chapter 2

Standard Model and Beyond

2.1 Standard Model of particle physics

The Standard Model of particle physics is a theory of electromagnetic, weak and strong interactions, which governs the dynamics of basic building blocks of universe. These building blocks do not possess any sub-structure, therefore are called elementary or fundamental particles. These elementary particles can be categorized into spin-0 scalar (Higgs) bosons, spin-1/2 fermions and spin-1 gauge bosons under the Lorentz symmetry of space-time. The fermions constitute the matter of universe while gauge bosons form force-carriers. Passings the tests of hundreds of scattering experiments in various channels, carried out over a dozen of collider experiments the SM has earned the distinction to the extreme accuracy. The SM has not failed a single test even at very high precision scale.

The SM is a paradigm of quantum field theory (QFT) constructed on $SU(2)_L \otimes U(1)_Y \otimes SU(3)_C$ group structure of local gauge symmetries, which exposes the underlying action of nature. Quantum field theory is the application of quantum mechanics to the dynamical system of fields physically operating on the continuous symmetry of space-time, namely, the Lorentz symmetry $SO(1,3)$. For the sake of completeness, the Lorentz symmetry is briefly recapitulated in Appendix A.3. The exotic extensions of SM incorporate additional particles, extra dimensions, elaborated internal and flavor symmetries to explain neutrino oscillations, dark matter, baryon asymmetry of the universe (BAU) etc.

The particle content of the SM is inscribed in Tab. 2.1. The Greek indices on the gauge boson depict their vectorial nature under Lorentz symmetry, while roman indices a and i represent their number which is same as dimension of adjoint representation (rep.) of the associated internal symmetry. The matter field is constituted by the fermions belonging to spinorial rep of Lorentz symmetry while Higgs boson is

Spin=1				
Hyperon	B_μ	(1,0,1)	$U(1)_Y$	g'
Weak Bosons	$W^i_\mu,\ i=1,2,3$	(3,0,1)	$SU(2)_L$	g
Gluons	$G^a_\mu,\ a=1,2\ldots8$	(1,0,8)	$SU(3)_C$	g_S
Spin=1/2				
Quarks	$(2,1/6,3)$	$\begin{pmatrix}u\\d\end{pmatrix}^\alpha_L$	$\begin{pmatrix}c\\s\end{pmatrix}^\alpha_L$	$\begin{pmatrix}t\\b\end{pmatrix}^\alpha_L$
	$(1,2/3,3)$	u^α_R	c^α_R	t^α_R
	$(1,-1/3,3)$	d^α_R	s^α_R	b^α_R
Leptons	$(2,-1/2,1)$	$\begin{pmatrix}\nu_e\\e\end{pmatrix}_L$	$\begin{pmatrix}\nu_\mu\\\mu\end{pmatrix}_L$	$\begin{pmatrix}\nu_\tau\\\tau\end{pmatrix}_L$
	$(1,-1,1)$	e_R	μ_R	τ_R
Spin=0				
Higgs	$(2,1/2,1)$	$\begin{pmatrix}H^+\\H^0\end{pmatrix}$		

Table 2.1: The Standard Model particles.

the scalar of the symmetry. The alliance of particles under the internal symmetries can be summarized by the set (r_2, Y, r_3), where r_2 and r_3 are the dimensions of reps of non-abelian internal symmetries $SU(2)_L$ and $SU(3)_C$, and Y is the hypercharge quantum number of the abelian symmetry $U(1)_Y$. All the left handed fermions and the Higgs boson stay in the fundamental rep of $SU(2)_L$, while the right handed fermions are its singlets. Quarks stay in fundamental rep of $SU(3)_C$, while leptons and Higgs stay unexposed to this symmetry. All the flavor generations of fermions under $SU(2)_L$ w symmetry are explicitly scripted. The index α on quark sector runs over three colors in the fundamental rep. Coulomb charges of all the particles can be estimated using Gellmann-Nishijima formula

$$Q = T_3 + Y \tag{2.1}$$

where T_3 is the diagonal generators of $SU(2)$ symmetry. The kinetic part of Lagrangian of Gauge ($\mathcal{L}_{GK}$) and Matter ($\mathcal{L}_{MK}$) fields can be written as

$$\begin{aligned}
\mathcal{L}_{GK} &= -\frac{1}{4}B_{\mu\nu}B^{\mu\nu} - \frac{1}{4}W^i_{\mu\nu}W^{\mu\nu\, i} - \frac{1}{4}G^a_{\mu\nu}G^{\mu\nu\, a} \qquad (2.2)\\
\mathcal{L}_{MK} &= i\sum_{i=1}^{3}\Big(L^\dagger_{Li}\sigma^\mu\mathcal{D}_\mu L_{Li} + e^\dagger_{Ri}\sigma^\mu\mathcal{D}_\mu e_{Ri} + Q^\dagger_{Li}\sigma^\mu\mathcal{D}_\mu Q_{Li}\\
&\quad + u^\dagger_{Ri}\sigma^\mu\mathcal{D}_\mu u_{Ri} + d^\dagger_{Ri}\sigma^\mu\mathcal{D}_\mu d_{Ri}\Big) \qquad (2.3)
\end{aligned}$$

where the corresponding field strengths can be expressed as

$$\begin{aligned}
B_{\mu\nu} &= \partial_\mu B_\nu - \partial_\nu B_\mu\,, \qquad (2.4)\\
W^i_{\mu\nu} &= \partial_\mu W^i_\nu - \partial_\nu W^i_\mu - g\,\epsilon^{ijk}W^j_\mu W^k_\nu\,, \qquad (2.5)\\
G^a_{\mu\nu} &= \partial_\mu G^a_\nu - \partial_\nu G^a_\mu - g_S\, f^{abc}G^b_\mu G^c_\nu. \qquad (2.6)
\end{aligned}$$

Here ϵ^{ijk} and f^{abc} are structure functions of $SU(2)_L$ and $SU(3)_C$ groups and $i, j, k = 1, 2, 3$; $a, b, c = 1, 2, \ldots 8.$, and g_S and g are $SU(3)_C$ and $SU(2)_L$ gauge field coupling strengths. Though non-abelian gauge field do, abelian gauge fields do not self-interact which is clear from eq. (2.4)-eq. (2.6). Abelian field strength appear only in fermion-gauge-fermion and scalar-gauge-scalar interactions, through covariant derivatives present in the fermion kinetic terms and scalar kinetic term, to be introduced later. Covariant derivative operator in general can be expressed as

$$\mathcal{D}_\mu = \partial_\mu 1 + i\sum_p g_p \sum_{l_p}^{n_p^2-1} A^{l_p}_\mu T^{l_p} \prod \delta_{\not p}. \qquad (2.7)$$

where p is index of internal symmetries present in a theory, l_p are indices over adjoint representation of internal symmetry p, and $\delta_{\not p}$ are the Kronecker delta for the internal symmetries other than p. For $U(1)_Y$ symmetry, $l_Y = 1$ and $T^{l_Y} = Y$. The explicit structure of covariant derivatives acting on fermion and Higgs fields are presented in Tab. 2.2.

The collider experiments have tested and confirmed the $SU(2)_L \otimes U(1)_Y$ gauge structure of the theory in the fermion weak boson and triple gauge boson interaction channels. If the gauge symmetry $SU(2)_L \otimes U(1)_Y$ remains unbroken neither the gauge bosons nor the fermions acquire masses. The bare mass terms for fermions and gauge bosons, $m_f\bar{\psi}_f\psi_f$ and $M_A^2 A_\mu A^\mu$, are not $SU(2)_L \otimes U(1)_Y$ invariant hence are forbidden. But, the weak gauge bosons are required to be massive to explain short range weak interaction while quarks and leptons have to be massive to explain the micro structure

Field	Multiplet	Covariant derivatives
Q_L	(2,1/6,3)	$\mathcal{D}_\mu Q_L = [(\partial_\mu \mathbf{1} + igW^i_\mu \frac{\sigma^i}{2} + i\frac{g'}{6}B_\mu \mathbf{1})\delta_{\alpha\beta} + ig_S G^a_\mu \frac{\lambda^a_{\alpha\beta}}{2}\mathbf{1}]Q_{L\beta}$
L_L	$(2, -1/2, 1)$	$\mathcal{D}_\mu L_L = (\partial_\mu \mathbf{1} + igW^i_\mu \frac{\sigma^i}{2} - i\frac{g'}{2}B_\mu \mathbf{1})L_L$
u_R	(1, 2/3,3)	$\mathcal{D}_\mu u_R = [(\partial_\mu + i\frac{2g'}{3}B_\mu)\delta_{\alpha\beta} + ig_S G^a_\mu \frac{\lambda^a_{\alpha\beta}}{2}]u_{R\beta}$
d_R	$(1, -1/3, 3)$	$\mathcal{D}_\mu d_R = [(\partial_\mu - i\frac{g'}{3}B_\mu)\delta_{\alpha\beta} + ig_S G^a_\mu \frac{\lambda^a_{\alpha\beta}}{2}]d_{R\beta}$
e_R	$(1, -1, 1)$	$\mathcal{D}_\mu e_R = (\partial_\mu - ig' B_\mu)e_R$
H	$(2, 1/2, 1)$	$\mathcal{D}_\mu H = (\partial_\mu \mathbf{1} + igW^i_\mu \frac{\sigma^i}{2} + i\frac{g'}{2}B_\mu \mathbf{1})H$

Table 2.2: Covariant derivatives of fermionic and Higgs fields under $SU(2)_L \otimes U(1)_Y \otimes SU(3)_C$ gauge structure. $\mathbf{1}$ is 2×2 identity matrix and α, β run over the three color indices. The index over quarks have been suppressed in the left-hand side.

of atoms. In fact! all the particles observed till date, except photons, are massive. Therefore the symmetry is broken badly. Thus, under $SU(2)_L \otimes U(1)_Y$ the current is conserved but particle states are not symmetric. This we call spontaneous breaking of symmetry. The novel mechanism to generate the masses for weak gauge bosons and charged fermions won the 2013 noble prize to Prof. Peter Higgs [6] and Prof. Francois Englert [5], and is called 'Higgs mechanism'. Earlie the predictions of SM ad their experimental tests won nobel prizes.

The masses of the gauge bosons and fermions are generated by the Higgs mechanism via spontaneous symmetry breaking (SSB). To preserve the Lorentz symmetry, the symmetry is spontaneously broken by scalar fields only. A $SU(2)_L$ doublet scalar field with non-zero $U(1)_Y$ charge is required to generate the invariant Yukawa term of fermions and scalar interaction. Hypercharge of left handed (LH) particles indoctrinates another symmetry through $Y = (B - L)/2$, while right handed (RH) ones seem arbitrary. With the introduction of a Higgs doublet we may write the Yukawa part of the SM Lagrangian as

$$\mathcal{L}_{Yuk} = -\sum_{f_1,f_2=1}^{3} \left[Y^l_{f_1 f_2} \overline{L}_{Lf_1} H e_{Rf_2} + Y^d_{f_1 f_2} \overline{Q}_{Lf_1} H d_{Rf_2} + Y^u_{f_1 f_2} \overline{Q}_{Lf_1} \tilde{H} u_{Rf_2} \right] + h.c. \quad (2.8)$$

where

$$\tilde{H} \equiv i\sigma_2 H^{\dagger *} = \begin{pmatrix} H^{0\dagger} \\ -H^- \end{pmatrix},^* \quad (2.9)$$

and $Y^{l,d,u}$ are arbitrary 3×3 matrices, eventually determining the fermion masses and flavor mixings. Sum over color and isospin indices have been ignored and f_1, f_2

run over the number of flavor generations.

2.2 SSB and Higgs mechanism

A vacuum state may or may not be invariant under the symmetry present in the Lagrangian. These modes of symmetry realization are called Wigner-Weyl or Nambu-Goldstone modes respectively. The symmetry realized in nature also depends on the properties of the vacuum state. Wigner-Weyl realization causes all the particles in a single multiplet to have degenerate masses while in Nambu-Goldstone realization the multiplet contains zero-mass particles, known as Nambu-Goldstone boson, equal to the number of broken generators. When the local gauge symmetries are broken spontaneously, the Nambu-Goldstone bosons disappear providing longitudinal modes to gauge fields making them massive.

The $SU(2)_L$ complex Higgs scalar doublet with SM quantum numbers (2,1/2,1) is denoted as,

$$H = \begin{pmatrix} H^+ \\ H^0 \end{pmatrix} \equiv \frac{1}{\sqrt{2}} \begin{pmatrix} H_1 + iH_2 \\ H_3 + iH_4 \end{pmatrix}. \tag{2.10}$$

The scalar part of SM Lagrangian is augmented as

$$\mathcal{L}_H = (\mathcal{D}_\mu H)^\dagger \mathcal{D}_\mu H - [\mu^2 H^\dagger H + \lambda (H^\dagger H)^2]. \tag{2.11}$$

Where the scalar potential is $V(H) = \mu^2 H^\dagger H + \lambda(H^\dagger H)^2$ acquires above structure due to $SU(2)_L \otimes U(1)_Y$ invariance and renormalizability condition. For $\mu^2 < 0$ electroweak symmetry breaks spontaneously, and $\lambda > 0$ is required to keep vacuum stable. Kinetic part of the Lagrangian gives the three and four point interactions between Higgs and gauge bosons, and the λ term describes quartic scalar self-interaction. Re-writing the scalar potential in real basis we get

$$V(H) = \frac{1}{2}\mu \left(\sum_i^4 H_i^2 \right) + \frac{1}{4}\lambda \left(\sum_i^4 H_i^2 \right)^2. \tag{2.12}$$

Without loss of generality we can choose the coordinates in this four dimensional space such that $\langle 0|H_i|0\rangle = 0$ for $i = 1, 2, 4$ and $\langle 0|H_3|0\rangle \geq 0$. Electromagnetic charge neutral component of the scalar field acquires vacuum expectation value (VEV), preserving $U(1)_Q$ symmetry of vacuum. Minimization of potential part yields

$$\left\langle H^\dagger H \right\rangle_0 = -\frac{\mu^2}{2\lambda} \equiv \frac{v_{EW}^2}{2} \rightarrow \langle 0|H|0\rangle = \frac{1}{\sqrt{2}}\begin{pmatrix} 0 \\ v_{EW} \end{pmatrix}, \tag{2.13}$$

called the Higgs field acquiring VEV. The complete transformation of Higgs field is

$$H \rightarrow e^{\frac{i}{2}(\alpha^i \sigma^i + i\beta)} H = \frac{1}{\sqrt{2}} \begin{pmatrix} 0 \\ v_{EW} + h \end{pmatrix}. \tag{2.14}$$

Then gauge transformation with, say, $\alpha_{1,2} = 0$ and $\alpha_3 = \beta$ will be a symmetry of vacuum. Thus, the generators $\sigma_{1,2}$ and $\frac{1}{2}\sigma_3 - Y\mathbf{1}$ are spontaneously broken since they give non-zero charge to vacuum. But, vacuum carries no quantum number for $Q = \frac{1}{2}\sigma_3 + Y\mathbf{1}$ thus $U(1)_Q$ symmetry stays unbroken. The scalar kinetic term with $H = H' + \langle H \rangle$ gives the relevant mass term

$$\begin{aligned} (\mathcal{D}_\mu \langle H \rangle)^\dagger (\mathcal{D}_\mu \langle H \rangle) \quad &\rightarrow \quad \frac{1}{2}(0, v_{EW}) \left| g W_\mu^i \frac{\sigma^i}{2} + \frac{g'}{2} B_\mu \mathbf{1} \right|^2 \begin{pmatrix} 0 \\ v_{EW} \end{pmatrix} \\ &= \quad \frac{1}{2}\frac{v_{EW}^2}{4} \left[g^2 W_\mu^+ W^{\mu -} + (-g W_\mu^3 + g' B_\mu)^2 \right] \end{aligned} \tag{2.15}$$

where

$$W_\mu^\pm = \frac{1}{\sqrt{2}}(W_\mu^1 \mp i W_\mu^2) \ \text{ with mass } \ m_W = g\frac{v_{EW}}{2} \tag{2.16}$$

$$Z_\mu = \frac{1}{\sqrt{g^2 + g'^2}}(g W_\mu^3 - g' B_\mu) \ \text{ with mass } \ m_Z = \sqrt{g^2 + g'^2}\frac{v_{EW}}{2} \tag{2.17}$$

Thus, the field orthogonal to Z_μ is electro-magnetic (EM) field $A_\mu = \frac{1}{\sqrt{g^2+g'^2}}(g' W_\mu^3 + g B_\mu)$, which remains massless. The EM and neutral weak boson fields are related as

$$\begin{pmatrix} Z_\mu \\ A_\mu \end{pmatrix} = \begin{pmatrix} \cos\theta_W & -\sin\theta_W \\ \sin\theta_W & \cos\theta_W \end{pmatrix} \begin{pmatrix} W_\mu^3 \\ B_\mu \end{pmatrix} \tag{2.18}$$

where $\theta_W = cos^{-1}\left(\frac{g}{\sqrt{g^2+g'^2}}\right)$ is called *Weinberg angle*. The relation $M_W^2 = M_Z^2 \cos^2\theta_W$ confirms the weak doublet nature of the Higgs particle. Fermionic mass terms are acquired trivially as

$$M_\psi = \frac{1}{\sqrt{2}} Y^\psi v_{EW}, \tag{2.19}$$

where $\psi = l, d, u$. The Yukawa couplings (Y^ψ) are not any special matrices hence can be diagonalized only using bi-unitarity transformation.

This mechanism introduced the natures complexity through 28 fundamental parameters namely 12 masses, 6 angles and 2 Dirac phases in quark and lepton sectors, and 2 Majorana phases in the neutrino sector. The parameters in the Bosonic sector are $\alpha, m_Z, v_{EW}, m_H, \alpha_S$ and θ_{QCD} where $\alpha_s = e^2/4\pi$ is electromagneic fine structure constant and θ_{QCD} is CP violating parameter for strong interaction. The allowed parameter space for Higgs mass was constrained to very limited region of parameter space, around 100 GeV, with the help of radiative corrections to gauge bosons due to presence of Higgs in the loop. This was further constrained by LEP, Tevatron direct search experiments and unitarity constraint on WW-scattering. The Higgs has been eventually discovered at LHC.

The spontaneous symmetry breaking and Higgs mechanism also help in making of a renormalizable theory with massive vector bosons. Breaking of gauge invariance explicitly by adding mass terms for gauge bosons results in a non-renormalizable theory.

2.3 Excellencies of the Standard Model

Gauge and fermionic kinetic terms together with Yukawa and Higgs Lagrangian complete the Lagrangian for SM, except the fact that while quantizing SM we need to add gauge fixing and Faddeev-Popov ghost terms. Since its origin the SM has been beautifully confirmed by all the experiments. It has a very simple structure and different forces of nature appear in same fashion, i.e., local gauge theories. The 58 objects (45 fermion fields, 12 gauge boson fields and 1 scalar boson field), 118 degrees of freedom (1 for Higgs, 2 for photons, 8×2 for gluons, 3×3 for massive electroweak gauge bosons, 3×4 for charged leptons, 3×2 for neutrinos, $6 \times 3 \times 4$ for quarks) and 28 free parameters (12 for fermion masses, 3 angles and 1 CP phase of Cabibbo-Kobayashi-Maskawa (CKM) matrix, 3 angles and 3 phases in Pontecorvo-Maki-Nakagawa-Sakata (PMNS) matrix, four in electroweak sector of bosons namely α, M_Z, v_{EW} and M_H and 2 in strong sector namely α_S and strong CP phase Θ_{QCD}) constitute the complete model. All these parameters have been experimentally measured except Θ_{QCD}, three phases of PMNS matrix, and absolute neutrino mass scale. For a nice summary of SM and beyond see [121].

Few of the world's major collider experiments are LEP (e^+e^-), SLC (e^+e^-), Tevatron ($p\bar{p}$), HERA (e^-p), PEP-II (e^+e^-), KEKB (e^+e^-) and the latest LHC (pp). These experiments have explored the energy scale from 10 GeV to 8 TeV. Leptonic collider experiments give clean signals at fixed energy suitable for detailed study.

Hadronic collider experiment signals are messy with unknown/variable energy but are suitable for discovery purposes due to high energy, involved nature and capability of producing large amount of signal. With the above structure, SM fits precisely the experimental findings of above experiments. To test a property of the theory we measure the associated parameter in various ways, compare the predicted and measured quantities. Once confirmed, fit the full parameter space of the model is fitted and checked for consistency. All the particles predicted by the SM since its origin, namely τ (1975), ν_τ (2000), c (1974), b (1977), t (1995), gluons (1979), W, Z (1983) and Higgs (2012) scalar, have not only been confirmed but also fit perfectly in the model framework.

2.4 Deficiencies of the Standard Model

With the recent discovery of Higgs particle in CMS [17] and ATLAS [16] detectors at LHC our quest for the SM parameters completes. Even ignoring the fact that it does not incorporate gravitational interaction, there are enough reasons for not believing it as a complete story. Few of the most crucial reasons behind the need of BSM physics are listed as follows

- **Neutrino Masses:** The most important and widely discussed experimental evidence of beyond standard model (BSM) physics is the observed neutrino masses and their peculiar mixings in innumerable oscillation experiments. Solar neutrino experiments (Homestake, Kamiokande, GALLEX/GNO, SAGE, Super-Kamiokande, SNO, BOREXINO) and reactor experiment KamLAND estimated $\Delta m^2_{sol} \simeq 7.5\times10^{-5}$ eV^2 and angle $\sin^2\theta_{sol} \simeq 0.3$. Atmospheric experiments (Kamiokande, IMB, Super-Kamiokande, MACRO, Soudan-2, MINOS) and long baseline experiments (K2K, MINOS and T2K) measured $\Delta m^2_{atm} \simeq 2.4\times10^{-3}$ eV^2 and a mixing angle $\sin^2\theta_{atm} \simeq 0.5$. The reactor experiments Daya Bay, RENO and Double Chooz recently confirmed non-zero reactor angle $\sin^2\theta_{rct} \simeq 0.02$. In the standard three generation framework $\Delta m^2_{sol} = \Delta m^2_{21}$, $\Delta m^2_{atm} = |\Delta m^2_{31}| \simeq |\Delta m^2_{32}|$ and $\theta_{sol} = \theta_{12}$, $\theta_{atm} = \theta_{23}$, $\theta_{rct} = \theta_{13}$ are chosen for convenience. The latest global fit for these parameters is listed Tab. 2.3 [122]. From a totally different scenario the cosmological bounds coming from WMAP constrain the sum of light neutrino masses to $\sum m_i < 0.19 - 1.19$ eV where Planck15 data [] gives $\sum m_i <$ eV at 2σ level [123]. Uncertainties in mass hierarchy and CP-phases are expected to be fixed in near future. From SM point of view neutrino masses must vanish if no right handed neutrinos existed, hence

Parameter	Case	Best fit	1σ range	2σ range	3σ range
$\frac{\delta m^2}{10^{-5}\ \mathrm{eV}^2}$	NH/IH	7.54	7.32 – 7.80	7.15 – 8.00	6.99 – 8.18
$\frac{\sin^2\theta_{12}}{0.1}$	NH/IH	3.08	2.91 – 3.25	2.75 – 3.42	2.59 – 3.59
$\frac{\Delta m^2}{10^{-3}\ \mathrm{eV}^2}$	NH	2.43	2.37 – 2.49	2.30 – 2.55	2.23 – 2.61
	IH	2.38	2.32 – 2.44	2.25 – 2.50	2.19 – 2.56
$\frac{\sin^2\theta_{13}}{0.01}$	NH	2.34	2.15 – 2.54	1.95 – 2.74	1.76 – 2.95
	IH	2.40	2.18 – 2.59	1.98 – 2.79	1.78 – 2.98
$\frac{\sin^2\theta_{23}}{0.1}$	NH	4.37	4.14 – 4.70	3.93 – 5.52	3.74 – 6.26
	IH	4.55	4.24 – 5.94	4.00 – 6.20	3.80 – 6.41
δ/π	NH	1.39	1.12 – 1.77	0.00 – 0.16 $\oplus$ 0.86 – 2.00	—
	IH	1.31	0.98 – 1.60	0.00 – 0.02 $\oplus$ 0.70 – 2.00	—

Table 2.3: Latest global best-fit and allowed 1, 2 and 3σ range analysis of 3ν mass-mixing parameters. The $\Delta m^2 = m_3^2 - (m_1^2 + m_2^2)/2$ for NH and $= -m_3^2 + (m_1^2 + m_2^2)/2$ for IH. The χ^2 for NH and IH are not very different ($\Delta\chi^2_{\mathrm{I-N}} = -0.3$) [122].

no Dirac mass term for neutrinos exist and lepton number is conserved. Another method to understand m_ν is to add a left-haded scalar triplet $\delta_L 3, -1, 1$ and assi it a tiny VEV which will be discussed in chapter 5. Charge neutralness of neutrinos leave other doubts like whether neutrinos are Dirac or Majorana type. If they are Dirac kind, Yukawa couplings will have to be $\sim 10^{-12}$, and there will not be any prediction for neutrinoless double beta decay. If they are Majorana type their masses might come through seesaw mechanism quite naturally.

- **Dark Matter:** There are cosmological and astrophysical evidences that most of the matter in the universe is not SM like, as it does not emit electromagnetic radiation and hence is dark. Neutrinos would also not emit electromagnetic radiation but relic density abundance of neutrinos disfavors its possibility of being cold Dark Matter. Implication for particle physics are such that there must exist cold dark matter which in non-baryonic. Till date the existence of cold Dark Matter, which is likely to have particle physics origin, is elevated only because of its gravitational interaction. See review by Drees and Gerbier in [124].

- **Baryon Asymmetry of Universe:** The imbalance in baryonic and anti-baryonic matter in the observable universe is known as baryon asymmetry problem. A system outside the thermal equilibrium is required to violate C,

CP and B-number, to generate such asymmetry [125]. These conditions are necessary, for theories in which $B = 0$ during the Big Bang, but not sufficient. All of these conditions are satisfied in the SM. B is violated by instantons when kT is of the order of the weak scale (but $B - L$ is conserved). CP is violated by the CKM phase and out of equilibrium conditions could be verified during the electroweak phase transition. A detailed quantitative analysis [126–129] shows that baryogenesis is not possible in the SM because there is not enough CP-violation and the phase transition is not sufficiently strong at first order, unless $m_H < 80$ GeV. Possibility of this mass had been ruled out by LEP and LHC experiments. The electroweak Higgs particle has been recently discovered at LHC and found to have $m_H \simeq 126$ GeV.

- **Flavor problem:** Despite the fact that all the SM fermions acquire their masses through a single spontaneous symmetry breaking mechanism, their masses exhibit strong hierarchical pattern. The symmetry of SM does not impose any constraint on the masses or mixings of fermions. Including the tiny but non-zero masses of neutrino, the ratio of heaviest to lightest fermion is $\sim 10^{12}$. There is no explanation of three generations. Even in theories beyond the SM there is no single, justifiable, minimal mechanism to correlate different Yukawa couplings at electroweak scale.

- **Fine tuning:** Once the dependency on the cut-off scale is absorbed in the redefinitions of masses and couplings, SM is a renormalizable theory. Higgs mass is not protected by any symmetry and receives large radiative correction from new-physics scale. This requires order by order fine tuning of extreme orders to make the Higgs mass stable. Best solution out of few is the introduction of SUSY at TeV scale.

- **Gauge symmetry problem:** The gauge structure and pattern of representations once discovered looks simple, but the origin of this structure and three different gauge couplings of totally different nature remains unexplained. A satisfactory theory should be able to explain the origin of these gauge symmetries and couplings. Evolution of these gauge couplings appear to be converging to a single origin, this behavior should also have some convincing explanation.

- **Charge quantization:** Gellmann-Nishijima equation is convincingly acquired while generation masses for gauge bosons, but it does not answer the question why all the particles have integer multiple of $Q_e/3$, where Q_e is charge of electron. More generically, why charges are quantized? From within the SM we do not get hint for Hypercharge quantum numbers.

- **Ultra High energy cosmic rays:** The highest energy cosmic rays observed have macroscopic energies up to several 10^{11} GeV. They may provide a good probe to physics and astrophysics at such a large energies, unattainable in terrestrial lab experiments. The origin of such an energetic cosmic rays is one of the unresolved problem, searching for an explanation in the variety of theories from astrophysical acceleration to BSM physics. For a review see [130].

The motive of our study is two folded: (1) To address some of the above mentioned open problems from grand unification point of view, and (2) to predict some new BSM physics within the reach of ongoing or future experiments. Unfortunately, all the precision data, extensive flavor physics programs at K and B factories, and direct collider searches indicate that there is no new physics at the electroweak scale.

Before we move to next level of our discussion let us have a look at the evolution of gauge couplings of SM and its minimal SUSY extension.

2.5 Evolution of gauge couplings and unification

The high energy behavior of the three gauge couplings of SM g_S, g and g' point towards the unification of the electro-weak and strong forces. This is one of the main motivation behind studying Grand Unification. Aesthetically too, we will prefer all the forces of nature to unify at certain very high energy. Fig. 2.2 and Fig. 2.3 describes the evolution of gauge couplings of SM and MSSM. The group theoretic formulations of one and two loop beta functions coefficients for a general $G_1 \times G_2$ gauge theory are listed in ref. [131,132] for both non-SUSY and SUSY scenarios. The renormalization group evolution (RGE) of gauge coupling with two loop correction can be expressed as [131, 132]

$$\mu\frac{\partial g_i}{\partial \mu} = \beta_i \equiv \frac{1}{16\pi^2}a_i g_i^3 + \frac{1}{(16\pi^2)^2}\sum_j a_{ij} g_i^3 g_j^2 + \text{Yukawa term} \tag{2.20}$$

where i run over the three symmetries, μ is the energy parameter, and $a_i\,(a_{ij})$ are one (two) loop beta function coefficients.

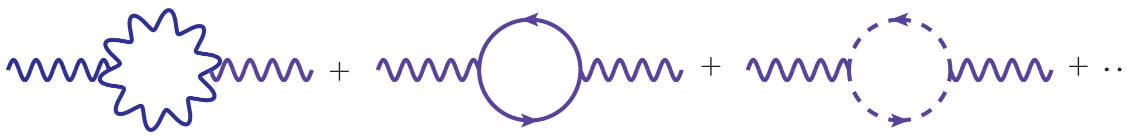

Figure 2.1: One loop correction to gauge boson propagator.

2.5.1 SM gauge coupling running

In the non-SUSY scenario the beta functions coefficients are [132]

$$
\begin{aligned}
a_i &= -\frac{11}{3}C_2(G_1) + \frac{2}{3}\theta T(R_1)d(R_2) + \frac{1}{6}\delta T(S_1)d(S_2) \\
a_{ii} &= -\frac{34}{3}\left[C_2(G_1)\right]^2 + \left[\frac{10}{3}C_2(G_1) + 2C_2(R_1)\right]\theta T(R_1)d(R_2) \\
&\quad + \left[\frac{1}{3}C_2(G_1) + 2C_2(S_1)\right]\delta T(S_1)d(S_2) \\
a_{i\neq j} &= 2\theta C_2(R_2)d(R_2)T(R_1) + 2\delta C_2(S_2)d(S_2)T(S_1)
\end{aligned} \tag{2.21}
$$

where $\theta = 1\,(2)$ for Weyl (Dirac) fermions and $\delta = 1\,(2)$ for real (complex) scalar fields. The fermionic and scalar multiplets transform according to the representations R_i and S_i with respect to the symmetry G_i. For an irreducible representation X we have

$$
\begin{aligned}
tr(M_a(X)M_b(X)) &= T(X)\delta_{ab}, \\
[M_a(X)M_a(X)]_{ij} &= C_2(X)\delta_{ij},
\end{aligned} \tag{2.22}
$$

where M_a is the matrix representation of the generators of the group. The $T(X)$ and $C_2(X)$ are called Dynkin index invariants and quadratic Casimir invariants, respectively, and are related by $C_2(X)d(X) = T(X)d_G$. Here $d(X)$ is the dimension of the representation X and d_G is the number of generators of the group. We have availed a brief discussion on Quadratic Casimir and Dynkin index invariants in Appendix A.2. If the theory has product of more than two group $d(X_2) = \prod_{i\geq 2} d(X_i)$ is assumed. $C_2(G)$ is the quadratic Casimir for the adjoint representation. For a representation of abelian symmetry $\mathrm{U}(1)_z$ we have $C_2(G) = 0$ and $C_2(X) = T(X) = z^2$, where z is the appropriately normalized charge associated to the $U(1)$ symmetry.

We will be frequently estimating these coefficients for various gauge groups under study, hence we have explicitly elaborated the way to calculate those in the following example.

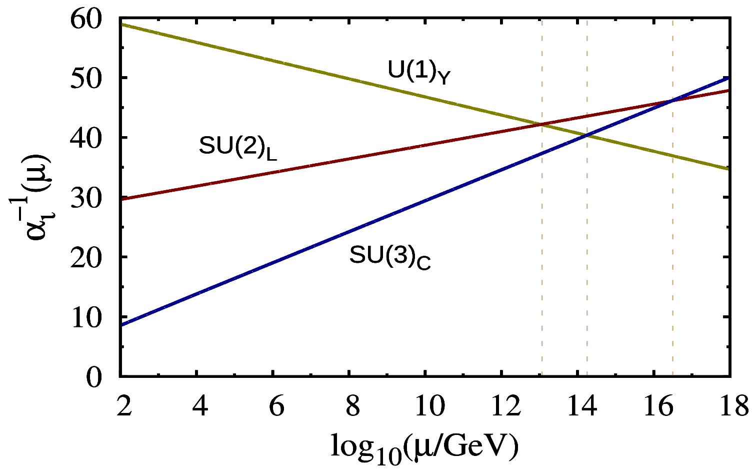

Figure 2.2: Standard Model gauge coupling running.

Example: Assume that we have quark doublet $(2, 1/6, 3)$, which is a Weyl fermion above electroweak restoration scale hence $\theta = 1$. This example is as general as required. One loop coefficient corresponding to this representation is

$$a_{(2,1/6,3)} = \frac{2}{3}\left(\frac{1}{2}\times 3,\ \frac{3}{5}\left(\frac{1}{6}\right)^2 \times 6,\ \frac{1}{2}\times 2\right) \times n_g \tag{2.23}$$

In the eq. (2.23) the common factor 2/3 is the impression of representation being fermionic. There are three terms inside the bracket corresponding to three groups. The first term has a Dynkin index for fundamental of isospin group $SU(2)_L$, i.e., $T(R_{SU(2)_L}) = 1/2$ and this isospin fundamental occurs thrice as the dimension of the rest part of the theory, $U(1)_Y \otimes SU(3)_C$, $d_{R_2} = 3$. In the second term the factor 3/5 is the renormalization factor in redefining the $U(1)_Y$ gauge coupling g' to the new gauge couplings g_1 as $g'Y = g_1 T_1$, such that the generator T_1 is normalized to 1/2 for a fundamental representation of the unifying group. This condition gives $g' = \sqrt{3/5}\, g_1$. Eventually, the comparison of the RGE of the two gauge couplings g' and g_1 gives $a_1 = (3/5)a_Y$. The term $(1/6)^2$ is the Dynkin index $(T = Y^2)$ for $U(1)_Y$ symmetry. This is further multiplied by the dimension (=6) coming from remaining symmetry $SU(2)_L \otimes SU(3)_C$. Similarly in the third term we have a $SU(3)_C$ fundamental and the dimension of rest of the theory, $SU(3)_C \otimes U(1)_Y$, $d_R = 3$. At last n_g is the number of flavor generations in the theory for this representation (for SM $n_g = 3$). Similarly we calculate two loop color-color beta coefficient for the above representation, which would be

$$\begin{aligned} a_{3C3C} &= \left[\left(\frac{10}{3}C_2(G_1) + 2C_2(R_1)\right)T(R_1)d(R_2)\right] \times n_g \\ &= \left[\left(\frac{10}{3} \times 3 \times \frac{1}{2} \times 2\right) + 2 \times \left(\frac{1}{2}\right)^2 \times \frac{8}{3} \times 2\right] \times 3, \end{aligned} \tag{2.24}$$

where $d_{R_1}C_2(R_1) = T(R_1)d_{G_1}$ have been used in the second term. $C_2(G) = 3,\ d_G = 8$ for $SU(3)_C$ and particles are in it's fundamental representation hence $d_{R_1} = 3$ and trivially $d_{R_2} = 2$. Similar calculations will be required for all other representations present in the theory over all generation of scalars and fermions.

The non-zero contributions of all particles to the gauge couplings at one loop level are depicted in the feynman diagrams of Fig. 2.1. We have listed one and two loop RGE beta coefficient in the first row of the Tab. B.1 in the Sec. A.3.1.

The Fig. 2.2 shows the nature of evolution of gauge couplings assuming the bare SM throughout the range of energy beyond electroweak scale. We find that the inverse fine structure constants of $SU(2)_L$ and $U(1)_Y$ crossing at 10^{13} GeV and those of $SU(3)_c$ and $U(1)_Y$ crossing at $10^{14.5}$ GeV. Similarly the inverse fine structure constants of $SU(2)_L$ and $SU(3)_c$ are found to meet at 10^{17} GeV. This generates a fine triangular region and the SM couplings do not unify at a single unification scale.

2.5.2 MSSM gauge coupling running

The SUSY is a symmetry which transforms boson (fermion) in to fermion (boson) and, thus, it contains fermi-bose symmetry. In the no-supersymmetric (non-SUSY) standard model the one-loop radiative correction to the Higgs mass as shown in Fig.2.4 which gives quadratic divergence for the Higgs mass. this causes the SM vacuum to be unstable. But when superpartners called Higgsinos are introduced as in MSSM, there is another one-loop diagram mediated by the Higgsino loop shown in Fig.2.5. The resultant contribution of Fig.2.4 and Fig.2.5 vanishes and the Higgs mass has no quadratically divergent contributions. Thus the major motivation of introducing supersymmetry is to remove the called "gauge hierarchy" problem and keep the SM vacuum stable. Without SUSY, however, the quadratic divergence is controlled by finetuning of parameters to energy loop order which is not so natural as the divergence cancellation in SUSY case. SUSY is required in certain kind of theories which integrate gravitation with internal symmetries of Standard Model. Usually, it is introduced at very high energy scales. The emancipation of SM from the fine tuning problem require the SUSY scale at TeV.

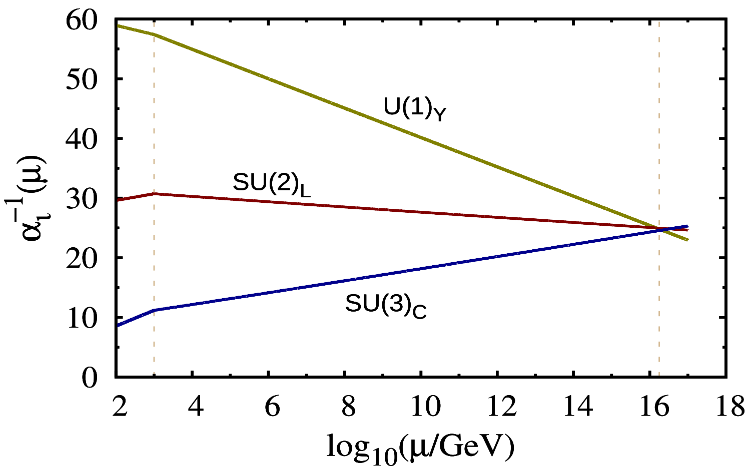

Figure 2.3: MSSM gauge coupling running.

SUSY pairs fermions and bosons hence every SM fermion is paired with their, yet to be discovered, super-partner. Gauge couplings acquire corrections due to super-partners of SM particles present at TeV scale. The gauge coupling meet at a point, around 2×10^{16} GeV. Evolution of gauge couplings is shown in Fig. 2.3 and corresponding one and two loop beta coefficients are listed in Tab. 2.4. Meeting

MSSM beta coefficients	
b_i	b_{ij}
$\begin{pmatrix} 33/5 \\ 1 \\ -3 \end{pmatrix}$	$\begin{pmatrix} 199/50 & 27/10 & 44/5 \\ 9/10 & 35/6 & 12 \\ 11/10 & 9/2 & -26 \end{pmatrix}$

Table 2.4: One and two loop gauge coupling beta coefficients.

of gauge coupling at a point may be another leading motivation for believing the existence of SUSY. To keep the gauge couplings unified beyond the meeting point we need to embed the MSSM in a higher theory like SUSY $SU(5)$ or SUSY $SO(10)$. The ongoing experiments at LHC have constrained the parameter space of MSSM [133] to the effect that masses of superpartners of quarks and gluons are bounded near or above TeV scale. This experimental result at LHC has cast doubts about the existence of SUSY at electroweak scale as a resolution of gauge hierarchy problem. Further extensions of a minimal SUSY GUT like $SU(5)$ will be required to explain neutrino masses.

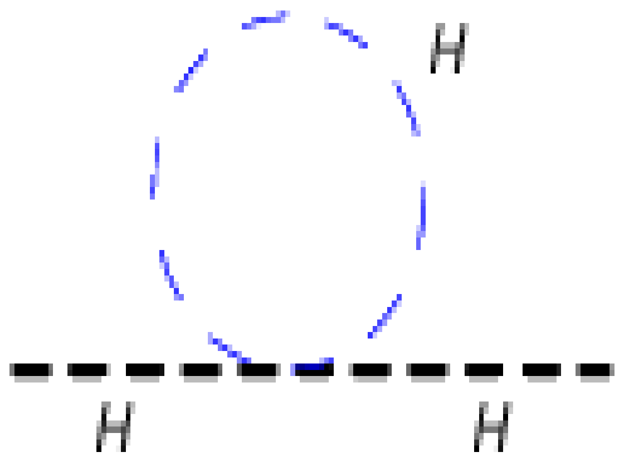

Figure 2.4: One loop correction to Higgs mass.

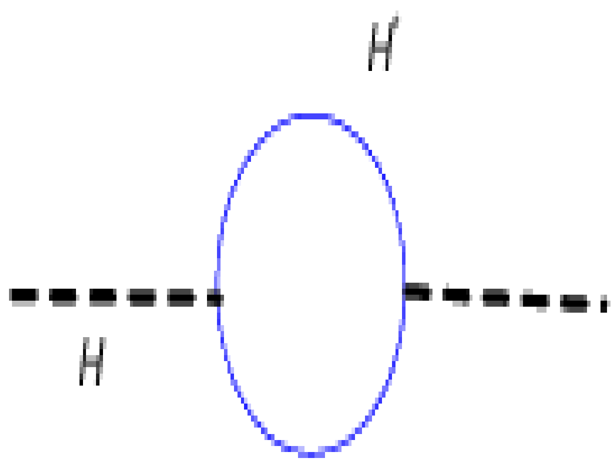

Figure 2.5: Higgsino mediated correction in MSSM.

Chapter 3

Grand Unified Theory

3.1 Motivations and constraints

The plausible convergence of the gauge couplings of SM, although with marked deviation as shown in Fig. 2.2, is one of the major aesthetic reason to believe in grand unification. Other motivations behind studying the grand unification are: (a) To reduce the number of arbitrary parameters of SM. (b) To address, if not all, some of the deficiencies of SM in a higher symmetry, possibly present at very high energy scale. (c) To find other beyond SM signature of which there have been no experimental evidence, and only bounds are available. The proton decay, LFV, non-unitarity, rare decays, etc. are just few examples from the list.

The basic mathematical requirement for GUT model construction is a simple Lie algebra (G) as the gauge group, similar to SM. This simple group should be large enough to have SM as its subgroup. The total number of commuting generators ($\equiv$ rank of the group) in SM is four. Hence, the G must be a rank ≥ 4 group. All the gauge couplings of theories below GUT symmetry restoration scale become equal to GUT gauge coupling, α_G, and above this scale we have only one gauge coupling α_G. The next requirement is that the reps of GUT model must correctly reproduce the particle content of the observed fermion spectrum of SM as well as the Higgs boson. Thus G must posses complex reps, as well as it (or the combination) must be free from anomaly in order not to spoil the renormalizability of GUT by an incompatibility of regularization and gauge invariance. The requirement of complex representation is based on the fact that embedding the known fermions in real representations would require mirror fermions, which must be very heavy making all SM fermions masses close to their scale. The above requirements constrain the possible algebras to $SU(5)$, $SU(6)$, $SO(10)$ and E_6. The smallest possible unification structure with rank four is $SU(5)$. The other most popular structure is $SO(10)$ w with rank=5. While $SU(5)$ enjoys being smallest and most predictive structure which can give SM after spontaneously breaking the $SO(10)$ is the smallest Lie group for which all the SM fermions of one generation can be accommodated in a single anomaly free irreducible representation (16 dimensional spinor), with the natural prediction of right handed neutrino. Having a larger structure $SO(10)$ offers enormous freedom in choosing the symmetry breaking pattern.

The model independent achievements of grand unification theories include: (a) A unique gauge coupling describing nature above the unification scale. (b) Because, quarks and leptons come together in rep(s) of G, the charge quantization is automatically achieved. (c) For the same reason quark-lepton Yukawa couplings get related as a consequence of GUT symmetry constraints. (d) The baryon and lepton number violating super-heavy gauge bosons open the channels for nucleon decay, specifically proton decay. The resolutions of other problems in SM like (i) Fine tuning problem, (ii) Dark matter content of the universe, (iii) Baryonic asymmetry of universe, and (iv) Highly flavored structure of the SM fermions etc. are usually tackled model dependently. In this report we have focused on $SO(10)$ based models at their variant forms.

3.2 $SU(5)$

The grand unification theory based on $SU(5)$ was first proposed by Georgi and Glashow in 1974 [32]. The $SU(5)$ group has only four generator in Cartan subalgebra hence the rank of this group is 4 and the rank of SM is also 4. The adjoint representation is $5^2 - 1 = 24$ dimensional, hence the number of generators and therefore number of gauge bosons is also 24. Because an adjoint representation is a bi-product of fundamental representation and its conjugate representation, $5 \times \bar{5} = 1 + 24$, hence it is an effectively two rank tensor and can be represented in 5×5 matrix form. Only 12 out of 24 gauge bosons belong to SM hence below $SU(5)$ scale only 12, belonging to SM, gauge bosons remain massless while rest acquire GUT scale masses. The fundamental representation, 5, of $SU(5)$ can be decomposed in to $SU(2)_L$ and $SU(3)_C$ like $5 = (2,1)_{1/2} + (1,3)_{-1/3}$, where the structures within bracket are fundamental representations of the respective groups and numbers at subscripts are associated hypercharges, such that $\sum Y = 0$ [135], i.e., no hypercharge quantum number in $SU(5)$. Any multiplicative number to the hypercharges is subject to normalization. The 15 Weyl field of each generation of SM

Reps	Origin	Anomaly	SM Decomposition
5	Fund.	1	$(1,-1/3,3)+(2,1/2,1)$
10	$(5\times 5)_a$	1	$(2,1/6,3)+(1,-2/3,\bar{3})+(1,1,1)$
15	$(5\times 5)_s$	9	$(2,1/6,3)+(1,-2/3,6)+(3,1,1)$
24	$(\bar{5}\times 5)_{tr=0}$	0	$(1,0,8)+(3,0,1)+(2,-5/6,3)$ $+(2,5/6,\bar{3})+(1,0,1)$

Table 3.1: Simple representations of $SU(5)$ and their decomposition in Standard Model.

can not be put in symmetric representation of $SU(5)$ because Adler anomaly is non-zero for this representation (see Appendix A.1) and this symmetric representation also contains a color sixtet of $SU(3)_C$ but, quarks come in color triplet only. The Higgs doublet of SM is put in 5 of $SU(5)$ as $5=(h_T, H)^T \equiv \Phi$. This whole multiplet has to be charge less hence each colored scalar acquires $Y = Q_{EM} = -1/3$. Weyl field are put in the form

$$\bar{5}_F = \begin{pmatrix} d^C \\ \epsilon_2 L \end{pmatrix}_L, \quad 10_F = \begin{pmatrix} \epsilon_3 u^C & Q \\ -Q^T & \epsilon_2 e^C \end{pmatrix}_L \tag{3.1}$$

Here Q represents the quark doublet, the superscript C means the charge conjugation, $\epsilon_2 A = \epsilon_{ij} A_j$ and $\epsilon_3 A = \epsilon_{ijk} A_k$. The ϵ_2 and ϵ_3 are the two and three index Levi-Civita antisymmetric tensors in $SU(2)_L$ and $SU(3)_C$ basis, respectively. Expanding the eq. (3.1) we get

$$\epsilon_2 e^C = \begin{pmatrix} 0 & e^C \\ -e^C & 0 \end{pmatrix}, \; \epsilon_2 L = \begin{pmatrix} e \\ -\nu_e \end{pmatrix} \; \& \; \epsilon_3 u^C = \begin{pmatrix} 0 & u_b^C & -u_g^C \\ -u_b^C & 0 & u_r^C \\ u_g^C & -u_r^C & 0 \end{pmatrix} \tag{3.2}$$

$$SU(5) \rightarrowtail \begin{pmatrix} SU(3) \\ SU(2) \end{pmatrix}, \; SU(5) \rightarrowtail \left(\begin{array}{c|c} SU(3)_C & SU(3)_C \otimes SU(2)_L \\ \hline SU(3)_C \otimes SU(2)_L & SU(2)_L \end{array} \right) \tag{3.3}$$

The distribution of $SU(5)$ in to $SU(3)$ and $SU(2)$ substructures for one and two index tensors is symbolically depicted in eq. (3.3), where the $U(1)_Y$ quantum numbers are ignored. From the Tab. 3.1 we see that decomposition of any of the $SU(5)$ representation smaller than adjoint (24) do not have SM singlet. Therefore, the smallest scalar multiplet which can break $SU(5)$ in to SM has to be the adjoint ($24_H \equiv \Sigma$) representation. Others will simply break the SM as well, or more critically the color symmetry $SU(3)$. A detail analysis of spontaneous symmetry breaking of $SU(n)$ can be found in [136, 137]. The minimal $SU(5)$ is considered as a prototype GUT model to depict the strength and limitations of grand unification and is a text book material today and has been addressed in [138–141] in good detail. Assigning VEV along the off diagonal fields of adjoint representation will again break both $SU(3)_C$ and $SU(2)_L$. Hence, we have the only choice of assigning VEV, which commutes with the generators of $SU(3)$ and $SU(2)$, is

$$\langle\Sigma\rangle \propto \left(\begin{array}{c|c} 2\times\mathbf{1_3} & 0 \\ \hline 0 & -3\times\mathbf{1_2} \end{array}\right) v_\Sigma. \tag{3.4}$$

Hence leaving the symmetry $SU(3)_C \otimes SU(2)_L$ preserved. Given the correct normalization factor, this VEV mimics exactly the hypercharge quantum numbers, hence also leaving the $U(1)_Y$ symmetry intact.

The most general potential, with additional simplifying Z_2 symmetry $\Sigma = -\Sigma$, which plays the role in the breaking of $SU(5)$ is

$$V(\Sigma) = -\frac{\mu^2}{2}\mathrm{Tr}\Sigma^2 + \frac{\lambda}{4}\mathrm{Tr}\Sigma^4 + \frac{\lambda'}{4}(\mathrm{Tr}\Sigma^2)^2. \tag{3.5}$$

where Σ can be also expanded as

$$\Sigma = \left(\begin{array}{c|c} \Sigma_O(1,0,8) & \Sigma_X(2,-5/6,3) \\ \hline \Sigma_{\overline{X}}(2,5/6,\overline{3}) & \Sigma_T(3,0,1) \end{array}\right) + \Sigma_S\,\langle\Sigma\rangle\,. \tag{3.6}$$

Putting the VEV $\langle\Sigma\rangle$ in the eq. (3.5) and estimating the mass term, we get scalar masses

$$m_O^2 = \frac{\lambda}{6}v_\Sigma^2,\ m_T^2 = \frac{2\lambda}{3}v_\Sigma^2,\ m_S^2 = 2\mu^2,\ m_{X,\bar{X}} = 0. \tag{3.7}$$

Therefore, $\lambda > 0$ is required to get an stable and viable solution. These twelve massless scalar bosons $\Sigma_{X,\overline{X}}$ are the Goldstone modes of the theory, which must be swallowed by twelve gauge bosons. The kinetic part of the Higgs under investigation will contribute to the masses of gauge bosons. The covariant derivative for Σ particles is

$$D_\mu\Sigma = \partial_\mu\Sigma + ig_5[A_\mu,\Sigma] \tag{3.8}$$

where

$$A_\mu = \left(\begin{array}{c|c} G(1,0,8) & (X,Y)(2,-5/6,3) \\ \hline (\overline{X},\overline{Y})(2,5/6,\overline{3}) & W(3,0,1) \end{array}\right)_\mu + B_\mu, \tag{3.9}$$

and $A_\mu = \sum_{a=1}^{24} A_\mu^a T^a$ is assumed. As per design, $\langle\Sigma\rangle$ commutes with the generators belonging to SM. Hence, the gluons G_μ, weak bosons W_μ, and Hyper-charge gauge boson B_μ stay massless at the $SU(5)$ breaking scale. However, the generators associated with twelve heavy gauge bosons, $(X,Y)_\mu \equiv (2,-5/6,3)$ and their conjugates, do not commute with the VEV $\langle\Sigma\rangle$ and therefore acquire the GUT scale, $\mathcal{O}(v_\Sigma)$, masses. These gauge bosons are required to be very heavy because they couple quarks with leptons through fermion$-$gauge boson$-$fermion interactions, violating baryon (B) and lepton (L) numbers (though accidentally preserving $B-L$) at the vertices. Therefore they mediate the nucleon decay processes. To satisfy the present bound on proton decay life time, masses of these gauge bosons must be $\geq 10^{15.5}$ GeV.

From Table.(3.1) we see that the fundamentl scalar representation $5_H = (1,-1/3,3)+(2,1/2,1)$ under the SM gauge group. Clearly it contains the standard Higgs doublet $\phi(2,1/2,1) = (\phi^+$
$\phi^0)$. Thus 5_H breaks $SM \to U(1)_{em} \times SU(3)_c$ with appropriate VEV.

The possible scalar multiplets which can generate fermion masses can be found from the decompositions of matter bilinears

$$\overline{5}\times\overline{5} = \overline{10}+\overline{15},\ \ \overline{5}\times 10 = 5+\overline{45},\ \ 10\times 10 = \overline{5}+45+50. \tag{3.10}$$

Not all the multiplets in the right hand side are allowed because $\overline{5}_F$ contains only one chiral component of the matter field hence Dirac mass term are not permitted. Hence, only $5_H, 45_H$ and 50_H are the possible candidates for generating masses of SM fermions. On the other hand 10_H and 15_H may give Majorana term, helpful for seesaw mechanism. In the minimal model, with only 5 as the Higgs boson, the Yukawa Lagrangian is

$$\mathcal{L}_Y = Y_{\overline{5}}\overline{5}^i_F C 10_{Fij}\overline{5}^j_H + \epsilon^{ijklm} 10_{Fij} C Y_{10} 10_{Fkl} 5_{Hm}. \tag{3.11}$$

Here we have ignored the generation index over the fermions. With three generations known in nature the Yukawa matrices $Y_{\overline{5},10}$ are 3×3 complex matrices. With $\langle\Phi\rangle = (0,0,0,0,v_{EW})^T$, we get the masses of fermions. But, $\langle\Phi\rangle$ preserves the $SU(4)$ symmetry so down quark and lepton masses are related at GUT scale. Also using the properties of antisymmetry of Levi-Civita tensor we get

$$Y_d = Y_e^T \quad Y_u = Y_u^T. \tag{3.12}$$

The above relations do not fit with the experimental findings. For example eq. (3.11) predict $m_d = m_e$ and $m_s = m_\mu$ out of which the later relation is badly violated. Although the representation 5_H is used to break the SM gauge theory spontanously, only its standard doublet component takes part in symmetry breaking process. The color takes part in the symmetry breaking process. The color triplet submultiplet $(1, -1/3, \bar{3})$ which is not needed for SSB acquires mass at the GUT scale by extended survival hypothesis. Thus the minimal $SU(5)$ predicts the same particle content as SM below the GUT scale with one loop coefficients $a_Y = 41/10$, $a_{2L} = -19/6$, and $a_{3c} = -7$. It fails to unify gauge couplings of SM as shown in fig.(2.2).

The minimal $SU(5)$ is an extremely predictive model with failed promises. Various extensions of minimal $SU(5)$ model have been popular to explain both experimental as well as philosophical questions. The gauge coupling unification is achieved in its SUSY extensions [142,143], together with the solution to hierarchy problem and the possibility of dark matter candidate. But this extension solicits the incorporation of neutrino mass generating extensions. On the other hand, the adjoint fermionic extension to the minimal $SU(5)$ model gives few-hundred GeV scale type-I+III seesaw, called Adjoint $SU(5)$ model [144, 145]. Major problem with such extensions of $SU(5)$ models is that very often we need to make additional fine tuning to generate different mass scales for the particle with different SM quantum numbers but sitting in the same $SU(5)$ multiplet (For example: the triplet color Higgs, h_T, can mediate the proton decay hence has to be very heavy closer to GUT scale). This is either done by adding extra multiplets [146] in the theory or by introducing higher dimensional operators [144, 145]. The discussion on minimal $SU(5)$ teaches us about the implementation of some crucial checks on GUT models to confirm its viability.

Any unification model based on $SU(5)$ does not satisfactorily predict the family structure of fermions. There is no chiral symmetry in $SU(5)$ at any scale. There is no prediction for RH neutrinos. Also, $SU(5)$ does not explain nature favoring $(V - A)$ current over $(V + A)$.

3.3 $SO(10)$

The next, most popular, candidate gauge group for grand unification is $SO(10)$, first proposed by Fritzsch and Minkowski [35] and Georgi [33]. With one unit larger rank (=5), the theory is phenomenologically more attractive due to larger degrees of freedom. All the SM fermions, together with an additional SM singlet, of one generation are beautifully accommodated in a single 16 dimensional, irreducible, spinor representation. The additional SM singlet is identified as the right handed

(RH) neutrino (N). This is where $SO(10)$ fits perfectly, for it unifies matter besides the interaction. The theory also suggest the LR symmetry of universe prior to any symmetry breakdown or at intermediate scales, which may give platform to explain the favor of $(V-A)$ current over $(V+A)$ at low energies. Thus $SO(10)$ can explain the origin of parity violation as monopoly of weak interaction.

The special orthogonal group $SO(10)$ is a group of 10×10 real orthogonal matrices, O obeying $O\,O^T = O^T O = 1$, with $\mathrm{Det}(O) = 1$. The algebra of $SO(N)$ has been extensively discussed in text books [138–140]. For the sake of completeness, a small recapitulation of the properties of special orthogonal groups is given in Appendix A.4. Since the low energy theory is based on unitary gauge groups, the $SO(10)$ invariants must be re-casted in to the unitary maximal subgroups. The two maximal subgroups of $SO(10)$ are $SU(5)\times U(1)$ and $SU(2)_L \times SU(2)_R \times SU(4)_C \cong SO(4)\times SO(6)$. The decomposition of $SO(10)$ algebra in the basis of $SU(5)\times U(1)$ and $SU(2)_L\times SU(2)_R\times SU(4)_C$ have been extensively discussed in [147,148] and [152], respectively. For the sake of completeness we have listed the table of decompositions of $SO(10)$ irreducible representations up to 210 in to various subgroups, from [153], in the Appendix E.1. The decomposition of $SO(10)$ invariants in to Pati-Salam symmetry has been extensively studied in [153, 155].

Forty five dimensional adjoint representation are orthogonal matrices corresponding to second rank antisymmetric tensor. Similarly $54\subset SO(10)$ in the second rank symmetric tensor. Because $SO(10)$ is a large symmetry, there can be many subgroups which are larger than SM and accommodate the structure of SM. The symmetries of these subgroups may appear at intermediate energy scales, unlike the $SU(5)$ GUT where we had one and only one way to reach SM. Some popular breaking schemes of $SO(10)$ to SM are depicted in Fig. 3.1, where

$$
\begin{aligned}
&G_{13} = U(1)_Q \otimes SU(3)_C\\
&G_{5/51} = SU(5)/SU(5)\otimes U(1)_X\\
&G_{213} = SU(2)_L \otimes U(1)_Y \otimes SU(3)_C \quad \text{(SM)}\\
&G_{214} = SU(2)_L \otimes U(1)_X \otimes SU(4)_C\\
&G_{224} = SU(2)_L \otimes SU(2)_R \otimes SU(4)_C \quad \text{(PS)}\\
&G_{2113} = SU(2)_L \otimes U(1)_{B-L} \otimes U(1)_R \otimes SU(3)_C\\
&G_{2213} = SU(2)_L \otimes SU(2)_R \otimes U(1)_{B-L} \otimes SU(3)_C \quad \text{(LR)}\\
&G_{2213D} = G_{2213}\otimes D \quad (g_{2L}=g_{2R}),\; G_{224D} = G_{224}\otimes D(g_{2L}=g_{2R}),
\end{aligned}
\tag{3.13}
$$

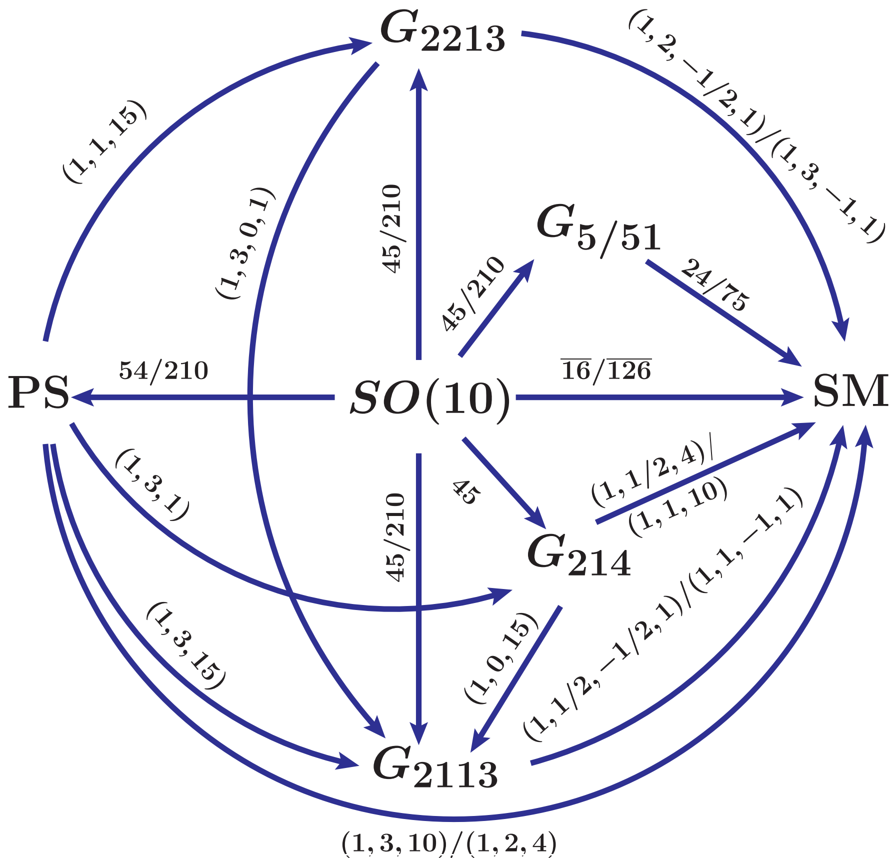

Figure 3.1: Popular and physically viable breaking chains of $SO(10)$ down to the SM [33, 38, 156–159].

and the scalar multiplets sitting near the arrows if given VEV will break the symmetries at the tail in to symmetries at the head. The $SO(10)$ origin of these multiplets can be found from the decomposition tables and are re-listed in Tab. 3.2. The SSB of $SO(10)$ to G_{224D} can be achieved by D-even PS singlet residing in 54 [38, 149, 150], while breaking to G_{224} is achieved by D-odd PS singlet residing in 210 [36, 37]. Also, the SSB of $SO(10)$/PS D-even symmetry to G_{2213D} is achieved by D-even LR singlet residing in $210/(1, 1, 15)$ [154], while breaking of $SO(10)$ or PS symmetry (D-odd or even) to G_{2213} is achieved by D-odd LR singlet residing in $45/(1, 1, 15)$ [149–151]. Rest of the sub-algebras are D-parity broken. The scalar multiplets breaking these sub-algebras are depicted in Fig. 3.1 and their $SO(10)$ origin can be read from the Tab. 3.2. Under the assumption of *extended survival hypothesis*, particles residing only in these representation acquire the masses of the order of symmetry breaking scale. For example 54 scalar breaks $SO(10)$ in to G_{224D} at GUT scale and does not participate in any breaking further hence all the scalars in 54 get the masses

$(1,1,15)_{G_{224}} \subset 45, 210$
$(1,3,0,1)_{G_{2213}} \subset (1,3,1)_{G_{224}} \subset 45$
$(1,0,15)_{G_{214}} \subset (1,3,15)_{G_{224}} \subset 210$
$(1,0,15)_{G_{214}} \subset (1,1,15)_{G_{224}} \subset 210$
$(1,3,0,1)_{G_{2213}} \subset (1,3,15)_{G_{224}} \subset 210$
$(1,1,-1,1)_{G_{2113}} \subset (1,1,10)_{G_{214}} \subset (1,3,10)_{G_{224}} \subset 126$
$(1,1,-1,1)_{G_{2113}} \subset (1,3,-1,1)_{G_{2213}} \subset (1,3,10)_{G_{224}} \subset 126$
$(1,1/2,-1/2,1)_{G_{2113}} \subset (1,1/2,4)_{G_{214}} \subset (1,2,4)_{G_{224}} \subset 16$
$(1,1/2,-1/2,1)_{G_{2113}} \subset (1,2,-1/2,1)_{G_{2213}} \subset (1,2,4)_{G_{224}} \subset 16$
$(2,1,-1,1)_{G_{2113}} \subset (2,1,4)_{G_{224}} \subset 16$

Table 3.2: The multiplets participating in SSB by acquiring VEVs in the invariant direction of the residual symmetry.

of $\mathcal{O}(M_{GUT})$. Similarly when (1,3,1) of 45 breaks PS symmetry to G_{214} or (1,3,15) of 210 breaks PS symmetry to G_{2113} the scalar particles residing in these multiplets (1,3,1) and (1,3,15) acquire the masses of PS (whether D-odd or even) breaking scale.

Once the additional symmetries are included to populate the grand desert, SUSY is not necessarily required for unification of gauge couplings. In addition, with intermediate gauge symmetries $SO(10)$ also predicts signals of new physics which can be probed at low or accelerator energies. The left-right (LR) [30, 31] symmetry is a finite gauge transformation under charge conjugation. Through Pati-Salam [28] intermediate symmetry left-right symmetry G_{224D} or through G_{2213D} is realized and the parity violation at low energy is understood as an artifact of the breaking of the left-right symmetry.

We note from the Tab. E.1 to Tab. E.7 that all representations except 10 and 120 contain SM singlets, but not all of them break $SO(10) \to$SM in a single step. The SM singlets of representations 45, 54 and 210 are also singlets of higher symmetry, so assigning VEV to the scalar fields in these representations will break $SO(10)$ to the corresponding higher symmetry.

On the other hand in addition to these, if SM singlets of $\overline{16}$ and $\overline{126}$ are assigned a VEV the symmetry of $SO(10)$ will spontaneously break to SM. If an intermediate symmetry is at work then sub-multiplets of $\overline{16}$ and $\overline{126}$ under the intermediate symmetry having SM singlets will do the job. For example In the case of 16_H it is the mutual component of RH doublet $(1, 2, -1, 1)_H$ and in the case of 126_H it is the neutral component of the RH triplet $\Delta_R(1, 3, -2, 1)$ that acquires VEV to break $G_{2213} \to SM$. The gauge coupling unification in non-SUSY $SO(10)$ grand unification desperately demands the presence of intermediate symmetries. Hence we require a combination of the appropriately chosen multiplets to generate the spontaneous symmetry breaking mechanism under study.

In the SUSY version of $SO(10)$, If $R\,[= (-1)^{3(B-L)+2S}]$ parity remains an exact symmetry at all scales the lightest SUSY partner will be stable, which may be an ideal candidate for the dark matter of the universe. This R-parity is predicted as a gauged discrete symmetry SUSY $SO(10)$ or SUSY G_{224D} models which maintains stability of dark matter. This R-parity is predicted as a gauged discrete symmetry SUSY $SO(10)$ or SUSY G_{224D} models which maintains stability of dark matter. Under R-parity $p \to p$ and $\tilde{p} \to \tilde{p}$, where p stands for particle and $\tilde{p}$ for its super-partner. In the non-SUSY LR model, Pati-Salam model, or non-SUSY SO(10) model, the matter parity $M = (-1)^{3(B-L)}$ is obviously equivalent to the R-parity becomes $(-1)^{2S} = 1$ for the physical Hamiltonians and only scalars with $S = 0$ are allowed to have non vanishing VEVs. Under matter parity $16 \to -16$ and $10 \to 10$. All other relations build out of 10, such as 45, 54, 120, 126, 210 etc., are even. Only representations with spinor content like 16, 144 etc. will be odd under matter parity.

The decomposition of $SO(10)$ spinor multiplet 16_F in to SM fermions plus additional RH neutrino is expressed as

$$\begin{array}{rcl} 16_F & = & \underset{Q_L}{(2, \frac{1}{6}, 3)} + \underset{L_L}{(2, -\frac{1}{2}, 1)} + \underset{u_L^C}{(1, -\frac{2}{3}, \bar{3})} + \underset{d_L^C}{(1, \frac{1}{3}, \bar{3})} + \underset{e_L^C}{(1, 1, 1)} + \underset{\nu_L^C .}{(1, 0, 1)} \end{array} \quad (3.14)$$

In the $SU(5)$ and PS basis this can be equivalently written as

$$\begin{aligned} 16_F &\equiv \bar{5}_F \oplus 10_F \oplus 1_F; \quad SU(5) \\ &\equiv (2, 1, 4) \oplus (1, 2, \overline{4})_F; \quad \text{PS}. \end{aligned} \quad (3.15)$$

Thus all fermions of one generation including RH neutrino (N) occur as left-right symmetric doublets in G_{224} or G_{2213}. The interesting features of $SO(10)$ GUTs is that the Majorana masses are dictated by Yukawa couplings and the SSB pattern implemented for gauge coupling unification. Since, the $SO(10)$ symmetry does not distinguish among the components of the decomposition, see eq. (3.15), the Yukawa couplings for neutrinos are closely related to charged fermions. The Yukawa Lagrangian which generates masses to the 16_F fermions of the model must have scalars in 10, 120 and $\overline{126}$ representations, in general, because

$$16 \otimes 16 = 10_s \oplus 120_{as} \oplus 126_s\,. \tag{3.16}$$

We can see that SM Higgs doublets are also present in these representations which further break SM in to $U(1)_Q \times SU(3)_C$ and generate fermion masses. A realistic $SO(10)$ GUT framework allows proper SSB of $SO(10)$ down to SM, and gauge and Yukawa interactions must be compatible with the current experimental results on quark and lepton masses and mixings. In (non-)SUSY case, at least (two)three Higgs representations are required to break $SO(10)$ down to $U(1)_Q \times SU(3)_C$, the low energy theory. As noted, the scalar representations which couple to fermionic bilinears are $10_H, 120_H$ and $\overline{126}_H$ which contain the SM like Higgs doublets. There can be $SU(2)_L$ Higgs doublets coming from the representations which do not directly couple to fermionic bilinears. Their superposition gives effective SM light Higgs doublet which can acquire electroweak VEV. A nice and detail description can be found in [153]. If tree-level Dirac neutrino mass is prevented by imposing some symmetry, then neutrino can acquire small Dirac masses at the loop level without extreme fine tuning of couplings.

Advantages of using $SO(10)$ over $SU(5)$ are: a) A single family of fermions are accommodated in a single 16-dimensional spinorial representation of $SO(10)$, with a prediction of right-handed neutrino. b) Both left and right handed fermions reside in a single representation, hence, left-right symmetry can be achieved through a finite gauge transformation in the form of charge conjugation. Thus the parity symmetry is a part of continuous gauge symmetry. c) Besides $SU(5) \times U(1)$, its other maximal subgroup is Pati-Salam symmetry, which explains the GUT scale mass relation $m_s = m_{\mu/3}$, up to certain extent. d) The gauge coupling unification can be achieved through intermediate symmetry even if the SUSY is absent. e) In the non-SUSY version, matter parity $M = (-1)^{B-L}$ is equivalent to the R-parity in SUSY $SO(10)$. It is possible to keep R intact if $SO(10)$ symmetry is broken appropriately by the Higgs representation 126_H instead of 16_H in SUSY (non-SUSY) case.

3.4 Majorana neutrinos and seesaw mechanism

3.4.1 Standard model extensions

Since, the neutrinos are electrically neutral they can be Dirac or Majorana fermions. If they are complex four component Dirac fields, as charge fermions, then neutrinos (ν) and antineutrinos ($\overline{\nu}$) would have same mass but opposite lepton number therefore ν-mass Lagrangian would be lepton number conserving. There is no lepton number preserving symmetry in the SM but there is a global lepton number symmetry. Violation of this accidental symmetry will allow the Majorana mass term in the Lagrangian, and neutrinos would be two component Majorana fields.

Extending the SM with three right handed singlet field ν_R we write Dirac mass Lagrangian for neutrino

$$\mathcal{L}^D = -\overline{\nu}_L M_D \nu_R + h.c. \tag{3.17}$$

where M_D= Dirac neutrino mass matrix=$Y_\nu v_{EW}$, and v_{EW} is electroweak VEV of standard Higgs doublet. For neutrinos to be as light as 1 eV, $Y_\nu \sim \mathcal{O}(10^{-12})$, which is extremely tiny and leads to fine tuning problem in the theory. However there has been also a number of interesting investigations suggesting neutrinos to be Dirac particles On the other hand Majorana mass term can be written as

$$\mathcal{L}^M = -\frac{1}{2}\overline{\nu}_L M_L^M \nu_L^C + h.c. \tag{3.18}$$

The smallness of M_L has also to be explained. With two lepton doublets, we need to make this term gauge and Lorentz invariant. The most elegant way to explain this is the seesaw mechanism [161]. From within the SM, Yukawa interactions augmented by higher dimensional terms are written like dimension-5 Weinberg operator [160]

$$\mathcal{L}_Y(d=5) = \lambda_{ij}\frac{({l_L}_i^T i\sigma_2 H)C(H^T i\sigma_2 l_{Lj})}{M_\Lambda} \tag{3.19}$$

where M_Λ is the cut-off scale of the theory, λ is couplings strength and i, j are flavour indices. When H acquires VEV we get

$$M_L^M = \lambda\frac{v_{EW}^2}{M_\Lambda}. \tag{3.20}$$

The other non-vanishing contributions, ignoring Lorentz index, can be

$$(l_L^T\sigma_2\overrightarrow{\sigma}l_L)(H^T\sigma_2\overrightarrow{\sigma}H) \tag{3.21}$$

$$(l_L^T\sigma_2\overrightarrow{\sigma}H)(H^T\sigma_2\overrightarrow{\sigma}l_L) \tag{3.22}$$

Closer look at the eq. (3.19), eq. (3.21) and eq. (3.22) suggests that the renormalizable Yukawa term with extended particle structure can reproduce the dim=5 invariants if heavy modes are integrated out

$$({l_L}^T\sigma_2 H)\nu_R,\ (l_L^T\sigma_2\overrightarrow{\sigma}l_L).\overrightarrow{\Delta},\ \&\ (l_L^T\sigma_2\overrightarrow{\sigma}H).\overrightarrow{\rho}, \tag{3.23}$$

where ν_R, Δ and ρ are SM singlet fermion, $SU(2)_L$ triplet (3,1,1) scalar and $SU(2)_L$ triplet (3,0,1) fermion, respectively, under $SU(2)_L\times U(1)_Y\times SU(3)_C$. The masses of these BSM particles are the cut-off scale. Integrating out the heavy modes generates the non-zero masses for light neutrinos and this mechanism to generate the masses for neutrinos is known as seesaw mechanism. These three types of generating masses of neutrinos are called type-I [39, 42], type-II [144, 145, 162] and type-III [43, 79, 162] seesaw, respectively.

With a gauge singlet chiral fermion per generation, the renormalizable Yukawa coupling follows

$$\Delta\mathcal{L} = Y_\nu \bar{l}_L\sigma_2 H^*\nu_R + \frac{M_R}{2}\nu_R^T C\nu_R + h.c. \tag{3.24}$$

with $\nu \equiv \nu_L + C\overline{\nu}_L^T$ and $N \equiv \nu_R + C\overline{\nu}_R^T$ we get the total mass matrix of neutral Lagrangian

$$M_\nu = \begin{pmatrix} 0 & M_D^T \\ M_D & M_R \end{pmatrix} \equiv U_\nu \begin{pmatrix} m_\nu & 0 \\ 0 & M_h \end{pmatrix} U_\nu^T, \tag{3.25}$$

where M_ν, U_ν are 6×6 matrices and rest of the matrices in eq. (3.25) are 3×3. For $M_D << M_R$ we have predominantly Majorana case such that the block diagonalized matrices are

$$m_\nu \simeq -M_D\frac{1}{M_R}M_D^T\ \&\ M_N \simeq M_R. \tag{3.26}$$

This is the canonical or type-I seesaw.

Now, if instead of fermionic singlet we have a scalar triplet, the relevant Yukawa part of Lagrangian is

$$\Delta\mathcal{L} = Y_\Delta^{ij} l_{L_i}^T C\sigma_2\Delta_L l_{L_j} + h.c. \tag{3.27}$$

and the associated scalar potential term is

$$\Delta V = \mu_\Delta H^T \sigma_2 \Delta_L^* H + M_\Delta^2 \mathrm{Tr} \Delta_L^\dagger \Delta_L + .. \tag{3.28}$$

where $\mu_\Delta \sim \mathcal{O}(M_\Delta)$ and $\Delta = \overrightarrow{\sigma} \cdot \overrightarrow{\Delta}$. The VEV $\langle\Delta\rangle$ results from cubic scalar part of the Lagrangian. Neutrinos get the mass

$$m_\nu = Y_\Delta \langle\Delta\rangle \tag{3.29}$$

with $\langle\Delta\rangle \simeq \frac{\mu_\Delta v_{EW}^2}{M_\Delta^2}$. This is known as type-II seesaw mechanism.

Similarly, addition of a triplet fermion gives the Lagrangian

$$\Delta\mathcal{L} = Y_\rho l_L^T C \sigma_2 \rho H + M_\rho \overrightarrow{\rho}^T C \overrightarrow{\rho} \tag{3.30}$$

where $\rho = \overrightarrow{\sigma} \cdot \overrightarrow{\rho}$ and the mass M_ρ is the scale of new physics. Similar to type-I seesaw for $M_\rho >> v_{EW}$

$$m_\nu = -Y_\rho \frac{1}{M_\rho} Y_\rho^T v_{EW}^2. \tag{3.31}$$

This mechanism to generate light neutrino masses is called type-III seesaw. While in type-II seesaw only one Δ is enough to get the general neutrino mass matrix, in type-I (III) seesaw the number of required singlet (triplet) is same as required number of non-zero light masses, i.e. at least two.

3.4.2 Seesaw mechanisms in GUTs

In the GUT framework, the multiplets giving type-I, type-II and type-III seesaw are part of suitable representations. For example in $SU(5)$ GUTs the RH neutrino N needed for type-I seesaw mechanism is SU(5) singlet fermion, the triplet scalar of SM giving type-II seesaw is a part of the symmetric representation of 15_H of $SU(5)$ of the triplet SM fermion giving type-III seesaw is a part of adjoint representation of 24_F of $SU(5)$, as we can see in Tab. 3.1. The $SU(5)$ singlet fermion (N) giving type-I may be part of some GUT multiplet. In $SO(10)$ we already have the additional fermion singlet as part of the fermionic family in the spinorial representation 16_F. In E_6 GUT it is a fundamental representation 27_F. The triplet scalars (vectors) giving type-II (III) seesaw come from $\overline{126}_H$ and 45_F multiplets of $SO(10)$. The advantage of $SO(10)$ over $SU(5)$ is that since extra fermion is part of the same multiplet in the former case as other SM fermions, the neutrino Dirac mass matrix is strongly correlated with the mass matrices of other fermions.

Chapter 4

Non-Canonical Seesaw Dominance: General Framework

4.1 Type-I and Type-II seesaw in LRS and SO(10) models

The most popular method of neutrino mass [163–168] generation has been through type-I or canonical seesaw mechanism [39–42] which was also noted to apply in the simplest extension of the SM through right-handed (RH) neutrinos encompassing family mixings [76, 77]. Most of the problems of the SM have potentially satisfactory solutions in the minimal left-right symmetric (LRS) [28–31, 43] grand unified theory based on SO(10) [36–38, 60, 61, 169–179].

A special feature of left-right gauge theories [28–31] and SO(10) grand unified theory (GUT) [36–38, 60, 61, 169, 170, 172] is that the canonical seesaw formula [39–42, 76, 77] for Majorana neutrino masses is usually accompanied by the type-II seesaw formula [43, 76, 79–82, 180]. The parameters entering into this hybrid seesaw formula have fundamentally appealing interpretations in Pati-Salam model [28, 29] or SO(10) GUT. In eq.(1.2) $M_D(M_N)$ is Dirac (RH-Majorana) neutrino mass, and in eq.(1.3) $v_L \sim \lambda \frac{v_{wk}^2 V_R}{M_{\Delta_L}^2}$ is the induced vacuum expectation value (VEV) of the LH triplet Δ_L, $V_R = SU(2)_R \times U(1)_{B-L}$ breaking VEV of the RH triplet Δ_R, and f is the Yukawa coupling of the triplets $\subset \overline{126}_H$ of SO(10). Here λ is the quartic coupling in the $\Delta_L - \Delta_R - \phi$ interaction term in the Higgs potential $V_{Higgs} = \lambda \Delta_L^\dagger \Delta_R \phi^\dagger \phi$ + ... where $\phi(2, 2, 0, 1)$ is the Higgs bidoublet $\subset 10_H$ of SO(10). The same Yukawa coupling f also defines the RH neutrino mass $M_N = fV_R$. Normally, because of the underlying quark-lepton symmetry in SO(10) or Pati-Salam model, M_D is of the same order as M_u, the up-quark mass matrix, that drives the canonical seesaw scale to be large, $M_N \sim 10^{14}$ GeV. In the LRS theory based upon $SU(2)_L \times SU(2)_R \times U(1)_{B-L} \times SU(3)_C (\equiv G_{2213})$, $M_D \sim M_l =$ charged lepton mass matrix. The neutrino oscillation data then pushes this seesaw scale to $M_N \sim 10^{10}$ GeV. Similarly the type-II seesaw scale is also around this mass. With such high seesaw scales in non-supersymmetric (non-SUSY) SO(10) model or LRS theory, there is no possibility of direct experimental verification of the seesaw mechanism or the associated W_R boson mass in near future. Likewise, the predicted LFV decay rates are far below the experimental limits.

The scope and applications of type-I seesaw to TeV scale W_R boson models have been discussed in the recent interesting review [181]. In such models D-Parity is at first broken at high scale that makes the left-handed triplet much heavier than the W_R mass, but keeps the $G_{2213}(g_{2L} \neq g_{2R})$ unbroken down to much lower scale [36–38]. This causes the type-II seesaw contribution of the hybrid seesaw formula of eq. (1.1) to be severely damped out in the LHC scale W_R models where type-I seesaw dominates. But because M_N is also at the TeV scale, the predicted type-I seesaw contribution to light neutrino mass turns out to be $10^6 - 10^{11}$ times larger than the experimental values unless it is adequately suppressed while maintaining its dominance over type-II seesaw. Such suppressions have been made possible in two ways:(i) using fine tuned values of the Dirac neutrino mass matrices M_D [181–187] ,(ii) introducing specific textures to the fermion mass matrices M_D and/or M_N [188–203].

Even without going beyond the SM paradigm and treating the added RH neutrinos in type-I seesaw as gauge singlet fermions at $\sim$ GeV scale, rich structure of new physics has been predicted including neutrino masses, dark matter, and baryon asymmetry of the universe. The fine-tuned value of the associated Dirac neutrino Yukawa coupling in these models is $y \sim 10^{-7}$ [204–206].

There are physical situations where type-II seesaw dominance, rather than type-I seesaw or inverse seesaw, is desirable [43–45, 47–50, 55, 76, 77, 79–82, 89–92, 94, 95, 180, 207, 208, 210, 211].

In the minimal case, being a mechanism driven by intermediate scale mass of LH triplet, type-II seesaw may not be directly verifiable; nevertheless it can be clearly applicable to TeV scale Z_R models in non-SUSY SO(10) to account for neutrino masses [208] provided type-I contribution is adequately suppressed. However, as in the fine-tuning of Dirac neutrino mass in the type-I seesaw case in LR models, the induced VEV needed for type-II seesaw can also be fine tuned using more than one electroweak bi-doublets reducing the triplet mass to lower scales accessible to accelerator tests. Looking to the eq.(1.1) and the structure of the induced VEV v_L, the most convenient method of suppressing type-I seesaw with respect to type-II seesaw is to make the type-I seesaw scale $M_N = fV_R$ larger and the triplet mass much smaller, $M_{\Delta_L} << M_N$. This requires the $SU(2)_R \times U(1)_{B-L}$ breaking scale or $M_{W_R} >> M_{\Delta_L}$. SUSY and non-SUSY SO(10) models have been constructed with this possibility and also in the case of split-SUSY [44, 45] where $M_{W_R} \simeq 10^{17}$ GeV. Obviously such models have no relevance in the context of TeV scale W_R or Z_R bosons accessible to LHC searches.

Whereas the pristine type-I or type-II seesaw are essentially high scale formulas inaccessible for direct verification and need fine tuning or textures to bring them down to the TeV scale, the well known classic inverse seesaw mechanism [212] which has been also discussed by a number of authors [213–222] is essentially TeV scale seesaw. It has the high potential to be directly verifiable at accelerator energies and also by ongoing experiments on charged lepton flavor violations [223–232, 232, 233].

As discussed above if type-I seesaw is the neutrino mass mechanism at the TeV scale, it must be appropriately suppressed either by finetuning or by introducing textures to the relevant mass matrices [181]. On the otherhand if type-II seesaw dominance in LR models or SO(10) is to account for neutrino masses, W_R, Z_R boson masses must be at the GUT-Planck scale in the prevailing dominance mechanisms [44, 45].

In view of this, it would be quite interesting to explore, especially in the context of non-supersymmetric SO(10), possible new physics implications when the would be dominant type-I seesaw cancels out exactly and analytically from the light neutrino mass matrix even without needing any fine tuning or fermion mass textures in M_D and/or M_N . The complete cancellation of type-I seesaw in the presence of heavy RH Majorana mass term $M_N NN$ was explicitly proved in ref. [234, 235] in the context of SM extension when both N_i and S_i are present manifesting in heavy RH neutrinos and lighter singlet fermions. We call this as gauge singlet fermion assisted extended seesaw dominance mechanism. Since then the mechanism has been utilised in explaining baryon asymmetry of the universe via low-scale leptogenesis [234, 235], the phenomenon of dark matter (DM) [236] along with cosmic ray anomalies [237]. More recently this extended seesaw mechanism for neutrino masses in the SM extension has been exploited to explain the keV singlet fermion DM along with low-scale leptogenesis [238].

In the context of LR intermediate scales in SUSY SO(10), this mechanism has been applied to study coupling unification and leptogenesis [239–241] under gravitino constraint. Application to non-SUSY LR theory originating from Pati-Salam model [242] and non-SUSY SO(10) with TeV scale W_R, Z_R bosons have been made [87, 88] with the predictions of a number of experimentally testable physical phenomena by low energy experiments and including the observed dilepton excess at LHC [243]. In these models the singlet fermion assisted type-I seesaw cancellation mechanism operates and the extended seesaw (or inverse seesaw) formula dominates.

This article is organised in the following manner. In Sec.4.2, we explain how the Kang-Kim mechanism [234, 235] operates within the SM paradigm extended by singlet fermions. In Sec.4.3, we show how a generalised neutral fermion mass matrix exists in the appropriate extensions of the SM, LR theory, or SO(10). In Sec.4.4, we show emergence of the other dominant seesaw mechanism including the extended or inverse seesaw and type-II seesaw and cancellation of type-I seesaw.

4.2 Mechanism of extended seesaw dominance

Using the explicit derivation of Kang and Kim [234], here we discuss how the type-I contribution completely cancels out paving the way for the dominance of extended seesaw mechanism. The SM is extended by introducing RH neutrinos $N_i (i = 1, 2, 3)$ and an additional set of fermion singlets $S_i (i = 1, 2, 3)$, one for each generation. After electroweak symmetry breaking, the Yukawa Lagrangian in the charged lepton mass basis gives for the neutral fermions

$$\mathcal{L}_{mass} = (M_D \overline{\nu} N + \frac{1}{2} M_N N^T N + M \overline{N} S + h.c) + \mu_S S^T S \tag{4.1}$$

where M_D = the Dirac neutrino mass matrix $= Y < \phi >$, Y being the Yukawa matrix. This gives the 9×9 neutral fermion mass matrix in the (ν, N^c, S) basis,

$$\mathcal{M}_\nu = \begin{pmatrix} 0 & M_D & 0 \\ M_D^T & M_N & M^T \\ 0 & M & \mu_S \end{pmatrix}. \tag{4.2}$$

The type-I seesaw cancellation leading to dominance of extended seesaw (or inverse seesaw) [212] proceeds in two steps: As $M_N >> M >> M_D, \mu_S$, it is legitimate to integrate out the RH N_i fields at first leading to the corresponding effective Lagrangian

$$-\mathcal{L}_{\text{eff}} = \left(M_D \frac{1}{M_N} M_D^T\right)_{\alpha\beta} \nu_\alpha^T \nu_\beta + \left(M_D \frac{1}{M_N} M^T\right)_{\alpha m} \left(\overline{\nu_\alpha} S_m + \overline{S_m} \nu_\alpha\right) + \left(M \frac{1}{M_N} M^T\right)_{mn} S_m^T S_n + \mu_S S^T S. \tag{4.3}$$

Then diagonalisation of the 9×9 neutral fermion mass matrix including the result of $\mathcal{L}_{\text{eff}}$ gives conventional type-I seesaw term and another of opposite sign leading to the cancellation.

It must be emphasized that the earlier realizations of the classic inverse seesaw formula [212] were possible [213–220,222] with vanishing RH Majorana mass $M_N = 0$ in eq.(4.2).

Under the similar condition in which the type-I seesaw cancels out the Majorana mass m_S of the sterile neutrino and its mixing angle θ_S with light neutrinos are governed by

$$m_S = \mu_S - M \frac{1}{M_N} M^T \sim -M \frac{1}{M_N} M^T,$$
$$\tan 2\theta_S = 2 \frac{M_D}{M}. \tag{4.4}$$

As μ_S is naturally small, it is clear that type-I seesaw now controls the gauge singlet fermion mass, although it has no role to play in determining the LH neutrino mass. These results have been shown to emerge [87, 88, 208, 239, 243, 244] from SO(10) with gauge fermion singlet extensions by following the explicit block diagonalisation procedure in two steps while safeguarding the hierarchy $M_N >> M > M_D, \mu_S$ with the supplementary condition $\mu_S M_N < M^2$.

4.3 Generalized neutral fermion mass matrix

A left-right symmetric (LRS) gauge theory $G_{2213D}(g_{2L} = g_{2R})$ at higher scale ($\mu = M_P$) is known to lead to TeV scale asymmetric LR gauge theory $G_{2213}(g_{2L} \neq g_{2R})$ via D-Parity breaking [36–38]. This symmetry further breaks to the SM gauge symmetry by the VEV of the RH triplet $\Delta_R(1, 3, -2, 1)$ leading to massive W_R, Z_R bosons and RH neutrinos at the intermediate scale M_R. Instead of $G_{2213D}(g_{2L} = g_{2R})$ it is possible to start directly from $SO(10)$ which has been discussed at length in a number of investigations that normally leads to the type-I$\oplus$type-II hybrid seesaw formula. In the absence of additional sterile neutrinos, the neutral fermion matrix is standard 6×6 form. Here we discuss how a generalised 9×9 neutral fermion mass matrix that emerges in the presence of additional singlet fermions contains the rudiments of various seesaw formulas. As noted in Sec. 4.1, the derivation of the minimal classic inverse seesaw mechanism [212] has been possible in theories gauge singlet fermion extensions of the SM are available [213–222, 245]. Extensive applications of this mechanism have been discussed and reported in a number of recent reviews [168, 247, 248, 250–252]. Exploring possible effects on invisible Higgs decays [253–255], prediction of observable lepton flavor violation as a hall mark of the minimal classic inverse seeaw mechanism has attracted considerable attention earlier and during recent investigations [256–259, 263–265]. The effects of massive gauge singlet fermions have been found to be consistent with electroweak precision observables [266,267] Earlier its impact on a class of left-right symmetric models have been examined [246, 268, 269]. Prospects of lepton flavor violation in the context of linear seesaw and dynamical left-right symmetric model have been also investigated earlier [245].

It is well known that 15 fermions of one generation plus a right handed neutrino form the spinorial representation 16 of SO(10) grand unified theory [169, 170]. In addition to three generation of fermions $16_i (i = 1, 2, 3)$, we also include one SO(10)-singlet fermion per generation $S_i (i = 1, 2, 3)$. We note that such singlets under the LR gauge group or the SM can originate from the non-standard fermion representations in SO(10) such as 45_F or 210_F.

Under G_{2213} symmetry the fermion and Higgs representations are,

Fermions

$$Q_L = \begin{pmatrix} u \\ d \end{pmatrix}_L \Big(2, 1, 1/3, 3\Big),\ Q_R = \begin{pmatrix} u \\ d \end{pmatrix}_R \Big(1, 2, -1/3, 3^*\Big),$$
$$L = \begin{pmatrix} \nu_l \\ l \end{pmatrix}_L \Big(2, 1, -1, 1\Big),\ R = \begin{pmatrix} N_l \\ l \end{pmatrix}_R \Big(1, 2, -1, 1\Big),$$
$$S_i = \Big(1, 1, -1, 1\Big).$$

Higgs

$$\phi = \begin{pmatrix} \phi_1^0 & \phi_2^+ \\ \phi_1^- & \phi_2^0 \end{pmatrix} \Big(2, 2, 0, 1\Big),\ \Delta_L = \begin{pmatrix} \Delta_L^+/\sqrt{2} & \Delta_L^{++} \\ \Delta_L^0 & -\Delta_L^+/\sqrt{2} \end{pmatrix} \Big(3, 1, -2, 1\Big),$$

$$\Delta_R = \begin{pmatrix} \Delta_R^+/\sqrt{2} & \Delta_R^{++} \\ \Delta_R^0 & -\Delta_R^+/\sqrt{2} \end{pmatrix} \Big(1, 3, -2, 1\Big),$$
$$\chi_L = \begin{pmatrix} \chi_L^0 \\ \chi_L^- \end{pmatrix} \Big(2, 1, -1, 1\Big),\ \chi_R = \begin{pmatrix} \chi_R^0 \\ \chi_R^- \end{pmatrix} \Big(1, 2, -1, 1\Big),$$
$$\eta_o(1, 1, 0, 1),$$
where η_o is a D-Parity odd singlet with transformation property $\eta_o \to -\eta_o$ under $L \to R$. When this singlet acquires VEV $< \eta_o >\sim M_P$, D-Parity breaks along with the underlying left-right discrete symmetry but the asymmetric LR gauge theory G_{2213} is left unbroken down to the lower scales. The G_{2213} gauge theory can further break down to the SM directly by the VEV of RH Higgs triplet $\Delta_R(1, 3, -2, 1) \subset 126_H \subset SO(10)$ or the RH Higgs doublet $\chi_R(1, 2, -1, 1) \subset 16_H \subset SO(10)$. The D-Parity odd (even) singlets $\eta_o(\eta_e)$ were found to occur naturally in $SO(10)$ GUT theory [36–38]. Designating the quantum numbers of submultiplets under Pati-Salam symmetry $SU(2)_L \times SU(2)_R \times SU(4)_C$ ($\equiv G_{224}$), the submultiplet $(1, 1, 1) \subset 210_H \subset SO(10)$ is η_o where as the submultiplet $(1, 1, 1) \subset 54_H \subset SO(10)$ is η_e. Likewise the neutral component of the submultiplet $(1, 1, 15) \subset 45_H \subset SO(10)$ behaves as η_o, but that in $(1, 1, 15) \subset 210_H$ behaves as η_e. Thus the GUT scale symmetry breaking $SO(10) \to G_{224D}$ can occur by the VEV of 54_H in the direction $< \eta_e >\sim M_{GUT}$, but $SO(10) \to G_{224}$ can occur by the VEV of 210_H in the direction $< \eta_o >\sim M_{GUT}$. Likewise $SO(10) \to G_{2213D}$ can occur by the VEV of the neutral component $(1, 1, 0, 1)_H \subset (1, 1, 15)_H \subset 210_H$, but $SO(10) \to G_{2213}$ can occur by the VEV of the neutral component of $(1, 1, 0, 1)_H \subset (1, 1, 15)_H \subset 45_H$. As an example, one minimal chain with TeV scale LR gauge theory in the context of like-sign dilepton signals observed at LHC is,

$$\begin{aligned} SO(10) \quad &\stackrel{(M_U=M_P)}{\longrightarrow} \quad SU(2)_L \times SU(2)_R \times U(1)_{B-L} \times SU(3)_C \quad [G_{2213}] \\ &\stackrel{(M_R)}{\longrightarrow} \quad SU(2)_L \times U(1)_Y \times SU(3)_C \quad [\mathrm{SM}] \\ &\stackrel{(M_Z)}{\longrightarrow} \quad SU(3)_C \times U(1)_Q. \end{aligned} \tag{4.5}$$

In this symmetry breaking pattern all LH triplets and doublets are near the GUT scale, but RH triplets or doublets are near the G_{2213} breaking intermediate scale M_R which could be $\sim$ (few $-$ 100) TeV. Out of two minimal models with GUT scale D-Parity breaking satisfying the desired decoupling criteria $M_N >> M >> M_D, \mu_S$ [208, 243], dominance of extended seesaw in the presence of gauge singlet fermions has been possible in ref. [243] with single G_{2213} intermediate scale corresponding to TeV scale W_R, Z_R bosons. The extended seesaw dominance in the presence of fermion singlets in SO(10) have been also realised including additional intermediate symmetries G_{2214D} and G_{224} where observable proton decay, TeV scale Z_R boson and RH Majorana neutrinos, observable proton decay, $n-\bar{n}$ oscillation, and rare kaon decay have been predicted. Interestingly the masses of W_R boson and lepto-quark gauge bosons of $SU(4)_C$ have been predicted at ~ 100 TeV which could be accessible to planned LHC at those energies where W_R boson scale $\sim (100-1000)$ TeV matching with observable $n-\bar{n}$ oscillation and rare kaon decay has been predicted. But the heavy RH neutrino and Z_R boson mass being near TeV scale have been predicted to be accessible to LHC and planned accelerators [87, 88]. That non-SUSY GUTs with two-intermediate scales permit a low mass Z_R boson was noted much earlier [116].

In eq.(4.5), instead of breaking directly to SM, the G_{2213} breaking may occur in two steps $G_{2213} \to G_{2113} \to SM$ where G_{2113} represents the gauge symmetry $SU(2)_L \times U(1)_R \times U(1)_{B-L} \times SU(3)_C$ $[G_{2113}]$. This promises the interesting possibility of TeV scale Z_R boson with the constraint $M_{W_R} >> M_{Z_R}$. Thus the model can be discriminated from the direct LR models if Z_R boson is detected at lower mass scales than the W_R-boson. There are currently ongoing accelerator searches for this extra heavy neutral gauge boson. This has been implemented recently with type-II seesaw dominance in the presence of added fermion singlets [208]. As we will discuss below both these types of models predict light neutrinos capable of mediating double beta decay rates in the $W_L - W_L$ channel saturating the current experimental limits. In addition resonant leptogenesis mediated by heavy sterile neutrinos has been realised in the model of ref. [208].

The G_{2213} symmetric Yukawa Lagrangian descending from $SO(10)$ symmetry can be written as

$$\begin{aligned}\mathcal{L}_{\rm Yuk} \quad &= \quad \sum_{i=1,2} Y_i^{\ell} \overline{\psi}_L \, \psi_R \, \Phi_i + f \, (\psi_R^c \, \psi_R \Delta_R + \psi_L^c \, \psi_L \Delta_L) + y_\chi \, (\overline{\psi}_R \, S \, \chi_R + \overline{\psi}_L \, S \, \chi_L) \\ &\quad + \text{h.c.}, \end{aligned} \tag{4.6}$$

where $\Phi_{1,2} \subset 10_{H_1,H_2}$ are two bidoublets, $(\Delta_L, \Delta_R) \subset 126_F$ and $(\chi_L, \chi_R) \subset 16_H$.

Including the induced VEV contribution to Δ_L, the Yukawa mass term can be written as

$$\mathcal{L}_{mass} = (M_D \overline{\nu} N + \frac{1}{2} M_N N^T N + M \overline{N} S + M_L \overline{\nu_L} S + h.c) + m_\nu^{II} \nu^T \nu + \mu_S S^T S. \tag{4.7}$$

Here the last term denotes the gauge invariant singlet mass term where naturalness criteria demands μ_S to be a very small parameter. In the (ν, S, N^C) basis the generalised form of the 9×9 neutral fermion mass matrix after electroweak symmetry breaking can be written as

$$\mathcal{M}_\nu = \begin{pmatrix} m_\nu^{II} & M_L & M_D \\ M_L^T & \mu_S & M^T \\ M_D^T & M & M_N \end{pmatrix}, \tag{4.8}$$

where $M_D = Y\langle\Phi\rangle$, $M_N = f v_R$, M $= y_\chi\langle\chi_R^0\rangle$,$M_L = y_\chi\langle\chi_L^0\rangle$. In this model the symmetry breaking mechanism and the VEVs are such that $M_N > M \gg M_D$. The LH triplet scalar mass M_{Δ_L} and RH neutrino masses being at the the heaviest mass scales in the Lagrangian, this triplet scalar field and the RH neutrinos have been at first integrated out leading to the effective Lagrangian at lower scales [208, 234],

$$\begin{aligned} -\mathcal{L}_{\text{eff}} &= \left(m_\nu^{II} + M_D \frac{1}{M_N} M_D^T\right)_{\alpha\beta} \nu_\alpha^T \nu_\beta + \left(M_L + M_D \frac{1}{M_N} M^T\right)_{\alpha m} \left(\overline{\nu_\alpha} S_m + \overline{S_m}\nu_\alpha\right) \\ &\quad + \left(M \frac{1}{M_N} M^T\right)_{mn} S_m^T S_n + \mu_S S^T S. \end{aligned} \tag{4.9}$$

4.4 Cancellation of Type-I seesaw and dominance of others

(a) Cancellation of Type-I seesaw

Whereas the heaviest RH neutrino mass matrix M_N separates out trivially, the other two 3×3 mass matrices $\mathcal{M}_\nu$, and $\mathcal{M}_S$ are extracted through various steps of block diagonalisation. The details of various steps are given in refs. [87, 88, 208, 209]

$$\begin{aligned} \mathcal{M}_\nu &= m_\nu^{II} + \left(M_D M_N^{-1} M_D^T\right) - (M_D M_N^{-1} M_D^T) + M_L (M^T M_N^{-1} M)^{-1} M_L^T \\ &\quad - M_L (M^T M_N^{-1} M)^{-1} (M^T M_N^{-1} M_D^T) - (M_D M_N^{-1} M)(M^T M_N^{-1} M)^{-1} M_L^T \\ &\quad + M_D M^{-1} \mu_S M_D M^{-1^T}, \\ \mathcal{M}_\mathcal{S} &= \mu_S - M M_N^{-1} M^T + ..., \\ \mathcal{M}_\mathcal{N} &= M_N. \end{aligned} \tag{4.10}$$

From the first of the above three equations, it is clear that the type-I seesaw term cancels out with another of opposite sign resulting from block diagonalisation. Then the generalised form of the light neutrino mass matrix turns out to be

$$\begin{aligned}\mathcal{M}_\nu &= fv_L + M_L M^{-1} M_N (M^T)^{-1} M_L^T \\ &\quad -[M_L M^{-1} M_D^T + M_D (M_L M^{-1})^T] + \frac{M_D}{M}\mu_S (\frac{M_D}{M})^T. \end{aligned} \tag{4.11}$$

In different limiting cases this generalised light neutrino mass matrix reduces to the corresponding well known neutrino mass formulas.

(b). Linear seesaw and double seesaw

With $M_L = y_\chi v_{\chi_L}$ that induces $\nu - S$ mixing, the second term in eq.(4.11) is the double seesaw formula,

$$\mathcal{M}_\nu^{(\text{double})} = M_L M^{-1} M_N (M^T)^{-1} M_L^T. \tag{4.12}$$

The third term in eq.(4.11) represents the linear seesaw formula

$$\mathcal{M}_\nu^{(\text{linear})} = -[M_L M^{-1} M_D^T + M_D (M_L M^{-1})^T]. \tag{4.13}$$

Similar formulas have been shown to emerge from single-step breaking of SUSY GUT models [270–272] which require the presence of three gauge singlet fermions.

Using the D-Parity breaking mechanism of ref. [36, 37], an interesting model of linear seesaw mechanism in the context of supersymmetric SO(10) with suceessful gauge coupling unification [274] has been suggested in the presence of three gauge singlet fermions. A special feature of this linear seesaw, compared to others [270, 270, 272] is that the neutrino mass formula is suppressed by the SUSY GUT scale but it is decoupled from the low $U(1)_{B-L}$ breaking scale. In addition to prediction of TeV scale superpartners, the model provides another important testing ground through manifestation of extra Z' boson at LHC or via low-energy neutrino scattering experiment [273].

(c). Type-II seesaw

When the assigned or induced VEV $< \chi_L >= 0$, or negligible and $\mu_S \to 0$, type-II seesaw dominates leading to

$$m_\nu \simeq f v_L. \tag{4.14}$$

As noted briefly in Sec.1, in the conventional models [44, 45] of type-II seesaw dominance in SO(10), the W_R, Z_R boson masses have to be at the GUT-Planck scale. As a phenomenal development, this singlet-fermion assisted type-II seesaw dominance permits $U(1)_{B-L}$ breaking scale associated with G_{2213} or G_{2113} breaking (i,e the W_R, Z_R boson masses) accessible to accelerator energies including LHC. At the same time the heavy $N-S$ mixing mass terms $M_i (i = 1,2,3)$ at the TeV scale are capable of mediating observable LFV decay rates closer to their current experimental values [223–232, 232, 233]. Consequences of this new Type-II seesaw dominance with TeV scale Z_R boson mass has been investigated in detail [208] in which charged triplet mediated LFV decay rates are negligible but singlet fermion decay rates are observable.

(d). Extended seesaw

It is quite clear that the classic inverse seesaw formula [212] for light neutrino mass emerges when the LH triplet mass is large and the VEV $<\chi_L>= 0$ which is possible in a large class of non-SUSY models with left-right, Pati-salam, and SO(10) gauge groups with $D - Parity$ broken at high scales [36–38]

As noted in Sec.1, the derivation of classic inverse seesaw mechanism [212–222] has $M_N = 0$ in eq.(4.2). More recent applications in LRS and GUTs have been discussed with relevant reference to earlier works in [86, 191, 275–280].

In this section we have discussed that, in spite of the presence of the heavy Majorana mass term of RH neutrino, each of the three seesaw mechanisms : (i) Extended Seesaw, (ii) Type-II seesaw , (iii) Linear Seesaw or Double seesaw, can dominate as light neutrino mass ansatz when the respective limiting conditions are satisfied. Also the seesaw can operate in the presence of TeV scale G_{2213} or G_{2113} gauge symmetry originating from non-SUSY SO(10) [87, 88, 208]. As the TeV scale theory spontaneously breaks to low-energy theory $U(1)_{em} \times SU(3)_C$ through the electroweak symmetry breaking of the standard model, these seesaw mechanisms are valid in the SM extensions with suitable Higgs scalars and three generations of N_i and S_i. For example without taking recourse to LR gauge theory, type-II seesaw can be embedded into the SM extension by inclusion of LH Higgs triplet $\Delta_L(3, -2, 1)$ with $Y = -2$. The induced VEV can be generated by the trilinear term $\lambda M_{tr}.\Delta_L^\dagger \phi^\dagger \phi^\dagger$ [281–283]. The origin of such induced VEV in the direct breaking of $SO(10) \to SM$ is well known.

(e). Hybrid seesaw

In the minimal SO(10), without extra fermion singlets, one example of hybrid seesaw with type-I$\oplus$type-II is given in eq.(1.1). There are a number of investigations where this hybrid seesaw has been successful in parametrising small neutrino masses with large mixing angles along with $\theta_{13} \sim 8^o$ in SUSY SO(10) [47–50, 94, 95] and LR models. But the present mechanism of type-I seesaw cancellation suggests a possible new hybrid seesaw formula as a combination of type-II$\oplus$Linear$\oplus$Extended seesaw as revealed from eq.(4.11). Neutrino physics phenomenology may yield interesting new results with this new combination with additional degrees of freedom to deal with neutrino oscillation data and leptogenesis covering coupling unification in SO(10) which has a very rich structure for dark matter.

Using the D-Parity breaking mechanism of ref. [36, 37], an interesting model of linear see saw mechanism in the context of supersymmetric SO(10) with suceessful gauge coupling unification [274] has been suggested in the presence of three gauge singlet fermions. A special feature of this linear seesaw, compared to others [270, 270] is that the neutrino mass formula is suppressed by the SUSY GUT scale but seedecoupled from the low $U(1)_{B-L}$ breaking scale which can be even at $\sim$ few TeV. This serves as a testing ground through manifestation of extra Z' boson at LHC or via low-energy neutrino scattering experiments [273]. Being a SUSY model it also predicts TeV scale superpartners expected to be visible at LHC.

(f). Common mass formula for sterile neutrinos

In spite of different types of seesaw formulas in the corresponding limiting cases the formula for sterile neutrino mass remains the same as in eq.(4.4) which does not emerge from the classic inverse seesaw [212–215] approach with $M_N = 0$

We conclude this section by noting that the classic inverse seesaw mechanism [212–215] was gauged at the TeV scale through its embedding in non-SUSY SO(10) with the prediction of experimentally accessible Z' boson, LFV decays, and non-unitarity effects [86]. The possibility of gauged and extended inverse seesaw mechanism with dominant contributions to both lepton flavor and lepton number non-conservation was at first noted in the context Pati-Salam model in ref. [242] and in the context of non-SUSY SO(10) in ref. [87,88] with type-I seesaw cancellation. The generalised form of hybrid seesaw of eq.(4.11) in non-SUSY SO(10) with type-I cancellation was realised in ref. [208]. As a special case of this model, the experimentally verifiable phenomena like extra Z' boson, resonant leptogenesis, LFV decays, and double beta decay rates closer to the current search limits were decoupled from the intermediate scale type-II seesaw dominated neutrino mass genaration mechanism. Proton lifetime prediction for $p \to e + \pi^0$ mode also turns out to be within the accessible range.

Chapter 5

New Mechanism for Type-II Seesaw Dominance in SO(10) with Low Mass Z' , RH Neutrinos, Verifiable LFV, and Proton Decay

A key ansatz to resolve the issue of large mixing in the neutrino sector and small mixing in the quark sector has been suggested to be through type-II seesaw dominance [284] via renormalization group evolution of quasi-degenerate neutrino masses that holds in supersymmetric quark-lepton unified theories [28, 29] or SO(10) and for large values of $\tan\beta$ which represents the ratio of vacuum expectation values (VEVs) of up-type and down type Higgs doublets. In an interesting approach to understand neutrino mixing in SUSY theories, it has been shown [285] that the maximality of atmospheric neutrino mixing is an automatic cosnsequence of type-II seesaw dominance and $b-\tau$ unification that does not require quasi-degeneracy of the associated neutrino masses. A number of consequences of this approach have been explored to explain all the fermion masses and mixings including type-II seesaw, or a combination of both type-I and type-II seesaw [49, 92, 93, 96–99, 286] through SUSY SO(10). As a further interesting property of type-II seesaw dominance, it has been recently shown [47, 50, 287] without using any flavor symmetry that the well known tri-bimaximal mixing pattern for neutrino mixings is simply a consequence of rotation in the flavor space. Although several models of type-II seesaw dominance in SUSY SO(10) have been investigated, precision gauge coupling unification is distorted in most cases.

Certain charged fermion mass fittings in the conventional one-step breaking of SUSY GUTs including fits to the neutrino oscillation data require the left-handed triplet to be lighter than the type-I seesaw scale. The gauge coupling evolutions being sensitive to the quantum numbers of the LH triplet $\Delta_L(3, -2, 1)$ under SM gauge group, tend to misalign the precision unification in the minimal scenario achieved without the triplet being lighter. Type-II seesaw dominance in one SUSY SO(10) [44] and another split SUSY or non-SUSY model [45] has been reviewed in chapter 1. The purpose of this work is to show that in a class of models descending from non-SUSY SO(10) or from Pati-Salam gauge symmetrty, type-II seesaw dominance at intermediate scales ($M_\Delta \simeq 10^8 - 10^9$ GeV) and $M_N \sim O(1) - O(10)$ TeV can be realised by cancellation of the type-I seesaw contribution but with a Z' boson at $\sim O(1) - O(10)$ TeV scale accessible to the large Hadron Collider (LHC) where $U(1)_R \times U(1)_{B-L}$ breaks spontaneously to $U(1)_Y$ through the vacuum expectation value (VEV) of the RH triplet component of Higgs scalar contained in 126_H that carries $B-L = -2$. We also discuss how the type-II seesaw contribution dominates over the linear seesaw formula. Whereas in all previous Type-II seesaw dominance models in SO(10), the RH Majorana neutrino masses have been very large and inaccessible for accelerator energies, the present model predicts these masses in the LHC accessible range. In spite of large values of the W_R boson and the doubly charged Higgs boson $\Delta_L^{++}, \Delta_R^{++}$ masses, it is quite interesting to note that the model predicts a new observable contribution to $0\nu\beta\beta$ decay in the $W_L - W_L$ channel. The key ingredients to achieve type-II seesaw dominance by complete suppression of type-I seesaw contribution are addition of one SO(10) singlet fermion per generation ($S_i, i = 1, 2, 3$) and utilization of the additional Higgs representation 16_H to generate the $N - S$ mixing term in the Lagrangian through Higgs-Yukawa interaction. The underlying leptonic non-unitarity effects lead to substantial LFV decay branching ratios and leptonic CP-violation accessible to ongoing search experiments. We derive a new formula for the half-life of $0\nu\beta\beta$ decay as a function of the fermion singlet masses and extract lower bound on the lightest sterile neutrino mass from the existing lower bounds on the half-life of different experimental groups. For certain regions of parameter space of the model, we also find the proton lifetime for $p \to e^+\pi^0$ to be accessible to ongoing or planned experiments.

Compared to earlier existing SO(10) based type-II seesaw dominant models whose RH neutrino masses are in the experimentally inaccessible range and new gauge bosons are in the mass range $10^{15} - 10^{17}$ GeV, the present model predictions on LHC scale Z', light and heavy Majorana type sterile neutrinos, RH Majorana neutrino masses in the range $\simeq 100 - 1000$ GeV accessible to LHC in the $W_L - W_L$ channel through dilepton production, the LFV branching ratios closer to experimental limits, and dominant $0\nu\beta\beta$ decay amplitudes caused by sterile neutrino exchanges provide a rich testing ground for new physics signatures.

This chapter is organized as follows: in Sec. 5.1 we briefly discuss the TeV scale left-right gauge theory with low-mass W_R, Z' bosons, light neutrino masses and associated non-unitarity effects. In Sec. 5.2, we have discussed the branching ratios for lepton flavor violating decays. In Sec. 5.3, we have implemented the idea in a $SO(10)$ grand unified theory and derive Dirac neutrino mass matrix at the TeV scale. In Sec. 5.4, we have briefly discussed the phenomenon of Z' boson.

5.1 Type-II seesaw dominance

5.1.1 The Model

More explicit discussions on Model-I and Model-II are given in Sec. 5.3. In Model-I, the first step of symmetry breaking takes place by assigning the GUT-scale VEV to the neutral component of the Higgs submultiplet $(1,1,15) \subset 210_H$ of $SO(10)$ under Pati-Salam gauge symmetry $SU(2)_L \times SU(2)_R \times SU(4)_C$. As this neutral component carries D-Parity even quantum number [36, 37], the GUT symmetry breaks without breaking D-Parity. In Model-II, the D-Parity itself breaks down at the GUT scale by assigning, in addition, the GUT scale VEV to the D-Parity odd singlet component $(1,1,1)_H \subset 210_H$ [36, 37]. The second step of symmetry breaking in both models is implemented by assigning intermediate scale VEV to the Higgs scalar component $\sigma(1,3,0,1) \subset 45_H$. The third step of symmetry breaking in both models is materialised by assigning TeV scale VEV to the neutral component of the RH scalar triplet $\Delta_R(1,3,-2,1)$ which generates the TeV scale Z'- boson and the RH neutrino masses. The Type-II seesaw dominance occurs in Model-I by the natural presence of the LH triplet $\Delta_L(3,1,-2,1) \subset 126_H$ that acquires the desired induced VEV needed to drive the seesaw mechanism. Type-II seesaw contribution dominates by suppressing the linear seesaw term with the help of appropriate finetuning of parameters. In Model-II the mass of the LH triplet $\Delta_L(3,1,-2,1)$ is kept at the intermediate scale by fine tuning of parameters to implement type-II seesaw seesaw dominance while the linear seesaw term is naturally suppressed in this case.

For subsequent discussions it is necessary to clarify about the various fermions and their charges under different gauge symmetries as shown in Table 5.1.

It is clear that a RH neutrino (N) and all 15 standard fermions of one generation are in different fundamental representations of LR gauge theory G_{2213}. Together

Field	*Family*	G_{2113}	G_{2213}	$SO(10)$
$\begin{pmatrix} u \\ d \end{pmatrix}_L$	3	$\big(2, 0, 1/3, 3\big)$	$\big(2, 1, 1/3, 3\big)$	16
$\begin{pmatrix} u \\ d \end{pmatrix}_R$	3	$\big(1, \pm 1/2, -1/3, 3\big)$	$\big(1, 2, -1/3, 3^*\big)$	16
$\begin{pmatrix} \nu \\ l \end{pmatrix}_L$	3	$\big(2, 0, -1, 1\big)$	$\big(2, 1, -1, 1\big)$	16
$\begin{pmatrix} N \\ l \end{pmatrix}_R$	3	$\big(1, \pm 1/2, -1, 1\big)$	$\big(1, 2, -1, 1\big)$	16
S_i	3	$\big((1, 0, -1, 1)\big)$	$\big(1, 1, -1, 1\big)$	1

Table 5.1: Standard fermions and RH neutrino (N) as fundamental representations of left-right gauge theory contained in the spinorial representation $16 \subset SO(10)$. The sterile neutrinos S_i are singlets under SM and all other gauge groups mentioned here.

they are in a single spinorial representation $16 \subset SO(10)$. For the purpose of implementing type-II seesaw dominance by cancelling out type-I seesaw, lepton flavour violation (LFV), lepton number violation (LNV), and leptogenesis, the model also introduces three additional fermions $S_i(i = 1,\, 2,\, 3)$ which are singlets under $SO(10)$ and all other subgroups including the SM. But each of them is contained in the fundamental representation $27 \subset E_6$ which decomposes under $SO(10)$ as $27 = 16+10+1$ and comprises of 10 more non-standard fermions. In our notation the symbol $\hat{S}_i(\hat{N}_i)$ denote the mass eigen states of $S_i(N_i)$ with the respective mass eigen value while the symbols without hats denote flavour states.

5.1.2 Type-II seesaw

We have added to the usual spinorial representations $16_{F_i}(i = 1, 2, 3)$ for fermion representations in $SO(10)$, one fermion singlet per generation $S_i(i = 1, 2, 3)$. The G_{2213} symmetric Yukawa Lagrangian descending from $SO(10)$ symmetry can be written as

$$\begin{aligned}
\mathcal{L}_{\text{Yuk}} &= \sum_{i=1,2} Y_i^{\ell} \left(\overline{\psi}_L\, \psi_R\, \Phi_i\right) + f(\, \psi_R^c\, \psi_R \Delta_R + \psi_L^c\, \psi_L \Delta_L) \\
&+ \; y_\chi \left(\overline{\psi}_R\, S\, \chi_R + \overline{\psi}_L\, S\, \chi_L\right) + (\text{h.c.})\,, \qquad (5.1)
\end{aligned}$$

where $\Phi_{1,2} \subset 10_{H_1,H_2}$ are two bidoublets, $(\Delta_L, \Delta_R) \subset 126_F$ and $(\chi_L, \chi_R) \subset 16_H$. As discussed in Sec.2, the spontaneous breaking of $G_{2213} \longrightarrow G_{2113}$, takes place by the VEV of the RH triplet $\sigma_R(1, 3, 0, 1) \subset 45_H$ carrying $B - L = 0$ which does not generate any fermion mass term. We introduce VEVs for Higgs scalars Φ_i, Δ_R and χ_R for spontaneous symmetry breakings leading to $G_{2113} \longrightarrow SM \longrightarrow U(1)_{em} \times SU(3)_C$. The quantity generating $N-S$ mixing term is $M = y_\chi \langle \chi_R^0 \rangle$. In addition $v_{\chi_L} = \langle \chi_L^0 \rangle$ and $v_L = \langle \Delta_L^0 \rangle$ are automatically induced even though the LH doublet χ_L and the RH triplet Δ_L are assigned vanishing VEVs directly. In models with inverse seesaw or extended seesaw [86, 87, 242, 288–292] mechanisms, a bare mass term of the singlet fermions $\mu_S S^T S$ occurs in the Lagrangian. Being unrestricted as a gauge singlet mass term in the Lagrangian, determination of its value has been left to phenomenological analyses in neutrino physics. Larger values of the parameter near the GUT-Planck scale [293] or at the intermediate scale [270, 271] have been also exploited. On the other hand, fits to the neutrino oscillation data through inverse seesaw formula require much smaller values of μ_S [83–87, 242, 258, 260–262]. Even phenomenological implications of its vanishing value have been investigated recently in the presence of other non-standard and non-vanishing fermion masses [295–298] in the 9×9 mass matrix. Very small values of μ_S is justified on the basis of 't Hooft's naturalness criteria representing a mild breaking of global lepton number symmetry of the SM [294]. While we consider the implication of this term later in this section, at first we discuss the emerging neutrino mass matrix by neglecting it. In addition to the VEVs discussed for gauge symmetry breaking at different stages, we assign the VEV to the neutral component of RH Higgs doublet of 16_H with $< \chi_R(1, 1/2, -1/2, 1) >= V_\chi$ in order to generate $N-S$ mixing mass term $\mathrm{M}\overline{N}S$ between the RH neutrino and the sterile fermion where the 3×3 matrix $\mathrm{M} = y_\chi V_\chi$. We define the other 3×3 mass matrices $M_D = Y^{(1)} v_u$ and $M_N = f V_R$. We also include induced small contributions to the vacuum expectation values of the LH Higgs triplet $v_L =< \Delta_L(3, 0, -2, 1) >$ and the LH Higgs doublet $v_{\chi_L} =< \chi_L(2, 0, -2, 1) >$ leading to the possibilities $\nu - S$ mixing with $M_L = y_\chi v_{\chi_L}$ and the induced type-II seesaw contribution to LH neutrino masses $m_\nu^{II} = f v_L$ given in eq.(5.8). The induced VEVs are shown in the left and right panels of Fig.5.1. We have also derived them by actual potential minimisation which agree with the diagramatic contribution. Including the induced VEV contributions, the mass term due to Yukawa Lagrangian can be written as eq.(4.7). In the (ν, S, N^C) basis the generalised form of the 9×9 neutral fermion mass matrix after electroweak symmetry breaking can be written as eq.(4.2). In this model the symmetry breaking mechanism and the VEVs are such that $M_N > M \gg M_D$. The RH neutrino mass being the heaviest fermion mass scale in the Lagrangian, this fermion is at first integrated out leading to the effective Lagrangian at lower scales [234,235,239,240] as in eq.(4.9). Whereas the heaviest RH neutrino mass matrix M_N separates out trivially, the other two 3×3 mass matrices $\mathcal{M}_\nu$, and m_S are extracted through various steps of block diagonalisation [87].The details of various steps are given in Appendix B and the results are

$$\begin{aligned}
\mathcal{M}_\nu &= m_\nu^{II} + \left(M_D M_N^{-1} M_D^T\right) - (M_D M_N^{-1} M_D^T) + M_L (M^T M_N^{-1} M)^{-1} M_L^T \\
&\quad - M_L (M^T M_N^{-1} M)^{-1} (M^T M_N^{-1} M_D^T) - (M_D M_N^{-1} M)(M^T M_N^{-1} M)^{-1} M_L^T \\
&\quad + M_D M^{-1} \mu_S M_D {M^{-1}}^T, \\
\mathcal{M}_\mathcal{S} &= \mu_S - M M_N^{-1} M^T + ..., \\
\mathcal{M}_\mathcal{N} &= M_N. \qquad (5.2)
\end{aligned}$$

From the first of the above three equations, it is clear that the type-I seesaw term cancels out [234, 235, 239, 240] with another of opposite sign resulting from block diagonalisation. Then the generalised form of the light neutrino mass matrix turns out to be

$$\begin{aligned}
\mathcal{M}_\nu &= f v_L + M_L M^{-1} M_N (M^T)^{-1} M_L^T \\
&\quad - [M_L M_D^T M^{-1} + M_L^T M_D (M^T)^{-1}]. \qquad (5.3)
\end{aligned}$$

With $M_L = y_\chi v_{\chi L}$ that induces $\nu - S$ mixing, the second term in this equation is double seesaw formula and the third term is the linear seesaw formula which are similar to those derived earlier [270, 271]. From the Feynman diagrams, the analytic expressions for the induced VEVs are

$$v_L \sim \frac{V_R}{M_{\Delta_L}^2}\left(\lambda_1 v_1^2 + \lambda_2 v_2^2\right), \qquad (5.4)$$

$$\begin{aligned}
v_{\chi_L} &\sim \frac{V_\chi}{M_{\chi_L}^2}\left(\lambda_1' M_1' v_1 + \lambda_2' M_2' v_2\right), \\
&= C_\chi \frac{V_\chi M_{R^+} v_{wk}}{M_{\chi_L}^2}, \qquad (5.5)
\end{aligned}$$

where $v_{wk} \sim 100$ GeV, and

$$C_\chi = \frac{(\lambda_1' M_1' v_1 + \lambda_2' M_2' v_2)}{(M_{R^+} v_{wk})}. \qquad (5.6)$$

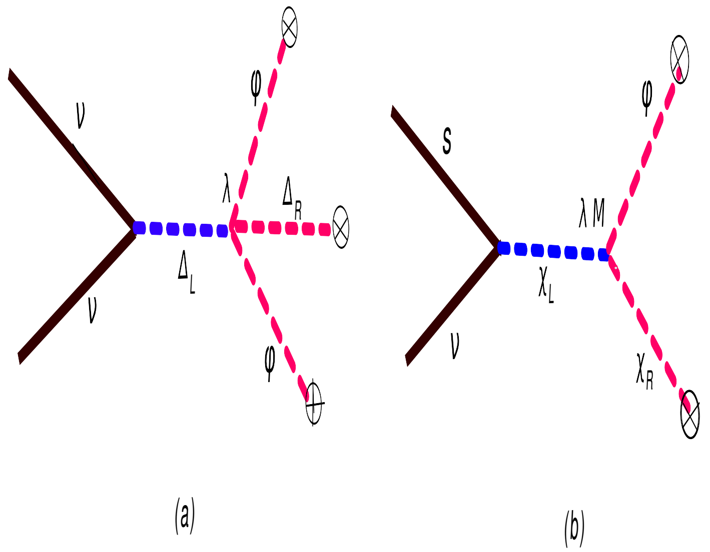

Figure 5.1: Feynman diagrams for induced contributions to VEVs of the LH triplet (diagram (a)) and the LH doublet (diagram (b)) in Model-I and Model-II.

In eq.(5.5), $v_i (i = 1, 2)$ are the VEVs of two electroweak doublets each originating from separate $10_H \subset SO(10)$ as explained in the following section, and M_1', M_2' are Higgs trilinear coupling masses which are normally expected to be of order M_{R^+}. In both the models $V_R = 5 - 10$ TeV and $V_\chi \sim 300 - 1000$ GeV. Similar expressions as in eq.(5.5) are also obtained by minimisation of the scalar potential.

5.1.3 Suppression of linear seesaw and dominance of type-II seesaw

Now we discuss how linear seesaw term is suppressed without fine tuning of certain parameters in Model-I but with fine tunning of the same parameters in Model-II. The expression for neutrino mass is given in eq.(5.3) where the first, second, and the third terms are type-II seesaw, double seesaw, and linear seesaw formulas for the light neutrino masses. Out of these, for all parameters allowed in both the models (Model-I and Model-II), the double seesaw term will be found to be far more suppressed compared to the other two terms. The structures of Model-I and Model-II are more explicitly illustrated in the following Sec. 5.3 and in Fig.(5.3) and in Fig.(5.3). Therefore we now discuss how the linear seesaw term is suppressed compared to the type-II seesaw term allowing the dominance of the latter. In Model-

I where LR discrete symmetry (parity) breaks at the GUT scale, gauge coupling unification has been achieved such that $M_P = M_{\chi_L} \sim M_U \geq 10^{15.6}$ GeV, $M_{\Delta_L} = 10^8$ GeV where $M'_1 \sim M'_2 \sim M_{R^+} \sim 10^9$ GeV. Using these masses in eq.(5.3), we find that even with $C_\chi \sim 0.1 - 1.0$

$$\begin{aligned} v_{\chi_L} &\sim 10^{-18}\text{ eV} - 10^{-17}\text{ eV}, \\ v_L &\simeq 0.1\text{ eV} - 0.5\text{ eV}, \end{aligned} \tag{5.7}$$

Such induced VEVs in the Model-I suppress the second and the third terms in eq.(5.3) making the model quite suitable for type-II seesaw dominance although the Model-II needs fine tuning in the induced contributions to the level of $C_\chi \leq 10^{-5}$ as discussed below.

In Model-II where parity breaks at the intermediate scale (M_P), $M_{\Delta_L} \sim M_{\chi_L} \sim M_P \sim 10^9$ GeV. Without any fine tuning of the parameters in eq.(5.4), we obtain $v_L \sim 10^{-10}$ GeV. From eq.(5.5) we get $v_{\chi_L} \sim C_\chi \times 10^{-6}$ GeV $\sim 10^{-7}$GeV for $C_\chi \sim 0.1$. With $(M_D)_{(3,3)} \leq 100$ GeV and $\frac{M_D}{M} \simeq 0.1 - 1$, the most dominant third term in eq.(5.3) gives $M_\nu \geq 10^{-8}$ GeV. This shows that fine tuning is needed in the parameters occuring to reduce $C_\chi \leq 10^{-5}$ to suppress linear seesaw and permit type-II seesaw dominance in Model-II whereas the type-II seesaw dominance is achieved in Model-I with $C_\chi \simeq 0.1 - 1.0$ without requiring any such fine tuning. In what follows we will utilise the type-II seesaw dominated neutrino mass formula to study neutrino physics neutrino-less double beta decay, and lepton flavor violations in the context of Model-I although they are similar in Model-II subject to the fine tuning constraint on C_χ. Thus the light neutrino mass is dominated by the type-II seesaw term in both models.

$$\mathcal{M}_\nu \simeq f v_L. \tag{5.8}$$

5.1.4 Right-handed neutrino mass prediction

Global fits to the experimental data [299–303] on neutrino oscillations have determined the mass squared differences and mixing angles at 3σ level

$$\begin{aligned}
&\sin^2\theta_{12} = 0.320, \quad \sin^2\theta_{23} = 0.427, \\
&\sin^2\theta_{13} = 0.0246, \;\; \delta_{CP} = 0.8\pi, \\
&\Delta m^2_{\text{sol}} = 7.58\times10^{-5}\text{eV}^2, \\
&|\Delta m_{\text{atm}}|^2 = 2.35\times10^{-3}\text{eV}^2.
\end{aligned} \tag{5.9}$$

For normally hierarchical (NH), inverted hierarchical (IH), and quasi-degenerate (QD) patterns, the experimental values of mass squared differences can be fitted by the following values of light neutrino masses

$$\begin{aligned}
\hat{m}_\nu &= (0.00127, 0.008838, 0.04978)\text{ eV (NH)} \\
&= (0.04901, 0.04978, 0.00127)\text{ eV (IH)} \\
&= (0.2056, 0.2058, 0.2)\text{ eV (QD)}
\end{aligned} \tag{5.10}$$

We use the diagonalising Pontecorvo-Maki-Nakagawa-Sakata (PMNS) matrix. U_{PMNS}

$$U_{\text{PMNS}} = \begin{pmatrix} c_{13}c_{12} & c_{13}s_{12} & s_{13}e^{-i\delta} \\ -c_{23}s_{12} - c_{12}s_{13}s_{23}e^{i\delta} & c_{12}c_{23} - s_{12}s_{13}s_{23}e^{i\delta} & s_{23}c_{13} \\ s_{12}s_{23} - c_{12}c_{23}s_{13}e^{i\delta} & -c_{12}s_{23} - s_{12}s_{13}c_{23}e^{i\delta} & c_{13}c_{23} \end{pmatrix}, \tag{5.11}$$

and determine it numerically using mixing angle and the leptonic Dirac phase from eq. (5.9)

$$U_{\text{PMNS}} = \begin{pmatrix} 0.814 & 0.55 & -0.12-0.09i \\ -0.35-0.049i & 0.67-0.034i & 0.645 \\ 0.448-0.057i & -0.48-0.039i & 0.74 \end{pmatrix}. \tag{5.12}$$

Now inverting the relation $\hat{m}_\nu = U^\dagger_{PMNS}\mathcal{M}_\nu U^*_{PMNS}$ where $\hat{m}_\nu$ is the diagonalised neutrino mass matrix, we determine $\mathcal{M}_\nu$ for three different cases and further determine the corresponding values of the f matrix using $f = \mathcal{M}_\nu/v_L$ where we use the predicted value of $v_L = 0.1$ eV. Noting that
$M_N = fV_R = \mathcal{M}_\nu V_R/v_L$, we have also derived eigen values of the RH neutrino mass matrix $\hat{M}_{N_i}$ as the positive square root of the i^{th} eigen value of the Hermitian matrix $M_N^\dagger M_N$.

NH

$$f = \begin{pmatrix} 0.117 + 0.022i & -0.124 - 0.003i & 0.144 + 0.025i \\ -0.124 - 0.003i & 0.158 - 0.014i & -0.141 + 0.017i \\ 0.144 + 0.025i & -0.141 + 0.017i & 0.313 - 0.00029i \end{pmatrix} \tag{5.13}$$

$$|\hat{M}_N| = \text{diag}(160, 894, 4870)\ \text{GeV}. \tag{5.14}$$

IH

$$f = \begin{pmatrix} 0.390 - 0.017i & 0.099 + 0.01i & -0.16 + 0.05i \\ 0.099 + 0.01i & 0.379 + 0.02i & 0.176 + 0.036i \\ -0.16 + 0.05i & 0.176 + 0.036i & 0.21 - 0.011i \end{pmatrix} \tag{5.15}$$

$$|\hat{M}_N| = \text{diag}(4880, 4910, 131)\ \text{GeV}. \tag{5.16}$$

QD

$$f = \begin{pmatrix} 2.02 + 0.02i & 0.0011 + 0.02i & -0.019 + 0.3i \\ 0.0011 + 0.02i & 2.034 + 0.017i & 0.021 + 0.21i \\ -0.019 + 0.3i & 0.021 + 0.21i & 1.99 - 0.04i \end{pmatrix} \tag{5.17}$$

For $v_L = 0.1$ eV, we have

$$|\hat{M}_N| = \text{diag}(21.46, 20.34, 18.87)\ \text{TeV} \tag{5.18}$$

but for $v_L = 0.5$ eV, we obtain

$$|\hat{M}_N| = \text{diag}(4.3, 4.08, 3.77)\ \text{TeV}. \tag{5.19}$$

These RH neutrino masses predicted with $v_L = 0.1$ eV for NH and IH cases and with $v_L = 0.5$ eV for the QD case are clearly verifiable by the LHC

The sterile neutrino mass matrix with a scaling property:

As a new oservation we point out a scaling property of sterile neutrino mass matrix.

The mass matrix of the sterile neutrino in the $\mu_S \to 0$ limit [294] is

$$m_S \;\; = -M \tfrac{1}{M_N} M^T, \tag{5.20}$$

where M is the $N - S$ mixing mass term in the Yukawa Lagrangian. Here we note a new interesting "scaling" property of m_s in view of its connection with G_{2113} gauge symmetry breaking, the RH neutrino mass M_N, and the $N - S$ mixing matrix M. This property has implications on sterile neutrino mass eigen values, leptogenesis, and dilepton production through displaced vertices.

"When the RH neutrino mass matrix M_N and the $N - S$ mixing matrix M are rescaled as

$$\begin{aligned} M_N &\to (X.M_N), \\ M &\to [(\sqrt{X}).M], \end{aligned} \tag{5.21}$$

the sterile neutrino mass matrix m_s and its mass eigen values are unchanged."

5.1.5 Neutrino parameters and non-unitarity condition

Using the constrained diagonal form of M as mentioned above, the mass matrix μ_S is determined using the gauged inverse seesaw formula and neutrino oscillation data provided that the Dirac neutrino mass matrix M_D is also known. The determination of M_D at the TeV scale, basically originating from high- scale quark-lepton symmetry G_{224D} or $SO(10)$ GUT, is carried out by predicting its value at the high scale from fits to the charged fermion masses of three generations and then running down to the lower scales using the corresponding RGEs in the top-down approach. It is to be noted that for fits to the fermion masses at the GUT scale, their experimental values at low energies are transported to the GUT scale using RGEs and the bottom-up approach [208, 304].

5.1.5.1 Determination of Dirac neutrino mass matrix

The RG extrapolated values at the GUT scale are [208, 304–306],
$\mu = \mathrm{M_{GUT}}$:

$$\begin{aligned} m_e^0 &= 0.00048\ \text{GeV}, m_\mu^0 = 0.0875\ \text{GeV}, m_\tau^0 = 1.8739\ \text{GeV}, \\ m_d^0 &= 0.0027\ \text{GeV}, m_s^0 = 0.0325\ \text{GeV}, m_b^0 = 1.3373\ \text{GeV}, \\ m_u^0 &= 0.001\ \text{GeV}, m_c^0 = 0.229\ \text{GeV}, m_t^0 = 78.74\ \text{GeV}, \end{aligned} \tag{5.22}$$

The V_{CKM}^0 matrix at the GUT scale is given by

$$V_{\text{CKM}}^0 = \begin{pmatrix} 0.97 & 0.22 & -0.0003 - 0.003i \\ -0.22 - 0.0001i & 0.97 & 0.036 \\ 0.008 - 0.003i & -0.035 + 0.0008i & 0.99 \end{pmatrix}. \tag{5.23}$$

For fitting the charged fermion masses at the GUT scale, in addition to the two complex $10_{H_{1,2}}$ representations with their respective Yukawa couplings $Y_{1,2}$, we also use the higher dimensional operator [208]

$$\frac{\kappa_{\mathbf{ij}}}{\mathbf{M_G^2}} \mathbf{16_i 16_j 10_H 45_H 45_H}, \tag{5.24}$$

In the above equation the product of three Higgs scalars acts as an effective $126_H^\dagger$ operator [83–85]. With $M_G \simeq M_{Pl}$ or $M \simeq M_{string}$, this is suppressed by $(M_U/M_G)^2 \simeq 10^{-3} - 10^{-5}$ for GUT-scale VEV of 45_H. Then the formulas for different charged fermion mass matrices are

$$\begin{aligned} M_u &= G_u + F, \quad M_d = G_d + F, \\ M_e &= G_d - 3F, \quad M_D = G_u - 3F. \end{aligned} \tag{5.25}$$

Following the procedure given in [208], the Dirac neutrino mass matrix at the GUT scale is found to be

$$M_D(M_{R^0}) = \begin{pmatrix} 0.014 & 0.04 - 0.01i & 0.109 - 0.3i \\ 0.04 + 0.01i & 0.35 & 2.6 + 0.0007i \\ 0.1 + 0.3i & 2.6 - 0.0007i & 79.20 \end{pmatrix} GeV. \tag{5.26}$$

This value of M_D will be utilized for all applications discussed subsequently in this work including the fit to the neutrino oscillation data through the inverse seesaw formula, predictions of effective mass parameters in $0\nu2\beta$, computation of non-unitarity

measure of non-unitarity	Expt. bound C0	C1	C2	C3
$\lvert\eta_{ee}\rvert$	2.0×10^{-3}	3.5×10^{-8}	2.7×10^{-7}	3.1×10^{-6}
$\lvert\eta_{e\mu}\rvert$	3.5×10^{-5}	3.9×10^{-7}	3.4×10^{-6}	1.5×10^{-5}
$\lvert\eta_{e\tau}\rvert$	8.0×10^{-3}	9.4×10^{-6}	2.8×10^{-5}	6.4×10^{-5}
$\lvert\eta_{\mu\mu}\rvert$	8.0×10^{-4}	4.7×10^{-6}	2.3×10^{-5}	6.9×10^{-5}
$\lvert\eta_{\mu\tau}\rvert$	5.1×10^{-3}	1.1×10^{-4}	2.2×10^{-4}	3.2×10^{-4}
$\lvert\eta_{\tau\tau}\rvert$	2.7×10^{-3}	2.7×10^{-3}	2.7×10^{-3}	2.7×10^{-3}

Table 5.2: Experimental bounds of the non-unitarity matrix elements $|\eta_{\alpha\beta}|$ (column $C0$) and their predicted values for degenerate (column $C1$), partially-degenerate (column $C2$), and non-degenerate (column $C3$) values of $M = \text{diag}\,(M_1, M_2, M_3)$.

and CP-violating effects, and lepton flavor violating decay branching ratios.

The light active Majorana neutrino mass matrix is diagonalized by the PMNS mixing matrix U_ν such that $U_\nu^\dagger m_\nu U_\nu^* = \hat{m}_\nu = \text{diag}\,(m_{\nu_1}, m_{\nu_2}, m_{\nu_3})$. The non-unitarity matrix at the leading order is still $\mathcal{N} \simeq (1-\eta)U_\nu$, see Appendix D for details.

Thus η is a measure of deviation from unitarity in the lepton sector on which there has been extensive investigations in different models [86–88]. Assuming M to be diagonal for the sake of simplicity, $M \equiv \text{diag}(M_1, M_2, M_3)$, gives $\eta_{\alpha\beta} = \frac{1}{2}\sum_k M_{D\alpha k} M_k^{-2} M^*_{D\beta k}$, but it can be written explicitly for the degenerate case ($M_1 = M_2 = M_3 = M_R$). The determination of the Dirac neutrino mass matrix $M_D(M_{R^0})$ at the TeV seesaw scale is done which was discussed in [86, 304–306].

5.1.5.2 Estimation of non-unitarity matrix

In order to study non-unitarity effects and lepton flavor violations, we assume the $N-S$ mixing matrix M to be diagonal for the sake of simplicity and also for exercising economy of parameters,

$$M = \text{diag}\,(M_1, M_2, M_3), \tag{5.27}$$

The non-unitarity deviation η is defined as

$$\begin{aligned} \eta &= \frac{1}{2} X.X^\dagger = M_D M^{-2} M_D^\dagger, \\ \eta_{\alpha\beta} &= \frac{1}{2} \sum_{k=1,2,3} \frac{M_{D_{\alpha k}} M^*_{D_{\beta k}}}{M_k^2}. \end{aligned} \tag{5.28}$$

which for the degenerate case, $M_i = M_{Deg}(i=1,2,3)$, gives,

$$\eta = \frac{1\text{GeV}^2}{M_{Deg}^2} \times \begin{pmatrix} 0.0394 & 0.146-0.403i & 4.17-11.99i \\ 0.146+0.403i & 3.602 & 105.8-0.002i \\ 4.173+11.9i & 105.805+0.002i & 3139.8 \end{pmatrix}. \tag{5.29}$$

For the general non-degenerate case of M, we saturate the upper bound $|\eta_{\tau\tau}| < 2.7\times10^{-3}$ [185] to derive

$$\frac{1}{2}\left[\frac{0.1026}{M_1^2} + \frac{7.0756}{M_2^2} + \frac{6762.4}{M_3^2}\right] = 2.7\times10^{-3}, \tag{5.30}$$

where numerical values i the LHS inside the square brackets are in GeV^2 and M_i's are in GeV. By inspection this equation gives the lower bounds
$M_1 > 4.35$ GeV, $M_2 > 36.2$ GeV, $M_3 > 1120$ GeV, and for the degenerate case $M_{Deg} = 1213$ GeV.
For the partial degenerate case of $M_1 = M_2 \neq M_3$ the solutions can be similarly derived as in ref [86] and one example is $M(100, 100, 1319.67)$ GeV .

5.2 Lepton flavor violation

In the present non-SUSY SO(10) model, even though neutrino masses are governed by high scale type-II seesaw formula, the essential presence of singlet fermions that implement the type-II seesaw dominance by cancelling out the type-I seesaw contribution give rise to experimentally observable LFV decay branching ratios through their loop mediation. The heavier RH neutrinos in this model being in the range of $\sim 1-10$ TeV mass range also contribute, but less significantly than the singlet fermions.

5.2.1 Branching ratio and CP violation

One of the most important outcome of non-unitarity effects is its manifestation through ongoing experimental searches for LFV decays such as $\tau\to e\gamma$, $\tau\to\mu\gamma$, $\mu\to e\gamma$. In these models the RH neutrinos and the singlet fermions contribute to the branching ratios [83–86, 307–310] Because of the condition $M_N >> M$, neglecting the RH neutrino exchange contribution compared to the sterile fermion singlet contributions [208], our estimations for different cases of M values are presented in Table 6.2. These values are many orders larger than the standard non-SUSY predictions for branching ratios, $Br \simeq 10^{-50}$. Our predictions are accessible to ongoing or planned searches [223–229, 232]. In these models contribution to the branching ratios due to the heavier the RH neutrinos is subdominant compared to the lighter singlet fermions

$$\mathrm{Br}\left(\ell_\alpha \to \ell_\beta + \gamma\right) = \frac{\alpha_{\mathrm{w}}^3\, s_{\mathrm{w}}^2\, m_{\ell_\alpha}^5}{256\,\pi^2\, M_W^4\, \Gamma_\alpha} \left|\mathcal{G}_{\alpha\beta}^N + \mathcal{G}_{\alpha\beta}^S\right|^2 , \tag{5.31}$$

$$\begin{aligned} \text{where} \quad \mathcal{G}_{\alpha\beta}^N &= \sum_k \left(\mathcal{V}^{\nu N}\right)_{\alpha k} \left(\mathcal{V}^{\nu N}\right)^*_{\beta k} \mathcal{I}\left(\frac{m_{N_k}^2}{M_{W_L}^2}\right) , \\ \mathcal{G}_{\alpha\beta}^S &= \sum_j \left(\mathcal{V}^{\nu S}\right)_{\alpha j} \left(\mathcal{V}^{\nu S}\right)^*_{\beta j} \mathcal{I}\left(\frac{m_{S_j}^2}{M_{W_L}^2}\right) , \\ \text{and} \quad \mathcal{I}(x) &= -\frac{2x^3+5x^2-x}{4(1-x)^3} - \frac{3x^3 \ln x}{2(1-x)^4} . \end{aligned} \tag{5.32}$$

Because of the condition $M_N >> M$, the RH neutrino exchange contribution is however damped out compared to the sterile fermion singlet contributions.

For the degenerate case

$$\begin{aligned} \Delta\Delta\mathcal{J}_{e\mu}^{12} &= -2.1 \times 10^{-6}, \\ \Delta\Delta\mathcal{J}_{e\mu}^{23} &= -2.4 \times 10^{-6}, \\ \Delta\Delta\mathcal{J}_{\mu\tau}^{23} &= 1.4 \times 10^{-4}, \\ \Delta\Delta\mathcal{J}_{\mu\tau}^{31} &= 1.2 \times 10^{-4}, \end{aligned} \tag{5.33}$$

we have the branching ratio

$$\begin{aligned} BR(\mu \to e\gamma) &= 6.43 \times 10^{-17}, \\ BR(\tau \to e\gamma) &= 8.0 \times 10^{-16}, \\ BR(\tau \to \mu\gamma) &= 2.41 \times 10^{-12}. \end{aligned} \tag{5.34}$$

Because of the presence of non-unitarity effects in the present model , the leptonic CP-violation can be written as [86, 185, 190, 311–317]. The moduli and phase of non-

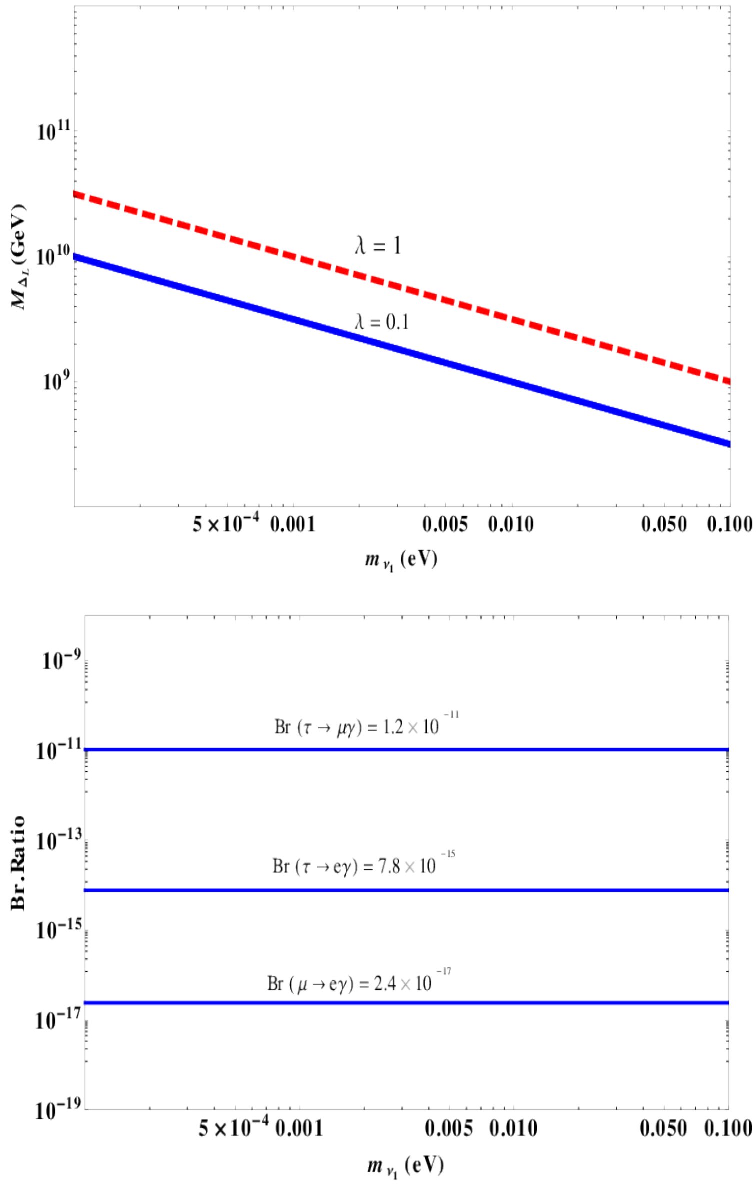

Figure 5.2: Variation of scalar triplet mass M_{Δ_L} (upper curve) and LFV branching ratio (lower curves) as a function of the lightest neutrino mass for different values of λ in a $type-II$ seesaw dominant model following normal ordering. The horizontal thick band represents separation of the vertcal axis between the upper and the lower figures. The three alomost horizontal lines represent the LFV branching ratios for $M = 1.3$ TeV.

unitarity and CP-violating parameter for the degenerate case is given in 5.35.

$$
\begin{aligned}
|\eta_{e\mu}| &= 2.73 \times 10^{-8}, \\
\delta_{e\mu} &= 1.920, \\
|\eta_{e\tau}| &= 4.54 \times 10^{-7}, \\
\delta_{e\tau} &= 1.78, \\
|\eta_{\mu\tau}| &= 2.31 \times 10^{-5}, \\
\delta_{\mu\tau} &= 2.39 \times 10^{-7}.
\end{aligned} \tag{5.35}
$$

Our estimation presented in 5.35 shows that in a wider range of the parameter space, the leptonic CP violation parameter could be nearly two orders larger than the CKM-CP violation parameter for quarks.

Our predictions for branching ratios as a function of the lightest neutrino mass are shown in in Fig.5.2 for the type-II dominance case. In this figure we have also shown variation of the LH triplet mass as expected from the type-II seesaw formula. But inspite of the large value of the triplet mass that normally predicts negligible LFV branching ratios, our model gives experimentally accessible values.

5.3 Implementation in specific SO(10) models

Symmetry breaking chain

To discuss the above phenomenology we have considered the two-step breaking of the LR gauge theory [208],

Model-I

$$SO(10) \to G_{2213D} \to G_{2113} \to SM. \tag{5.36}$$

Model-II

$$SO(10) \to G_{2213} \to G_{2113} \to SM. \tag{5.37}$$

In the Model-II, $SU(2)_L \times SU(2)_R \times U(1)_{B-L} \times SU(3)_C \times D\ [\equiv G_{2213D}](g_{2L} = g_{2R})$ is obtained by breaking the GUT-symmetry and by giving vacuum expectation value (VEV) to the D-Parity even singlet $(1,1,0,1) \subset (1,1,15) \subset 210_H$ [36–38] where the first, second, and the third set of quantum numbers of the scalar components are under G_{2213P}, the Pati-Salam symmetry G_{224}, and $SO(10)$, respectively. As a result, the Higgs sector is symmetric below $\mu = M_U$ leading to equality between the gauge couplings $g_{2L}(M_R^+)$ and $g_{2R}(M_R^+)$. In this case the LR discrete symmetry ($\equiv$ Parity) survives down to the intermediate scale ,$M_{R^+} = M_P$. The second step of symmetry breaking is implemented by assigning VEV to the neutral component of the right-handed (RH) Higgs triplet $\sigma_R(1, 3, 0, 1) \subset 45_H$ that carries $B - L = 0$. The third step of breaking to SM is carried out by assigning the order $5 - 10$ TeV VEV to the G_{2113} component $\Delta_R^0(1, 1, -2, 1)$ contained in the RH triplet $\Delta_R(1, 3, -2, 1) \subset 126_H$ carrying $B - L = -2$. This is responsible for RH Majorana neutrino mass generation $M_N = f v_R$ where $v_R = \langle \Delta_R^0 \rangle$ and f is the Yukawa coupling of $126^\dagger$ with SO(10) spinorial fermionic representation :$f\mathbf{16}.\mathbf{16}.\mathbf{126}^\dagger_\mathbf{H}$. We introduce $SO(10)$ invariant $N - S$ mixing mass via $y_\chi \mathbf{16}.\mathbf{1}.\mathbf{16}^\dagger_\mathbf{H}$ and obtain the mixing mass $M = y_\chi V_\chi$ where $V_\chi = \langle \chi_R^0 \rangle$ by noting that under G_{2113} the submultiplet $\chi_R^0(1, 1/2, -1, 1)$ is contained in the G_{2213} doublet $\chi_R(1, 2, -1, 1) \subset 16_H$. The symmetry breaking in the last step is implemented through the SM Higgs doublet contained in the bidoublet $\phi(2, 2, 0, 1) \subset 10_H)$ of SO(10). This is the minimal Higgs structure of the model, although we will utilise two different Higgs doublets $\phi_u \subset 10_{H_1}$ and $\phi_d \subset 10_{H_2}$ for fermion mass fits. In Model-I, the GUT symmetry breaks to LR gauge symmetry $G_{2213}(g_{2L} \neq g_{2R})$ in such a way that the D-parity breaks at the GUT scale and is decoupled from $SU(2)_R$ breaking that occurs at the intermediate scale. This is achieved by giving GUT scale VEV to the D-parity odd singlet scalar component in $(1, 1, 0, 1)_H \subset (1, 1, 15)_H \subset 45_H$ where the first, second , and third submultiplet is under G_{2213}, the Pati-Salam symmetry G_{224}, and $SO(10)$, respectively. In this case by adopting the D-Parity breaking mechanism [36, 37] in $SO(10)$ normally the LH triplet component $\Delta_L(3, 1, -2, 1) \subset 126_H$ and the LH doublet component $\chi_L(2, 1, -1, 1) \subset 16_H$ acquire masses at the GUT scale while the RH triplet and RH doublet components, $\Delta_R(1, 3, -2, 1) \subset 126_H$ $\chi_R(1, 2, -1, 1) \subset 16_H$, can be made much lighter. We have noted that in the presence of color octet at lower scales, found to be necessary in this Model-I as well as in Model-II, precision gauge coupling is achieved even if the the parameters of the Higgs potential are tuned so as to have the LH triplet mass at intermediate scale, $M_{\Delta_L} \simeq 10^8 - 10^9$ GeV. The presence of $\Delta_L(3, 1, -2, 1)$ at the intermediate scale plays a crucial role in achieving Type-II seesaw dominance as would be explained in the following section. The necessary presence of lighter LH triplets in GUTs with or without vanishing $B - L$ value for physically appealing predictions was pointed out earlier in achieving observable matter anti-matter oscillations [396, 397], in the context of low-scale leptogenesis [240], and type-II seesaw dominance in SUSY, non-SUSY and split-SUSY models [44, 45], and also for TeV scale LR gauge theory originating from SUSY $SO(10)$ grand unification.

In what follows, while safeguarding precise unification of gauge couplings at the GUT scale, we discuss allowed solutions of renormalisation group equations for the mass scales M_U, M_{R^+}, and M_{R^0} as a funtion of the mass M_C of the lighter color octet $C_8(1,1,0,8) \subset 45_H$. The renormalization group coefficients for the minimal cases have been given in Appendix A to which those due to the color octet scalar in both models and the LH triplet Δ_L in Model-I in their suitable ranges of the running scale have been added.

Model-I:

As shown in Table 5.3 for Model-I, with $M_{\Delta_L} = 10^8$ GeV the G_{2213} symmetry is found to survive down to $M_{R^+} = (10^8 - 10^{10})$ GeV with larger or smaller unification scale depending upon the color octet mass. In particular we note one set of solutions,

$$\begin{aligned} M_{R^0} &= 10 \text{ TeV},\ M_{R^+} = 10^{9.7}\text{GeV},\ M_U = 10^{15.62}\text{GeV}, \\ M_{\Delta_L} &= 10^8 \text{ GeV},\ M_C = 10^{10.9}\text{GeV}. \end{aligned} \tag{5.38}$$

As explained in the following sections, this set of solutions are found to be attractive both from the prospects of achieving type-II seesaw dominance and detecting proton decay at Hyper-Kamiokande. with $M_U = 6.5 \times 10^{15}$ GeV when the color octet mass is at $M_C \sim 10^{11}$ GeV. As discussed below the proton lifetime in this case is closer to the current experimental limit. With allowed values of $M_{R^0} = (5 - 10)$ TeV, this model also predicts $M_{Z'} \simeq (1.2 - 3.5)$ TeV in the accessible range of the Large Hadron Collider. Because of the low mass of the Z' boson associated with TeV scale VEV of V_R, the type-II seesaw mechanism predicts TeV scale RH neutrino masses with known mixings among them. These RH neutrinos can be testified at the LHC or future high energy accelerators. The RG evolution of gauge couplings for the set of mass scales given in eq.(5.38) is presented in Fig.5.3 showing clearly the unification of the four gauge couplings of the G_{2213} intermediate gauge symmetry.

Model-II:

As shown in Table 5.4 for Model-II, the G_{2113D} symmetry is found to survive down to $M_{R^+} = M_P = 10^{8.2}$ GeV with $M_U = 6.5 \times 10^{15}$ GeV when the color octet mass is at $M_C = 10^8$ GeV. As discussed below the proton lifetime in this case is closer to the current experimental limit. One example of RG evolution of gauge couplings

M_R^0 (TeV)	M_C (GeV)	M_R^+ (GeV)	M_G (GeV)	α_G^{-1}	τ_p (Yrs.)
10	$10^{4.5}$	10^9	$10^{16.9}$	41.1	5.4×10^{39}
10	10^5	$10^{8.9}$	$10^{16.74}$	41.4	1.1×10^{39}
10	10^7	10^9	$10^{16.4}$	41.7	8.4×10^{37}
10	$10^{10.9}$	$10^{9.7}$	$10^{15.63}$	41.9	3.2×10^{34}
5	$10^{7.8}$	$10^{8.8}$	$10^{16.4}$	41.5	9×10^{37}

Table 5.3: Allowed mass scales as solutions of renormalization group equations for gauge couplings for Model-I with fixed value of the LH triplet mass $M_\Delta = 10^8$ GeV,

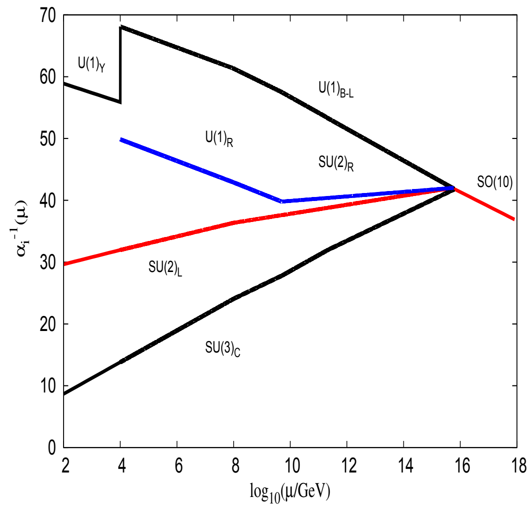

Figure 5.3: Two loop gauge coupling unification in the $SO(10)$ symmetry breaking chain with $M_U = 10^{15.62}$ GeV and $M_R^+ = 10^{9.7}$ GeV, $M_{\Delta_L} = 10^8$ GeV with a low mass Z' boson at $M_R^0 = 10$ TeV for Model-I.

M_R^0 (TeV)	M_C (GeV)	M_R^+ (GeV)	M_G (GeV)	α_G^{-1}	τ_p (Yrs.)
10	$10^{4.5}$	$10^{7.886}$	$10^{16.15}$	40.25	4.3×10^{36}
10	$10^{5.5}$	$10^{7.89}$	$10^{16.04}$	40.64	1.6×10^{36}
10	10^8	$10^{8.789}$	$10^{15.62}$	41.49	3.9×10^{34}
10	$10^{8.5}$	$10^{8.8}$	$10^{15.5}$	41.69	1.12×10^{34}
5	$10^{5.8}$	$10^{7.2}$	$10^{15.83}$	41.15	2.3×10^{35}

Table 5.4: Allowed mass scales as solutions of renormalisation group equations for Model-II as described in the text.

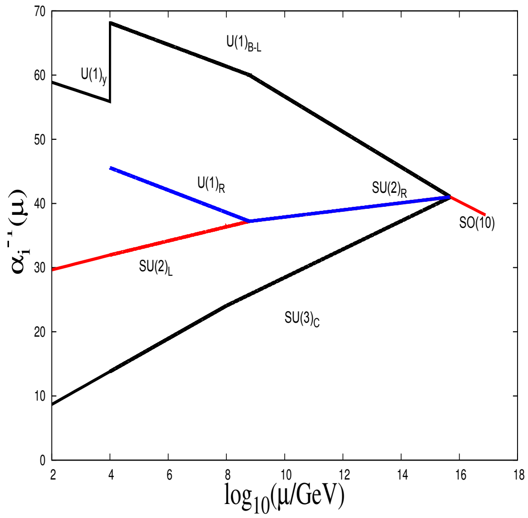

Figure 5.4: Two loop gauge coupling unification in the $SO(10)$ symmetry breaking chain with $M_U = 10^{15.62}$ GeV and $M_{R^+} = 10^{8.7}$ GeV with a low mass Z' boson at $M_R^0 = 10$ TeV for Model-II.

is shown in Fig.5.4 for $M_{R^0} = 10$ GeV, $M_{R^+} = 10^{8.7}$ GeV, $M_C = 10^8$ GeV, and $M_U = 6.5 \times 10^{15}$ GeV. Clearly the figure shows precise unifucation of the three gauge couplings of the intermediate gauge symmetry G_{2213P} at the GUT scale. For all other solutions given in Table-I the RG evolutions and unification of gauge couplings are similar. In both the models, with allowed values of $M_{R^+} \gg M_{R^0} = 5 - 10$ TeV, the numerical values of gauge couplings g_{2L}, g_{1R} and g_{B-L} predict [85, 105–111],

$$M_{Z'} = (1.2 - 3.5)\text{TeV}. \tag{5.39}$$

5.3.1 Proton lifetime prediction

In this section we discuss predictions on proton lifetimes in the two models and compare them with the current Super-Kamiokande limit and reachable limits by future experiments such as Hyper-Kamiokande [318–321]. Currently, the Superkamiokande detector has reached the search limit

$$(\tau_p)_{expt.}(p \to e^+\pi^0) \geq 1.4 \times 10^{34} \text{ yrs}, \tag{5.40}$$

The proposed 5.6 Megaton years Cherenkov water detector at Hyper-Kamiokane, Japan is expected to probe into lifetime [318–321],

$$(\tau_p)_{Hyper-K.}(p \to e^+\pi^0) \quad \geq \quad 1.3 \times 10^{35} \quad \text{yrs}, \tag{5.41}$$

The width of the proton decay for $p \to e^+\pi^0$ is expressed as [146, 322, 323]

$$\begin{aligned} \Gamma(p \to e^+\pi^0) \quad &= \quad \left(\frac{m_p}{64\pi f_\pi^2}\right) \times \left(\frac{{g_G}^4}{{M_U}^4}\right) \\ &\quad |A_L|^2 |\bar{\alpha_H}|^2 (1+D+F)^2 \times R. \end{aligned} \tag{5.42}$$

where $R = [(A_{SR}^2 + A_{SL}^2)(1 + |V_{ud}|^2)^2]$ for $SO(10)$, $V_{ud} = 0.974 =$ the $(1,1)$ element of V_{CKM} for quark mixings, $A_{SL}(A_{SR})$ is the short-distance renormalization factor in the left (right) sectors and $A_L = 1.25 =$ long distance renormalization factor. $M_U =$ degenerate mass of 24 superheavy gauge bosons in $SO(10)$, $\bar{\alpha}_H =$ hadronic matrix element, $m_p =$ proton mass $= 938.3$ MeV, $f_\pi =$ pion decay constant $= 139$ MeV, and the chiral Lagrangian parameters are $D = 0.81$ and $F = 0.47$. With $\alpha_H = \bar{\alpha_H}(1+D+F) = 0.012\ \text{GeV}^3$ obtained from lattice gauge theory computations, we get $A_R \simeq A_L A_{SL} \simeq A_L A_{SR} \simeq 2.726$ for both the models. The expression for the inverse decay rates for the models is expressed as,

$$\begin{aligned} \tau_p = \Gamma^{-1}(p \to e^+\pi^0) \quad &= \quad \frac{64\pi f_\pi^2}{m_p} \left(\frac{{M_U}^4}{{g_G}^4}\right) \times \\ &\quad \frac{1}{|A_L|^2 |\bar{\alpha_H}|^2 (1+D+F)^2 \times R}. \end{aligned} \tag{5.44}$$

where the factor $F_q = 2(1 + |V_{ud}|^2)^2 \simeq 7.6$ for $SO(10)$. Now using the given values of the model parameters the predictions on proton lifetimes for both the models are given in Table 5.3 and Table 5.4. We find that for proton lifetime predictions accessible to Hyper-Kamiokande detector [318–321], it is necessary to have a intermediate value of the color octet mass $M_C \geq 10^{8.6}$GeV in Model-II and $M_C \geq 10^{10.8}$GeV in Model-I. The predicted proton lifetime as a function of the color octet mass is shown in Fig. 5.5 both for Model-I and for Model-II. These analyses suggest that low color octet mass in the TeV scale and observable proton lifetime within Hyper-Kamiokande limit are mutually exclusive. If LHC discovers color octet within its achievable enegy range, proton decay searches would need far bigger detector than the Hyper-K detector. On the other hand the absence of color octet at the LHC would still retain the possibility of observing proton decay within the Hyper-K limit.

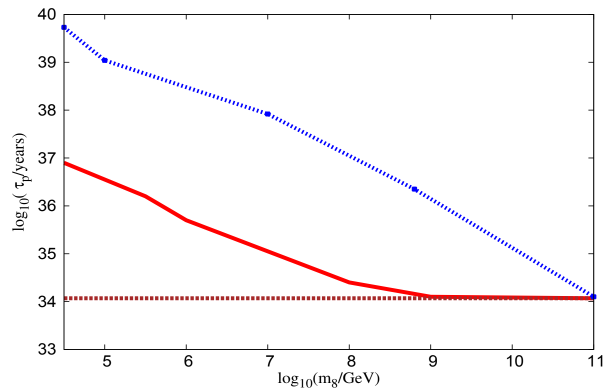

Figure 5.5: Variation of proton lifetime as a function of color octet mass M_C for Model-I (upper curve) and Model-II (lower curve). The horizontal line is the present experimental limit.

5.4 Brief discussion on low mass Z' boson.

Although in our model the Z' boson is present at TeV scale, there is no effect of this boson on the electroweak precision observables, STU parameters and other electroweak constraints. We also point out occurence of small $Z - Z'$ mixings while indicating briefly a possible application for dilepton production.

In the allowed kinematical region, we have estimated the partial decay widths,

$$\Gamma(Z \to S_i S_i) = \Gamma_Z^{\nu\bar{\nu}}[\sum_\alpha |\left(\mathcal{V}_{\alpha,i}^{\nu S}\right)|^4]\,(i = 1, 2), \tag{5.45}$$

where the standard value $\Gamma_Z^{\nu\bar{\nu}} = 0.17$ GeV and $\mathcal{V}_{\alpha,i}^{\nu S} = (M_D/M)_{\alpha,i}$ with $\alpha = \nu_e, \nu_\mu, \nu_\tau$ and $i = 1, 2, 3$. We then obtain $\Gamma(Z \to S_1 S_1) = 1.2 \times 10^{-14}$ GeV for NH, IH, and QD cases, and $\Gamma(Z \to S_2 S_2) = 6.6 \times 10^{-11}$ GeV for QD case only. Similarly we have estimated the partial decay width

$$\Gamma(W \to l S_i) = \Gamma_W^{l\nu}[\sum_\alpha |\left(\mathcal{V}_{\alpha,i}^{\nu S}\right)|^2]\,(i = 1, 2), \tag{5.46}$$

and obtained $\Gamma(W \rightarrow eS_1) \simeq \Gamma(W \rightarrow eS_2) = 3.5 \times 10^{-9}$ GeV, $\Gamma(W \rightarrow \mu S_1) \simeq \Gamma(W \rightarrow \mu S_2) = 1.8 \times 10^{-7}$ GeV, and $\Gamma(W \rightarrow \tau S_1) \simeq \Gamma(W \rightarrow \tau S_2) = 1.0 \times 10^{-5}$ GeV. These and other related estimations cause negligible effects on electroweak precision observables [324] primarily because of small $\nu - S$ mixings determined by the model analyses. In addition to these insignificant tree level corrections, new physics effects may affect the electroweak observables indirectly via oblique corrections through loops leading corrections to the Peskin-Takeuchi S, T, U parameters [266,267,325]. In this model the neutral generator corresponding to heavy Z' is a linear combinations of $U(1)_R$ and $U(1)_{B-L}$ generators while the other orthogonal combination is the $U(1)_Y$ generator of the SM [85, 105–111, 116–118]. The $Z - Z'$ mixing in such theories is computed through the generalised formula $\tan^2\theta_{zz'} = \frac{M_0^2 - M_Z^2}{M_{Z'}^2 - M_0^2}$ where $M_0 = \frac{M_W}{\sqrt{\rho_0}\cos\theta_W}$. In our model since the LH triplet $\Delta_L(3, -1, 1)$ has a very small VEV $v_L = 0.1 - 0.5$ eV $<< V_{\rm ew}$, the model is consistent with the tree level value of the ρ- parameter. $\rho_0 = 1$. The radiative corrections due to the 125 GeV Higgs of the SM and the top quark yield $\rho \simeq 1.009$ [326]. The new neutral gauge boson Z' in principle may have additional influence on the electroweak precision parameters as well as the $Z-$pole parameters if $M_{Z'} << \mathcal{O}(1)$ TeV [85, 105–111, 329, 330]. The most recent LHC data has given the lower bound $M_{Z'} \geq 1.6$ TeV [328]. Since our model is based on extended seesaw mechanism, we require $V_R >> V_{ew} = 246$ GeV and this implies $M_{Z'} >> M_Z$ but accessible to LHC. Under this constraint $M_{Z'} \sim \mathcal{O}(5-10)$ TeV are the most suitable predictions of both the models discussed in this work. As some examples, using such values of $M_{Z'}$ and the most recently reported values from Particle Data Group [331,332] of $\sin^2\theta_W = 0.23126 \pm 0.00005$, $M_W = 80.385 \pm 0.015$GeV, $M_Z = 91.1876 \pm 0.0021$ GeV, $\rho_0 = 1.01$, we obtain $\theta_{zz'} = 0.00131 \pm 0.0003,\ 0.0005 \pm 0.00012,\ 0.0003 \pm 0.00008,$ and 0.0002 ± 0.00006 for $M_{Z'} = 2.0$ TeV, 5.0 TeV, 7.5 TeV, and 10 TeV, respectively. Because of the smallness of the values, these mixings are consistent with the electroweak precision observables including the $Z-$ pole data [85, 105–111, 329, 330, 334, 335]. Some of these masses may be also in the accessible range of the ILC [333]. Details of experimental constraints on $Z - Z'$ mixings as a function of Z' masses would be investigated elsewhere.

Chapter 6

Neutrinoless Double Beta Decay and Resonant Leptogenesis

A basic feature of our type-II seesaw dominance model which we discuss in this chapter is that, it gives a new contribution to neutrinoless double beta decay in the $W_L - W_L$ channel although the W_R boson mass is $\simeq 10^8$ GeV. In addition, our model provides a mechanism for resonant leptogenesis [189] mediated by TeV scale quasi-degenerate pair of sterile neutrinos. Two different cases have been identified. In the Case (a) while the light sterile neutrino S_1 of first generation mediates dominant contribution to double beta decay and like-sign dilepton events with displaced vertices in the channels $eejj$, $e\mu jj$, and $\mu\mu jj$, resonant leptogenesis is allowed to be mediated by heavy quasi-degenerate sterile neutrino pairs S_2 and S_3 belonging to the second and the third generations. In another class of solutions identified as the alternative Case (b), dominant double beta decay and dilepton events with displaced vertices are mediated by the allowed lighter mass of S_2 while resonant leptogenesis is mediated by the heavy quasi-degenerate sterile neutrino pairs, S_1 and S_3. In addition to QD hierarchy of light neutrino masses, most important fact is that we also show how all these results hold in the presence of NH neutrino masses. This result might be important if the recent cosmological bound [336] is finally established.This chapter is organized as below. In Sec.6.1 we discuss the phenomenon of neutrinoless double beta decay. Neutrinoless double beta decay half life and effective mass parameter are discussed in Sec.6.2. In Sec.6.3 we discuss the mechanism of leptogenesis.

6.1 Neutrinoless double beta decay

Even with the vanishing bare mass term $\mu_S = 0$ in the Yukawa Lagrangian of eq.(5.1), the singlet fermions $S_i (i = 1, 2, 3)$ acquire Majorana masses over a wide range of values and, in the leading order, the corresponding mass matrix given in eq.(5.2) is $m_S = -M \frac{1}{M_N} M^T$. As far as light neutrino mass matrix is concerned, it is given by the type-II seesaw formula of eq.(5.8) which is independent of the Majorana mass matrix m_S of singlet fermions. But the combined effect of substantial mixing between the light neutrinos and the singlet fermions, and the Majorana neutrino mass insertion m_S due to the singlet fermions, the Feynman diagram of Fig.(6.1) gives rise to new contributions to the amplitude and the effective mass parameter for $0\nu\beta\beta$ in the $W_L - W_L$ channel. This may be contrasted with conventional type-II seesaw dominated non-SUSY $SO(10)$ models with only three generations of standard fermions in $\mathbf{16_i} (i = 1, 2, 3)$ where there are negligible contributions to $0\nu\beta\beta$ decay due to non-standard particle exchanges. The charged current interaction Lagrangian for leptons in the present model in the flavor basis is

$$\mathcal{L}_{\rm CC} = \frac{g}{\sqrt{2}} \sum_{\alpha=e,\mu,\tau} \left[\overline{\ell}_{\alpha\, L}\, \gamma_\mu \nu_{\alpha\, L}\, W_L^\mu + \overline{\ell}_{\alpha\, R}\, \gamma_\mu N_{\alpha\, R}\, W_R^\mu \right] + \text{h.c.} \qquad (6.1)$$

In the present model the $W_R^\pm$ bosons and the doubly charged Higgs scalars, both left-handed and right handed, are quite heavy with $M_{W_R} \sim M_\Delta \simeq 10^8 - 10^9$ GeV that make negligible contributions to the RH current effects and Higgs exchange effects for the $0\nu\beta\beta$ decay amplitude. The most popular standard and conventional contribution in the $W_L^- - W_L^-$ channel is due to light neutrino exchanges. But one major point in this work is that even in the $W_L^- - W_L^-$ channel, the singlet fermion exchange allowed within the type-II seesaw dominance mechanism, can yield much more dominant contribution to $0\nu\beta\beta$ decay rate. For the exchange of singlet fermions $(\hat{S}_j)$, the Feynman diagram is shown in the Fig.6.1. The heavier RH neutrino exchange contributions are found to be negligible compared to the singlet fermion exchange contributions since $m_{N_i} >> m_{s_i}$. To visualise this clearly we note that every neutrino flavour state ν_α is a superposition of mass eigen states $\hat{\nu}_i$, $\hat{S}_i$, and $\hat{N}_i$, (i=1,2,3).

$$\nu_\alpha = V^{\nu\nu}_{\alpha i} \hat{\nu}_i + V^{\nu s}_{\alpha i} \hat{S}_i + V^{\nu N}_{\alpha i} \hat{N}_i \qquad (6.2)$$

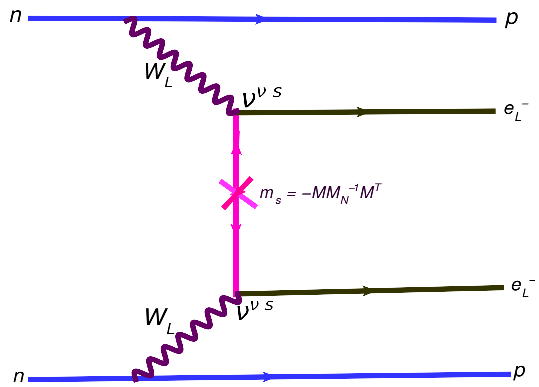

Figure 6.1: Feynman diagrams for neutrinoless double beta decay contribution with virtual Majorana neutrinos $\hat{\nu}_i$, and $\hat{S}_i$ in the $W_L - W_L$-channel.

, where (i=1,2,3) and ($\alpha = e$,μ,τ). In the mass basis, the contributions to the decay amplitudes by ν, S ans N exchanges are estimated as

$$A_\nu^{LL} \propto \frac{1}{M_{W_L}^4} \sum_{i=1,2,3} \frac{\left(\mathcal{V}_{e\,i}^{\nu\nu}\right)^2\, m_{\nu_i}}{p^2} \tag{6.3}$$

$$A_S^{LL} \propto \frac{1}{M_{W_L}^4} \sum_{j=1,2,3} \frac{\left(\mathcal{V}_{e\,j}^{\nu S}\right)^2}{m_{S_j}} \tag{6.4}$$

$$A_N^{LL} \propto \frac{1}{M_{W_L}^4} \sum_{j=1,2,3} \frac{\left(\mathcal{V}_{e\,j}^{\nu N}\right)^2}{m_{N_j}}, \tag{6.5}$$

where $|p| \simeq 190$ MeV represents the magnitude of neutrino virtuality momentum [337–346]. Using uncertainities in the nuclear matrix elements [343–346] we have found it to take values in the range $|p| = 120\text{MeV} - 200\text{MeV}$. In order to understand physically how the singlet fermion Majorana mass insertion terms as a new source of lepton number violation contributes to $0\nu\beta\beta$ process, we draw the Feynman diagram Fig.6.1. with mass insertion. In this model, the Majorana mass matrix for the singlet fermion after block diagonalisation is $m_S = -MM_N^{-1}M^T$. Then exchanges of such singlets generate dominant contribution through their mixings with active neutrinos and this mixing is proportional to the Dirac neutrino mass M_D. Similarly

$$
\begin{aligned}
V_{ej}^{\nu s} &= \left(\frac{M_D}{M}\right)_{ej}, \\
V_{ej}^{\nu N} &= \left(\frac{M_D}{M_N}\right)_{ej}.
\end{aligned} \tag{6.6}
$$

It is important to note that in SO(10), $M_D \simeq M_u$ the up-quark mass matrix. This is another factor in enhancing neutrinoless double beta decay contribution. It is clear from the Fig. 6.1 that the singlet fermion exchange amplitudes are derived [87] to have the same form as in eq.(6.4).

6.1.1 Nuclear matrix elements and normalized effective mass parameters

By now it is well known that different particle exchange contributions for $0\nu2\beta$ decay discussed above are also modified by the corresponding nuclear matrix elements which depend upon the chirality of the hadronic currents involved [343–346]. Including all relevant contributions except those due to heavy doubly charged Higgs exchanges, and using eq. (6.3) - eq. (6.5), we express the inverse half-life in terms of effective mass parameters with proper normalization factors. Thus after taking into account the nuclear matrix elements [343–346] leads to the half-life prediction

$$\left[T_{1/2}^{0\nu}\right]^{-1} = G_{01}^{0\nu}\left\{|\mathcal{M}_\nu^{0\nu}|^2|\eta_\nu|^2 + |\mathcal{M}_N^{0\nu}|^2|\eta_{N_R}^L|^2 + |\mathcal{M}_N^{0\nu}|^2|\eta_{N_R}^R|^2\right. \tag{6.7}$$

$$+ \left.|\mathcal{M}_\lambda^{0\nu}|^2|\eta_\lambda|^2 + |\mathcal{M}_\eta^{0\nu}|^2|\eta_\eta|^2\right\} + \text{interference terms.} \tag{6.8}$$

where the dimensionless particle physics parameters are

$$
\begin{aligned}
|\eta_\nu| &= \left|\frac{\sum_i \mathcal{V}_{ei}^{\nu\hat{\nu}^2}\, m_{\nu\, i}}{m_e}\right| \\
|\eta_N^R| &= m_p \left(\frac{M_{W_L}}{M_{W_R}}\right)^4 \left|\frac{\mathcal{V}_{ei}^{N\hat{N}^2}}{m_{N_i}}\right| \\
|\eta_N^L| &= m_p \left|\frac{V_{ei}^{N\hat{\nu}}}{m_{N_i}} + \frac{V_{ei}^{S\hat{\nu}}}{m_{S_i}}\right| \\
|\eta_\lambda| &= \left(\frac{M_{W_L}}{M_{W_R}}\right)^2 \left|U_{ei}\left(\frac{M_D}{M_N}\right)_{ei}\right| \\
|\eta_\eta| &= \tan\zeta_{LR} \left|U_{ei}\left(\frac{M_D}{M_N}\right)_{ei}\right|.
\end{aligned} \tag{6.9}
$$

In eq. (6.9), m_e (m_i)= mass of electron (light neutrino), and m_p = proton mass. In eq. (6.8), $G^{0\nu}_{01}$ is the the phase space factor. Besides different particle physics parameters, it contains the nuclear matrix elements due to different chiralities of the hadronic weak currents such as ($\mathcal{M}^{0\nu}_\nu$) involving left-left chirality in the standard contribution, and ($\mathcal{M}^{0\nu}_\nu$) due to heavy neutrino exchanges involving right-right chirality, ($\mathcal{M}^{0\nu}_\lambda$) for the λ-diagram, and $\left(\mathcal{M}^{0\nu}_\eta\right)$ for the η-diagram. Explicit numerical values of these nuclear matrix elements discussed in ref. [343–346] are given in Tab. 6.1.

Isotope	$G^{0\nu}_{01}$ $[10^{-14}$ yrs$^{-1}]$ refs. [343–346]	$\mathcal{M}^{0\nu}_\nu$	$\mathcal{M}^{0\nu}_N$	$\mathcal{M}^{0\nu}_\lambda$	$\mathcal{M}^{0\nu}_\eta$
^{76}Ge	0.686	2.58–6.64	233–412	1.75–3.76	235–637
^{82}Se	2.95	2.42–5.92	226–408	2.54–3.69	209–234
^{130}Te	4.13	2.43–5.04	234–384	2.85–3.67	414–540
^{136}Xe	4.24	1.57–3.85	160–172	1.96–2.49	370–419

Table 6.1: Phase space factors and nuclear matrix elements with their allowed ranges as derived in refs. [343–346]

In order to arrive at a common normalization factor for all types of contributions, at first we use the expression for inverse half-life for $0\nu2\beta$ decay process due to only light active Majorana neutrinos, $\left[T^{0\nu}_{1/2}\right]^{-1} = G^{0\nu}_{01}\,|\mathcal{M}^{0\nu}_\nu|^2\,|\eta_\nu|^2$.

6.2 Effective mass parameter and half-life

Adding together the $0\nu\beta\beta$ decay amplitudes arising out of light-neutrino exchanges, singlet fermion exchanges, and the heavy RH neutrino exchanges in the $W_L - W_L$ channel from eq.(6.3), eq.(6.4), eq.(6.5) and using suitable normalisations [343–346], we express the inverse half life

$$\begin{aligned}\left[T^{0\nu}_{1/2}\right]^{-1} &\simeq G^{0\nu}_{01}|\frac{\mathcal{M}^{0\nu}_\nu}{m_e}|^2|(\mathbf{m}^{ee}_\nu + \mathbf{m}^{ee}_S + \mathbf{m}^{ee}_N)|^2, \\ &= K_{0\nu}|(\mathbf{m}^{ee}_\nu + \mathbf{m}^{ee}_S + \mathbf{m}^{ee}_N)|^2, \\ &= K_{0\nu}|\mathbf{m}_{\rm eff}|^2. \end{aligned} \tag{6.10}$$

In the above equation $G^{0\nu}_{01} = 0.686 \times 10^{-14}$yrs^{-1}, $\mathcal{M}^{0\nu}_\nu = 2.58 - 6.64$, $K_{0\nu} = 1.57 \times 10^{-25}$yrs^{-1}eV^{-2}, and the three effective mass parameters for light-neutrino, singlet fermion, and heavy RH neutrino exchanges are

$$\mathbf{m}_{\nu}^{\rm ee} = \sum_i \left(\mathcal{V}^{\nu\nu}_{e\,i}\right)^2\, m_{\nu_i}, \tag{6.11}$$

$$\mathbf{m}_{S}^{\rm ee} = \sum_i \left(\mathcal{V}^{\nu S}_{e\,i}\right)^2\, \frac{|p|^2}{m_{S_i}}, \tag{6.12}$$

$$\mathbf{m}_{N}^{\rm ee} = \sum_i \left(\mathcal{V}^{\nu N}_{e\,i}\right)^2\, \frac{|p|^2}{m_{N_i}}, \tag{6.13}$$

with

$$\mathbf{m}_{\rm eff} = \mathbf{m}_{\nu}^{ee} + \mathbf{m}_{S}^{ee} + \mathbf{m}_{N}^{ee}. \tag{6.14}$$

Here m_{S_i} is the eigen value of the $S-$ fermion mass matrix m_S, and the magnitude of neutrino virtuality momentum $|p| = 120$ MeV-200 MeV. As the predicted values of the RH neutrino masses carried out in Sec. 5.1.4 have been found to be large which make their contribution to the $0\nu\beta\beta$ decay amplitude negligible, we retain only contributions due to light neutrino and singlet fermion exchanges. The estimated values of the effective mass parameters due to the $S-$ fermion exchanges and light neutrino exchanges are shown separately in Fig. 6.2 where the magnitudes of corresponding mass eigen values used have been indicated.

6.2.1 Numerical estimations of effective mass parameters

Using the equations of normalized mass parameters [87], we estimate numerically the nearly standard contribution due to light neutrino exchange and the dominant non-standard contributions due to singlet fermion exchanges.

A.Nearly standard contribution

In this model the new mixing matrix $\mathcal{N} \equiv \mathcal{V}^{\nu\nu} = (1-\eta)\, U_\nu$ contains additional non-unitarity effect due to non-vanishing η [87] Using $M_{Deg} = 1213$ GeV the N-S mixing mass in the degenerate case, we estimate

$$\mathcal{N}_{ei} = \ (0.81437,\ 0.54858,\ 0.1267 + 0.0922i). \tag{6.15}$$

Since all the $\eta-$ parameters are constrained by $|\eta_{\alpha\beta}| < 10^{-3}$, it is expected that

$|\mathcal{N}_{ei}| \simeq |U_{ei}|$ for any other choice of M. In the leading approximation by neglecting the $\eta_{\alpha i}$ contributions, the effective mass parameter in the the $W_L - W_L$ channel with light neutrino exchanges is expressed as

$$\begin{aligned} m_\nu^{\rm ee} &= \sum_i \mathcal{N}_{ei}^2 \hat{m}_i \\ &\simeq (c_{12}c_{13})^2 \hat{m}_1 e^{i\alpha_1} + (s_{12}c_{13})^2 \hat{m}_2 e^{i\alpha_2} + s_{13}^2 e^{i\delta} \hat{m}_3, \end{aligned} \tag{6.16}$$

where we have introduced two Majorana phases α_1 and α_2. As discussed subsequently in this section, they play crucial roles in preventing cancellation between two different effective mass parameters. Using $\alpha_1 = \alpha_2 = 0$ and the experimental values of light neutrino masses and the Dirac phase $\delta = 0.8\pi$ from eq.(5.9), the light neutrino exchanges have their well known values,

$$|m_\nu^{\rm ee}| = \begin{cases} 0.0039\,\text{eV} & \text{NH}, \\ 0.04805\,\text{eV} & \text{IH}, \\ 0.23\,\text{eV} & \text{QD}. \end{cases} \tag{6.17}$$

B. Dominant non-standard contributions

The (ei) element of the $\nu - S$ mixing matrix is [87]

$$\mathcal{V}_{ei}^{\nu S} = (\frac{M_D}{M})_{ei}. \tag{6.18}$$

where the Dirac neutrino mass matrix M_D has been given in eq.(5.26) and $M = diag(M_1, M_2, M_3)$. We derive the relevant elements of the mixing matrix $\mathcal{V}^{\nu S}$ using the structures of the the Dirac neutrino mass matrix M_D given in eq.(5.26) and values of the diagonal elements of $M = diag(M_1, M_2, M_3)$ satisfying the non-unitarity constraint in eq.(5.30). The eigen values of the $S-$ fermion mass matrix m_S are estimated for different cases using the structures of the RH Majorana neutrino mass matrices given in eq.(5.14), eq.(5.16), and eq.(5.18) in the formula $m_S = -M \frac{1}{M_N} M^T$. It is clear that in the effective mass parameter the non-standard contribution due to sterile fermion exchange has a sign opposite to that due to light neutrino exchange and also its magnitude is inversely proportional to the sterile fermion mass eigen values. In the NH case the estimated effective mass parameters are shown in Fig.6.2 where the values of diagonal elements of M and the eigen values of m_s have been specified. For comparison the effective mass parameters in the standard case without singlet fermions have been also given. It is clear that for allowed masses of the model, the non-standard contributions to effective mass parameters can be much more dominant compared to the standard values irrespective of the mass patterns of light neutrino masses, in NH, IH or QD cases.

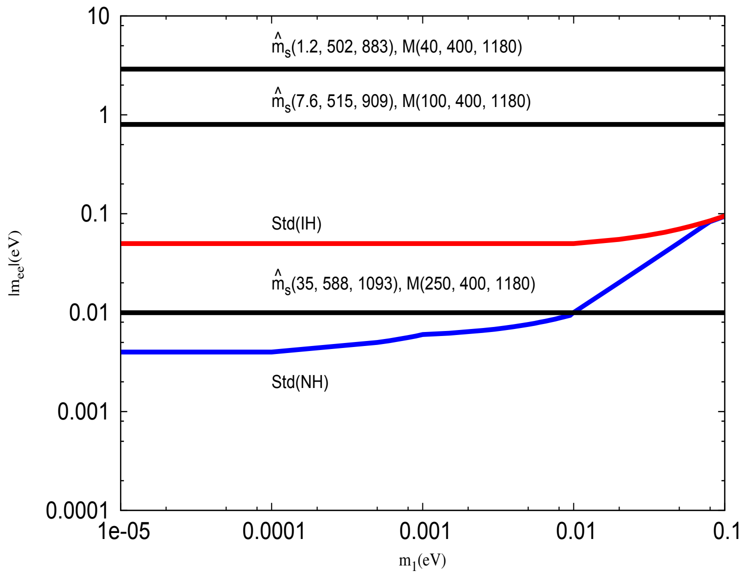

Figure 6.2: Variation of the effective mass parameters with lightest LH neutrino mass. The dominant non-standard contributions due to fermion singlet contributions are shown by three horozontal lines with corresponding mass values in GeV units. The subdominant effective mass parameters due to NH and IH cases shown are similar to the standard values.

6.2.2 Cancellation between effective mass parameters

When plotted as a function of singlet fermion mass eigen value m_{S_1}, the resultant effective mass parameter shows cancellation for certain region of the parameter space, the cancellation being prominent in the QD case. Like the light neutrino masses, the singlet fermion masses m_{S_i} are also expected to have two Majorana phases. When all Majorana phases are absent, both in the light active neutrino as well as in the singlet fermion sectors, it is clear that in the sum of the two effective mass parameter there will be cancellation between light active neutrino and the singlet fermion contributions because of the inherent negative sign of the non-standard contribution. Our estimations for NH, IH, and QD patterns of light neutrino mass hierarchies are discussed separately.

A. Effective mass parameter for NH and IH active neutrino masses

In Fig. 6.3, we have shown the variation of the resultant effective mass parameter with m_{S_1} for NH and IH patterns of active light neutrino masses. It is clear that for lower values of m_{S_1}, the singlet fermion exchange term continues to dominate . For larger values of m_{S_1} the resultant effective mass parameter tends to be identical to the light neutrino mass contribution due to the vanishing non-standard contribution. We note that the values $|m_{eff}| = 0.5 - 0.1$ eV can be easily realised for $|m_{S_1}| = 3 - 5$ GeV in the NH case but for $|m_{S_1}| = 1 - 2$ GeV in the IH case.

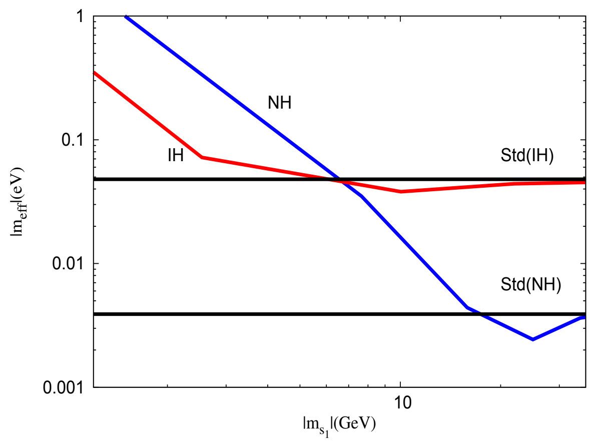

Figure 6.3: Variation of effective mass of $0\nu\beta\beta$ decay with the mass of the lightest singlet fermion for the value of $|p| = 190$ MeV .

B. Effective mass parameter for QD active neutrinos

The variation of effective mass with m_{S_1} for the QD case with one experimentally determined Dirac phase $\delta = 0.8\pi$ and assumed values of two unknown Majorana phases is given in Fig. 6.4. The left-panel of Fig. 6.4 shows the variation with $\alpha_1 = \alpha_2 = 0$ for different choices of the common light neutrino mass $m_0 = 0.5$ eV, 0.3 eV , and 0.2 eV for the upper, middle, and the lower curves, respectively, where cancellations are clearly displayed in the regions of $m_{s_1} = 0.4 - 1.5$ GeV. However, before such cancellation occurs, the dominance of the singlet exchange contribution has been clearly shown to occur in the regions of lower values of m_{S_1}. For larger values of $m_{S_1} > 5$ GeV, the singlet exchange contribution tends to be negligible and the light QD neutrino contribution to m_{eff} is recovered. In the right panel of Fig. 6.4, the upper curve corresponds to $\alpha_1 = \pi$, $\alpha_2 = \pi$ at $m_0 = 0.2$ eV. The middle line corresponds to $\alpha_1 = \pi$, $\alpha_2 = 0$ at $m_0 = 0.5$ eV .The lower line corresponds to $\alpha_1 = 0$, $\alpha_2 = \pi$ at $m_0 = 0.3$ eV. We find that because of introduction of appropriate Majorana phases the dips in two curves have disappeared.

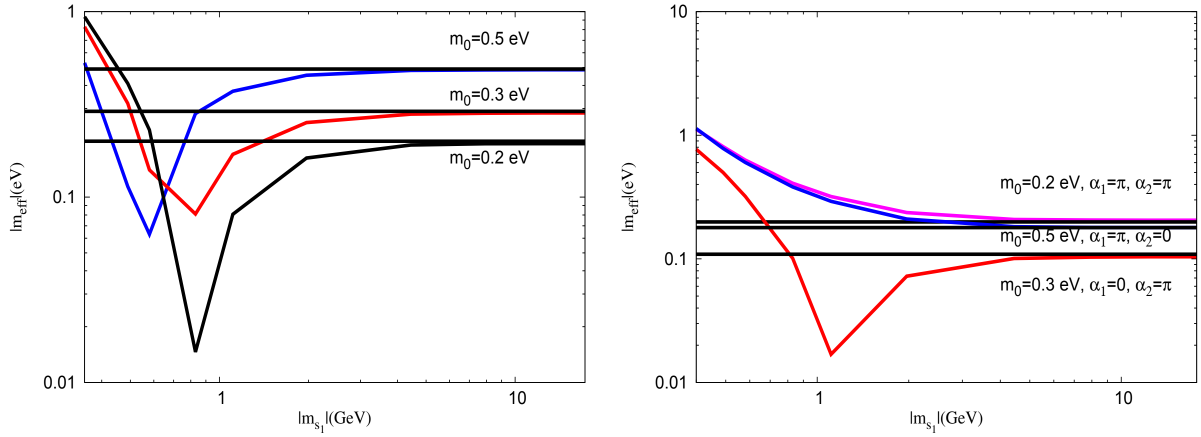

Figure 6.4: Variation of effective mass of $0\nu\beta\beta$ decay with the mass of the lightest singlet fermion for QD light neutrinos with one Dirac phase (left) and one Dirac phase and two Majorana phases (right).

6.2.3 Half-life as a function of singlet fermion masses

In order to arrive at a plot of half-life against the lightest singlet fermion mass in different cases, at first we estimate the mass eigen values of the three singlet fermions for different allowed combinations of the $N-S$ mixing matrix elements satisfying the non-unitarity constraint of eq.(5.30) and by using the RH neutrino mass matrices predicted for NH, IH, and QD cases from eq.(5.14), eq.(5.16), eq.(5.18), and eq.(5.19). These solutions are shown in Table 6.2.

We then derive expressions for half-life taking into account the contributions of the two different amplitudes or effective mass parameters arising out of the light neutrino and the singlet fermion exchanges leading to

$$\left[T_{1/2}^{0\nu}\right] = \frac{m_{s1}^2}{K_{0\nu}|p|^4 {(M_D/M)_{e1}}^4}\left[|1+X+Y|\right]^{-2}, \tag{6.19}$$

where

$$X = \frac{{(M_D/M)_{e2}}^2}{{(M_D/M)_{e1}}^2}\frac{m_{S_1}}{m_{s_2}} + \frac{{(M_D/M)_{e3}}^2}{{(M_D/M)_{e1}}^2}\frac{m_{S_1}}{m_{S_3}}, \tag{6.20}$$

$$Y = \mathbf{m}_\nu^{ee}\frac{m_{S_1}}{p^2 (M_D/M)_{e1}^2}. \tag{6.21}$$

Here we have used the expression for $\mathbf{m}_\nu^{ee}$ given in eq.(6.11). In eq.(6.19), $Y=0$ gives complete dominanace of the singlet fermion exchange term. However this formula of half-life is completely different from the one obtained using inverse seesaw dominance

M (GeV)	$\hat{m_s}(NH)$ (GeV)
(40,400,1180)	(1.2,502,883)
(100,400,1180)	(7.65,515,909))
(150,400,1180)	(16,533,951)
(200,400,1180)	(25,558,1011)
(250,400,1180)	(35,588,1093)
(300,400,1180)	(43,622,1200)
(350,400,1180)	(50,659,1331)

M (GeV)	$\hat{m_s}(IH)$ (GeV)
(40,450,1280)	(0.4,54.32,7702)
(60,450,1280)	(0.9,54.4,7705)
(70,450,1280)	(1.2,54.4,7706)
(100,450,1280)	(2.5,55,7715)
(300,450,1280)	(22,56,7831)
(400,450,1280)	(36.2,59,7933)
(450,450,1280)	(42,64,7996)

M (GeV)	$\hat{m_s}(QD)$ (GeV)
(100,600,1500)	(0.5,17.7,109))
(130,600,1500)	(0.8,17.7,109)
(200,600,1500)	(1.97,17.7,109)
(300,600,1500)	(4.4,17.7,109)
(350,600,1500)	(6.05,17.7,109)
(400,600,1500)	(8,17.7,109)
(500,600,1500)	(12.3,17.7,109)
(600,600,1500)	(17.7,17.7,109)

Table 6.2: Eigen values for singlet fermion mass matrix for different allowed $N-S$ mixing matrix elements for NH, IH, and QD patterns of light neutrino masses

in SO(10) [88]. In this model half-life depends directly to the square of the lightest singlet fermion mass and it is independent of the right-handed neutrino mass which is non-diagonal. But in [88], the half-life of neutrino less double beta decay is directly proportional to the fourth power of the lightest singlet fermion mass and square of the lightest right handed neutrino mass leading to a different result.

A. Half-life in the NH and IH cases

We have computed the half-life for NH and IH patterns of active neutrino masses, taking the contributions of singlet fermion as well as light active neutrino exchanges. This is shown in the left-panel for NH case and in the right panel for IH case in Fig.6.5. Taking both X term and Y term in eq.(6.19) , we find that for smaller value of m_{S_1} ,the contribution due to sterile neutrino is dominated for both NH and IH. But with the increase in the value of m_{S_1}, the half-lfe increases showing its decreasing strength. The predicted half-life curve satuarates the experimental data at $m_{S_1} \simeq 3$ GeV and $m_{S_1} \simeq 2$ GeV, for NH and the IH cases, respectively. The interesting predictions are that if the lightest sterile neutrino mass satisfies the bound $m_{S_1} \leq 3GeV$, then the $0\nu\beta\beta$ decay should be detected with half-life close to the current experimental bound even if the light neutrino masses have NH pattern of masses. Similarly the corresponding bound for the IH case is $m_{S_1} \leq 2$ GeV. But in [88] which has inverse seesaw dominant formula for m_ν, the corresponding bound for the NH and IH case is $m_{S_1} \leq 14$ GeV.

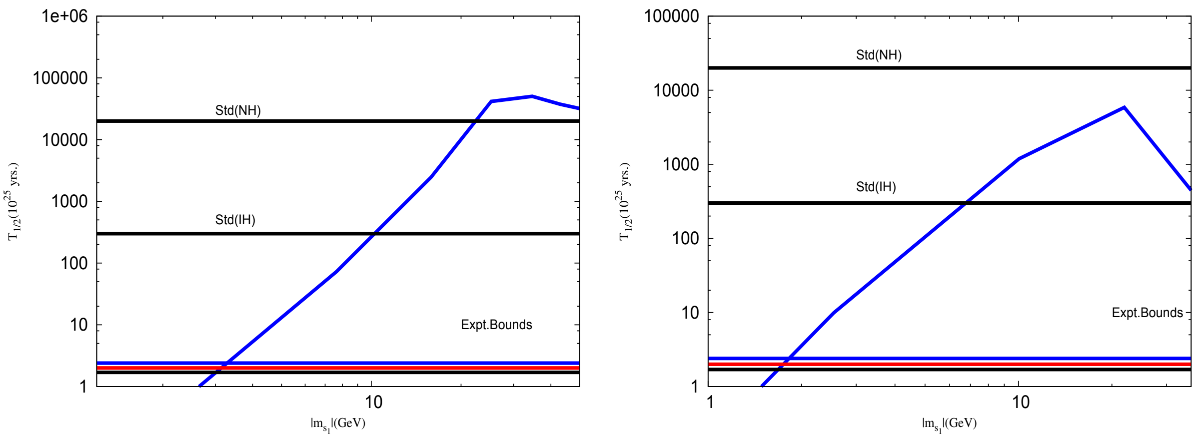

Figure 6.5: Variation of half-life of $0\nu\beta\beta$ decay with the sterile neutrino mass for NH(left) and IH(right) patterns of light active neutrino masses for $|p| = 190$ MeV.

B. Lifetime prediction with QD neutrino masses.

For QD masses of light active neutrinos we considered the X term and Y term of eq.(6.19) i.e including both the sterile neutrino exchange and light neutrino exchange contributions. For the light-neutrino effective mass parameter occuring in Y, we have considered three different cases with common light-neutrino mass values $m_0 = 0.2\text{eV}, 0.3\text{eV}$, and 0.5eV resulting in three different curves shown in the left- and the right- panels of Fig. 6.6. In the left-panel only the experimentally determined Dirac phase $\delta = 0.8\pi$ has been included in the PMNS mixing matrix for light QD neutrinos while ignoring the two Majorana phases($\alpha_1 = \alpha_2 = 0$). In the right panel while keeping $\delta = 0.8\pi$ for all the three curves, the Majorana phases have been chosen as indicated against each of them. As the sterile neutrino exchange amplitude given in eq.(6.11) is inversely proportional to the eigen value of the corresponding sterile neutrino mass m_{S_i}, even in the quasi-degenerate case this contribution is expected to dominate for allowed small values of m_{S_i}. This fact is reflected in both the figures given in Fig.6.6. When Majorana phases are ignored, this dominance gives half-life less than the current bounds for $m_{S_1} < 0.5$ GeV when $m_0 = 0.5$ eV, but for $m_{S_1} < 0.7$ GeV when $m_0 = 0.2 - 0.3$ eV. When Majorana phases are included preventing cancellation between the two contributions, these crossing points are changed to $m_{S_1} < 0.7$ GeV when $m_0 = 0.3$ eV, but $m_{S_1} < 1.0$ GeV when $m_0 = 0.2 - 0.5$ eV. In one of the paper [88] which is inverse seesaw dominant, the corresponding bound for the QD case is $m_{S_1} \leq 12.5$ GeV. The peaks in the half-life prediction in the curves appear because of cancellation between the two effective parameters. Inclusion of Majorana phases annuls cancellation resulting in constructive addition of the two effective mass parameters and reduced values of half-life accessible to ongoing searches. For larger values of $m_{S_1} >> 20$ GeV, the sterile neutrino contribution to $0\nu\beta\beta$ amplitude becomes negligible and the usual contributions due to light quasi-degenerate neutrinos are recovered.

5

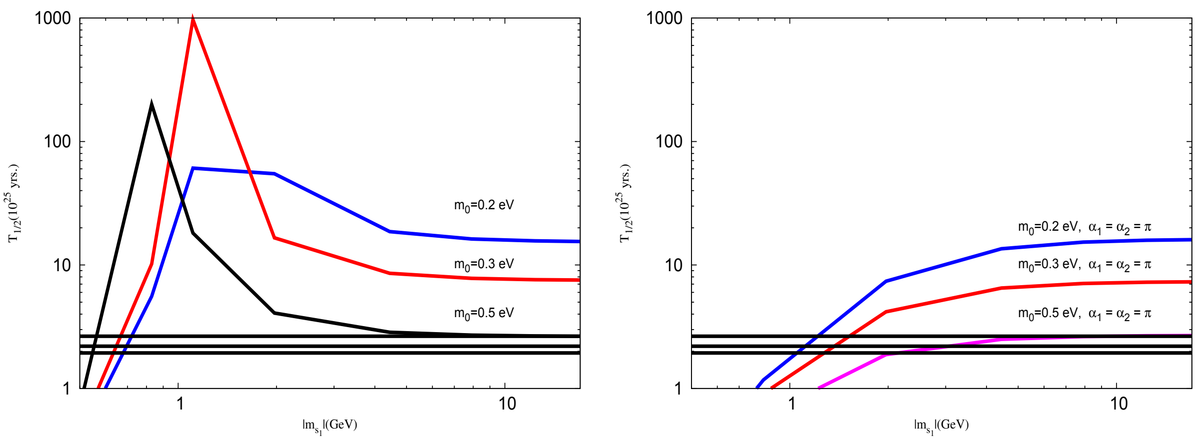

Figure 6.6: Variation of half-life of $0\nu\beta\beta$ decay with the mass of the lightest singlet fermion for QD light neutrinos with one Dirac phase (left) and with one Dirac phase and two Majorana phases (right).

6.2.4 Scattered plots for singlet fermion exchange dominated half-life

The nonstandard contributions to half life of double beta decay as a function of sterile neutrino mass has been discussed in [86–88,208,243]. The models predict $\nu - S$ mixing and sterile neutrino masses which have been used to predict the half-life in the case of different hierarchies of light neutrino masses:NH, IH, and QD. Using the estimations of ref. [88] which are also applicable to models of refs. [87,208,242,243], scattered plots for the predicted half-life are shown in Fig.6.7, Fig.6.8, and Fig.6.9 for the three types of neutrino mass hierarchies.

In Fig.6.10 we show predictions in the QD case excluding and including the CP phases of Majorana type sterile neutrinos. The cancellations between light neutrino

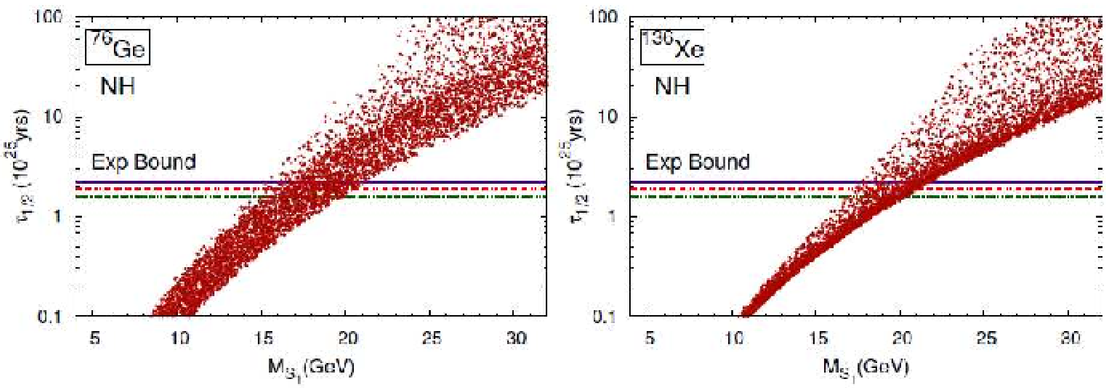

Figure 6.7: Scattered plots for half-life prediction of double beta decay as a function of neutral singlet fermion mass in the case of normal hierarchy (NH) of light neutrino masses from ^{76}Ge nucleus (left-panel) and from ^{136}Xe nucleus right panel.

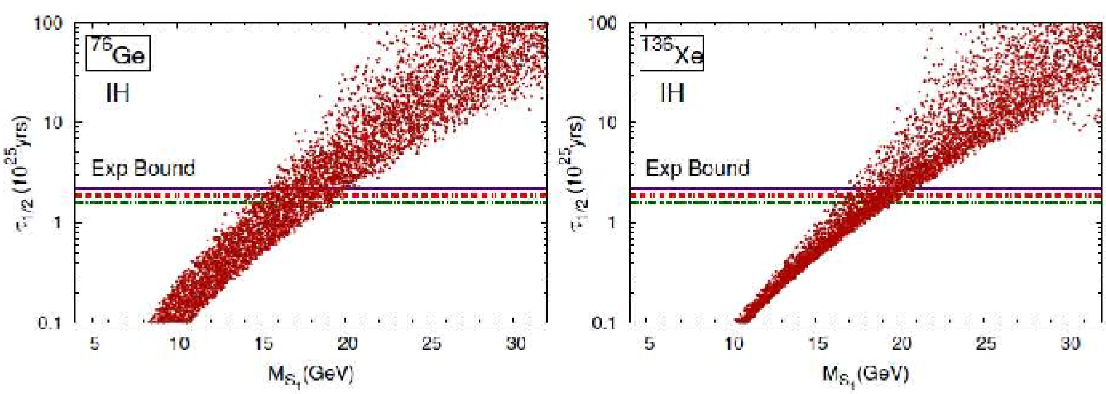

Figure 6.8: Same as Fig.6.7 but for inverted hierarchy (IH) of light neutrino masses.

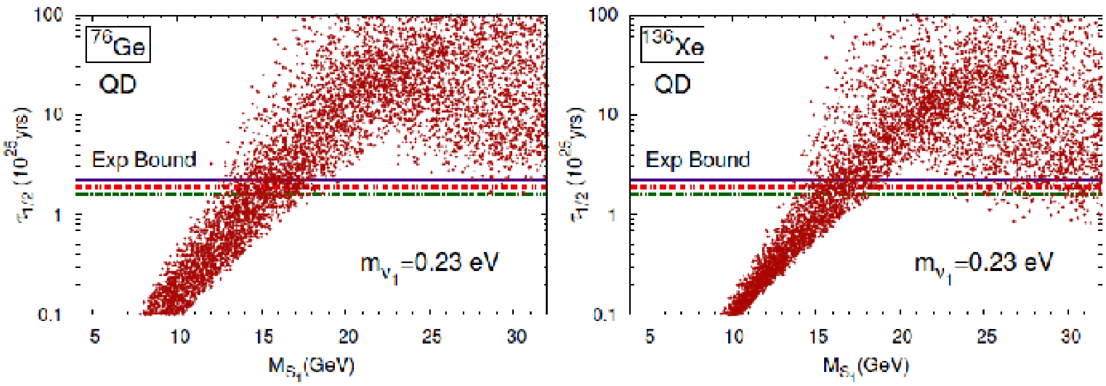

Figure 6.9: Same as Fig.6.7 but for quasi degenerate (QD) type light neutrino masses.

exchange amplitude and the sterile neutrino exchange amplitude is shown by the two peaks. When CP phases associated with the Majorana type sterile neutrino mass eigen value(s) are included, the peaks are smoothened as shown by dotted lines [88].

6.2.5 Sterile neutrino mass prediction from double beta decay half-life

In Fig.6.11 estimations on the lightest sterile neutrino masses are predicted which saturate the current experimental limit on the observed double beta decay half life using Ge−76 and Xe−136 nuclei for three different light neutrino mass hierarchies in each case. The uncertainties in the predicted masses correspond to the existing uncertainty in the neutrino virtuality momentum $|p| = 120 - 200$ MeV. The green horizontal line represents the average value

$$\hat{m}_{S_1} = 18 \pm 4 \quad \text{GeV}, \tag{6.22}$$

of the lightest sterile neutrino mass determined from double beta decay experimental bound [88]. Lower values of this mass has been obtained using light neutrino assisted type-II seesaw dominance [208].

These predictions suggest that sterile neutrino exchange contribution dominates the double beta decay rate even when the light neutrino masses have NH or IH type of mass hierarchies. To predict double beta decay saturating the current experimental bounds, it is not necessary that light neutrinos should be quasi-degenerate in mass.

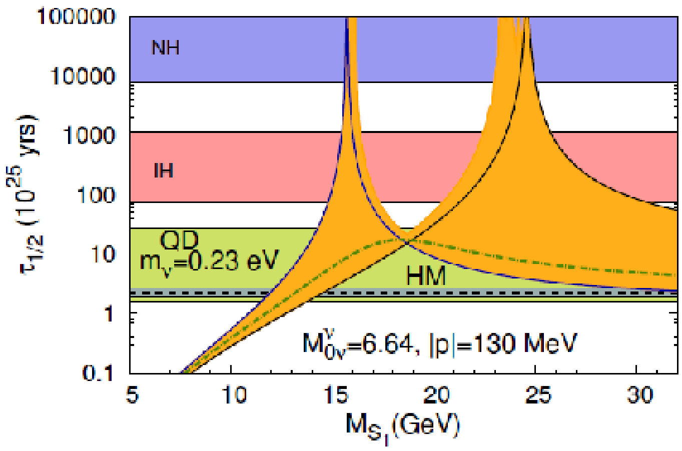

Figure 6.10: Prediction of half-life for double beta decay as a function of sterile neutrino mass in the case of QD type mass hierarchy with the common mass parameter $m_0 = 0.23$ eV. The peaks correspond to cancellation between light neutrino and sterile neutrino exchange amplitudes when Majorana CP phases of sterile neutrino is ignored. The dotted line shows the absence of peaks when CP phases are included [88]

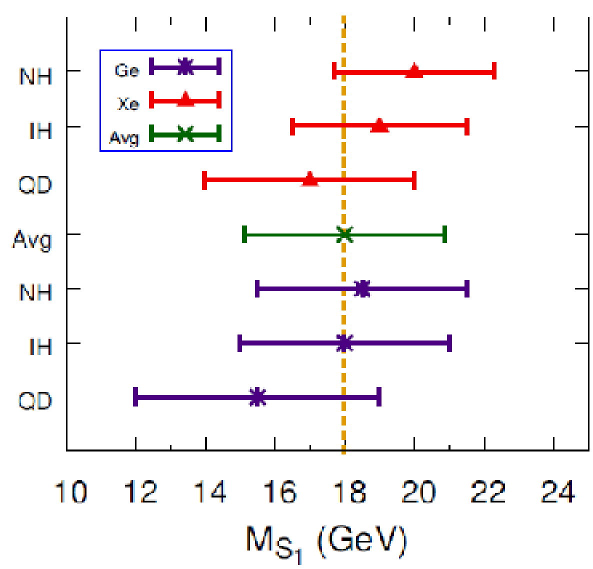

Figure 6.11: Prediction of light sterile neutrino mass from the saturation of experimental decay rates of ongoing searches for different active neutrino mass hierarchies. The horizontal green line indicates the average value of all results.

On the other hand if double-beta decay is not found with half-life close to the current limits, then the solutions with light sterile neutrino masses in the range $\sim (2-15)$ GeV are ruled out, but the model with larger mass eigen values easily survives.

6.3 Leptogenesis

6.3.1 Singlet fermion assisted resonant leptogenesis in non-SUSY SO(10)

An extensive review of thermal leptogenesis with reference to LFV is available in [347]. With the neutrino mass following a modified type-I seesaw at a scale $\geq 10^8$ GeV, thermal leptogenesis has been investigated. It is well known that TeV scale RH neutrinos can participate in resonant leptogenesis contributing to enhanced generation of leptonic CP-asymmetry that is central to generation of baryon asymmetry of the universe via sphaleron interactions. The experimental value of baryon asymmetry of the universe is $8.66 \pm 11 \times 10^{-11}$ [348]. Here we briefly discuss a recent work [208] where quasi-degenerate sterile neutrinos at the TeV scale in non-SUSY SO(10) have been shown to achieve resonant leptogenesis through their decays. The Feynman diagrams at the tree level and with vertex and self energy corrections are shown in Fig.6.12.

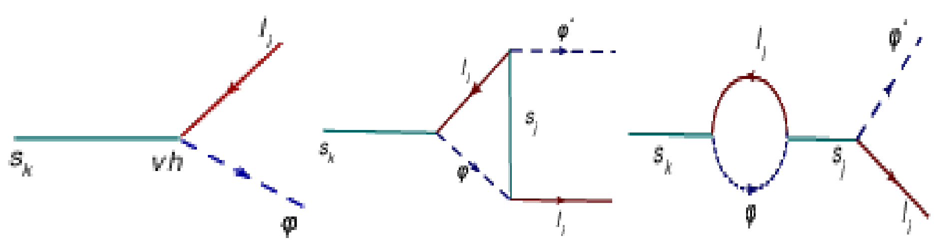

Figure 6.12: Tree and one-loop diagrams for the S_k decay contributing to the CP-asymmetry. All fermion-Higgs couplings in the diagrams are of the form Vh where $h = N - l - \Phi$ Yukawa coupling and $V \simeq M/M_N$.

The CP-asymmetry formula for the resonant leptogenesis is [208]

$$\varepsilon_{S_k} = \sum_j \frac{\mathcal{I}m[(y^\dagger y)^2_{kj}]}{|y^\dagger y|_{jj}|y^\dagger y|_{kk}} R_{kj}, \quad (6.23)$$

where

$$R_{kj} \;=\; \frac{(\hat{m}^2_{S_k} - \hat{m}^2_{S_j})\hat{m}_{S_k}\Gamma_{S_j}}{(\hat{m}^2_{S_k} - \hat{m}^2_{S_j})^2 + \hat{m}^2_{S_k}\Gamma^2_{S_j}}\,, \tag{6.24}$$

$y = (M/M_N)h$, $h = M_D/V_{\rm wk}$, and $V_{\rm wk} \simeq 174$ GeV. This leads to the baryon asymmetry

$$Y_B \;\simeq\; \frac{\varepsilon_{S_k}}{200 K_k}, \tag{6.25}$$

where

$$K_k \;=\; \frac{\Gamma_{S_k}}{H(\hat{m}_{S_k})}, \tag{6.26}$$

In eq.(6.26) $H(\hat{m}_{S_k})$ is the Hubble parameter at temperature $\hat{m}_{S_k}$.

$$H(\hat{m}_{s_k}) = 1.66 g_*^{1/2}\frac{\hat{m}^2_{s_k}}{M_{Planck}}, \tag{6.27}$$

where $g_* \simeq 107$. In eq.(6.26) the singlet fermion decay width is

$$\Gamma_{s_k} = \frac{1}{8\pi}\hat{m}_{s_k}(y^+ y)_{kk} \tag{6.28}$$

Defining

$$\delta_i = \frac{|\hat{m}_{S_i} - \hat{m}_{S_j}|}{\Gamma_{S_i}}(i \neq j), \tag{6.29}$$

the depleted washout factor is [349]

$$K_i^{\rm eff} \simeq \delta_i^2 K_i. \tag{6.30}$$

Here we discuss two cases for the sterile neutrino contribution towards leptogenesis and baryon asymmetry: (a) $\hat{m}_{s_1}$ is light, $\hat{m}_{s_2}$ and $\hat{m}_{s_3}$ are quasi-degenerate; (b) $\hat{m}_{s_2}$ is light, $\hat{m}_{s_1}$ and $\hat{m}_{s_3}$ are quasi-degenerate.

Case (a). $\hat{m}_{s_1}$ light, $\hat{m}_{s_2}$ and $\hat{m}_{s_3}$ heavy and quasi-degenerate.

Using an allowed interesting region of the parameter space $M \simeq \text{diag.}(146, 3500, 3500)$

m_{s_1} (GeV)	m_{s_2} (GeV)	m_{s_3} (GeV)	Baryon asymmetry	$T^{0\nu}_{1/2}$ ($10^{25} yrs.$)
1	500	500	8.0×10^{-11}	2.72
10	500	500	8.1×10^{-11}	16.01
500	1	500	8.1×10^{-11}	0.0494
500	3	500	8.2×10^{-11}	2.19

Table 6.3: Predictions for baryon asymmetry and double-beta decay half-life as a function of sterile neutrino masses.

GeV, $V_R = 10^4$ GeV, and $M_N = f V_R$ we get

$$\hat{m}_{S_i} = \text{diag.}(1.0, 595.864.., 595.864..)\text{GeV}, \quad (6.31)$$

leading to $K_2 = 4.0 \times 10^7$. Using $(\hat{m}_{S_2} - \hat{m}_{S_3}) \simeq 4 \times 10^{-7}$ GeV, we obtain

$$\begin{aligned} \varepsilon_{S_2} &= 0.512, \\ Y_B &= 8.0 \times 10^{-11}. \end{aligned} \quad (6.32)$$

Case (b) $\hat{m}_{s_2}$ light, $\hat{m}_{s_1}$ and $\hat{m}_{s_3}$ heavy and quasi-degenerate.

Choosing another allowed region of the parameter space $M \simeq \text{diag.}(3200, 146, 3200)$ GeV, similarly we get

$$\hat{m}_{S_i} = \text{diag.}(500.567.., 1.0, 500.567..)\text{GeV}, \quad (6.33)$$

leading to $K_1 = 8 \times 10^6$. Using $(\hat{m}_{S_1} - \hat{m}_{S_3}) \simeq 9 \times 10^{-5}$ GeV, we obtain

$$\begin{aligned} \varepsilon_{S_1} &= 0.128, \\ Y_B &= 8.1 \times 10^{-11}. \end{aligned} \quad (6.34)$$

In Case (a) with $\hat{m}_{S_1} \sim \mathcal{O}(1)$ GeV, the lightest sterile neutrino acts as the most dominant source of $0\nu\beta\beta$ decay whereas the heavy quasi-degenerate pair of sterile neutrinos S_2 and S_3 mediate resonant leptogenesis. Similarly in the alternative scenario of Case (b) with $\hat{m}_{S_2} \sim \mathcal{O}(1)$ GeV, the second generation light sterile neutrino acts as the mediator of dominant double beta decay while the heavy quasi-degenerate pair of the first and the third generation sterile neutrinos mediate resonant leptogenesis. Because of the resonant leptogenesis constraint, we note that either Case (a) or Case (b) is permitted, but not both.

Our predictions for the double beta decay half-life and the baryon asymmetry in Case (a) and Case (b) are presented in Table .6.3. It is clear that for smaller mass eigen values of sterile neutrinos in Case (a) or Case (b), it is possible to saturate current experimental limit on the double-beta decay half-life while explaining the right order of magnitude of the baryon asymmetry. Thus, in addition to the Case (a) found in ref. [208], we have shown another possible alternative scenario as Case (b).

Before concluding this section certain interesting results on thermal leptogenesis derived earlier are noted. Thermal leptogenesis with a hybrid seesaw and RH neutrino dark matter have been proposed by introducung additional $U(1)$ gauge symmetry [201]. Thermal leptogenesis in extended seesaw models have been investigated earlier [198, 350–353] which are different from our cases reported here and earlier [184, 208]. Possibilities of falsyfying high-scale leptogenesis on the basis of certain LHC results and also on the basis of LFV and $0\nu\beta\beta$ decay results have been suggested [354, 355] . Prospects of dark matter in the minimal inverse seesaw model has been also investigated in ref. [356, 357]

6.3.2 Resonant leptogenesis with light NH masses

As noted earlier, the motivation for this analysis is based upon the possibility that light neutrino masses may be NH type rather than QD type as suggested from recent cosmological bound [336] with

$$\sum m_\nu \quad < \quad 0.15\text{eV}, \tag{6.35}$$

and more stringent bound [358]

$$\sum m_\nu \quad < \quad 0.12\text{eV}. \tag{6.36}$$

Although such cosmological bounds may need further confirmation by laboratory experiments on earth, it is worth while to see if our models may be able to account for BAU even if NH hierarchy is adopted.

We have choose an interesting region of the parameter space $M \simeq \text{diag.}(38.27, 752.1, 1219.0)$ GeV. Then using the RH neutrino mass matrix M_N derived in ref. [208] in the NH case, we get

$$\hat{m}_{S_i} \quad = \quad \text{diag.}(1.2, 1348.86.., 1348.86...)\text{GeV}. \tag{6.37}$$

containing the desired mass patterns. In this case using eq.(6.28), we have derived the two decay widths

$$\Gamma_{S_3} = 8.63\text{GeV}, \tag{6.38}$$

$$\Gamma_{S_2} = 0.009\text{GeV}. \tag{6.39}$$

Noting the corresponding value of the Hubble parameter

$$H(\hat{m}_{S_3}) = 2.91 \times 10^{-12}\text{GeV}, \tag{6.40}$$

the washout factor due to the S_3 decay is estimated using eq.(6.26)

$$K_3 = 2.96 \times 10^{12}. \tag{6.41}$$

Using $|\hat{m}_{S_2} - \hat{m}_{S_3}| \simeq 0.003$ GeV and eq.(6.23), the CP-asymmetry

$$\varepsilon_{S_3} \quad = \quad 0.00583. \tag{6.42}$$

Using eq.(6.29), we have calculated damping factor or the depletion factor for this large washout

$$\delta_3 = 0.0003. \tag{6.43}$$

Leading to the effective washout factor through eq.(6.30)

$$K_{eff} = 405367. \tag{6.44}$$

With this depleted washout, the baryon asymmetry formula of eq.(6.25) that turns to be

$$Y_{BD} \quad \simeq \quad \frac{\varepsilon_{S_k}}{200 K_{eff}}. \tag{6.45}$$

gives

$$Y_B \quad = \quad 8.0 \times 10^{-11}. \tag{6.46}$$

With the value of $\hat{S}_1$ mass given in eq.(6.37) we have verified that the double beta decay lifetime is predicted with a value close to the current experimental limit.

Thus we have shown that for NH pattern of light neutrino masses that favours the recent cosmological bound [336], a light sterile neutrino mass ~ 1.2 GeV allowed in both the $SO(10)$ models mediates dominant double beta decay. In this case resonant leptogenesis is implemented by a pair of quasi-degenerate heavy masses $\simeq 1348.86$ GeV of the sterile neutrinos of the second and the third generations which is also permitted within the allowed parameter space. In this case also the scaling law of eq.(5.21) can be applied to examine the validity of resonant leptogenesis for a wider range of Z' boson masses. In the next two sections we have shown how the lightest sterile neutrino mediates displaced vertices for like-sign dilepton production in the channels $pp \to eejj$ and $pp \to \mu\mu jj$ at LHC.

6.3.3 Leptogenesis in extended MSSM and SUSY SO(10)

In the conventional type-I seesaw based leptogenesis models where heavy RH neutrino decays give rise to the desired lepton asymmetry [359], the Davidson-Ibarra bound [360, 361] imposes a lower limit on the scale of leptogenesis, $M_{N_1} > 4.5 \times 10^9$ GeV [360, 361]. This also suggests the lower bound for the reheating temperature after inflation, $T_{RH} \geq 10^9$ GeV, that would lead to overproduction of gravitinos severely affecting the relic abundance of light nuclei since the acceptable limit has been set as $T_{RH} \leq 10^7$ GeV [362]. Several attempts have been made to evade the gravitino constraint on leptogenesis where sterile neutrino assisted results are interesting. Obviously gravitino constraint is satisfied in models with TeV scale resonant leptogenesis [363]. Also in the singlet fermion extended SUSY SO(10) where RH neutrinos are heavy pseudo Dirac neutrinos and neutrino mass formula is through inverse seesaw [212], there is no problem due to gravitino constraint [83–85, 292]. We discuss the cases where all the three types of neutrinos are Majorana fermions.

6.3.4 Leptogenesis with extended seesaw dominance

With extended seesaw realisation of leptogenesis in two types of SUSY models have been investigated under gravitino constraint:(i)MSSM extension with fermion singlets [234–238], and (ii) Singlet extension of SO(10) with intermediate scale G_{2213} gauge symmetry. [239, 240]. We discuss their salient features.

6.3.4.1 MSSM extension with fermion singlets

The Dirac neutrino mass matrix is identified with the charged lepton mass matrix in this model where MSSM is extended with the addition of heavy RH neutrinos N_i as well as additional singlets S_i [234,235], one for each generation. As already explained in the limit $M_N > M >> M_D, \mu_S$ extended seesaw formula, which is the same as the inverse seesaw formula for active neutrino mass. In this case resonant leptogenesis is implemented via quasi-degenerate RH neutrino decays at the TeV scale. It is well known that such resonant leptogenesis scenario with $M_{N_1} \sim M_{N_2} \sim 1$ TeV implemented through canonical seesaw, needs a very small mass splitting between the RH neutrinos $\frac{(M_{N_2}-M_{N_1})}{(M_{N_2}+M_{N_1})} \sim 10^{-6}$. With the the tension arising out of fitting the neutrino oscillation data being transferred from type-I seesaw to extended seesaw in the presence of additional sterile fermions, it is not unimaginable that this fine tuning associated with very tiny RH neutrino mass splitting could be adequately alleviated. The fermion singlets S_i give rise to a new self-energy contribution and using this successful resonant leptogenesis has been found to be possible for a much larger mass ratio $\frac{M_{N_2}}{M_{N_1}} \sim 10$. Possibilities of ~ 100 MeV to ~ 10 GeV mass range for light sterile neutrinos have been pointed out. In a separate analysis the possibility of singlet Majorana fermion or singlet scalar as candidates of dark matter has been pointed out [236]. Realisation of doubly coexisting dark matter candidates in the context of extended seesaw framework has been pointed out [237].

6.3.4.2 Leptogenesis in SUSY SO(10)

In non-SUSY minimal LR models where M_D is similar to charged lepton mass matrix successful leptogenesis emerges with intermediate scale hierarchical RH neutrino masses [364]. In SUSY SO(10) the underlying quark-lepton unification forces the Dirac neutrino mass to be similar to the up-quark mass matrix. This pushes the type-I seesaw scale closer to the GUT scale, $M_R \geq 10^{14}$ GeV and rules out the possibility of low scale W_R bosons accessible to accelerator searches in foreseeable future unless the canonical seesaw ansatz is given up, for example, in favour of inverse seesaw with TeV scale pseudo Dirac neutrinos and W_R bosons [83–85, 292]. With heavy right-handed Majorana neutrinos and GUT-scale LR breaking scale, successful leptogenesis has been implemented in realistic SUSY SO(10) [365]. With the help of an effective dim.5 operator ansatz which originates from renormalisable interactions at GUT-Planck scale in SUSY SO(10) (without using 126_H) both thermal and non-thermal leptogenesis [367–369] have been discussed with heavy hierarchical RH neutrino masses [370,371]. Possible solutions to the allowed parameterspace to evade gravitino constraint have been also discussed in this work.

Apart from the models with resonant leptogenesis, possibility of leptogenesis under gravitino constraint in SUSY SO(10) has been realised with hierarchical RH neutrinos assisted by sterile neutrinos. As already noted above, in these cases the extended seesaw formula controls the neutrino mass as a result of cancellation of type-I seesaw contribution. Gauge coupling unification in these SO(10) models requires the G_{2213} symmetry to occur at the intermediate scale in the renormalizable model [240]. A common feature of both these models [239, 240] is the generation of lepton asymmetry through the decay of hierarchical sterile neutrinos through their respective mixings with heavier RH neutrinos which are also hierarchical.

An important and specific advantage of heavy gauge-singlet neutrino decay to achieve leptonic CP asymmetry is the following: The singlet neutrino of mass $\sim 10^5$ GeV which decays to $l\phi$ though its mixing with RH neutrino of mass $\sim 10^{10}$ GeV has a small mixing angle $\sim 10^{-5}$. This small mixing ensures out-of-equilibrium condition by making the decay rate smaller than the Hubble expansion rate in arriving at CP asymmetry at lower temperatures ~ 300 GeV.

Chapter 7

Sterile Neutrino Mediated Dilepton Events with Displaced Vertices, and its Collider Phenomenology

In our type-II seesaw dominant model production in SO(10) discussed in earlier chapters, both the Z' boson and the right handed neutrino are present at TeV scales. Quite recently, as an interesting and novel manifestation of Majorana type of RH neutrino that drives type-I seesaw, it has been pointed out that if W_R boson is at the TeV scale and a RH neutrino mass needed for the seesaw is sufficiently light, it would mediate $0\nu\beta\beta$ decay while like-sign di-electron signals caused due to displaced vertices mediated by the RH neutrino mass in the range $1-80$ GeV would provide more interesting model signatures through $eejj$ events devoid of standard model backgrounds [182, 372] without missing energy. It is worthwhile to point out that the mechanism of like sign dilepton production at accelerators was at first suggested by Keung and Senjanovic [373]. Then these like-sign di-electron signals and $0\nu\beta\beta$ decay events would indicate the presence of the gauge theory at the TeV scale. Even if there is no W_R gauge boson at the TeV scale, this approach predicts the novel possibility of like-sign dilepton events which can be observed at ATLAS or CMS detectors. In such a type-I seesaw model as the associated RH neutrino is sufficiently light, it is necessary to fine-tune the associated Dirac neutrino Yukawa coupligs to small values, $10^{-7}-10^{-6}$ to fit the neutrino oscillation data. Secondly, it may be difficult to implement TeV scale resonant leptogenesis for which two quasi-degenerate heavy masses of RH neutrinos of two other generations may be needed and this possibility needs further investigation. Also such a single RH neutrino model may not adequately mediate detector events at CMS or ATLAS in the channels $pp \to \mu\mu jjX$, or $pp \to e\mu jjX$ for which much heavier RH neutrino masses appear to be needed. In addition, the heavy-light neutrino mixings in this model can be anywhere bounded by the DELPHI [374] and the double beta decay experimental limits.

In this chapter we discuss how the two non-SUSY $SO(10)$ models discussed in our paper [208], as indicated by eq.(5.36) and eq.(5.37), predict a rich structure of like-sign di-electron and di-muon events with displaced vertices at LHC detectors along with dominant contributions to double beta decay. These can materialise when the prevailing LFV constraints and heavy RH neutrino masses allow one of the singlet fermions ($\equiv$ sterile neutrinos) to be sufficiently light. In contrast to models along this line including those of ref. [182, 372] where heavy -light neutrino mixings are assumed under the DELPHI [374] and the double beta decay constraints , these mixings in our models are predicted from all charged fermion mass fit at the GUT scale and the LFV constraints. The Dirac neutrino mass matrix derived in this manner serves as important ingredient for predictions of LFV, LNV, and dilepton production events. Two different cases have been identified. In the Case (a)while the light sterile neutrino S_1 of first generation mediates dominant contribution to double beta decay and like-sign dilepton events with displaced vertices in the channels $eejj$, $e\mu jj$, and $\mu\mu jj$, resonant leptogenesis is allowed to be mediated by heavy quasi-degenerate sterile neutrino pairs S_2 ans S_3 belonging to the second and the third generations. Identified as the alternative Case (b), dominant double beta decay and dilepton events with displaced vertices are mediated by the allowed lighter mass of S_2 while resonant leptogenesis is mediated by the heavy quasi-degenerate sterile neutrino pairs, S_1 and S_3. We also explore detection possibilities of the extra Z' boson predicted by these two models at the Large Hadron Collider (LHC) and the International Linear Collider (ILC). We further predict heavy RH Majorana neutrino production cross sections through the like-sign dilepton production at the LHC detectors in the $W_L - W_L$ channel.

In Sec.7.1 below we have discussed heavy-light neutrinos mixings and predictions for new physics effects. In Sec.7.2 we have discussed dilepton signals with displaced vertices. Dilepton signature of RH neutrinos is discussed in Sec.7.3. In Sec.7.4 we have discussed the collider phenomenology of Z' boson.

7.1 Heavy-light neutrinos mixings and predictions for new physics effects

We mention briefly how the matrix elements for $\nu - S$ and $\nu - N$ mixings have been derived from all charged fermion mass fits at the GUT scale and by utilising $N - S$ mixing matrix M from LFV constraint and the M_N matrix from fits to neutrino oscillation data.

(i) The $\nu - S$ mixing:

In predicting the LFV branching ratios we have used the simplifying diagonal structure for the $N - S$ mixing matrix M,

$$M = \text{diag.}\ (M_1, M_2, M_3), \tag{7.1}$$

As shown in eq.(5.26), the Dirac neutrino mass matrix resulting from charged fermion mass fit at the SO(10) unification scale is

$$M_D(M_{R^0}) = \begin{pmatrix} 0.014 & 0.04 - 0.01i & 0.109 - 0.3i \\ 0.04 + 0.01i & 0.35 & 2.6 + 0.0007i \\ 0.1 + 0.3i & 2.6 - 0.0007i & 79.20 \end{pmatrix} GeV. \tag{7.2}$$

Noting that out ν-s mixing matrix [208]

$$V^{\nu s} = \frac{M_D}{M}, \tag{7.3}$$

using eq.(7.1) and eq.(5.26) in eq.(7.3) we get the elements of the $\nu_l - S$ mixing matrix

$$V^{(lS)} = \begin{pmatrix} M_{De1}/M_1 & M_{De2}/M_2 & M_{De3}/M_3 \\ M_{D\mu1}/M_1 & M_{D\mu2}/M_2 & M_{D\mu3}/M_3 \\ M_{D\tau1}/M_1 & M_{D\tau2}/M_2 & M_{D\tau3}/M_3 \end{pmatrix}. \tag{7.4}$$

(ii) The $\nu - N$ mixing matrix:

Similarly the $\nu - N$ mixing matrix, for generalised class of non-diagonal matrices M_D and M_N can be written as

$$V^{\nu s} = \frac{M_D}{M_N}, \tag{7.5}$$

$$V^{(lN)} = \begin{pmatrix} (M_D/M_N)_{e1} & (M_D/M_N)_{e2} & (M_D/M_N)_{e3} \\ (M_D/M_N)_{\mu 1} & (M_D/M_N)_{\mu 2} & (M_D/M_N)_{\mu 3} \\ (M_D/M_N)_{\tau 1} & (M_D/M_N)_{\tau 2} & (M_D/M_N)_{\tau 3} \end{pmatrix}. \tag{7.6}$$

Using eq.(5.26) and eq.(5.14) we find that, in the case of NH masses of light active neutrinos, the elements of the $\nu - N$ mixing matrix are

$$V^{(lN)} = \begin{pmatrix} -0.7+2i & 0.16-0.26i & 0.98-2.01i \\ -13.31-16.76i & 8.1-11.52i & 15.94+3.409i \\ -718-492i & -46-352i & 510+141i \end{pmatrix} \times 10^{-4} \tag{7.7}$$

As we discuss in Sec.7.2 and Sec.7.3, these mixings are needed to predict dilepton signals with displaced vertices (DLSD) in the $W_L - W_L$ channel mediated by lighter sterile neutrinos and like-sign dilepton production cross sections mediated by heavy RH neutrinos in the channel $pp \to l^\pm l^\pm jjX$ at different LHC energies.

7.2 Dilepton signals with displaced vertices

In the first part of this section we discuss decay width, half-life, and displaced lengths of sterile neutrinos. In the second part we make predictions on DLSD events in our models.

7.2.1 Decay width, half-life, and displaced lengths

The Feynman diagram for the production of like-sign dileptons along with two jets in the $W_L - W_L$ channel is given in Fig.(7.1). When the RH Majorana neutrino has mass near the TeV scale or heavier and very short lifetime and path length, almost instantly it mediates like sign dilepton (LSD) production events some of which have been observed at the LHC detectors [375]. The standard model background is a major source of uncertainty in identifying such events. But when the mass of the sterile neutrino ($\equiv$ singlet fermion) is $\mathcal{O}(1-10)$ GeV and its mixing with active light neutrinos is small, then it is expected to cause DLSD events with negligible standard model background uncertainties and with no missing energy [182, 376, 378–383]. If the neutrino transverse decay length lies between 1 mm and 1 m, a DLSD signal could be recorded at ATLAS or CMS [379]. As already explained in Sec.7.1, because of the $SO(10)$ model predictions of heavy-light mixing matrix elements $V_{ei}, V_{\mu i}$ $(i = 1, 2)$, either S_1 or S_2 could be capable of mediating the displaced vertices resulting in the

like-sign dilepton events $eejj$, $\mu\mu jj$, and $e\mu jj$ provided that the signal strength is strong enough under different cut conditions.
The decay width of the i-th light sterile neutrino $S_i(i = 1$ or $2)$ which would be required in estimating collider signals is defines as [182, 372, 377]

$$\Gamma_{S_i} = \frac{3G_F^2}{32\pi^3} m_{s_i}^5 \sum_l |V_{ls_i}|^2, \tag{7.8}$$

where $G_F =$ Fermi coupling constant and V_{ls_i} is the element of $\nu - s$ mixing matrix defined through eq.(7.4).

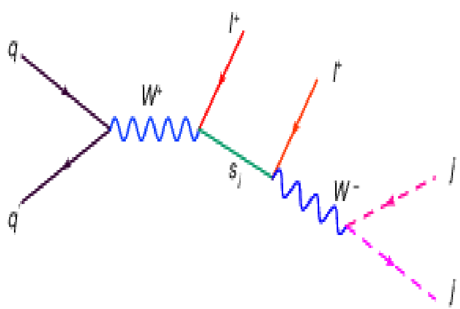

Figure 7.1: Feynman diagram for like-sign dilepton production process $l^{\pm}l^{\pm}jj$ in the $W_L - W_L$ channel in the pp collision process at LHC

At LHC the sterile neutrino ($\equiv$ singlet fermion) mediated dilepton production cross section can be expressed in terms of bare cross section and heavy-light mixing [377]

$$\begin{aligned} \sigma(pp \to Sl^{\pm} \to l^{\pm}l^{\pm}jj) &= (2 - \delta_{l1l2}) S_{l1l2} \sigma_0(S), \\ S_{l_1 l_2} &= \frac{|V_{l_1 s} V_{l_2} s|^2}{\sum_{l=e,\mu,\tau} |V_{ls}|^2}, \end{aligned} \tag{7.9}$$

where $l = e$ or μ and $\sigma_0(S)$ is the bare cross section arising out of the exchange of the sterile neutrino S. In addition to ref. [377], the cross section has been also estimated in ref. [182] and the two sets of results have been found to agree. The number of events within the displaced length limit can be defined through the formula [372]

$$\begin{aligned} N &= \mathcal{L} \times \sigma(pp \to Sl^{\pm} \to l^{\pm}jj) \times A_{CUT} \times PN, \\ PN &= e^{-d_1/L} - e^{-d_2/L}, \end{aligned} \tag{7.10}$$

where $\mathcal{L}$ is the beam luminosity, A_{CUT} = Acceptance factor under a cut condition [384], L = sterile neutrino decay length defined below, PN = probability of the sterile neutrino to decay within the distances between d_1 and d_2. For example we have chosen below $d_1 = 10^{-3}$ m and $d_2 = L = 1$ m to compute the predicted events via displaced vertices. Thus the number of events decreases considerably due to the imposition of the cut, smallness of heavy-light mixings, and the factor PN. The cut acceptance factor has been estimated which can be easily inferred from Fig.1 and Fig.2 of ref. [182].

In our Model-I and Model-II, the heavy light mixings as well as the sterile neutrino masses are predicted by the underlying mechanism in $SO(10)$. We investigate how these model predictions are accommodated in the almost model-independent approach of ref. [182]. We also predict the number of events that can be produced through displaced vertices in other channels like $e\mu jj$, $\mu\mu jj$, and $e\tau jj$. In each case considered within our models, in addition to the lightest sterile Majorana neutrino of mass $\sim \mathcal{O}(1)$ GeV, there are two sterile neutrinos and three RH Majorana neutrinos all of which have masses $\sim \mathcal{O}(1)$ TeV or larger. Thus compared to the lightest sterile neutrino exchange, all other contributions to the dilepton production are treated as negligible. This assumption is consistent with the results of ref. [377] which predict very large (very small) cross sections for very light (very heavy) sterile neutrino mass.

Using eq.(7.8) we have the corresponding half-life $\tau_{S_i} = \Gamma^{-1}_{S_i}$. For average energy E_i of the i-th sterile neutrino, taking into account the time-dilatation factor $\bar{\gamma}_i = E_i/\hat{m}_{s_i}$ on the half life, the boosted decay length is

$$\begin{aligned} L &= c\bar{\gamma}_i\tau_{s_i} \\ &= 4875\bar{\gamma}_i(\frac{GeV}{\hat{m}_{S_i}})^5\frac{10^{-7}}{|V_{ls_i}|^2}. \end{aligned} \tag{7.11}$$

For large transverse momentum value compared to mass

$$\bar{\gamma}_i \sim |\vec{p}^{\,T}_{S_i}|/\hat{m}_{S_i}, \tag{7.12}$$

and the formula of eq.(7.11) reduces to the one given in ref. [379].

We find from eq.(7.11) that for a given average value of E_i, the decay length L and $\bar{\gamma}_i$, the plot $\log(|V^2_{ls_i}|)$ vs. $\log(\hat{m}_{S_i})$ gives a straight line curve with a negative slope and curves with four different values of $L = 1$mm, $L = 0.01, 0.1$ m and 1 m yield four parallel straight lines where the upper most (lower most) one correspond to the smallest (largest) of the four lengths. But in the $\log(|V_{lS_i}^2|)$ vs. $\hat{m}_{S_i}$ plot, i,e in the semi-logarithmic plot, instead of straight lines, the corresponding curves appear with concavity towards the right-hand side as shown in Fig.7.2. The pink coloured shaded region indicates the parameter space for which at most five dilepton events are observable at LHC.

We follow the strategy of ref. [182] in showing the constraints due to various cut conditions. The dashed lines of Fig.7.2 are the superposed images of the corresponding lines of Fig.1(a) signifying different cut conditions imposed upon the primary and the secondary leptons but without imposing any cut on the two jets. Fig.7.3 is drawn in a similar fashion as Fig.7.2 but they carry the superimposed images of dashed lines of Fig.1(b) of ref. [182] where both leptonic and jet cut conditions have been imposed.

The two solid lines in each of Fig.7.2 and Fig.7.3 are the upper and lower limits of experimental measurements on double beta decay half life. The upper most green coloured line in both the figures represent the experimental limit from DELPHI [374] measurement.

Fixing the expected number of events as ≤ 5 for the luminosity $\mathcal{L} = 300\text{fb}^{-1}$ and noting the limiting value of heavy-light mixing V_{lS_i} to which the LHC measurement would be sensitive under a given cut condition as displayed in Fig.7.2 or Fig.7.3, we estimate the value of A_{CUT} using the results of ref. [377], the formula of eq.(7.9) and eq.(7.10) for each value of mass $\hat{m}_{S_i}$ in the intersection region of the dashed line and the pink coloured region. Since the estimated bare cross cross section is almost constant over the range of $\hat{m}_{S_i}$ within the shaded region, the values of A_{CUT} obtained for different points are nearly equal.

Thus using the computational results [182, 377], luminousity $\mathcal{L} = 300fb^{-1}$ and $p_T^{e_1} > 30$ and $|\eta^e| < 2.5$, the values are $A_{CUT} \simeq 1, 0.1, 0.01$ and 0.001 for $p_T^{e_2} > 7$ GeV, $p_T^{e_2} > 30$ GeV, $p_T^{e_2} > 35$ GeV, and $p_T^{e_2} > 45$ GeV, respectively. For the same luminosity, $p_T^{e_1}$, $p_T^{e_2} > 7$ GeV, and $|\eta^{e,j}| < 2.5$, the derived values are $A_{CUT} \simeq 0.05, 0.1, 0.003$ and 0.001 for $p_T^j = 10$ GeV, $p_T^j = 10$ GeV, $p_T^j = 15$ GeV, and $p_T^j = 20$ GeV, respectively. Fixing $p_T^j > 15$ GeV and $|\eta^{e,j}| < 2.5$ for $p_T^{e_1} > 30$ GeV, and $p_T^{e_2} > 7$ GeV gives $A_{CUT} \simeq 0.005$ for the three values of the luminosity $\mathcal{L}$ =50 fb^{-1}, 300 fb^{-1}, and $3000fb^{-1}$ corresponding to $|V_{ls}|^2 = 10^{-5}, 10^{-6}$, and 10^{-7}, respectively.

In what follows we we will use these numerical results on A_{CUT} to make predictions in our models in different channels where the sterile neutrino masses and heavy-light mixings are predicted by the two SO(10) models.

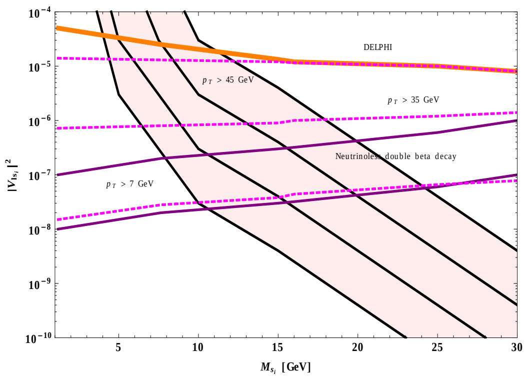

Figure 7.2: Constraints on active-sterile neutrino mixings including DELPHI and neutrinoless double beta decay limits. The lower-most solid line of the pink colored shadow region having upward concavity corresponds to $L = 1$ m and the upper-most line corresponds to $L = 0.001$ m where the displaced vertex search at LHC is expected to be sensitive. The dashed lines correspond to different p_T cuts: $p_T^{e_1} > 40$ GeV, $p_T^{e_2} > 7$ GeV, $p_T^{e_1} > 40$ GeV, $p_T^{e_1} > 45$ GeV and $|\eta^e| < 2.5$ with luminosity $300 fb^{-1}$. The two lower solid curves with positive slopes indicate the double beta decay limits.

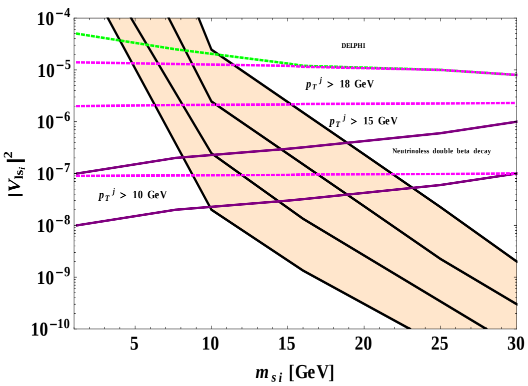

Figure 7.3: Constraints on active-sterile neutrino mixings including DELPHI and neutrinoless double beta decay limits. The lower-most solid line of the pink colored shadow region having upward concavity corresponds to $L = 1$ m and the upper-most line corresponds to $L = 0.001$ m where the displaced vertex search at LHC is expected to be sensitive. The dashed lines correspond to different p_T cuts: $p_T^{e_1} > 30$ GeV, $p_T^{e_2} > 7$ GeV, $p_T^{j} >$10, 15, and 18 GeV and $|\eta^{e,j}| < 2.5$ with luminosity $300 fb^{-1}$. The two lower solid curves with positive slopes indicate the double beta decay limits.

7.2.2 Prediction of dilepton signals with displaced vertices

Utilising the formulas of eq.(7.9), eq.(7.10), and eq.(7.11) in Sec.7.2.1 we have identified in an almost model-independent manner, the allowed region in the $|V_{lS_i}|^2$ vs. $\hat{m}_{S_i}$ plane where detection of like-sign dilepton events with displaced vertices is possible. In this section we specify correlations of these model-independent results with the actual model parameters and observables allowed within Model-I and Model-II. An important point shown in this section is that the heavy-light mixings predicted by our Mode-I and Model-II based on $SO(10)$ which have been used to predict double beta decay life or leptogenesis as discussed above are noted to fall in the sensitive region of the model-independent search identified in Sec.7.2.1. The connection of dilepton events with resonant leptogenesis and BAU is noted for the first time in this work. These solutions are shown in Table 7.1, Table 7.2, and Table 7.3. In Table 7.1 assuming QD hierarchy of light neutrino masses as in Case (a) and fixing the value of $M = (142.548, 3521.91, 3259.1)$ GeV, we have obtained three sets of solutions for the mass eigen values of eq.(5.20) corresponding to three different values of $V_R = (10, 5, 3.3)$ TeV and $M_{Z'} = (5.95, 2.975, 1.963)$ TeV. These three sets predict the three different mass eigen values of the first generation sterile neutrino $\hat{m}_{S_1} = (5,\ 10,\ 15)$ GeV and for all these values the predicted modulus square of mixing is $|V_{es_1}^2| = 10^{-8}$. It can be clearly recognised from Fig.7.2 these are the desired solutions in the pink coloured shaded region where both dominant double beta decay and observable dilepton events with displaced vertices are predicted. In addition, since each set of solutions is associated with heavy quasi-degenerate sterile neutrino masses of the second and the third generations, resolution of the issue of BAU is also accommodated.

As the solutions reported in Table 7.1 do not conform to jet cut conditions, in Table 7.2 we report three sets of solutions corresponding to $\hat{m}_{S_2} = (5, 10, 15)$ GeV expected to mediate dominant double beta decay and observable dilepton events with displaced vertices for $|V_{es_2}^2| = 2 \times 10^{-7}$ which fall in the identified in the pink coloured shaded region of Fig.7.3. These solutions are consistent with the respective leptonic and jet cut conditions. Further a pair of quasi-degenerate heavy sterile neutrinos of first and the third generations would ensure BAU generation by resonant leptogenesis.

Quite interestingly, in the case of NH hierarchy of light neutrino masses consistent with recent cosmological bounds [336, 358], the solutions to parameter values corresponding to dominant double beta decay, BAU generation by resonant leptogenesis, and observable dielectron production through displaced vertices are shown in Table

7.3 which match with the corresponding pink coloured shaded region of Fig.7.3 in conformity with the desired cut conditions on leptons and jets.

Compared to the DLSD events in the channel $pp \to eejj$, those in the case of $pp \to \mu\mu jj$ are expected to be more prominent even at $\mathcal{L} = 50\text{fb}^{-1}$ because of the high value of the predicted quantity $|V_{\mu_{s_2}}|^2 = 10^{-5}$. Naturally for stronger luminosity like $\mathcal{L} = 300\text{fb}^{-1}$, the event rates are expected to be six times larger. Lower p_T cuts would further increase these event rates.

$\hat{m}_s$ (GeV)	V_R (GeV)	Events at $\mathcal{L}(300)$ (fb^{-1})	$M_{Z'}$ (TeV)
(5, 2805.6, 2805.6)	10^4	6	5.95
(10, 5611.2, 5611.2)	5×10^3	6	2.975
(15, 8501.9, 8501.9)	3.3×10^3	6	1.963

Table 7.1: Prediction of like sign dielectron events via displaced vertices in the $eejj$ channel as a function of sterile neutrino mass $\hat{m}_{s_1} = 5, 10,$ and 15 GeV for M = (142.548, 3521.91, 3259.1) GeV, v_L=0.5 eV in the QD case of light neutrino masses, momentum cut $p_T^{e_2} > 7$ GeV, $p_T^{e_1} > 30$ GeV, $|\eta^e| < 2.5$, $A_{CUT} = 1$, and $|V_{es_1}^2| = 10^{-8}$.

$\hat{m}_s$ (GeV)	V_R (GeV)	Events at $\mathcal{L}(300)$ (fb^{-1})	$M_{Z'}$ (TeV)
(2494.03, 5, 2494.03)	10^4	6	5.95
(4988.06, 10, 4988.06)	5×10^3	6	2.975
(7557.67, 15, 7557.67)	3.3×10^3	6	1.963

Table 7.2: Prediction of like sign dielectron events via displaced vertices in the $eejj$ channel as a function of sterile neutrino mass $\hat{m}_{s_2} = 5, 10,$ and 15 GeV for M = (3088.52, 142.37, 3294.86) GeV, v_L=0.5 eV in the QD neutrinos, momentum cut $p_T^{e_2} > 7$ GeV, $p_T^{e_1} > 30$ GeV, $p_T^j > 10$ GeV $|\eta^{e,j}| < 2.5$, $A_{CUT} = 0.05$, and $|V_{es_2}^2| = 2 \times 10^{-7}$.

$\hat{m}_s$ (GeV)	V_R (GeV)	Events at $\mathcal{L}(300)$ (fb^{-1})	$M_{Z'}$ (TeV)
(5, 5535.96, 5535.96)	10^4	6	5.95
(10, 11071.8, 11071.8)	5×10^3	6	2.975
(15, 16624.5, 16624.5)	3.3×10^3	6	1.963

Table 7.3: Prediction of like sign dielectron events via displaced vertices in the $eejj$ channel as a function of sterile neutrino mass $\hat{m}_{s_1}$ for M = (34.6726, 681.403, 1104.41) GeV, v_L=0.5 eV in the NH neutrinos, momentum cut $p_T^{e_2} > 7$ GeV, $p_T^{e_1} > 30$ GeV, $p_T^j > 10$ GeV, $|\eta^{e,j}| < 2.5$, $A_{CUT} = 0.05$, and $|V_{es_1}^2| = 2 \times 10^{-7}$.

7.3 Dilepton signature by heavy RH neutrino exchange

After discussing the manifestation of sterile neutrinos in Model-I and Model-II of [208] through various physical processes like double beta decay, dilepton signals with displaced vertices, and resonant leptogenesis, in this section we investigate if the TeV scale RH neutrinos present in both the models may manifest at the LHC, particularly, through the like-sign dilepton [387–389, 391] production events that may materialise inside the ATLAS or the CMS detectors. Since the W_R boson mass is quite heavy $M_{W_R} > 10^8$ GeV, only the $W_L - W_L$ channel is dominant for the process $pp \to l^{\pm}l^{\pm}X$ where $l = e, \mu$. The heavy RH Majorana neutrino exchange cross section is given by [203]

$$\begin{aligned}\sigma(pp \to Nl^{\pm} \to l^{\pm}jj) = \sigma_{prod}(pp \to W_L \to Nl^{\pm})\\ \times BR(N \to l^{\pm}jj)\end{aligned} \tag{7.13}$$

We use the parton level differential cross section [297]

$$\frac{d\hat{\sigma}_{LHC}}{dcos\theta} = \frac{k\beta}{32\pi\hat{s}}\frac{\hat{s}+M^2}{\hat{s}}\frac{g^4}{48}\frac{(\hat{s}^2-M^4)(2+\beta cos^2\theta)}{(\hat{s}-M_W^2)^2+M_W^2\Gamma_W^2}, \tag{7.14}$$

where $k = 3.89 \times 10^8$ pb and $\beta = \frac{\hat{s}^2-M^2}{\hat{s}^2+M^2}$.
With the identification $Q = \sqrt(\hat{s})$ and $s = E_{CM}^2$, the total production cross section is given by [243, 297]

$$\begin{aligned}\sigma_{prod} = \frac{kg^4}{768\pi s}\int_{\tau_0}^{1}\gamma\frac{d\tau}{\tau}\int_{\tau}^{1}\frac{dx}{x}[f_u(x,Q)f_{\bar{d}}(\frac{\tau}{x},Q)+\\ (u \to \bar{d}, \bar{d} \to u)],\end{aligned} \tag{7.15}$$

where

$$\tau = \frac{\hat{s}}{E_{CM}^2}, \gamma = \frac{\hat{s}+M^2}{\hat{s}} \times \frac{(\hat{s}^2-M^4)(2+\beta/3)}{(\hat{s}-M_W^2)^2+M_W^2\Gamma_W^2} \tag{7.16}$$

For computation of the production cross section we have utilized the CTEQ6M parton distribution functions [393] in eq.(7.15).

The branching ratio is estimated using

$$BR(N \to l^{\pm}jj) = \frac{\Gamma(N \to l^{\pm}W)}{\Gamma_N^{tot}} \times BR(W \to jj) \qquad (7.17)$$

with $BR(W \to jj) = 0.676$. The total width is calculated by sum of all the partial widths [203]

$$\begin{aligned} \Gamma(N \to l^{\pm}W) &= \frac{g^2|V_{\nu N}|^2}{64\pi}\frac{{M_N}^3}{{M_W}^2}(1-\frac{{M_W}^2}{{M_N}^2})^2 \\ &\quad \times(1+\frac{2{M_W}^2}{{M_N}^2}), \end{aligned} \qquad (7.18)$$

$$\begin{aligned} \Gamma(N \to \nu_l Z) &= \frac{g^2|V_{\nu N}|^2}{128\pi Cos^2\theta_w}\frac{{M_N}^3}{{M_Z}^2}(1-\frac{{M_Z}^2}{{M_N}^2})^2 \\ &\quad \times(1+\frac{2{M_Z}^2}{{M_N}^2}), \end{aligned} \qquad (7.19)$$

$$\Gamma(N \to \nu_l h) = \frac{g^2|V_{\nu N}|^2}{128\pi}\frac{{M_N}^3}{{M_W}^2}(1-\frac{{M_h}^2}{{M_N}^2})^2 \qquad (7.20)$$

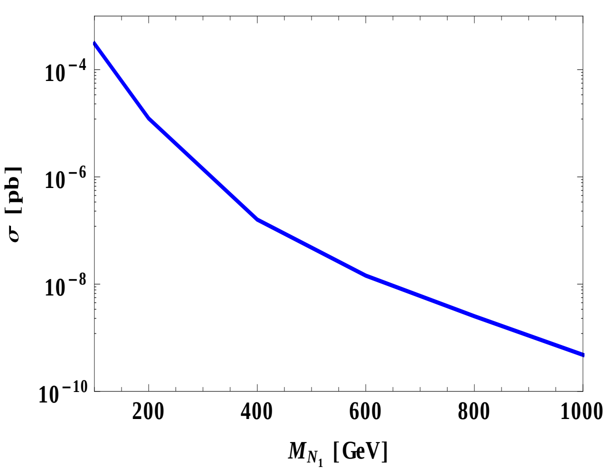

Figure 7.4: The prediction of signal cross section for the heavy RH neutrino mediated dimuon production at run-II of LHC with $\sqrt{s} = 14$ TeV.

The heavy-light neutrino mixing plays a crucial role in calculating the signal cross section. In our model the heavy-light neutrino mixing matrix for heavy RH neutrinos is $\frac{M_D}{M_N}$, where M_D is the Dirac neutrino mass matrix and M_N is the RH neutrino mass matrix. An interesting aspect of the models is that both the matrices, M_D and M_N, are already predicted by TeV scale gauge symmetry breaking, the neutrino oscillation data, and charged fermion mass fits at the GUT scale.

In the case of vanilla seesaw model investigated in [203], the heavy-light neutrino mixing is $V_{lN}^2 = m_\nu/M_N$ which is quite small and gives rise to a cross section $\sigma(pp \to \mu\mu jjX) \simeq 10^{-16}$ pb in the $W_L - W_L$ channel for exchanged heavy RH neutrino mass $\simeq 100$ GeV. On the other hand if the heavy-light mixing is assumed to be as large as $V_{lN}^2 = 3 \times 10^{-3}$ [203], the cross section is also large leading to $\sigma(pp \to \mu\mu jjX) \sim 6 \times 10^{-2}$ pb. However we do not assume any such large mixings here. In our type-II seesaw dominant models where all the heavy-light neutrino mixings are predicted, the estimated value of dimuon signal cross section in the $W_L - W_L$ channel turns out to be $\simeq 5\times10^{-4}(2\times10^{-5})$ pb for the mass of $M_{N_1} = 100(200)$ GeV resulting in nearly 24(12) events for beam luminosity $\mathcal{L} = 300\text{fb}^{-1}$ after including the cuts [377]. This result is shown in fig.(7.4). Thus if the RH neutrino masses are within $M_{N_1} \leq 300$ GeV, they are detectable at LHC run-II at $\sqrt{s} = 14$ TeV for projected beam luminosity $\mathcal{L} = 3000$ fb^{-1}, although the RH neutrino masses $M_{N_1} \leq 200$ GeV are detectable with beam luminosity $\mathcal{L} = 300$ fb^{-1}. In these models the larger values of RH neutrino masses, $M_{N_1} > 500$ GeV, are likely to escape detection at LHC through like-sign dilepton production signals. These conclusions remain valid after imposing the various cut conditions applicable to the $pp \to l^\pm l^\pm jjX$ channels [203, 377]. In the case of M_{N_2} we have similar conclusion.

7.4 Z' detection at colliders

One important and interesting feature of this work is the prediction of extra neutral Z' boson at the TeV scale accessible for detection at LHC, International Linear Collider [ILC], and future collider experiments. In this section we estimate relevant cross sections which may help in identifying the Z'-boson signals.

7.4.1 Cross section of Z' production at LHC

In this section we discuss the possible signatures of the Z' boson at LHC experiment through opposite sign dilepton production cross sections. In the dilepton channel we compare our estimated Z' production cross section with those obtained by CMS experiment [390] in the channel $pp \to Z'X \to l^+l^-X$ where $l = e, \mu$.

The resonant production cross section for the opposite sign dilepton production mediated by Z' boson resonance is [392, 395]

$$\sigma(pp \to Z' \to f\bar{f}) = \frac{\pi}{48s}[c_u w_u(s, M_{Z'}^2) \\ + c_d w_d(s, M_{Z'}^2)], \tag{7.21}$$

where

$$c_u = g'^2(g_V^{u^2} + g_A^{u^2})Br(l^+l^-), \tag{7.22}$$

$$c_d = g'^2(g_V^{d^2} + g_A^{d^2})Br(l^+l^-), \tag{7.23}$$

and $Br(l^+l^-)$ is the branching ratio defined through

$$\begin{aligned} Br(l^+l^-) &= \frac{\Gamma(Z' \to l^+l^-)}{\Gamma_{Z'}}, \\ \Gamma(Z' \to l^+l^-) &= \frac{g'^2 M_Z' [g_v^{l^2} + g_A^{l^2}]}{48\pi}, \\ \Gamma_{Z'} &= \frac{g'^2 M_Z'}{48\pi}[9(g_V^{u^2} + g_A^{u^2}) + 9(g_V^{d^2} + g_A^{d^2}) \\ &\quad +3(g_V^{e^2} + g_A^{e^2}) + 3(g_V^{\nu^2} + g_A^{\nu^2})]. \end{aligned} \tag{7.24}$$

The numerical values of different quantities occurring in eq.(7.22), eq.(7.23), and eq.(7.24) are [392]

$$\begin{aligned} g_V^u = 0.329; \quad g_V^d = -0.591, \quad g_A^u = -0.46, \\ g_A^d = 0.46, \quad g_V^e = 0.068, \quad g_V^\nu = 0.196, \\ g_A^e = 0.46, \quad g_A^\nu = 0.196, \quad g' = 0.59.. \end{aligned} \tag{7.25}$$

In eq.(7.21) $w_{u(d)}$ is related to the parton luminosities $\frac{dL_{u\bar{u}}}{dM_{z'^2}}$ and $\frac{dL_{d\bar{d}}}{dM_{z'^2}}$. Therefore they depend only upon the collider energy and the Z' mass [392, 395],

$$
\begin{aligned}
w_{u(d)} &= \sum_{q=u,c(d,s,b)} \int_0^1 \mathrm{d}x_1 \int_0^1 \mathrm{d}x_2 \int_0^1 \mathrm{d}z f_{q/P}(x_1, M_{z'}^2) \\
&\quad f_{q/P}(x_2, M_{z'}^2)\Delta_{qq}(z, M_{z'}^2) + f_{g/P}(x_1, M_{z'}^2) \\
&\quad [f_{q/P}(x_2, M_{z'}^2) + f_{q/P}(x_2, M_{z'}^2)]\Delta_{gq}(z, M_{z'}^2) \\
&\quad +(x_1 \leftrightarrow x_2, P \leftrightarrow P)\delta(\frac{M_{z'}^2}{s} - zx_1x_2), \qquad (7.26)
\end{aligned}
$$

where $f_{i/P}(x, M^2)$ is the parton distribution function (PDF) for the proton,

$$
\begin{aligned}
\Delta_{gq}(z, M_{z'}^2) &= \delta(1-z) + \frac{\alpha_s(M_{z'}^2)}{\pi} C_F \Bigg[\delta(1-z)\left(\frac{\pi^2}{3} - 4\right) \\
&\quad +4\left(\frac{ln(1-z)}{1-z}\right)_{+z[0,1]} - 2(1+z)ln(1-z) \\
&\quad -\frac{1+z^2}{1-z} lnz\Bigg], \qquad (7.27)
\end{aligned}
$$

$$
\begin{aligned}
\Delta_{gq}(z, M_{z'}^2) &= \frac{\alpha_s(M_{z'}^2)}{2\pi} T_F \Bigg[(1-2z+2z^2)ln\frac{(1-z^2)}{z} \\
&\quad +\frac{1}{2} + 3z - \frac{7}{2}z^2\Bigg], \qquad (7.28)
\end{aligned}
$$

with $C_F = 4/3$ and $T_F = 1/2$.

The production cross section in the channel $pp \to Z'X \to l^{\pm}l^{\mp}X$ as a function of invariant dilepton mass ($= M_{Z'}$) is shown in Fig.7.5. This result suggests that at $\sqrt{s} = 14$ TeV the number of Z' production events could be as large as 250 in the region of $M_{Z'} \sim 1$ TeV even for 30 fb^{-1} beam luminousity. However to get sizeable number of events in the region of $M_{Z'} \sim 2-3$ TeV, the beam luminousity has to increase beyond several 1000 fb^{-1}.

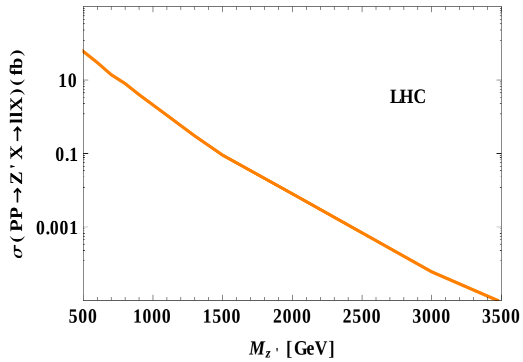

Figure 7.5: The signal cross section for the the Z' boson resonance mediated cross section as function of its mass, $M_{Z'}$, in the production channel $pp \to Z'X \to l^{\pm}l^{\mp}X$.

7.4.2 Ratio of Z$'$ signal-Z signal cross section at LHC

The CMS collaboration [390] has measured the cross section ratio

$$\sigma(pp \to Z' \to l^{\pm}l^{\mp}X)/\sigma(pp \to Z \to l^{\pm}l^{\mp}X) \tag{7.29}$$

as shown in Fig. 7.6 as a function of the Z' mass $M_{Z'}$. Our prediction using $l = e$ is shown by almost a slanted linear curve with falling value of the ratio with increasing value of $M_{Z'}$ plotted along the X-axis. The solid (dotted) black lines denote the observed (expected) ratios. The yellow (green) region shows the expected values at 95% (68%) From this Fig.7.6 by comparison with the CMS data we find that in our model the lower limit of the Z' mass is predicted to be $M_{Z'} \sim 2.8$ TeV.

7.4.3 Z-Z' mixing angle and $pp \to W^+W^- + X$ at LHC

In this subsection we discuss possible signature of Z' boson through the production of W^+W^- pairs for different values of $Z - Z'$ mixings at the LHC. The Z-Z' mixing in the SO(10) embedding of two step breaking of left-right gauge symmetry has been computed through the formula

$$\tan^2\phi_{zz'} = \frac{M_0^2 - M_Z^2}{M_{Z'}^2 - M_0^2}, \tag{7.30}$$

where $M_0 = \frac{M_W}{\sqrt{\rho_0}\cos\theta_W}$ [208]. In our model since the LH triplet $\Delta_L(3,1,-2,1)$ has a very small VEV $v_L = 0.1 - 0.5$ eV $<< V_{\rm ew}$, the model is consistent with the tree

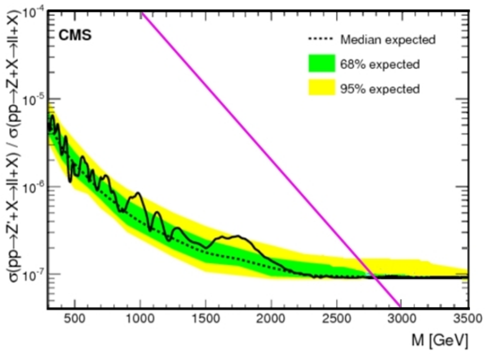

Figure 7.6: The ratio of the Z' boson and Z boson signal cross sections as a function of Z' mass. The CMS data [390] is shown at different confidence levels of expectations by the dark bands . The solid zig-zag curve denotes observed fluctuations about the median which has been shown by the dotted line. The falling behavior indicated by the red linear curve is our prediction as a function of $M = M_{Z'}$ plotted along the X-axis.

level value of the rho-parameter, $\rho_0 = 1$. The radiative corrections due to the 125 GeV Higgs of the SM and the top quark yield $\rho \simeq 1.009$ [208].

The potential of LHC to discover $Z - Z'$ mixing effects in the channel $pp \to W^+W^- + X$ has been investigated [394]. In this paper we estimate the variation of differential cross section with respect to the invariant mass $M_{W^+W^-} \equiv M$ of the produced W^+W^- pair for different $Z - Z'$ mixings. The corresponding differential cross section for the process $pp \to W^+W^- + X$ averaged over quark colors can be obtained starting from the basic W^+W^- production cross section by quark-antiquark annihilation $q\bar{q} \to W^+W^-$ mediated by Z' boson [394]

$$\begin{aligned}\frac{d\hat{\sigma}^{Z'}}{dcos\theta} &= \frac{\pi\alpha^2 cot^2\theta_w}{48}\beta_w^3(V_{2,f}^2 \\ &\quad + A_{2,f}^2)sin^2\phi\frac{\hat{s}}{(\hat{s}-M_{Z'}^2)^2 + M_{Z'}^2\Gamma_{Z'}^2} \\ &\quad \times(\frac{\hat{s}^2}{M_w^4}sin^2\theta \\ &\quad + 4\frac{\hat{s}}{M_w^2}(4 - sin^2\theta) + 12 sin^2\theta),\end{aligned} \tag{7.31}$$

where Γ'_Z is the decay width of Z', $\beta_W = \sqrt{1 - 4M_W^2/\hat{s}}$, ϕ is the Z-Z' mixing angle, v_f and a_f are the vector and axial vector coupling, $\hat{s}$ is the Mandelstam variable for square of c.m. energy, and θ is the angle between W^- and the quark in the W^+W^- center of mass frame [394].

$$\begin{aligned} V_{1f} &= g_V^f cos\phi + g_V^{f'} sin\phi, \\ V_{2f} &= g_V^{f'} cos\phi - g_V^f sin\phi, \\ A_{1f} &= g_A^f cos\phi + g_A^{f'} sin\phi, \\ A_{2f} &= g_A^{f'} cos\phi - g_A^f sin\phi, \\ g_V^{f'} &= \frac{cos\beta}{cos\theta_w * \sqrt{6}}, \\ g_A^{f'} &= \frac{cos\phi + \sqrt{5/3} sin\beta_W}{2cos\theta_w * \sqrt{6}}. \end{aligned} \tag{7.32}$$

The values of g_V^f and g_A^f are given in eq.(7.25).

$$\begin{aligned} \frac{d\sigma_{q\bar{q}}}{dMdydz} \quad = \quad & K\frac{2M}{s}\sum[f_{q/p_1}(\eta_1)f_{\bar{q}/p_2}(\eta_2) \\ & +f_{\bar{q}/p_1}(\eta_1)f_{q/p_2}(\eta_2)] \\ & \times\frac{d\hat{\sigma}_{q\bar{q}}}{dz}, \end{aligned} \tag{7.33}$$

where s = center of mass energy, $z = \cos\theta$, and θ = angle between quark and W boson, and $f_{q/p_1}(\eta_1, M)$ and $f_{\bar{q}/p_2}(\eta_2, M)$ are PDFs for protons P_1 and P_2, respectively. We have taken $K = 1.2$ [394] and use CTEQ-6L1 parton distribution functions for numerical computation.

By integrating the right hand side of eq.(7.33) over Z, the rapidity of $W^\pm$ pair y and invariant mass M around the resonance peak $(M_R - \delta M/2, M_R + \delta M/2)$, we get

$$\begin{aligned} \sigma(pp \to W^+W^- \to X) \quad = \quad & \int_{M_R-\delta M/2}^{M_R+\delta M/2} dM \int_{-Y}^{Y} dy \\ & \times \int_{-z_{cut}}^{z_{cut}} dz[\frac{d\sigma_{q\bar{q}}}{dMdydz}]. \end{aligned} \tag{7.34}$$

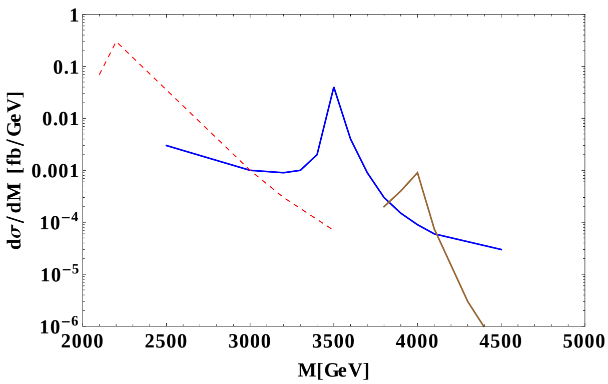

Figure 7.7: Invariant mass distribution of W pairs in $pp \to W^+W^- + X$ at the LHC with $\sqrt{S} = 14$ TeV. The red, blue, and the brown curves are for the values of the $Z - Z'$ mixing angle ϕ at 1.2×10^{-3}, 0.9×10^{-3}, and 0.7×10^{-3}, respectively.

In our model the computed values of mixings are $\sin\phi = 1.2 \times 10^{-3}$, 0.9×10^{-3}, and 0.7×10^{-3} at invariant mass values of 2.3 TeV, 3.5 TeV, and 4 TeV respectively.

The distribution curves are shown in fig.(7.7) for these three sets of values. Our predicted results give the value of $\frac{d\sigma}{dM} = 0.52$ (fb/GeV) for $M_{Z'} = 3.5$ TeV, $\frac{d\sigma}{dM} = 0.3$ (fb/GeV) for $M_{Z'} = 2.3$ TeV, $\frac{d\sigma}{dM} = 0.001$ (fb/GeV) for $M_{Z'} = 4.0$ TeV. The predicted values of the peak positions at 2.3 TeV and 4 TeV can also provide a test of the models if such a Z' is present in nature.

7.4.4 Z' cross section at ILC

The international linear collider (ILC) is expected to provide a rigorous experimental verification of various Z' models as far as their predicted masses are concerned. In our model, the variation of the predicted annihilation cross section via Z' resonance with center of mass energy of the colliding lepton beams is given in Fig.7.8. To estimate this cross section we have used the total decay width of Z' boson [392] defined through eq.(7.24) and eq.(7.25).

The signal cross section at ILC is given by

$$\begin{aligned} \sigma(l^+l^- \to Z' \to f^+f^-) &= \frac{12\pi}{M_{Z'}^2}\Gamma_{ll}\Gamma_{ff} \\ &\times \frac{s}{(s - M_{Z'}^2)^2 + M_{Z'}^2\Gamma_{Z'}^2} \end{aligned} \tag{7.35}$$

The signal cross section is found to be 70 pb at the center of mass energy $\sqrt{s} =$ 2800 GeV which corresponds to the Z' mass. Therefore its presence can be easily

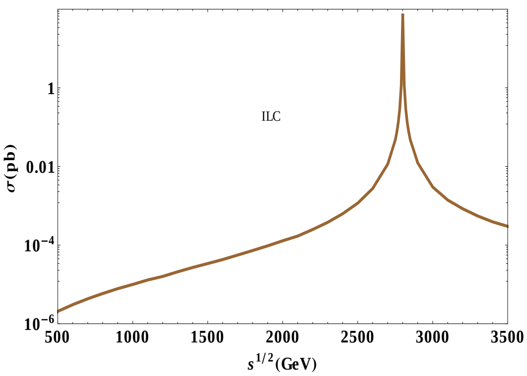

Figure 7.8: The signal cross section of the Z' boson as a function of its center of mass energy at ILC.

detected even for as low a luminousity as $\mathcal{O}(1)$ pb^{-1}.

Chapter 8

Summary and Conclusion

In this thesis we have investigated the prospects of experimentally verifiable beyond standard model physics in a type-II seesaw motivated non-SUSY SO(10) grand unification framework. The type-II seesaw mechanism can be successfully implemented with a low mass Z' boson which can be accessible at LHC and planned accelerators. The type-II scenario for explaining light neutrino masses and mixings may emerge from the suggested texture of 9×9 neutrino mass matrix. The unification theories based upon SO(10) group are particularly interesting. All the SM fermions of one generation plus a right handed neutrino can be accommodated in the irreducible 16 dimension representation. Since SO(10) is a large group, its spontaneous symmetry breaking to SM may pass through various intermediate symmetries. Once intermediate symmetries are present in the theory, gauge coupling unify nicely without any requirement of supersymmetry.

In Chapter 1 we have motivated the need to study non-SUSY unification model with experimentally reachable BSM predictions. We have also presented the scheme of investigation, briefly. In Chapter 2 we recapitulated the SM and its ineptitude in explaining various BSM phenomena. In Chapter 3 we motivated and briefly discussed the SU(5) and SO(10) GUT prototypes. We also briefly described the conventional seesaw mechanisms (type-I, II and III) which can explain small neutrino masses very naturally. Interestingly, in Chapter 4 we have discussed the mechanism where the type-I seesaw term is cancelled out in the presence of SO(10) singlet fermions. After the block diagonalization of 9×9 neutrino mass matrix, there are two type-I seesaw terms with opposite signs resulting in the cancellation that results due to the addition of these three extra fermion singlets, one per generation. Depending upon the choice of various parameters suitably we have also shown, the possibility of dominance of different seesaw mechanisms. We have discussed the condition for inverse seesaw dominance, type-II seesaw dominance, double seesaw dominance and linear seesaw dominance. In Chapter 5 we have investigated the prospects of type-II seesaw mechanism for neutrino masses in a non-SUSY SO(10) GUT model which passes through two intermediate symmetries (G_{2213} at 10^8 GeV and G_{2113} at TeV) to reach to SM. A SO(10) singlet fermion (S) per generation is introduced to get type-II seesaw. At TeV scale, Z' boson acquires mass through spontaneous breaking of $U(1)_R \times U(1)_{B-L}$ gauge symmetries into $U(1)_Y$ generated predominantly through Higgs representation 126_H. The left-right gauge theory is restored at the G_{2213} intermediate energy scale. The Dirac neutrino mass matrix M_D is the necessary input to estimate lepton number and lepton flavor violating contributions, non-unitarity effects as well as leptonic CP-violation. This matrix has been explicitly computed using the associated renormalization group equations in the presence of G_{2213} and G_{2113} intermediate gauge symmetries via bottom-up and top-down iterative methods, and by implementing the model constraints on the fermion masses at GUT scale. The $N-S$ mixing matrix M is estimated using the current non-unitarity experimental constraint. The predominant Dirac mass matrix together with TeV scale heavy neutrino masses $N-S$ mixing matrix M give the branching ratio predictions only few orders less than the current bound. The LFV branching ratios calculated in our model are $Br(\mu \rightarrow e\gamma) = 6.43 \times 10^{-17}$, $Br(\tau \rightarrow e\gamma) = 8 \times 10^{-16}$, $Br(\tau \rightarrow \mu\gamma)$ $= 2.41 \times 10^{-12}$.

The predicted proton-lifetime in this model is found to be $\tau_p(p \rightarrow e^+\pi^0) \simeq 2.0 \times 10^{34\pm1.0\pm0.34}$yrs where the first (second) uncertainty is due to GUT-threshold effects (experimental errors). This lifetime is accessible to ongoing and planned experiments. Thus, even though the model does not have low-mass RH $W_R^{\pm}$ bosons in the accessible range of LHC, it is associated with interesting signatures on lepton flavor, lepton number and baryon number violations. The predicted values of these phenomena are in concordance with the predictions in the previous chapters.

In Chapter 6 we have discussed the phenomenon of neutrinoless double beta decay and resonant leptogenesis through type-II seesaw framework in SO(10). Although the W_R boson is present at a high scale, there is a new contribution to the $0\nu\beta\beta$ decay amplitude in the $W_L - W_L$ channel due to the presence of extra fermion singlet. The model is designed in such a way that the first generation sterile neutrino as well as second generation sterile neutrino can contribute to the $0\nu\beta\beta$ decay . If the first generation sterile neutrino is made light by the suitable choice of $N-S$ mixing term M, then the first light singlet fermion exchange contributes to the $0\nu\beta\beta$ decay. Similarly if the second generation sterile neutrino is made light, then it can mediate

$0\nu\beta\beta$ decay in the $W_L - W_L$ channel. The model predicts the half life close to the experimental bound at m_s= 0.5 GeV for QD neutrinos, m_s = 3 GeV for NH neutrinos, and m_s = 2 GeV for IH neutrinos.

In this Chapter 6 we have also discussed the generation of baryon asymmetry of the universe in a novel fashion. Baryon asymmetry of the universe is achieved due to the resonant leptogenesis of two quasi degenerate sterile neutrino pairs allowed in the present model. For the case of QD type active neutrinos, we have showed that the lightest singlet fermion of first generation mediates the $0\nu\beta\beta$ process as discussed above, while the heavy quasidegenerate sterile fermions of second and third generation mediate resonant leptogenesis leading to right value of baryon asymmetry of the universe. In the alternative possibility the lightest second generation singlet fermion assists $0\nu\beta\beta$ but the heavy quasidegenerate singlet fermion of first and third generations mediate resonant leptogenesis leading to baryon asymmetry of the universe. In case of the NH type active neutrino masses, only the lightest singlet fermion of first generation is noted to mediate dominant $0\nu\beta\beta$ while heavier quasidegenerate singlet fermion of second and third generations mediate resonant leptogenesis leading to the right order of baryon asymmetry of the universe.

In Chapter 7 we have discussed the phenomenon of collider signature in a type-II seesaw dominant model. In our model since the RH neutrino is present at TeV scale, its signature can be verified experimentally in the PP collision through $W_L - W_L$ channel resulting in the production of dilepton events. In this model the Z' boson is present at TeV scale. So the signature of Z' boson can be detected at different collider experiments such as LHC and ILC.

Another interesting fact is that in this Chapter we have discussed the collider signature of sterile neutrino through displaced vertex. Dilepton events can be observed in the $W_L - W_L$ channel during PP collision. Because of the SO(10) model predictions of heavy-light mixing matrix elements, either first generation or second generation sterile neutrino could be capable of mediating the displaced vertices resulting in the like-sign dilepton events eejj, $\mu\mu jj$, and $e\mu jj$. Since in our model the Dirac neutrino mass matrix M_D and right handed neutrino mass matrix M_N are diagonal, we can detect the signature of dielectrons and dimuons in the PP collision. In the displaced vertex since the background strength signal is very weak, 3-4 events are sufficient to detect the signature of the sterile neutrino experimentally.

The above discussed model is self sufficiet enough to challenge some of the demerits of standard model such as non-zero neutrino mass, lepton flavour violation, neutrinoless double beta decay, baryon asymmetry. The collider signature of right handed neutrino, sterile neutrino and Z' boson are discussed with predictions on significant number of events. Our proposed model has attractive qualities of verifiability or falsifiability through different types of ongoing experiments.

Bibliography

[1] H. Weyl, Electron and Gravitation. 1. (In German), Z. Phys., **56** (1929) 330-352.

[2] Chen-Ning Yang and Robert L. Mills, Conservation of Isotopic Spin and Isotopic Gauge Invariance, Phys. Rev., **96** (1954) 191-195.

[3] S. L. Glashow, Partial Symmetries of Weak Interactions, Nucl. Phys., **22** (1961) 579-588.

[4] Julian S. Schwinger, A Theory of the Fundamental Interactions, Annals Phys., **2** (1957) 407-434.

[5] F. Englert and R. Brout, Broken Symmetry and the Mass of Gauge Vector Mesons, Phys. Rev. Lett., **13** (1964) 321-323.

[6] Peter W. Higgs, Broken Symmetries and the Masses of Gauge Bosons, Phys. Rev. Lett., **13** (1964) 508-509.

[7] Abdus Salam, Weak and Electromagnetic Interactions, Conf.Proc., **C680519** (1968) 367-377.

[8] Steven Weinberg, A Model of Leptons, Phys. Rev. Lett., **19** (1967) 1264-1266.

[9] David J. Gross and Frank Wilczek, Ultraviolet Behavior of Nonabelian Gauge Theories, Phys. Rev. Lett., **30** (1973) 1343-1346.

[10] H. David Politzer, Reliable Perturbative Results for Strong Interactions?, Phys. Rev. Lett., **30** (1973) 1346-1349.

[11] L. Brown, M. Dresden, L. Hoddeson and M. Riordan, The Rise of the Standard Model -History of Particle Physics from 1964 to 1979, Cambridge University Press, Cambridge.

[12] G. 't Hooft, Renormalizable Lagrangians for Massive Yang-Mills Fields, Nucl. Phys. B, **35** (1971) 167-188.

[13] G.'t Hooft, Gerard and M.J.G. Veltman, Regularization and Renormalization of Gauge Fields, Nucl. Phys. B, **44** (1972) 189-213.

[14] Fred Jegerlehner, Renormalizing the standard model, Conf. Proc., **C900603** (1990) 476-590.

[15] Elisabeth Kraus, The Renormalization of the electroweak standard model to all orders, Annals Phys., **262** (1998) 155-259.

[16] Georges Aad and others, Observation of a new particle in the search for the Standard Model Higgs boson with the ATLAS detector at the LHC, ATLAS Collaboration, Phys. Lett. B, **716** (2012) 1-29.

[17] Serguei Chatrchyan and others, Observation of a new boson at a mass of 125 GeV with the CMS experiment at the LHC, Phys. Lett. B, **716** (2012) 30-61, CMS Collaboration, arXiv:1207.7235[hep-ex].

[18] Guido Altarelli, Theoretical Models of Neutrino Mixing: Recent Developments, (2009) 377-396.

[19] Guido Altarelli, Status of Neutrino Masses and Mixing in 2010, "PoS", HRMS2010, (2010) 022.

[20] Guido Altarelli, Perspectives in Neutrino Physics, (2011) 383-391.

[21] Ernest Ma, Verifiable radiative seesaw mechanism of neutrino mass and dark matter, Phys. Rev. D, **73** (2006) 077301.

[22] R. N. Mohapatra, S. Antusch, K. S. Babu, G. Barenboim, Mu-Chun Chen and others, Theory of neutrinos: A White paper, Rept. Prog. Phys., **70** (2007) 1757-1867.

[23] R. N. Mohapatra, Neutrino mass and unification, Prog. Part. Nucl. Phys., **64** (2010) 307-312.

[24] S. Raby, and T. Walker, K. S. Babu, H. Baer, A. B. Balantekin, DUSEL Theory White Paper, "SLAC-PUB-14734, FERMILAB-PUB-08-680-T", 2008.

[25] Ernest Ma, Neutrino Mass: Mechanisms and Models, "UCRHEP-T468", (2009), arXiv:0905.0221 [hep-ph].

[26] Ernest Ma, Neutrino Mass Seesaw Version 3: Recent Developments, AIP Conf.Proc., **1116** (2009) 239-246, arXiv:0810.5574 [hep-ph].

[27] Hans Hettmansperger, Manfred Lindner, and Rodejohann, Werner, Phenomenological Consequences of sub-leading Terms in See-Saw Formulas, JHEP, **1104** (2011) 123, arXiv:1102.3432 [hep-ph].

[28] Jogesh C. Pati and Abdus Salam, Unified Lepton-Hadron Symmetry and a Gauge Theory of the Basic Interactions, Phys. Rev. D, **8** (1973) 1240-1251.

[29] Jogesh C. Pati, and Abdus Salam, Lepton Number as the Fourth Color, Phys. Rev. D, **10** (1974) 275-289.

[30] R. N. Mohapatra, J. C. Pati, Left-Right Gauge Symmetry and an Isoconjugate Model of CP Violation, Phys. Rev. D, **11** 566 (1975) 2558.

[31] G. Senjanović, R. N. Mohapatra, Exact left-right symmetry and spontaneous violation of parity, Phys. Rev. D, **12** (1975) 1502.

[32] H. Georgi and S. L. Glashow, Unity of All Elementary Particle Forces, Phys. Rev. Lett., **32** (1974) 438-441.

[33] H. Georgi, The State of the Art - Gauge Theories. (Talk)", AIP Conf. Proc., **23** (1975) 575-582.

[34] A. De Rujula, Howard Georgi, and S. L. Glashow, Hadron Masses in a Gauge Theory, Phys. Rev. D, **12** (1975) 147-162.

[35] Harald Fritzsch and Peter Minkowski, Unified Interactions of Leptons and Hadrons, Annals Phys., **93** (1975) 1193.

[36] D. Chang, R. N. Mohapatra and M. K. Parida, Decoupling parity and left-right symmetry breaking scales: A new approach to left-right symmetric models, Phys. Rev. Lett., **52** (1984) 1072.

[37] D. Chang, R. N. Mohapatra and M. K. Parida, A new approach to left-right symmetriy breaking in unified gauge theories, Phys. Rev. D, **30** (1984) 1052.

[38] D. Chang, R. N. Mohapatra, J. Gipson, R. E. Marshak, M. K. Parida, Experimental tests of new SO(10) grand unification, Phys. Rev. D, **31** (1985) 1718.

[39] T. Yanagida in Workshop on Unified Theories, KEK Report 79-18, p. 95, 1979.

[40] M. Gell-Mann, P. Ramond and R. Slansky, Supergravity, p. 315. Amsterdam: North Holland, 1979.

[41] S. L. Glashow, 1979 Cargese Summer Institute on Quarks and Leptons, p. 687, New York: Plenum, 1980.

[42] R. N. Mohapatra and G. Senjanovic, Neutrino Mass and Spontaneous Parity Violation, Phys. Rev. Lett., **44** (1980) 912.

[43] R. N. Mohapatra and G. Senjanovic, Neutrino masses and mixings in gauge models with spontaneous parity violation, Phys. Rev. D, **23** (1981) 165.

[44] H. S. Goh, and R. N. Mohapatra, S. Nasri, SO(10) symmetry breaking and type II seesaw, Phys. Rev. D, **70** (2004) 075022.

[45] R. N. Mohapatra, M. K. Parida, Type II Seesaw Dominance in Non-supersymmetric and Split Susy SO(10) and Proton Life Time, Phys. Rev. D, **84** (2011) 095021.

[46] Alejandra Melfo, Alba Ramirez, Goran Senjanovic, Type II see-saw dominance in SO(10), Phys. Rev. D, **82** (2010) 075014.

[47] G. Altarelli, G. Blankenburg, Different SO(10) Paths to Fermion Masses and Mixings, J. High Energy Phys., **1103** (2011) 133.

[48] B. Bajc, G. Senjanovic, F. Vissani, How Neutrino and Charged Fermion Masses are Connected Within Minimal Supersymmetric SO(10), hep-ph/0110310.

[49] S. Bertolini, M. Frigerio, M. Malinsky, Fermion masses in supersymmetric SO (10) with type II seesaw mechanism: A nonminimal predictive scenario, Phys. Rev. D, **70** (2004) 095002.

[50] P. S. Bhupal Dev, R. N. Mohapatra, M. Severson,Neutrino Mixings in SO(10) with Type II Seesaw and θ_{13} Phys. Rev. D, **84** (2011) 053005, arXiv:1107.2378.

[51] K. S. Babu and R. N. Mohapatra, Predictive neutrino spectrum in minimal SO(10) grand unification, Phys. Rev. Lett., **70** (1993) 2845-2848, hep-ph/9209215.

[52] B. Brahmachari and R. N. Mohapatra, Unified explanation of the solar and atmospheric neutrino puzzles in a minimal supersymmetric SO(10) model, Phys. Rev. D, **58** (1998) 015001, hep-ph/9710371.

[53] Takeshi Fukuyama and Nobuchika Okada, Neutrino oscillation data versus minimal supersymmetric SO(10) model, JHEP, **0211** (2002) 011, hep-ph/0205066.

[54] Noriyuki Oshimo, Antisymmetric Higgs representation in SO(10) for neutrinos, Phys. Rev. D, **66** (2002) 095010, hep-ph/0206239.

[55] Borut Bajc and Goran Senjanovic and Francesco Vissani, b-tau unification and large atmospheric mixing: A Case for noncanonical seesaw, Phys. Rev. Lett., **90518020** (2003) 051802, hep-ph/0210207.

[56] J. William Marciano and Goran Senjanovic, Predictions of Supersymmetric Grand Unified Theories, Phys. Rev. D, **25** (1982) 3092.

[57] Ugo Amaldi, Wim de Boer, Hermann Furstenau,Comparison of grand unified theories with electroweak and strong coupling constants measured at LEP, Phys. Lett. B, **260** (1991) 447-455.

[58] Paul Langacker and Ming-xing Luo, Implications of precision electroweak experiments for M_t, ρ_0, $\sin^2\theta_W$ and grand unification, Phys. Rev. D, **44** (1991) 817-822.

[59] N. G. Deshpande and E. Keith and Palash B. Pal, Implications of LEP results for SO(10) grand unification, Phys. Rev. D, **46** (1993) 2261-2264.

[60] R. N. Mohapatra and M. K. Parida, Threshold effects on the mass scale predictions in SO(10) models and solar neutrino puzzle, Phys. Rev. D, **47** (1993) 264-272, hep-ph/9204234.

[61] D. G. Lee, R. N. Mohapatra, M. K. Parida and Merostar Rani, Predictions for proton lifetime in minimal nonsupersymmetric SO(10) models: An update, Phys. Rev. D, **51** (1995) 229-235, hep-ph/9404238.

[62] H. V. Klapdor-Kleingrothaus, A. Dietz, L. Baudis, G. Heusser, I.V. Krivosheina, S. Kolb, B. Majorovits, H. Pas, H. Strecker, V. Alexeev, A. Balysh, A. Bakalyarov, S.T. Belyaev, V.I. Lebedev, S. Zhukov (Kurchatov Institute, Moscow, Russia), Latest results from the Heidelberg-Moscow double beta decay experiment, Eur.Phys.J. A, **12** (2001) 147.

[63] C. Arnaboldi et al. [CUORICINO Collaboration], Results from a search for the $0\nu\beta\beta$ decay of 130_{Te}, Phys. Rev. C, **78** (2008) 035502.

[64] C. E. Aalseth et al. [IGEX Collaboration], Phys. Rev. D, **65** (2002) 092007.

[65] J. Argyriades et al. [NEMO Collaboration], Measurement of the double beta decay half life of 150-Nd and seach for neutrinoless decay modes with the NEMO3 detector, Phys. Rev. C, **80** (2009) 032501.

[66] I. Abt, M. F. Altmann, A. Bakalyarov, I. Barabanov, C. Bauer, E. Bellotti, S. T. Belyaev, L. B. Bezrukov et al., A new 76_{Ge} double beta decay experiment at LNGS, [hep-ex/0404039]

[67] S. Schonert et al. [GERDA Collaboration], Nucl. Phys. Proc. Suppl., **145** (2005) 242 ; C. Arnaboldi et al. [CUORE Collaboration], Nucl. Instrum. Meth. A, **518** (2004) 775

[68] H. V. Klapdor-Kleingrothaus, I. V. Krivosheina, A. Dietz, O. Chkvorets, Phys. Lett. B, **586** (2004) 198 .

[69] H. V. Klapdor-Kleingrothaus, I. V. Krivosheina, Mod. Phys. Lett. A, **21** (2006) 1547 .

[70] A. K. Alfonso et al. [CUORE Collaboration], Phys. Rev. Lett., **115** (2015) 102502.

[71] S.Schonert *et al.* (GERDA collaboration), The Germanium Detector Array (Gerda) for the search of neutrinoless $\beta\beta$ decays of 76_{Ge} at LNGS, Nucl. Phys. Proc. Suppl.,**145** (2005) 242.

[72] R. Arnold *et al.*(NEMO-3 Collaboration), Results of the search for neutrinoless double- beta deay in 100_{MO} with the NEMO-3 experiment, Phys. Rev. D, **92** (2015) 7 072011.

[73] A. Gando *et al* (KAMLAND-Zen collaboration), Limits on Majoron-emitting double beta decays of 136_{Xe} in the KamLand-Zen experiment, Phys. Rev.C, **86**, (2012) 021601.

[74] A. Gando *et al* (KAMLAND-Zen collaboration),Limit on Neutrinoless double beta decay of 136_{Xe} from the First Phase of KamLAND-Zen and Comparison with the Positive Claim in 76_{Ge}, Phys. Rev. Lett.,**110** (2013) 062502.

[75] M. Auger *et al.*, Search for Neutrinoless Double-Beta Decay in 136_{Xe} with EXO-200, (EXO collaboration), Phys. Rev. Lett.,**109** (2012) 032505.

[76] J. J. Schechter and J. W. F. Valle, Neutrinoless double beta decay in $SU(2) \times U(1)$ theories, Phys. Rev. D, **25** (1982) 774.

[77] D. Aristizabal Sierra, M. Tortola, J. W. F. Valle, and A.Vicente, Leptogenesis with a dynamical seesaw scale, JCAP, **07** (2014) 052, arXiv:1405.4706V2 [hep-ph].

[78] Y. Fukuda et al. (SuperKamiokande Collaboration), Evidence for oscillation of atmospheric neutrinos, Phys. Rev. Lett. **81** (1998) 1562-1567.

[79] M. Magg, C. Wetterich, Neutrino mass problem and gauge hierarchy, Phys. Lett. B, **94** (1980) 61.

[80] T. P. Cheng, L. F. Li, Neutrino masses, mixings and oscillations in $SU(2) \times U(1)$ models of electroweak interactions, Phys. Rev. D, **22** (1980) 2860.

[81] G. Lazaridis, Q. Shafi and C. Wetterich, Proton lifetime and fermion masses in SO(10), Nucl. Phys. B, **181** (1981) 287.

[82] J. J. Schechter and J. W. F. Valle, Neutrino masses in $SU_2 \times U_1$ theories Phys. Rev. D, **22** (1980) 2227.

[83] P. S. Bhupal Dev and R. N. Mohapatra, TeV scale inverse seesaw in SO(10) and leptonic non-unitarity effects, Phys. Rev. D, **81** (2010) 013001.

[84] P. S. Bhupal Dev and R. N. Mohapatra, Electroweak symmetry breaking and proton decay in SO(10) SUSY GUT with TeV W_R, Phys. Rev. D, **82** (2010) 035014.

[85] Tao Han, P. Langacker, Zhen Liu, Lian-Tao Wang, Diagnosis of a new neutral gauge boson at the LHC and ILC for snowmass 2013, arXiv:1308.2738[hep-ph].

[86] R. L. Awasthi, M. K. Parida, Inverse seesaw mechanism in non-supersymmetric SO(10), proton lifetime, non-unitarity effects and a low mass Z' boson, Phys. Rev. D, **86** (2012) 093004, arXiv:1112.1826[hep-ph].

[87] R. L. Awasthi, M. K. Parida, S. Patra, Neutrino masses, dominant neutrinoless double beta decay, and observable lepton flavor violation in left-right models and SO(10) grand unification with low-mass W_R, Z_R bosons, JHEP, **08** (2013) 122, arXiv:1302.0672 [hep-ph].

[88] M. K. Parida, Ram Lal Awasthi, P. K. Sahu, Proton decay and new contributions to $0\nu2\beta$ decay in SO(10) with low-mass Z' boson, observable $n-\bar{n}$ oscillation, lepton flavor violation, and rare kaon decay, JHEP, **1501** (2015) 045, arXiv:1401.1412[hep-ph].

[89] R. N. Mohapatra, M. K. Parida, G. Rajasekaran, High scale mixing unification and large neutrino mixing angle, Phys. Rev. D, **69** (2004) 053007, arXiv:0301234 [hep-ph].

[90] R. N. Mohapatra, M. K. Parida, G. Rajasekaran, Threshold effects on quasi-degenerate neutrinos with high scale mixing unification, Phys. Rev. D, **71** (2005) 057301, arXiv: hep-ph/0501275.

[91] S. Agrawalla, M. K. Parida, R. N. Mohapatra, G. Rajasekaran, Neutrino mixings ad leptonic CP violation from CKM matrix and Majorana phases, Phys. Rev. D, **75** (2007) 033007, arXiv:hep-ph/0611225.

[92] B. Dutta, Y. Minura, R. N. Mohapatra, Origin of quark-lepton flavor in SO(10) with type-II seesaw, Phys. Rev. D, **80** (2009) 095021.

[93] A. Joshipura, B. P. Kodrani, K. M. Patel, Fermion masses and mixings in a $\mu-\tau$ symmetric SO(10), Phys. Rev. D, **79** (2009) 115017 .

[94] H. S. Goh, R. N. Mohapatra, S. P. Ng, Minimal SUSY SO(10), $b-\tau$ unification at large neutrino mixings, Phys. Lett.B, **570** (2003) 215, hep-ph/0303055.

[95] H. S. Goh, R. N. Mohapatra, S. P. Ng, Minimal SUSY SO(10) model and predictions for neutrino mixings and leptonic CP violation, Phys. Rev. D, **68** (2003) 115008, hep-ph/0308197.

[96] K. S. Babu, C. Macesanu, Neutrino masses and mixings in a minimal SO(10) model, Phys. Rev. D, **72** (2005) 115003.

[97] B. Dutta, Y. Mimura, R. N. Mohapatra, CKM CP violation in a minimal SO(10) model for neutrinos and its implications, Phys. Rev. D, **69** (2004) 115014.

[98] S. Bertollini, T. Schwetz, M. Malinsky, fermion masses and mixings in SO(10) models and the neutrino challenge to supersymmetric grand unified theories, Phys. Rev. D, **73** (2006) 115012.

[99] C. S. Aulakh, S. K. Garg, The new minimal supersymmetric GUT: spectra, RG analysis and fermion fits, Nucl. Phys. B, **857** (2012) 101, arxiv.0807.0917[hep-ph].

[100] D. Chang, R. N. Mohapatra, Comment on the seesaw mechanisms for small neutrino masses, Phys. Rev. D, **32** (1985) 1248.

[101] H. Nishino and others, Search for Nucleon Decay into Charged Anti-lepton plus Meson in Super-Kamiokande I and II, Super-Kamiokande collaboration, Phys. Rev. D, **85** (2012) 112001, aXiv:1203.4030 [hep-ph].

[102] Jennifer L. Raaf, Recent Nucleon Decay Results from Super-Kamiokande, Super-Kamiokande Collaboration, Nucl. Phys. Proc. Suppl. 229-232, (2012) 559.

[103] J.L. Hewett and H. Weerts and R. Brock, and J.N. Butler,and B.C.K. Casey, and others, Fundamental Physics at the Intensity Frontier, (2012), FERMILAB-CONF-12-879-PPD, arXiv:1205.2671 [hep-ex].

[104] K.S. Babu and E. Kearns and U. Al-Binni and S. Banerjee and D.V. Baxter and others, Baryon Nunber Violation, (2013), arXiv:1311.5285[hep-ph].

[105] P. Langacker, The physics of heavy Z' gauge bosons, Rev. Mod. Phys., **81** (2009) 1199, arXiv:0801.1345[hep-ph].

[106] P. Langacker, R. W. Robinet, J. L. Rosner, New heavy gauge bosons in PP and P anti P collisions, Phys. Rev. D, **30** (1984) 1470.

[107] P. Langacker, Bounds on mixing between light and heavy gauge bosons, Phys. Rev. D, **30** (1984) 2008.

[108] J. Erler, P. Langacker, S. Munir, and E. Roja, Improved constraints on Z' bosons from electroweak precision data, JHEP, **08** (2009) 017; arXiv:0906.2435[hep-ph].

[109] J. Erler and P. Langacker, Z bosons from E(6): collider and electroweak constraints, arXiv:1108.0685[hep-ph].

[110] M. -C Chen, B. A. Dobrescu, FERMILAB-PUB-08-676-T.

[111] A. Cakir, Prospects of new physics searches using high Lumi-LHC, arXiv:1412.8503.

[112] CMS Collaboration, V. Khachatryan et al., Search for physics beyond the standard model in dilepton mass spectra in proton-proton collision at $\sqrt{s} = 8$ TeV, JHEP, **04** (2015) 025, arXiv:1412.6302[hep-ex].

[113] A. E. Faraggi, M. Guzzi, Extra Z's and Ws in heteotic-string deived models, arXiv: 1507.07406.

[114] A. E. Faraggi, J. Rizos, A light Z' heterotic-string derived model, Nucl. Phys. B, **895** (2015) 233.

[115] Paul. Langacker,The Physics of New U$(1)'$ Gauge Bosons, AIP Conf.Proc.1200, (2010) 55-63,arXiv:0909.3260[hep-ph].

[116] For earlier work on Z' boson in GUTs embedding two-step breaking of left-right gauge symmetry, see M. K. Parida, A. Raychaudhuri, Low-mass parity restoration, weak-interaction phenomenology, and grand unification, Phys. Rev. D, **26** (1982) 2364.

[117] M. K. Parida, C. C. Hazra, Are N Anti- oscillation and proton decay mutually exclusive, Phys. Lett. B, **121** (1983) 355.

[118] M. K. Parida, C. C. Hazra, Superheavy Higgs scalar effects in effective gauge theories from SO(10) grand unification with low mass right-handed gauge bosons, Phys. Rev. D, **40** (1989) 3074.

[119] O.J.P. Eboli and J. Gonzalez-Fraile, and M.C. Gonzalez-Garcia, Present Bounds on New Neutral Vector Resonances from Electroweak Gauge Boson Pair Production at the LHC, Phys.Rev. D, **85** (2012) 055019, arXiv:1112.0316[hep-ph].

[120] A. Falkowski and C. Grojean and A. Kamiska and S. Pokorski and A. Weiler, If no Higgs then what?, JHEP, **111** (2011) 028, arXiv:1108.1183[hep-ph].

[121] Guido Altarelli, The Standard model and beyond, Nucl. Phys. B - Proceedings Supplements, **75** (1999) 37-45, arXiv:hep-ph/9809532.

[122] F. Capozzi, G. L. Fogli, G.L. and E. Lisi,and A. Marrone, and D. Montanino and others, Status of three-neutrino oscillation parameters, circa 2013, (2013), arXiv:1312.2878[hep-ph].

[123] G. L. Fogli, E. Lissi, and A. Marrone and A. Melchiorri and A. Palazzo and others, Observables sensitive to absolute neutrino masses. II,Phys.Rev. D, **78** (2008) 033010, arXiv:0805.2517 [hep-ph].

[124] J. Beringer et. al., Review of Particle Physics, 2012-2013. Review of Particle Properties, Phys. Rev. D, **86** (2012) 010001, Particle Data Group. Berkeley.

[125] A. D. Sakharov, Violation of CP Invariance, CP Asymmetry, and Baryon Asymmetry of the Universe, Pisma Zh.Eksp.Teor.Fiz.5, (1967), 32-35.

[126] Andrew G. Cohen and D.B. Kaplan and A.E. Nelson, Progress in electroweak baryogenesis, Ann. Rev. Nucl. Part. Sci., **43** (1993) 27-70,arXiv: hep-ph/9302210.

[127] M. Quiros, Field theory at finite temperature and phase transitions, Helv.Phys.Acta, **67** (1994) 451-583.

[128] V. A. Rubakov and M. E. Shaposhnikov, Electroweak baryon number nonconservation in the early universe and in high-energy collisions, Usp. Fiz. Nauk, **166** (1996) 493-537, arXiv: hep-ph/9603208.

[129] Marcela S. Carena and M. Quiros and C.E.M. Wagner, Electroweak baryogenesis and Higgs and stop searches at LEP and the Tevatron, Nucl. Phys. B, **524** (1998) 3-22, arXiv: hep-ph/9710401.

[130] Gunter Sigl, Ultrahigh-energy cosmic rays: A Probe of physics and astrophysics at extreme energies, Science, **291** (2001) 73-79, astro-ph/0104291.

[131] D.R.T. Jones, Two Loop Diagrams in Yang-Mills Theory, Nucl. Phys. B, **75** (1974) 531.

[132] D.R.T. Jones, The Two Loop beta Function for a $G(1) \times G(2)$ Gauge Theory, Phys. Rev. D, **25** (1982) 581.

[133] Amol Dighe and Diptimoy Ghosh and Ketan M. Patel and Sreerup Raychoudhuri, Testing Times for Supersymmetry: Looking Under the Lamp Post, Int. J. Mod. Phys. A, **28** (2013) 1350134, arXiv:1303.0721 [hep-ph].

[134] Paul Langacker, The Standard Model and Beyond, CRC Press, New York (2009).

[135] Paul Langacker, Grand Unified Theories and Proton Decay, Phys.Rept., **72** (1981) 185.

[136] Li Ling-Fong, Group Theory of the Spontaneously Broken Gauge Symmetries, Phys. Rev. D, **9** (1974) 1723.

[137] V. Elias, S. Eliezer,and A. R. Swift, Comment on Group Theory of the Spontaneously Broken Gauge Symmetries, Phys. Rev. D, **12** (1975) 3356.

[138] R. N. Mohapatra, Unification and Supersymmetry:The Frontiers of Quark-Lepton Physics, 2002, Springer, New York.

[139] H. Georgi, Lie Algebras In Particle Physics: From Isospin To Unified Theories, 1999, Frontiers in Physics, Westview Press, New York.

[140] Graham G. Ross, Grand Unified Theories, 1984, Frontiers in Physics, Westview Press,New York.

[141] Borut Bajc, Grand Unification and Proton Decay,Lectures given in ICTP summer school on Particle Physics (2011).

[142] Savas Dimopoulos, Howard Georgi, Softly Broken Supersymmetry and SU(5), Nucl. Phys. B, **193** (1981) 150.

[143] N. Sakai, Naturalness in Supersymmetric Guts, Z. Phys. C, **11** (1981) 153.

[144] Borut Bajc and Goran Senjanovic, Seesaw at LHC, JHEP, **0708** (2007) 014, arXiv:hep-ph/0612029.

[145] Borut Bajc and Miha Nemevsek and Goran Senjanovic, Probing seesaw at LHC, Phys. Rev. D, **76** (2007) 055011, arXiv:hep-ph/0703080.

[146] P. Nath, P. F. Perez, Proton stability in grand unified theories, in strings and in branes, Phys. Rept., 441 (2007) 191.

[147] Rabindra N. Mohapatra and B. Sakita, SO(2n) Grand Unification in an SU(N) Basis, Phys. Rev. D, **21** (1989) 1062.

[148] Pran Nath and Raza M. Syed, Analysis of couplings with large tensor representations in SO(2N) and proton decay, Phys. Lett. B, **506** (2001) 68-76, arXiv:hep-ph/0103165.

[149] K.S. Babu and Ernest Ma, Symmetry Breaking in SO(10): Higgs Boson Structure, Phys. Rev. D, **31** (1985) 2316.

[150] Masaki Yasue, How to break SO(10) via $SO(4) \times SO(6)$ down to $SU(2)_L \times SU(3)_C \times U(1)$, Phys. Lett. B, **103** (1981) 33.

[151] Masaki Yasue, Symmetry Breaking of SO(10) and Constraints on Higgs Potential. 1. Adjoint (45) and Spinorial (16), Phys. Rev. D, **24** (1981) 1005.

[152] Charanjit S. Aulakh and Aarti Girdhar, SO(10) a la Pati-Salam, Int. J. Mod. Phys. A, **20** (2005) 865-894, arXiv:hep-ph/0204097.

[153] Takeshi Fukuyama and Amon Ilakovac and Tatsuru Kikuchi, and Stjepan Meljanac and Nobuchika Okada, SO(10) group theory for the unified model building, J. Math. Phys., **46** (2005) 033505, arXiv: hep-ph/0405300.

[154] D. Chang and A. Kumar, Symmetry Breaking of SO(10) by 210-dimensional Higgs Boson and the Michel's Conjecture, Phys. Rev. D, **33** (1986) 2695.

[155] R.Slansky, Group Theory for Unified Model Building, Phys. Rept., **79** (1981) 1-128.

[156] John M. Gipson and R.E. Marshak, Intermediate Mass Scales in the New SO(10) Grand Unification in the One Loop Approximation, Phys. Rev. D, **31** (1985) 1705.

[157] Stefano Bertolini and Luca Di Luzio and Michal Malinsky, Intermediate mass scales in the non-supersymmetric SO(10) grand unification: A Reappraisal, Phys. Rev. D, **80** (2009) 015013, arXiv:0903.4049 [hep-ph].

[158] Stephen M. Barr, A New Symmetry Breaking Pattern for SO(10) and Proton Decay, Phys. Lett. B, **112** (1982) 219.

[159] Howard Georgi and Dimitri V. Nanopoulos, Ordinary Predictions from Grand Principles: T Quark Mass in O(10), Nucl. Phys. B, **155** (1979) 52.

[160] Steven Weinberg, Baryon and Lepton Nonconserving Processes, Phys. Rev. Lett., **43** (1979) 1566-1570.

[161] Peter Minkowski, $\mu \to e\gamma$ at a Rate of One Out of 1-Billion Muon Decays?, Phys. Lett. B, **67** (1977) 421.

[162] R. Foot, H. Lew, X. G. He, G. C. Joshi, See-saw neutrino masses induced by a triplet of leptons, Z. Phys. C, **44** (1989) 441.

[163] For more recent reviews see G. Altarelli, Neutrinos Today: An Introduction, in Proceedings: 49th Recontres de Moriond on Electroweak Interactons and Unified Theories, Thuile, Italy, March 15-22, (2014).

[164] A. Yu. Smirnov, Theories of Neutrino Masses and Mixings, Nuovo Cim.C, **037** (2014) no.3, 29-37.

[165] G. Senjanovic, Origin of Neutrino Mass, Pos PLANCK2015 (2016) 141; R. N. Mohapatra, From Old Symmetries to New Symmetries: Quarks, Leptons, and B-L, in "50 Years of Quarks" pp 245-263 (World Scientific, 2015).

[166] R. N. Mohapatra, Neutrino Mass as a Signal for TeV Scale Physics, Nucl. Phys. B, **908** (2016) 423-435.

[167] J. W. F. Valle, Status and Implications of Neutrino Mass: A Brief Panorama, Int. J. Mod. Phys. A, **30** (2015) **no.3** 1530034.

[168] O. G. Miranda, J. W. F. Valle, Neutrino Oscillation and Seesaw Origin of Neutrino Masses, Nucl. Phys. B, **908** (2016) 436-455.

[169] H. Georgi, Unified Gauge Theories, In *Coral Gables 1975, Proceedings, Theories and Experiments In High Energy Physics*, New York 1975, 329-339.

[170] H. Fritzsch and P. Minkowski, Unified Interactions of Leptons and Hadrons, Annals Phys. **93** (1975) 193.

[171] X. Chu, A. Yu Smirnov, Neutrino mixing and masses in SO(10) GUTs with hidden sector and flavor symmetries, JHEP, **1605** (2016) 135; arXiv:1604.03977.

[172] M. K. Parida, Intermediate left-right gauge symmetry, unification of couplings and fermion masses in SUSY SO(10)XS(4), Phys. Rev. D, **78** (2008) 053004, arXiv:0804.4571[hep-ph].

[173] M. K. Parida, K. Bora, P. K. Sahu, Flavor unification, dark matter, proton decay and other observable predictions with low-scale S(4) symmetry, Phys. Rev. D, **83** (2011) 093004, arXiv:1011.4577.

[174] C. Hagedorn, T. Ohlsson, S. Riad, M. A. Schmidt, Unification of gauge couplings in radiative neutrino mass models, JHEP, **09** (2016) 111, arXiv: 1605.03986.

[175] M. Kadastic, K. Kanike, M. Raidal, Dark matter as the signal of grand unification, Phys. Rev. D, **80** (2009) 085020; Erratum: Phys. Rev. **D 81** (2010) 029903.

[176] M. Kadastic, K. Kanike, M. Raidal, Phys. Rev. D, **81** (2010) 015902.

[177] T. Hambye, On the stability of particle dark matter, arXiv:1012.4587.

[178] M. Frigerio, T. Hambye, Dark matter stability and unification without supersymmetry, Phys. Rev. D, **81** (2010) 075002.

[179] Y. Mambrini, M. Nagata, K. Olive, J. Quevillon, J. Zhang, Phys. Rev. D, **91** (2015) **no.9** 09500

[180] J. Schecter, J. W. F. Valle, Neutrinoless double beta decay in $SU(2) \times U(1)$ theories, Phys. Rev. D, **25** (1982) 2951.

[181] R. N. Mohapatra, Neutrino mass as a signal of TeV scale physics, Nucl. Phys. B, **908** (2016) 423-435.

[182] J. C. Helo, M. Hirsch, S. Kovalenko, Heavy neutrino searches at LHC with displaced vertices, Phys. Rev. D, **89** (2014) 073005, arXiv:1312.2900 [hep-ph].

[183] S. Antusch, E. Cazzato, O. Fischer, Displaced vertex searches for sterile neutrinos at future lepton colliders, arXiv:1604.02420[hep-ph].

[184] Bidyut Prava Nayak, M. K. Parida, Dilepton events with displaced vertices, double beta decay, and type-II seesaw dominance, TeV scale Z' and heavy neutrinos, arXiv:1509.06192 and references therein.

[185] S. Antusch, J. P. Baumann, and E. Fernandez-Martinez, Non-standard neutrino interactions with matter from physics beyond the standard model, Nucl. Phys. B, **180** (2009) 369, arXiv:0807.1003[hep-ph].

[186] S. Antush, C. Biggio, E. Fernandez-Martinez, M. Belen Gavela, J. Lopez-Pavon, Unitarity of the leptonic mixing matrix, J. High Energy Phys., **10** (2006) 084, arXiv:hep-ph/0607020.

[187] D.V. Forero, S. Morisi, M. Tartola and J. W. F. Valle, Lepton flavour violation and non-unitarity lepton mixing in low scale type-I seesaw, J. High Energy Phys., **09** (2011) 142, arXiv:1107.6009[hep-ph].

[188] B. Dutta, R. N. Mohapatra, Lepton flavor violation and neutrino mixings in 3X2 seesaw model, Phys. Rev. D, **68** (2003) 056006, hep-ph/0305059.

[189] A. Pilaftsis, T. E. J. Underwood, Resonant leptogenesis, Nucl. Phys. B, **692** (2004) 303, hep-ph/0309342.

[190] J. Kersten, A. Yu. M. Smirnov, Right-handed neutrinos at LHC and the mechanism of neutrini mass generation, Phys. Rev. D, **76** (2007) 073005, arXiv:0705.3522[hep-ph].

[191] C. H. Lee, P.S. Bhupal Dev, R. N. Mohapatra, Natural TeV scale left-right seesaw mechanism for neutrinos and experimental tests, Phys. Rev. D, **88** (2013) 093010, arXiv:1309.0774[hep-ph].

[192] Carl H. Albright, S.M. Barr, Leptogenesis in type-III seesaw mechanism, Phys. Rev. D, **69** (2004) 073010, arXiv:hep-ph/0312224.

[193] C. H. Albright, S. M. Barr, Predicying quark and lepton masses ad mixings, Phys. Lett. B, **452** (1999) 287.

[194] C. H. Albright, K. S. Babu, S. M. Barr, A minimality condition and atmospheric neutrino oscillations, Phys. Rev. Lett., **81** (1998) 1167.

[195] P -H. Gu, M. Hirsch, U. Sarkar, J. W. F. Valle, Neutrino masses.leptogenesis and dark matter in hybrid seesaw, Phys. Rev.D, **79** (2009) 03310, arXiv:0811.0953.

[196] S. Goswami, S. Khan, A. Watanabe, Neutrino model, leptogenesis and dark matter in hybrid seesaw, Phys. Lett. B, **693** (2010) 249, arXiv:0811.4744.

[197] Shao-Long Chen, M. Frigerio, E. Ma, Hybrid seesaw neutrino masses with A_4 family symmetry, Nucl. Phys. B, **724** (2005) 423, hep-ph/0504181.

[198] P. -H. Gu, U. Sarkar, Leptogenesis with linear, inverse or double seesaw, Phys. Lett. B, **694** (2011) 226, arXiv:1007.2323[hep-ph].

[199] M. Hirsch, S. Morisi, J. W. F. Valle, A4 based tri-bimaximal mixing within inverse and linear seesaw, Phys. Lett. B, **679** (2009) 454, arXiv:0905.3056[hep-ph].

[200] J. Chakrabortty, A. S. Joshipura, P. Mehta, S. K. Vempati, Conf. Proc. **C0908171** (2010) 493.

[201] F. P. Deppisch, W. -C. Huang, Dark matter and leptogenesis in a hybrid neutrino mass model, JHEP, **1501** (2015) 066; arXiv:1411.2922[hep-ph].

[202] S. T. Petcov, W. Rodejohann, T. Shindou, Y. Takanishi, The seesaw mechanism, neutrino Yukawa couplings, LFV decays l(i) $\rightarrow$ l(j)+gamma and leptogenesis, Nucl. Phys. B, **739** (2006) 208, hep-ph/0510404.

[203] Chien-Yi Chen, P. S. Bhupal Dev, R. N. Mohapatra, Probing heavy-light neutrino mixing in left-right seesaw models at the LHC, Phys. Rev. D, **88** (2013) 033014.

[204] S. N. Gninenko. D. S. Gorbunov, M. E. Shaposhnikov, Search for GeV scale sterile neutrinos responsible for active eutrino oscillations and baryon asymmetry of the universe, Adv. High Enegy Phys. **2012** (2012) 718259.

[205] L. Canetti, M. Drewes, M. Shaposhnikov, Sterile neutrinos as the origin of dark and baryonic matter, Phys. Rev. Lett. **110** (2013) no.6 061801, arXiv:1204.3902[hep-ph].

[206] L. Canetti, M. Drewes, T. Hochsch, T. Frossard, M. Shaposhnikov, Dark matter, baryogenesis and neutrino oscillations from right handed neutrinos, Phys. Rev. D, **D 87** (2013) 093008, arXiv:1208.4607[hep-ph].

[207] Shao-Long Chen, R. N. Mohapatra, S. Nussinov, R-parity breaking via type-II seesaw, decaying gravitino dark matter and PAMELA positron excess, Phys. Lett. B, **677** (2009) 311, arXiv:0903.2562[hep-ph].

[208] B. P. Nayak, M. K. Parida, New mechanism for Type-II seesaw dominance in SO(10) with low mass Z', RH neutrinos,and verifiable LFV, LNV and proton decay, Eur. Phys. J. C, **75** (2015) 183, arXiv:1312.3185 .

[209] B. P. Nayak, M. K. Parida, Singlet fermion assisted dominant seesaw with lepton flavor, and number violation, and leptogenesis, Adv. High Energy Phys. 2017 **4023493**, arXiv:1607.07236[hep-ph].

[210] A. Melfo, M. Nemevsek, F. Nesti, G. Senjanovic, Y. Zhang, Type-II seesaw at LHC: the roadmap, Phys. Rev. D, **85** (2012) 055018, arXiv:1108.4416.

[211] G. Bambhaniya, P. S. Bhupal Dev, S. Goswami, The scalar triplet contribution to lepton flavor violation and neutrinoless double beta decay in left-right symmetric model, JHEP, **1604** (2016) 046.

[212] R.N. Mohapatra, J. W. F. Valle, Neutrino mass and baryon number nonconservation in superstring models, Phys. Rev. D, **34** (1986) 1642 .

[213] R. N. Mohapatra, Mechanism of understanding small neutrino masses in superstring theories, Phys. Rev. Lett., **56** (1986) 561.

[214] R. N. Mohapatra, Status of neutrino masses in supersymmetric and superstring theories, Presented at conference **C 86-06-11** (Osaka Beta Symposium 1986:0042).

[215] R. N. Mohapatra, Small neutrino masses in gauge theories", Published in HEIDELBERG 1987, PROCEEDINGS NEUTRINO PHYSICS 27-43 (1987).

[216] C. H. Albright, search for solutions of superstring neutrino mass problem, Phys. Lett. B, **178** (1986) 219.

[217] E. Witten, New issues in manifolds with SU(3) holonomy, Nucl. Phys. B, **268** (1986) 79.

[218] S. Nandi, U. Sarkar, A solution to neutrino mass problem in superstring E_6 theory, Phys. Rev. Lett., **56** (1986) 564.

[219] J. W. F. Valle, Gauge theories and the physics of neutrino mass, Prog. Part. Nucl. Phys., **26** (1991) 91-171.

[220] D. Wyler, L. Wolfenstein, Massless neutrinos in left-right symmetric models, Nucl. Phys. B, **218** (1983) 205.

[221] J. Bernabeau, A. Santamaria, J. Vidal, A. Mendez, J. W. F. Valle, Lepton flavor nonconservation at high energies in a superstring inspired standard model, Phys. Lett. B, **187** (1987) 303.

[222] E. Ma, Lepton number nonconservation in E(6) inspired superstring models, Phys. Lett. B, **191** (1987) 287.

[223] J. Adam *et al.* (MEG Collaboration), New limit on the lepton flavour violating decay $\mu \to$ e gamma, Phys. Rev. Lett., **107** (2011) 171801, arxiv: 1107.5547[hep-ex].

[224] K. Hayasaka *et al,* (Belle Collaboration), New search for tau $\to \mu$ gamma and tau $\to$ e gamma decay at Belle, Phys. Lett. B, **666** (2008) 16, arxiv:0705.0650 [hep-ex].

[225] U. Bellgardt *et al.*, (SINDRUM Collaboration), Search for the decay $\mu^+ \rightarrow e^+e^+e^-$, Nucl. Phys. B, **299** (1988) 1.

[226] W. H. Bertl *et al.*, (SINDRUM II Collaboration), A search for μ-e conversion in muonic gold, Eur. Phys. J. C, **47** (2006) 337.

[227] M. L. Brooks et al. (MEG Collaboration), Phys. Rev. Lett., **83** (1999) 1521.

[228] Y. Kuno (PRIME Working Group), Nucl. Phys. B. Proc. Suppl. **149** (2005) 376.

[229] For a review of earlier results see F. R. Joaquim, A. Rossi, Nucl. Phys. B, **765**, (2007) 71.

[230] J. Adam *et al.*,(MEG Collaboration), New constraint on the existence of $\mu^+ \rightarrow e^+$ gamma decay, Phys. Rev. Lett., **110** (2013) 201801, arXiv:1303.0754.

[231] A. M. Baldini *et al.*, (MEG Collaboration), Search for the lepton flavor violating decay $\mu^+ \rightarrow e^+\gamma$ with the full dataset of the MEG experiment, Eur. Phys. J. C, **76** (2016) no.8 434 arXiv:1605.05081.

[232] B. Aubert *et al.* (BABAR Collaboration), Search for lepton flavor violation in the decays $\tau \rightarrow e\gamma$ and $\tau \rightarrow \mu\gamma$, Phys. Rev. Lett., **104** (2010) 021802, arXiv:0908.2381.

[233] R. H. Bernstein, P. S. Cooper, Charged lepton flavor violation: An experimenter's guide, Phys. Rept., **532**, (2013) 27, arXiv:1307.5687.

[234] S. K. Kang and C. S. Kim, Extended double seesaw model for neutrino mass spectrum and low scale leptogenesis, Phys. Lett. B, **646** (2007) 248, arXiv:hep-ph/0607072.

[235] J. Ellis, D. V. Nanopoulos and K. Olive, Flipped heavy neutrinos from the solar neutrino problem to baryogenesis, Phys. Lett. B, **300** (1993) 121, arXiv:hep-ph/9211325 .

[236] H. S. Cheon, S. K. Kang, C. S. Kim, Low scale leptogeesis and dak matter candidates in an extended seesaw model, JCAP, **0805:004** (2009), arXiv:0710.2416v4 [hep-ph].

[237] H. S. Cheon, S. K. Kang, C. S. Kim, Phys. Lett. B, **675** (2009) 203-209.

[238] S. K. Kang, A. Patra, KeV sterile neutrino dark matter ad low scale leptogenesis, arXiv:1412.4899v2 [hep-ph].

[239] S. K. Majee, M. K. Parida, and A. Raychaudhuri, Neutrino mass and low scale leptogenesis in a testable SUSY SO(10) model, Phys. Lett., **668** (2008) 299.

[240] M. K. Parida and A. Raychaudhuri, Inverse seesaw, leptogenesis, observable proton decay and Δ_R^{++}in SUSY SO(10) with heavy W_R, Phys. Rev. D, **82** (2010) 093017, arXiv:1007.5085[hep-ph].

[241] S. K. Majee, M. K. Parida, A. Raychaudhuri, and U. Sarkar, Low intermediate scales for leptogenesis in supersymmetic SO(10) grand unified theories, Phys. Rev. **D 75**, (2007) 075003.

[242] M. K. Parida, S. Patra, Left-right models with light neutrino mass prediction and dominant neutrinoless double beta decay rate, Phys. Lett. B, **718** (2013) 1407-1412, arXiv:1211.5000[hep-ph].

[243] M. K. Parida, B. Sahoo, Planck-scale induced left-right gauge theory at LHC and experimental tests, Nucl. Phys. B, **906** (2016) 77-104, arXiv:1411.6748[hep-ph].

[244] B. Sahoo, M. K. Parida, Low mass right-handed gauge bosons from minimal grand unified theories, Nucl. Part. Phys. Proc. **273-275** (2015) 2672-2644, arXiv:1510.01096.

[245] E. Akhmedov, M. Lindner, E. Schnapka, J. W. F. Valle, Dynamical left-right symmetry breaking, Phys. Rev. D, **53** (1996) 2752, hep-ph/9509255.

[246] E. Kh. Akhmedov, A. S. Josipura, S. Ranfone, J. W. F. Valle, Nucl. Phys. B, **441** (1995) 61.(LRS model with additional spontaneously broken U(1) global symmetry: $\nu_\tau \to \nu + J(Majoron)$ leading to nonvanishing m_{nu} (due to S-ν mixing . Gives low W_R scale. Charged LFV Majoron decays: Br.$(l_i \to l_j + J) > 10^{-4} - 10^{-6}$).

[247] S. Morisi, J. W. F. Valle, Neutrino masses and mixing: a flavor symmetry roadmap, Fortsch. Phys., **61** (2013) 466-492, arXiv:1206.6678.

[248] F. Deppisch, Lepton flavor violation and flavor symmetries, Fortsch. Phys., **61** (2013) 622, arXiv:1206.5212[hep-ph].

[249] A. de Gouvea, P. Vogel, Lepton Flavor and Number Conservation Beyond the Standard Model, Prog. Part. Nucl. Phys., **71** (2013) 75, arXiv:1303.4097[hep-ph].

[250] S. Boucenna, S. Morisi, J. W. V. F. Valle, The low scale approach to neutrino masses, Adv. High Energy Physics, **2014** (2014) 831598, arXiv:1404.3751[hep-ph]

[251] F. Deppisch, Neutrino physics and LHC physics, Acta Phys. Polon. B, **46** (2015) **no.11** 2301.

[252] F. Deppisch, Neutrinos and coliider physics, New J. Phys., **17** (2015) **no.3** 036005, arXiv:1502.06541[hep-ph].

[253] A. Joshipura, J. W. F. Valle, Invisible Higgs decays and neutrino physics, Nucl. Phys. B, **397** (1993) 105.

[254] M. Diaz, M. Garcia-Jarena, D. Restrepo, J. W. F. Valle, Seesaw Majoron model of neutrino mass and novel signals in Higgs boson production at LEP, Nucl. Phys. B, **527** (1998) 44, hep-ph/9803362.

[255] C. Bonilla, J. W. F. Valle, J. C. Romao, Neutrino mass and invisible Higgs decays at the LHC, Phys. Rev. D, **91 no.11** (2015) 113015, arXiv:1502.01649[hep-ph].

[256] J. Heeck, Interpretation of Lepton Flavor Violtion, arXiv:1610.07623[hep-ph].

[257] F. Deppisch, J. W. F. Valle, Enhanced lepton flavor violation in supersymmetric inverse seesaw model, Phys. Rev. D, **76** (2005) 036001, hep-ph/0406040.

[258] F. Deppisch, T. Kosmas, J. W. F. Valle, Enhanced $\mu - e$-conversion in nuclei in the inverse seesaw model, Nucl. Phys. B, **752** (2006) 80, hep-ph/0512360.

[259] F. Deppisch, N. Desai, J. W. F. Valle, Is charged lepton flavor violation a high-energy phenomenon, Phys. Rev. D, **89** (2013) 051302(R), arXiv:1308.6789[hep-ph].

[260] J. Garoya, M. C. Gonjalez-Gartia, and N. Rius, J. High Energy Phys., **02** (2007) 021.

[261] C. Arina, F. Bazzochi, N. Forengo, J. C. Romao, and J. W. F. Valle, Minimal supergravity sneutrino dark matter and inverse seesaw neutrino masses, Phys. Rev. Lett., **101** (2008) 161802, arXiv:0806.3225[hep-ph].

[262] M. Malinsky, T. Ohlsson, Z. -z. Xing, and H. Zhang, Phys. Lett. B, **679**1 (2009) 242.

[263] A. Abada, M. E. Krauss, W. Porod, F. Staub, A. Vicente, C. Weiland, Lepton flavor violation in low-scale seesaw model: SUSY and non-SUSY contributions, JHEP, **11** (2014) 048, arXiv:1408.0138[hep-ph].

[264] S. Boucenna, J. W. F. Valle, A. Vicente, Predicting chrged lepton flavor violation from 3-3-1 gauge symmetry, Phys. Rev. D, **92** (2015) no.5 053001, arXiv:1502.077546[hep-ph].

[265] V. Cirigliano, A. Kurylov, M. J. Ramsey-Musolf, P. Vogel, Neutrinoless double beta decay and lepton flavor violation, Phys. Rev. Lett., **93** (2004) 231802.

[266] M. E. Peskin, T. Takeuchi, New constraint on a strongly interacting Higgs sector, Phys. Rev. Lett., **65** (1990) 964; Estimation of oblique electroweak corrections, Phys. Rev. D, **46** (1992) 381.

[267] G. Altarelli, R. Barbieri, Vacuum polarization effects of new physics on electroweak processes, Phys. Lett. B, **253** (1991) 161.

[268] A. Kumar, R. N. Mohapatra, A model for neutrino decays, Phys. Lett. B, **150** (1995) 191.

[269] E. Akhmedov, M. Lindner, E. Schnapka, J. W. F. Valle, Left-right symmetry breaking in NJL approach, Phys. Lett. B, **368** (1996) 270, hep-ph/9507275.

[270] S. M. Barr, A different seesaw formula for neutrino masses, Phys. Rev. Lett., **92** (2004) 101601, hep-ph/0309152.

[271] S. M. Barr, B. Kyae, A general analysis of corrections to standard seesaw formulas in grand unified models, Phys. Rev. D, **70** (2004) 075005, arXiv:hep-ph/0407154.

[272] T. Fukuyama, T. Kikuchi, T. Osaka, J. Cosmol. Astropart. Phys. **0703** (2007) 018.

[273] E. A. Garces, O. Miranda, M. Tartola, J. W. F. Valle, Low-energy neutrino-electron scattering as a standard model probe: The potential of LENA as case study, Phys. Rev. D, **85** (2012) 073006, arXiv:1112.3633[hep-ph].

[274] M. Malinsky, J. C. Romao, J. W. F. Valle, Novel supersymmetric SO(10) seesaw mechanism, Phys. Rev. Lett., **95** (2005) 161801, arXiv:hep-ph/0506296.

[275] A. Das, N. Okada, Inverse seesaw neutrino ignatures at LHC and ILC, Phys. Rev. D, **88** (2013) 113001, arXiv:1207.3734.

[276] A. Vicente, Lepton flavor violation in SUSY left-right symmetric theories, J. Phys. Conf. Ser. **259** (2010) 012065, arXiv:1010.0799[hep-ph].

[277] A. Abada, M. Lucente, Looking for the minimal inverse seesaw realisation, Nucl. Phys. B, **885** (2014) 651, arXiv:1401.1507[hep-ph].

[278] C. Weiland, Effects of fermionic singlet neutrinos on high- and low-energy observables, Ph. D. Thesis, arXiv:1311.5860[hep-ph].

[279] M. Lindner, M. Platscher, F. Queiroz , A call for new physics: The muon magnetic moment, and lepton flavor violation, arXiv:1610.06587[hep-ph].(both in SM and LRS extn, MSSM)

[280] C. Bonilla, M. E. Krauss, T. Opterkuch, W. Porod, Perspectives of detecting lepton flavor violation in left-right symmetric models, JHEP, **1703** (2017) 027, arXiv:1611.07025[hep-ph].

[281] E. Ma, U. Sarkar, Neutrino masses and leptogenesis with heavy Higgs triplet, Phys. Rev. Lett., **80** (1998) 5716, hep-ph/9802445.

[282] E. Ma, Neutrino mass from triplet and doublet scalars at the TeV scale, Phys. Rev. D, **66** (2002) 037301, arXiv:hep-ph/0204013.

[283] T. Hambye, E. Ma, U. Sarkar, Supersymmetric triplet Higgs model of neutrino masses and leptogenesis, Nucl. Phys. B, **602** (2001) 23.

[284] R. N. Mohapatra, M. K. Parida, and G. Rajasekaran, High scale mixing unification and large neutrino mixing angles, Phys. Rev. D, **72** (2004) 013002.

[285] B. Bajc, G. Senjanovic, F. Vissani, b-tau unification and large atmospheric mixing: a case for non-canonical see-saw, Phys. Rev. Lett., **90** (2003) 051802.

[286] H. S. Goh, R. N. Mohapatra, S. P. Ng, Minimal SUSY SO(10) model and predictions for neutrino mixings and leptonic CP violation, Phys. Rev. D, **68** (2003) 11508.

[287] P. S. Bhupal Dev, B. Dutta, R. N. Mohapatra, M. Severson,θ_{13} and Proton Decay in a Minimal SO(10) $\times S_4$ model of Flavor, Phys. Rev. D, **86** (2012) 035002, arxiv:1202.4012 [hep-ph].

[288] W. Grimus, L. Lavoura, The seesaw mechanism at arbitrary order: disentangling the small scale from the large scale, JHEP, **0011** (2000) 042, arXiv:0008179 [hep-ph].

[289] M. Mitra, G. Senjanovic, F. Vissani, Neutrinoless double beta decay and heavy sterile neutrinos, Nucl. Phys. B, **856** (2012) 26, arXiv:1108.0004 [hep-ph].

[290] M. Hirsch, H. V. Klapdor-Kleingrothaus, O. Panella, Double beta decay in left-right symmetric models, Phys. Lett. B, **374** (1996) 7, arXiv: 9602306 [hep-ph].

[291] S. Pascoli, M.Mitra, Steven Wong, The effect of cancellation in neutrinoless double beta decay, Phys. Rev. D, **90** (2014) 093005, arxiv:1310.6218 [hep-ph].

[292] S. Blanchet, P. S. Bhupal Dev, R. N. Mohapatra, Leptogenesis with TeV scale inverse seesaw model in SO(10), Phys. Rev. D, **82** (2010) 115025.

[293] M. Lindner, M. A. Schmidt, A. Yu. Smirnov, Screening of Dirac flavor structure in the seesaw and neutrino mixing, JHEP, **0507** (2005) 048, hep-ph/0505067.

[294] G. 't Hooft, in Proceedings of the 1979 Cargese Summer Institute on Recent Developments in Gauge Theories, edited by G. t Hooft et al. (Plenum Press, New York, 1980).

[295] M. B. Gavela, T. Hambye, D. Hernandez, P. Hernandez, Minimal flavour seesaw models, J. High Energy Phys., **09** (2009) 038, arXiv:0906.1461[hep-ph].

[296] A. Das, N. Okada, Inverse seesaw neutrino signatures at the LHC and ILC, Phys. Rev. D, **88** (2013) 103001, arXiv:1207.3734[hep-ph].

[297] P. S. Bhupal Dev, A. Pilaftsis, Minimal radiative neutrino mass mechanism for inverse seesaw models, Phys. Rev. D, **86** (2012) 113001, arxiv:1209.4051 [hep-ph].

[298] A. Das, P. S. Bhupal Dev, N. Okada, Direct bounds on electroweak scale pseudo-Dirac neutrinos from $\sqrt{s}$= 8 TeV LHC data, Phys. Lett. B, **735** (2014) 364, arXiv:1405.0177[hep-ph].

[299] G. L. Fogli, E. Lisi, A. Marrone, A. Palazzo, and A. M. Rotuno, Nucl. Phys. B. Proc. Suppl., **188** (2009) 27.

[300] T. Schwetz, M. Tartola and J. W. F. Valle, here we are on θ_{13} :addendum to global neutrino data and recent reactor fluxes: status of three-flavour oscillation parameters, New J. Phys., **13** (2011) 063004, arXiv:hp-ph/1108.1376.

[301] D. V. Forero, M. Tartola and J. W. F. Valle, Global status of neutrino oscillation parameter after neutrino-2012, Phys. Rev.D, **86** (2013) 073012, arXiv:1205.4018[hep-ph].

[302] K. Abe *et al.*, [T2K collaboration], Indication of electron neutrino appearance from an accelerator produced off axis muon neutrino beam, Phys. Rev. Lett., **107** (2011) 041801 ; arxiv:1106.2822

[303] M. Gonzalez-Garcia, M. Maltoni, T. Schwetz, Global analyses of neutrino oscillation experiments, Nucl. Phys. B, **908** (2016) 199, arXiv:1512.06856[hep-ph].

[304] C. R. Das and M. K. Parida, New formulas and predictions for running fermion masses at higher scales in SM, 2HDM and MSSM, Eur. Phy. J. C, **20** (2001) 121, arXiv:hep-ph/0010004.

[305] M. K. Parida and B. Purkayastha, New formulas and predictions for running masses at higher scales in MSSM, Eur. Phy. J. C, **14** (2000) 159, arXiv:hep-ph/9902374.

[306] M. K. Parida and N. N. Singh, Low energy formulas for neutrino masses with tan beta dependent hierarchy, Phys. Rev. D, **59** (1999) 32022, arXiv:hep-ph/9710328.

[307] A. Ilakovac, A. Pilaftsis, Flavour violating charged lepton decays in seesaw type models, Nucl. Phys. B, **437** (1995) 491, [hep-ph/9403398].

[308] F. Deppisch, J. W. F. Valle, Enhanced lepton flavour violation in the supersymmetric inverse seesaw model, Phys. Rev. D, **72** (2005) 036001, [hep-ph/0406040].

[309] M. Malinsky, T. Ohlsson, Z. -z. Xing, H. Zhang, Non-unitary neutrino mixing and CP violation in the minimal inverse seesaw model, Phys. Lett. B, **679** (2009) 242-248, arXiv:0905.2889 [hep-ph].

[310] M. Hirsch, T. Kernreiter, J. C. Romao, A. Villanova del Moral, Minimal supersymmetric inverse seesaw: neutrino masses,lepton flavour violation and LHC phenomenology, JHEP **1001** (2010) 103, arXiv:0910.2435 [hep-ph].

[311] E. Fernandez-Martinez, M. B. Gavela, J. Lopez-Pavon and O. Yasuda, CP-violation from non-unitary leptonic mixing, Phys. Lett. B, **649** (2007) 427, arXiv: hep-ph/0703098.

[312] K. Kanaya, Neutrino mixing in the minimal SO(10) model, Prog. Theor. Phys.,**64** (1980) 2278.

[313] M. Malinsky, T. Ohlsson, H. Zhang, Nonunitarity effects in a realistic low-scale seesaw model, Phys. Rev. D, **79** (2009) 073009, arXiv:0903.1961[hep-ph].

[314] G. Altarelli and D. Meloni, CP violation in neutrino oscillations and new physics, Nucl. Phys. B, **809** (2009) 158 , arXiv:0809.1041[hep-ph].

[315] F. del Aguila and J. A. Aguilar-Saavedra and J. de Blas, Trilepton signals: the golden channel for seesaw searches at LHC, Acta Phys. Polon. B, **40** (2009) 2901, arXiv:0910.2720 [hep-ph].

[316] A. van der Schaaf, J. Phys. G, **29** (2003) 2755; Y. Kuno, Nucl. Phys. B Proc. Suppl., **149** (2005) 376.

[317] F. del Aguila, J. A. Aguilar-Saavedra, Electroweak scale seesaw and heavy Dirac neutrino signals at LHC, Phys. Lett. B, **672** (2009) 158, arXiv:0809.2096 [hep-ph].

[318] K. S. Babu *et al.*, Baryon number violation, arXiv:1311.5285[hep-ph].

[319] A. de Gouvea *et al.*, Neutrinos, arXiv:1310.4340[hep-ex].

[320] K. Abe *et al.*, A search for nucleon decay via $n \to \bar{\nu}\pi^0$ and $p \to \bar{\nu}\pi^+$ in Super-Kamiokande Phys. Rev. Lett, **113** (2014) 121802, arXiv:1305.4391[hep-ex].

[321] K. Abe *et al.*, Nuclear Inst. And Methods in Physics Research A, 737C (2014) 253, arXiv:1307.0162[hep-ex].

[322] B. Bajc, I. Dorsner, M. Nemevsek, Minimal SO(10) splits supersymmetry, J. High Energy Phys., **0811** (2008) 007, arXiv:0809.1069[hep-ph].

[323] P. Langacker, Grand unified theories and proton decay, Phys. Rept.,**72** (1981) 185 .

[324] M. Ciuchini, E. Franco, S. Mishima, ans L. Silvestrini, Electroweak Precision Observables, New Physics and the Nature of a 126 GeV Higgs Boson, JHEP, **08** (2013) 106, arXiv:1306.4644[hep-ph].

[325] T. Appelquist, B. A. Dobrescu, A. R. Hopper, Nonexotic Neutral Gauge Bosons, Phys. Rev. D, **68** (2003) 035012; arxiv:hep-ph/0212073.

[326] F. Jegerlehner, M. Yu. Kalmykov, B. Kniehl, On the difference between the pole and the MSbar masses of the top quark at the electroweak scale, Phys. Lett. B, **722** (2013) 123, arxiv:1212.4319[hep-ph].

[327] K. A. Olive *et al.* (Particle Data Group), Chin. Phys. C, **38** (2014) 090001.

[328] CMS Collaboration, Measurements of the Properties of the New Boson with a Mass Near 125 GeV, CMS-PAS-HIG-13-005; ATLAS Collaboration, Combined Measurement of the Mass and Signal Strength of the Higgs Like Boson with the ATLAS detector Using up to $25 fb^{-1}$ of Proton-Proton Collision Data, ATLAS-CONF-2013-014; Search for Direct Top Squark Pair Production in Events with a Z Boson, b-Jets and Missing Transverse Momentum in $21 fb^{-1}$ of Proton-Proton Collisions at $\sqrt{s} = 8TeV$ with the ATLAS Detector, ATLAS-COM-CONF-2013-025 .

[329] J. Erler, P. Langacker, S. Munir, and E. Roja, Improved Constraints on Z' Bosons from Electroweak Precision Data, JHEP, **08** (2009) 017, arXiv:0906.2435[hep-ph].

[330] J. Erler and P. Langacker, Z' Bosons from $E(6)$: Collider and Electroweak Constraints, arXiv:1108.0685[hep-ph].

[331] C. Amsler *et al.* (Particle Data Group), Phys. Lett., **667** (2008) 1.

[332] K Nakamura *et al.* (Particle Data Group), J. Phys. G, **37** (2010) 075021.

[333] V. V. Andreev, G. M. Pick, P. Osland, Discriminating Z' from anamolous trilinear gauge coupling signatures in the $e^+e^- \to W^+W^-$ at ILC with polarized beams, Eur. Phys. J. C, **72** (2012) 2147, arXiv: hep-ph/9707235.

[334] J. C. Montero and V. Pleitez, Gauging $U(1)$ symmetries and the number of rifht handed neutrinos, Phys. Lett. B, **765** (2009) 64, arXiv:0706.0473[hep-ph].

[335] E.C.F.S. Fortes, J. C. Montero, and V. Pleitez, Asymmetries in $e^+e^- \to f\bar{f}$ processes at ILC for models with an extral neutral vector boson Z', Phys. Rev. D, **82** (2010) 114007 , arXiv:1005.2991[hep-ph].

[336] N. Palanque-Delabrouille *et al.*, Constraint on neutrino masses from SDSS-III/BOSS Lyα and other cosmological probes, JCAP,**1502** (2015) 02 045; arXiv:1410.7244.

[337] R. N. Mohapatra, Limits on the Mass of the Right-handed Majorana Neutrinos, Phys. Rev. D, **34** (1986) 909.

[338] M. Doi and T. Kotani, Double beta Decay and Majorana Neutrino, Prog. Theor. Phys., **83** (1985) 1.

[339] K. Muto,E. Bender, and H. V. Klapdor-Kleingrothaus, Effects on Ground State Correlations on 2 Neutrino Beta Beta Decay Rates and Limitations of the Qrpa Approach, Z. Phys. A, **334** (1989) 177.

[340] M. Hirsch, K. Muto, T. Oda, and H. V. Klapdor-Kleingrothaus, Nuclear structure calculations of beta$^+$ beta$^+$, beta$^+$ /EC and EC/EC decay matrix elements, Z. Phys.A, **347** (1994) 151.

[341] J. J. Gomez-Cadenas, J. Martin-Albo, M. Mezzetto, F. Monrabal, and M. Sorel, The search for neutrinoless double beta decay, Riv. Nuovo Cim., 35 (2012) 29 , arXiv:1109.5515 [hep-ex].

[342] J. Lopez-Pavon, S. Pascoli and Chan-fai Wong, Can heavy neutrinos dominate neutrinoless double beta decay ?, Phys. Rev. D, **87** (2013) 093007, arXiv:1209.5342 .

[343] G. Pantis, F. Simkovic, J. Vergados, and A. Faessler, Neutrinoless Double Beta Decay within QRPA with proton-neutron Pairing, Phys. Rev. C, **53** (1996) 695, arXiv:nucl-th/9612036 [nucl-th].

[344] J. Suhonen and O. Civitarese, Weak interaction and nuclear-stucture aspects of nuclear double beta decay, Phys. Rept., **300** (1998) 123.

[345] J. Kotila and F. Iachello, Phase space factors for double *beta* decay, Phys. Rev. C, **85** (2012) 034316 , arXiv:1209.5722 [nucl-th].

[346] A. Faessler, A. Meroni, S. T. Petcov, F. Simkovic, and J. Vergados, Uncovering multiple CP- no conserving mechanisms of double beta decay, Phys. Rev. D, **83** (2011) 113003, arXiv:1103.2434 [hep-ph].

[347] For a review of leptogenesis and LFV processes see E. Molinaro,CP violation in the lepton sector, thermal leptogenesis and lepton flavor violation, Ph. D. Thesis, SISSA, Italy (2010).

[348] Planck 2015 results. XIII. Cosmological parameters, A A, **594** (2016) A13, arXiv:1502.01589[astro-ph.CO].

[349] S. Blanchet, T. Hambye, F. X. Josse-Michaux, Reconciling Leptogenesis with Observable $\mu \to e$ Gamma Rates, JHEP, **1004** (2010) 023, arXiv: 0912.3153[hep-ph].

[350] M. Hirsch *et al.*, Thermal leptogenesis in extended supersymmetric seesaw, Phys. Rev. D, **75** (2007) 011701.

[351] P. -H. Gu, U. Sarkar, Leptogenesis with linear, inverse or double seesaw, Phys. Lett. B, **694** (2011) 226, arXiv:1007.2323.

[352] P. -H. Gu, M. Hirsch, U. Sarkar, J.W.F. Valle, Neutrino masses, leptogenesis and dark matter in hybrid seesaw, Phys. Rev. D, **79** (2009) 033010.

[353] E. Ma, N. Sahu, U. Sarkar, Leptogenesis in an extended NMSSM model, J. Phys.G, **34** (2007) **no.4** 741, hep-ph/0611257.

[354] F. Deppisch, J. Harz, M. Hirsch, W. -C. Huang, Falsifying high-scale leptogenesis at LHC, Phys. Rev. Lett.,**112** (2014) 221601, arXiv:1312.4447[hep-ph];

[355] F.Deppisch, J. Harz, M. Hirsch, W. -C. Huang, H. Pas, Falsifying high-scale baryogenesis with neutrinoless double beta decay and lepton flavor violation, Phys. Rev. D, **92** (2015) **no.3** 036005, arXiv:1503.04825[hep-ph].

[356] A. Abada, G. Arcadi, M. Lucente, Dark matter in the minimal inverse seesaw mechanism, JCAP, **1410** (2014) 001, arXiv:1406.6556[hep-ph].

[357] A. Abada, S. Nasri, Renormalisation group equations of a cold dark matter, Phys. Rev. D, **88** (2013) **no.1** 016006, arXiv:1304.3917[hep-ph].

[358] N. Palanque-Delabrouille *et al.*, Neutrino masses and cosmology with Lyman-alpha forest power spectrum, JCAP **1511** (2015) 011, arXiv:1506.05976.

[359] M. Fukugita, T. Yanagida, Barygenesis without grand unification, Phys. Lett. B, **74** (1986) 45.

[360] S. Davidson, A. Ibarra, A lower bound on the right-handed neutrino mass from leptogenesis, Phys. Lett. B, **535** (2002) 25.

[361] T. Hambye, G. Senjanovic, Consequences of Triplet Seesaw for Leptogenesis, Phys. Lett. B, **582** (2004) 73, arXiv:hep-ph/0307237.

[362] M. Yu. Khlopov, Andrei D Linde, Is It Easy to Save the Gravitino?, Phys. Lett. B, **138** (1984) 265-268.

[363] L. Boubekeur, T. Hambye, G. Senjanovic, Low-scale leptogenesis and soft supersymmetry breaking, Phys. Rev. Lett., **93** (2004) 111601.

[364] K. S. Babu, A. Bachri, H. Aissoui, Leptogenesis in Minimal Left-Right Symmetric Models, Nucl. Phys. B, **738** (2006) 76.

[365] X. Ji, Y. Li, R. N. Mohapatra, S. Nasri, Y, Zhang, Leptogenesis in realistic SO(10) models Phys. Lett. B, **651** (2007) 195.

[366] K. Kumekawa, T, Moroi, T. Yanagida, Flat Potential for Inflaton with a Discrete R-invariance in Supergravity, Prog. Theor. Phys., **92** (1994) 437.

[367] G. F. Giudice, M. Peleso, A. Riotto, T. Tkachev, Production of Massive Fermions at Preheating and Leptogenesis, JHEP, **9908** (1999) 014, arXiv:9905242[hep-ph].

[368] T. Asaka, K. Hamaguchi, M.Kawasaki, T. Yanagida, Leptogenesis in Inflaton Decay, Phys. Lett. B, **464** (1999) 12, arXiv:9906366[hep-ph].

[369] R. Jannernot, S. Khalil, G. Lazaridis, Q. Shafi, Inflation and monopoles in supersymmetric $SU(4)_c \times SU(2)_L \times SU(2)_R$, JHEP, **010** (2000) 012; arXiv:0002151[hep-ph].

[370] J. C. Pati, Phys. Rev. D, **68** (2003) 072002; J. C. Pati, Leptogenesis and Neutrino Oscillations Within A Predictive $G(224)$/SO(10)-Framework, arXiv:0209160[hep-ph].

[371] J. C. Pati, Int. J. Mod. Phys. **A18** (2003) 4135-4156, Subnucl. Ser. **40** (2003) 194-236.

[372] O. Castillo-Felisola, C. O.Dib, J. C. Helo, S. G. Kovalenko, S. E. Ortiz, Left-Right Symmetric Models at the High-Intensity Frontier, Phys. Rev. D, **92** 013001 (2015), arxiv: 1504.02489 [hep-ph].

[373] For the suggestion to observe like-sign dilepton signals at LHC via heavy RH Majorana neutrino exchange in the $W_R - W_R$ channel see W. -Y. Keung and G. Senjanovic, Phys. Rev. Lett. B, **50** (1983) 1427 .

[374] DELPHI Collaboration, P. Abreu et.al., Search for neutral heavy leptons produced in Z decays, Z. Phys, C, **74** (1997) 57 .

[375] F.del Aguila, J. Aguilar-Saavedra, Distinguishing seesaw models at LHC with multi-lepton signals, Nucl. Phys. B, **813** (2009) 22, arXiv:0808.2468 [hep-ph].

[376] Eder Izaguirre, Brian Shuve, Multilepton and Lepton Jet Probes of Sub-Weak-Scale Right-Handed Neutrinos, Phys. Rev. D, **91** (2015) 093010, arXiv:1504.02470 [hep-ph].

[377] Anupama Atre, Tao Han, Silvia Pascoli, Bin Zhang, The Search for Heavy Majorana Neutrinos, J. High Energy Phys., **0905** (2009) 030 , arXiv:0901.3589 [hep-ph].

[378] Csaba Csaki, Eric Kulflik, Salvator Lombardo, Oren Slone, Searching for Displaced Higgs Decays, Phys. Rev. D, **92** (2015) 073008, arXiv:1508.01522v2[hep-ph].

[379] Alberto M. Gago, Pilar Hernandez, Joel Jones-Perez, Marta Losada, Alexander Moreno Briceni, Probing the Type I Seesaw Mechanism with Displaced Vertices at the LHC, arXiv: 1505.05880 [hep-ph].

[380] Matthew J. Strassle, Kathryn M. Zurek, Discovering the Higgs Through Highly-Displaced Vertices, Phys.Lett. B, **661** (2008) 263-267, hep-ph/0605193.

[381] M. Gronau, C. N. Leung, J L. Roser, Extending limits on neutral heavy leptons, Phys. Rev. D, **29** (1984) 2539 .

[382] ATLAS Collaboration(G. Aad et al), Search for massive, long-lived particles using multitrack displaced vertices or displaced lepton pairs in pp collisions at $\sqrt{s} = 8$ TeV with the ATLAS detector, Phys. Rev. D, **92** (2015) 072004, arXiv:1504.05162[hep-ex].

[383] CMS Collaboration, V. Khachatryan et al, Search for long-lived neutral particles decaying to quark-antiquark pairs in proton-proton collisions at $\sqrt{s} = 8$ TeV Phys. Rev. D, **91** (2015) 012007, arXiv:1411.6530 [hep-ex]

[384] ATLAS Collaboration, Triggers for displaced decays of long-lived neutral particles in the ATLAS detector, JINST, **8** (2013) 07015.

[385] CMS Collaboration, S. Chatrchyan et al., Search for Heavy Neutrinos and W_R Bosons with Right-Handed Couplings in a Left-Right Symmetric Model in pp Collisions at $\sqrt{s} = 7$ TeV, Phys. Rev. Lett., **109** (2012) 261802.

[386] CMS Collaboration, V. Khachatryan et al., Search for heavy neutrinos and W bosons with right-handed couplings in proton-proton collisions at $\sqrt{s} = 8$ TeV, Eur. Phys. J. C, **74** no.11 (2014) 311, arXiv:1407.3683.

[387] Issac Hueing, Garbriel Samach, David Tucker Smith, phys. Rev. D, **90** (2014) 075016.

[388] Antonio Uras, Low mass dilpton production with ALICE at the LHC, Nucl. Phys. A, **932** (2014) 218-223.

[389] Debajyoti Choudhury, Rohini M Godbole, G Polesello, Measuring R-parity violating couplings in dilepton production at the LHC, J. High Energy Phys., **0208** (2002) 004, arXiv:hep-ph/0207248.

[390] E. Accomando, A. Belyaev, J. Fiaschi, S. Moretti, K. Mimasu, C. Shepherd-Themistocleous, Forward-Backward Asymmetry as a Discovery Tool for Z' Bosons at the LHC, arXiv:1503.02672 [hep-ph].

[391] ATLAS Collaboration (Aad, Georges et al), Phys. Rev. D, **90** (2014) 05200.

[392] E. Accomando, A. Belyaev, L. Fedeli, S. F. King, C. Shepherd-Themistocleous, Z' physics with early LHC data, Phys. Rev. D, **83** (2011) 075012, arXiv:1010.6058 [hep-ph].

[393] J.Pumplin, D. R. Stump, J. Huston, H. L. Lai, P. Nadolsky, and W. K. Tung, New Generation of Parton Distributions with Uncertainties from Global QCD Analysis JHEP, **07** (2002) 012, arXiv: hep-ph/0201195.

[394] V. V. Andreev, P. Osland, A. A. Pankov, Precise determination of Z-Z' mixing at the CERN LHC, Phys. Rev. D, **90** (2014) 055025, arXiv:1406.6776 [hep-ph].

[395] M. Carena, A. Daleo, B. A. Doberscu, and Tim M. P. Tait, Z' Gauge Bosons at the Tevatron, Phys. Rev. D, **70** (2004) 093009, hep-ph/0408098.

[396] M. K. Parida, Natural mass scales for observable matter-antimatter oscillations in SO(10), Phys. Lett. B, **126** (1983) 220.

[397] M. K. Parida, Phys. Rev. D, **17** (1983) R2383.

[398] Howard Georgi and Sheldon L. Glashow, Gauge theories without anomalies, Phys.Rev.D, **6** (1972) 429.

[399] J. Banks and H. Georgi, Comment on Gauge Theories Without Anomalies, Phys.Rev. D, **14** (1976) 1159.

[400] Susumu Okubo, Gauge Groups Without Triangular Anomaly, Phys.Rev. D, **16** (1977) 3528.

[401] Frank Wilczek and A.Zee, Families from Spinors, Phys.Rev. D, **25** (1982) 553.

[402] Raza M. Syed, Couplings in SO(10) grand unification,(2005), arXiv:hep-ph/0508153.

[403] M. K. Parida and P.K. Patra, Useful theorem on vanishing threshold contribution to $\sin^2(\theta_W)$ in a class of grand unified theories

[404] M.K. Parida and P. K. Patra, Theorem on vanishing multiloop radiative corrections to $\sin^2(\theta_W)$ in grand unified theories at high ma scales, Phys.Rev.Lett., **68** (1992) 754.

[405] M. K. Parida, Vanishing corrections on intermediate scale and implications for unification of forces., Phys.Rev.D, **57** (1998) 2736, arXiv:hep-ph/9710246.

Appendix A

Some Aspects of Grand Unified Theories

A.1 Anomalies

It happens sometimes that a symmetry of Lagrangian gets broken by quantum effects, i.e the symmetry of Lagrangian is not a symmetry of quantized theory. Anomalies appear in those symmetries involving both axial and vector currents, and reflect the impossibility of regularizing the quantum theory (the divergent loop) in a way which preserves symmetry. The grand unifications gauge groups, being non-abelian Lie groups, are likely to meet triangular anomalies. We either choose a gauge group which is either anomaly free or we fix it by canceling the anomaly as suggested by [398–400] where we find that all SO(n) groups with $n \neq 6$ are anomaly free and all the SU(n) groups with $n \geq 3$ are anomalous. For an example in SU(5) GUTs the representation space chosen for cancelling anomaly are $\overline{5}$ and 10. While considering extension of such SU(n) theories the cancellation of anomaly has to be taken care of. Here we list strength of anomaly for few representations of general SU(n) and SU(4) being isomorphic to SO(6) it applies there as well.

A.1.1 Adler Anomalies for a SU(n) representation

As described above all the SU(n) groups with $n \geq 3$ are anomalous groups, we need to study the order of anomaly of the representations in general. Adler anomalies for left handed fermion representations of SU(n) are as follows

- For totally antisymmetric left handed fermionic representation with m antisymmetric indices, the anomaly is

$$A_a = \frac{(n-3)!(n-2m)}{(n-m-1)!(m-1)!} \tag{A.1}$$

Young Tableaux	**Dimension**	**Anomaly**
$\square$	n	1
$\square\square$	$n(n+1)/2$	$n+4$
$\square\square\square$	$n(n+1)(n+2)/3!$	$(n+3)(n+6)/2$
$\begin{array}{c}\square\\\square\end{array}$	$n(n-1)/2$	$n-4$
$\begin{array}{c}\square\\\square\\\square\end{array}$	$n(n-1)(n-2)/3!$	$(n-3)(n-6)/2$
$\begin{array}{ll}\square&\square\\\square&\end{array}$	$(n+1)n(n-1)/3$	$(n-3)(n+3)$
$n-1\left\{\begin{array}{ll}\square&\square\\\vdots&\\\square&\end{array}\right.$	(n^2-1) Adj. rep.	0

Table A.1: Adler anomalies for few simple representations in SU(n) gauge theories. All $SO(n)$, $n \neq 6$, theories are anomaly free. Anomalies for right-handed fermion representations and corresponding complex conjugate representation will change the sign.

- For totally symmetric left handed fermionic representation with m symmetric indices, the anomaly is

$$A_s = \frac{(n+m)!(n+2m)}{(n+2)!(m-1)!} \tag{A.2}$$

For the two representations R_1 and R_2, $A(R_1+R_2) = A(R_1) + A(R_2)$ and $A(R_1 \otimes R_2) = D(R_1)A(R_2) + D(R_2)A(R_1)$ following the additive rule. Using these relations we can calculate anomaly due to a mixed representation. To complete this subsection we list few representations in Young tableaux form write their dimension and list anomaly in SU(n) Lie group.

A.2 Quadratic Casimir and Dynkin index invariants in SU(n)

In a group $G = \mathrm{SU}(n)$ group no of generators is n^2-1. We denote generators of this group in a specific representation R by $M_a(R)$. The quadratic Casimir invariance is defined as

$$\delta_{ij}C_2(R) = \sum_a \sum_k (M_a(R))_{ik}(M_a(R))_{kj} \tag{A.3}$$

where $a = 1, 2...d_G$; $i, j, k = 1, 2, ...d_R$ and $d_G\,(= n^2-1)$, d_R are the dimensions of group G and representation R in the group, respectively. The Dynkin index invariance is defined as

$$\delta_{ab}T(R) = \mathrm{Tr}[M_a(R)M_b(R)] \tag{A.4}$$

Obviously $d_R C_2(R) = d_G T(R)$. The properties of Dynkin index invariance are

$$T(R^*) = T(R) \tag{A.5}$$

$$T(R_1 + R_2) = T(R_1) + T(R_2) \tag{A.6}$$

$$T(R_1 \otimes R_2) = d_{R_1}T(R_2) + d_{R_2}T(R_1) \tag{A.7}$$

$$T\left(\square\right) = 1/2 \tag{A.8}$$

$$T\left(\left.\begin{array}{|c|}\hline \\ \hline \vdots \\ \hline \\ \hline\end{array}\right\}\mathrm{m-boxes}\right) = \frac{1}{2}\frac{(n-2)!}{(m-1)!(n-m-1)!} \tag{A.9}$$

$$T\left(\underbrace{\begin{array}{|c|c|c|}\hline \; & \ldots & \; \\ \hline\end{array}}_{\mathrm{m-boxes}}\right) = \frac{1}{2}\frac{(n+m)!}{(n+1)!(m-1)!} \tag{A.10}$$

Using the above properties we can calculate $C_2(R)$, $T(R)$ for any representation R. $C_2(G) = n$ is the quadratic Casimir for the adjoint representation. For a representation of $U(1)_X$ we have $C_2(G) = 0$, and $C_2(R) = T(R) = X^2$, where X is the appropriately normalized charge of the symmetry.

The best way to get the Dynkin indexes of a group $SU(n)$ is to first evaluate them for $SU(2)$ and then achieve rest iteratively. Like, the adjoint representation of $SU(2)$ can be easily estimated, $T(Adj)_{SU(2)} = 2$. Now, since adjoint of $SU(n+1)$ can be decomposed into $SU(n)$ representations as as

$$Adj(n+1) = \begin{pmatrix} Adj(n) & n \\ \bar{n} & 1. \end{pmatrix} \tag{A.11}$$

Therefore the Dynkin indexes are related as

$$\begin{aligned} T[Adj(n+1)] &= T[Adj(n)] + T[n] + T[\bar{n}] + T[1] \\ &= T[Adj(n)] + 1 \equiv n+1. \end{aligned} \tag{A.12}$$

Similarly for two index (anti)-symmetric representations we have

$$T[(n+1)\times(n+1)]_{(A)S} = T[n\times n]_{(A)S} + T[n]. \tag{A.13}$$

We remember that two index antisymmetric and symmetric representations in $SU(2)$ are singlet and adjoint representations also and their Dynkin index $T(AS) = 0$ and $T(S) = 2$, respectively. Therefore

$$T[n\times n]_{(A)S} = (0)2 + (n-2)/2. \tag{A.14}$$

A.3 Lorentz group

A point in four dimensional space-time manifold of Minkowaski space is denoted by $x^\mu = (t, \vec{x})$, where the laws of physics are invariant under Lorentz group. Vectorial transformation in this group are denoted as $x'^\mu = \Lambda^\mu{}_\nu x^\nu$, leading to the quadratic form $x^2 = x^\mu x_\mu = \eta_{\mu\nu}x^\mu x^\nu$ invariant. Hence Lorentz group is a non-trivial real orthogonal group of 4×4 real orthogonal matrices obeying

$$\eta_{\mu\nu}\Lambda^\mu{}_\rho\Lambda^\nu{}_\sigma = \eta_{\rho\sigma} \equiv \Lambda^T\eta\Lambda = \eta \tag{A.15}$$

with $det(\Lambda) = +1$. The invariance of Lorentz symmetry can also be written as

$$x_\alpha x^\alpha = (\gamma_\mu x^\mu)(\gamma_\nu x^\nu) \tag{A.16}$$

This requires that $\{\gamma_\mu, \gamma_\nu\} = 2\eta_{\mu\nu}$. This γ_μ defines a rank four clifford algebra. It's obvious that ${\gamma_0}^2 = 1_4$ and ${\gamma_i}^2 = -1_4$. And $\gamma^\mu = \Lambda^\mu{}_\nu\gamma^\nu$ and $\gamma_\mu = \eta_{\mu\nu}\gamma^\nu$, $tr(\gamma^\mu) = 0$. First and second condition on γ_μ^2 requires the hermiticity condition as $\gamma_0 = \gamma_0^\dagger$ and $\gamma_i = -\gamma_i^\dagger$. Hence eigen values are either ±1 or $\pm i$ and they occur in pair. We require the dimension of these matrices to be at least $2^2\times 2^2$ as there are only three such γ matrices in 2×2 dimension i.e. Pauli matrices themselves, and higher dimensional matrices will be reducible. Hence we find that the dimension of fundamental representation is same as spinor representation, but their generators are quite different. Out of different possible representation we write them in the form

$$\gamma_0 = \sigma_1 \otimes 1_2,\ \ \gamma_k = i\sigma_2 \otimes \sigma_k \tag{A.17}$$

known as Weyl representation. The Weyl basis has simple chiral projections. One more γ matrix we can define is the product of all four gamma matrices.

$$\gamma^5 = i\gamma^0\gamma^1\gamma^2\gamma^3 \tag{A.18}$$

and the chiral projections are read as

$$\psi_{\substack{R\\L}} = \frac{1}{2}\left(1 \pm \gamma^5\right)\psi \tag{A.19}$$

$$\gamma^0 = \begin{pmatrix} 0 & 1_2 \\ 1_2 & 0 \end{pmatrix},\ \gamma^k = \begin{pmatrix} 0 & \sigma^k \\ \sigma^k & 0 \end{pmatrix},\ \gamma^5 = \begin{pmatrix} 1_2 & 0 \\ 0 & -1_2 \end{pmatrix},\ \psi = \begin{pmatrix} \psi_L \\ \psi_R \end{pmatrix} \tag{A.20}$$

where ψ_L and ψ_R are the left-handed and right-handed two-component Weyl spinors.

$$\gamma'^{\mu} = \Lambda^{\mu}{}_{\nu}\gamma^{\nu} \tag{A.21}$$

generating the Clifford algebra for $\gamma\,'$ matrices. Transformation of a 2^2 dimensional spinor under the above transformation of γ matrices is

$$\psi'(x') = S(\Lambda)\psi(x) \tag{A.22}$$

γ^{μ}'s are $2^2 \times 2^2$ matrix forms of spinor representation hence transform like

$$\gamma'_{\mu} = S(\Lambda)\gamma_{\mu}S^{-1}(\Lambda) \tag{A.23}$$

we construct the explicit form of the transformation matrix, $S(\Lambda) = e^{-\frac{i}{4}a_{\alpha\beta}\Sigma_{\alpha\beta}}$. Simplification of infinitesimal rotation gives

$$\Sigma_{\mu\nu} = \frac{i}{2}\left[\gamma_{\mu}, \gamma_{\nu}\right] \tag{A.24}$$

The generators $\Sigma_{0,2}$ and $\Sigma_{1,3}$ can be simultaneously diagonalised therefore we define chirality operator as

$$\gamma_5 = i\Sigma_{02}\Sigma_{13} = i\gamma^0\gamma^1\gamma^2\gamma^3. \tag{A.25}$$

One can easily verify the following properties of chirality operator

$$\gamma_5^\dagger = \gamma_5, \;\; tr(\gamma_5) = 0, \;\; \{\gamma_5, \gamma_\mu\} = 0, \;\; \gamma_5^2 = 0, \;\; [\gamma_5, \Sigma_{\mu\nu}] = 0. \tag{A.26}$$

Thus a 4-dimensional spinor representation is reducible in to two 2-dimensional representations. The generators of the reduced representations are $\frac{1}{2}(1 \pm \gamma_5)\Sigma_{\mu\nu}$. Charge conjugation operators can be found to be product $\gamma_0\gamma_2$ or $\gamma_1\gamma_3$.

A.3.1 Lorentz scalar and vector constructs

If ψ is a Dirac spinor

Lorentz Scalars

$$\begin{aligned}
\bar{\psi}\psi &= \overline{\psi^C}\psi^C = \bar{\psi}_L\psi_R + \bar{\psi}_R\psi_L \\
\overline{\psi^C}\psi &= \psi_L^T C \psi_L + \psi_R^T C \psi_R \\
\bar{\psi}\psi^C &= \overline{\psi_L} C \overline{\psi_L}^T + \overline{\psi_R} C \overline{\psi_R}^T
\end{aligned} \tag{A.27}$$

Lorentz Vectors

$$\begin{aligned}
\bar{\psi}\gamma_\mu\psi &= \bar{\psi}_L\gamma_\mu\psi_L + \bar{\psi}_R\gamma_\mu\psi_R \\
\overline{\psi^C}\gamma_\mu\psi &= \psi_L^T C\gamma_\mu C\bar{\psi}_L^T + \psi_R^T C\gamma_\mu C\bar{\psi}_R^T \\
\overline{\psi^C}\gamma_\mu\psi &= \psi_L^T C\gamma_\mu\psi_R + \psi_R^T C\gamma_\mu\psi_L \\
\bar{\psi}\gamma_\mu\psi^C &= \bar{\psi}_L\gamma_\mu C\bar{\psi}_R^T + \bar{\psi}_R\gamma_\mu C\bar{\psi}_L^T
\end{aligned} \tag{A.28}$$

where

$$\bar{\psi} = \psi^\dagger\gamma_0, \;\; \psi^C = C\bar{\psi}^T, \;\; \psi = \psi_L + \psi_R \tag{A.29}$$

A.4 SO(2n) Algebra

The special orthognal group, $SO(2n)$ is a group of $2n \times 2n$ real orthogonal matrices, O obeying

$$O^T O = OO^T = \mathbf{1}, \qquad \det(O) = +1 \tag{A.30}$$

A real $2n$-dimensional column vector x transforms as

$$x_i' = O_{ij}x_j \;;\;\; i, j = 1, 2, \ldots 2n. \tag{A.31}$$

such that

$$x'^T x' = (Ox)^T Ox = x^T O^T Ox = x^T x. \tag{A.32}$$

The transformation matrix, O can be parametrized as

$$O(a) = exp\left(\frac{i}{2} a_{ij} L_{ij}\right), \quad \text{such that} \quad a_{ij} = -a_{ji} \tag{A.33}$$

The real numbers a_{ij} are the rotation parameters and under the local symmetry transformation depend on space-time coordinate, and L_{ij} are $2n \times 2n$ linearly independent matrices and the generators of the group. Putting eq. (A.33) in the eq. (A.30) and eq. (A.31) we get

$$L_{ij}^T = -L_{ji}. \quad \text{and} \quad (L_{ij})_{kl} = -i(\delta_{ik}\delta_{jl} - \delta_{il}\delta_{jk}); \quad 1 \leq k < l \leq 2n. \tag{A.34}$$

which gives $tr(L_{ij}) = 0$ and the matrix is antisymmetric therefore it's easy to write the explicit form of generators. The generators L_{ij} have *zeros* everywhere except at the positions (i, j) and (j, i), which are occupied by $-i$ and $+i$ respectively, and additionally we have $L_{ij} = -L_{ji} = L_{ij}^{\dagger}$. Therefore, the algebra of the real representation can be calculated using the definition of generators, eq. (A.34) as

$$[L_{ij}, L_{kl}] = -i\left(\delta_{jk} L_{il} + \delta_{il} L_{jk} - \delta_{ik} L_{jl} - \delta_{jl} L_{ik}\right) \tag{A.35}$$

The higher rank tensors can be defined which transform as

$$A'_{i_1 i_2 \ldots i_p} = O_{i_1 j_1} O_{i_2 j_2} \ldots O_{i_p j_p} A_{j_1 j_2 \ldots j_p} \tag{A.36}$$

The invariants of the group are second rank δ_{ij} and $2n^{th}$ rank Levi-Civita tensor. The later can be proved using the definition of determinant, ie.

$$\det(O) = \frac{1}{2n!} \epsilon_{i_1 i_2 \ldots i_{2n}} \epsilon_{j_1 j_2 \ldots j_{2n}} O_{i_1 i_2 \ldots i_{2n}, j_1 j_2 \ldots j_{2n}} \tag{A.37}$$

A higher rank tensor is reducible if it's contraction with Kroncker delta or Levi-Civita tensor gives a tensor of lower rank. The dimensionality of second rank anti-symmetric tensor and second rank symmetric traceless tensor are $n(2n-1)$ and $[n(2n+1)-1]$. Their transfornation follow the definition of eq. (A.36) for two indices. The dimension of second rank antisymmetric tensor, which is also the adjoint representation of the group, is same as the number of generators. Therefore, the transformation of Lorentz-vectors under $SO(2n)$ adjoint representation follow the similar properties with additional Lorentz index on gauge boson.

A.4.1 SO(2n) spinor representation

Similar to the Lorentz algebra in Minkowaski space, the invariant quadratic form of $SO(2n)$ symmetry is given by eq. (A.32). The quadratic form as square of linear form can be written as

$$x_1^2 + x_2^2 + \cdots + x_{2n}^2 = (x_1\Gamma_1 + x_2\Gamma_2 \cdots + x_{2n}\Gamma_{2n})^2 \tag{A.38}$$

if

$$\{\Gamma_i, \Gamma_j\} = 2\delta_{ij}\mathbf{1}; \quad i,j = 1,2,\ldots,2n \tag{A.39}$$

This $2n$ rank Clifford algebra gives

$$\Gamma_i^2 = \mathbf{1} \;\; \text{(no sum)}, \quad \text{and} \;\; \mathrm{tr}(\Gamma_\mathrm{i}) = 0 \tag{A.40}$$

We can prove by explicit iterative construction that "there exist $2n$ Hermitian matrices $\Gamma_i,\ i = 1,2,\ldots,2n$, which are $2^n \times 2^n$ and satisfy the $2n$ rank Clifford algebra" [401]. Thus from eq. (A.40) we see that their eigenvalues are $+1$ and -1 which come in pair.

The invariance of linear term, $\sum_i x_i\Gamma_i$ demands the transformation of Γ as

$$\Gamma_i \to \Gamma_i' = O_{ij}\Gamma_j. \tag{A.41}$$

The transformation of $SO(2n)$ spinor is written as

$$\Psi(x) \to \Psi'(x') = S(O)\Psi(x) \;\; \text{and} \;\; \Gamma_i' = S(O)\,\Gamma_i\,S^{-1}(O) = O_{ij}\Gamma_j. \tag{A.42}$$

where Ψ is a 2^n dimensional spinor. The Γ's follow the same Clifford algebra. The explicit form of the transformation matrix

$$S(O) = exp\left(\frac{i}{2}a_{ij}\Sigma_{ij}\right). \tag{A.43}$$

Here Σ_{ij} are the generators in the spinorial basis. Putting $S(O)$ in eq. (A.42) and using $O_{ij} = \delta_{ij} + a_{ij}$ we get

$$\Sigma_{ij} = \frac{i}{4}\left[\Gamma_i, \Gamma_j\right] \tag{A.44}$$

These antisymmetric ($\Sigma_{ij} = -\Sigma_{ji}$) and Hermitian ($\Sigma_{ij} = \Sigma_{ij}^\dagger$) generators satisfy the

$SO(2n)$ Lie algebra

$$[\Sigma_{ij}, \Sigma_{kl}] = -i\left(\delta_{ik}\Sigma_{jl} - \delta_{il}\Sigma_{jk} - \delta_{jk}\Sigma_{il} + \delta_{jl}\Sigma_{ik}\right), \tag{A.45}$$

which is the usual commutation relation of $SO(2n)$ generators in real representation, eq. (A.35). The cartan subalgebra consist of n generators, say

$$\text{Cartan subalgebra} = [\Sigma_{1\,2}, \Sigma_{3\,4}, \ldots, \Sigma_{2n-1\,2n}] \tag{A.46}$$

We can write, analogous to γ_5 in Dirac theory, the group chirality operator using the Cartan subalgebra

$$\Gamma_{\mathrm{P}} \equiv \prod_{i=1}^{n} \Sigma_{2i-1\,2i} = (-1)^n \Gamma_1 \Gamma_2 \ldots \Gamma_{2n} \tag{A.47}$$

with the properties

$$\Gamma_{\mathrm{P}}^2 = \mathbf{1}, \quad \Gamma_{\mathrm{P}} = \Gamma_{\mathrm{P}}^{\dagger}, \quad tr(\Gamma_{\mathrm{P}}) = 0, \quad [\Gamma_{\mathrm{P}}, \Sigma_{ij}] = 0, \quad \{\Gamma_{\mathrm{P}}, \Gamma_i\} = 0. \tag{A.48}$$

Thus since $\Gamma_{\mathrm{P}} \neq const.\mathbf{1}$ and $[\Gamma_{\mathrm{P}}, S(O)] = 0$, Schurs lemma suggests that 2^n representation is reducible, and $\Gamma_{\mathrm{P}}^2 = \mathbf{1}$ and $tr(\Gamma_{\mathrm{P}}) = 0$ suggest that this representation can reduce as $2^n = 2^{n-1} \oplus 2^{n-1}$ with opposite eigenvalues. Using the projection operator

$$\Gamma_{\pm} \equiv \frac{1 \pm \Gamma_{\mathrm{P}}}{2} \tag{A.49}$$

we get

$$\Psi_{\pm} = \Gamma_{\pm}\Psi. \tag{A.50}$$

Demanding the condition

$$\Psi^T B \Psi = \text{invariance} \Leftrightarrow \Psi^C = B\Psi^* \tag{A.51}$$

we get $\Sigma^T B + B\Sigma = 0$ leading to two possible solutions

$$B = \prod_{i}^{n} \Gamma_{2i} \quad \text{and} \quad B = \prod_{i}^{n} \Gamma_{2i-1}. \tag{A.52}$$

A.4.2 Bilinears and invariant constructs

From $\Psi'(x') = S(O)\Psi(x)$ and unitarity of $S(O)$, $S^{-1}(O) = S^{\dagger}(O)$ we immediately get bilinear structure

$$\Psi^{\dagger}\Psi \qquad \text{Scalar} \tag{A.53}$$

$$\Psi^{\dagger}\Gamma_i\Psi \qquad \text{Vector} \tag{A.54}$$

$$\Psi^{\dagger}\Gamma_i\Gamma_j\Psi \qquad 2^{\text{nd}} \text{ rank tensor} \tag{A.55}$$

$$\Psi^{\dagger}\Gamma_{i_1}\Gamma_{i_2}\ldots\Gamma_{i_r}\Psi \qquad r^{\text{th}} \text{ rank tensor} \tag{A.56}$$

Where $r \leq n$. An antisymmetric combinations of these bilinears can be extracted out by choosing the antisymmetric combinations of Γ matrices, $\Gamma_{[i_1}\Gamma_{i_2}\ldots\Gamma_{i_r]}$. These bilinears can be decomposed in terms of irreducible representations using the projection operator $\Gamma_{\pm}$ such that $\Psi = \Psi_+ + \Psi_-$. The surviving odd and even rank antisymmetric tensors would be

$$\Psi^{\dagger}_{\pm}\Gamma_{[i_1}\Gamma_{i_2}\ldots\Gamma_{i_r]}\Psi_{\mp}\ ; \qquad r - \text{odd} \tag{A.57}$$

$$\Psi^{\dagger}_{\pm}\Gamma_{[i_1}\Gamma_{i_2}\ldots\Gamma_{i_r]}\Psi_{\pm}\ ; \qquad r - \text{even.} \tag{A.58}$$

For $r = n$ they will form complex and real self dual and antiself dual. We assign left-handed and right-handed CP-conjugate chirality to Ψ_+ and Ψ_- respectively. To incorporate the Lorentz symmetry we insert γ^0 and $\gamma^0\gamma^{\mu}$ to make them Lorentz scalar and vectors respectively. Thus the scalar and vector couplings of these bispinors look like

$$\begin{aligned} \mathcal{K}_{ab}\ \overline{\Psi}_{\pm a}\Gamma_{[i_1}\Gamma_{i_2}\ldots\Gamma_{i_r]}\Psi_{\mp b}\Phi^{(\text{asym})}_{i_1 i_2\ldots i_r}\ ; &\qquad r - \text{odd} \\ \mathcal{K}'_{ab}\ \overline{\Psi}_{\pm a}\gamma^{\mu}\Gamma_{[i_1}\Gamma_{i_2}\ldots\Gamma_{i_r]}\Psi_{\pm b}V^{(\text{asym})}_{\mu i_1 i_2\ldots i_r}\ ; &\qquad r - \text{even,} \end{aligned} \tag{A.59}$$

respectively. Here a, b are generation indices, μ is Lorentz index, $\mathcal{K}, \mathcal{K}'$ are coupling constants, and Φ, V are Lorentz scalar and vectors of $SO(2n)$ antisymmetric (asym) tensors of rank r. The symmetries of $\mathcal{K}, \mathcal{K}'$ are decided by the properties of γ and Γ matrices.

The demand for invariance of term constructed by Ψ^T and Ψ in eq. (A.51) can be trivially implemented for writing bilinears using Ψ^T and Ψ. Now vector and scalar couplings are

$$\begin{aligned}
\mathcal{K}_{ab}\ \Psi^T{}_{\pm\, a} C B^T \Gamma_{[i_1}\Gamma_{i_2}\ldots\Gamma_{i_r]}\Psi_{\pm\, b}\Phi^{(\mathrm{asym})}_{i_1 i_2 \ldots i_r}\ ; &\qquad r-\text{even} \\
\mathcal{K}'{}_{ab}\ \Psi^T{}_{\pm\, a} C\gamma^{\mu} B^T \Gamma_{[i_1}\Gamma_{i_2}\ldots\Gamma_{i_r]}\Psi_{\mp\, b} V^{(\mathrm{asym})}_{\mu i_1 i_2 \ldots i_r}\ ; &\qquad r-\text{odd},
\end{aligned} \tag{A.60}$$

for n-even, and for n-odd $(r-\text{even}) \leftrightarrow (r-\text{odd})$ in the eq. (A.60). A detailed discussion on $SO(2n)$ group with GUT orientation can be found in [152, 402].

Appendix B

One and Two Loop Beta Function Coefficients for RG Evolution of Gauge Couplings

Symmetry	a_i	b_{ij} (GeV)
G_{213}	$\left(-19/6, 41/10, -7\right)$	$\begin{pmatrix} 199/50, 27/10, 44/5 \\ 9/10, 35/6, 12 \\ 11/10, 9/2, -26 \end{pmatrix}$
G_{2113}	$\left(-3, 57/12, 37/8, -7\right)$	$\begin{pmatrix} 8, 1, 3/2, 12 \\ 3/2, 33/57, 63/8, 12 \\ 9/2, 63/8, 209/16, 4 \\ 9/2, 3/2, 1/2, 26 \end{pmatrix}$
G_{2213}	$\left(-2, -3/2, 29/4, -7\right)$	$\begin{pmatrix} 31, 6, 39/2, 12 \\ 6, 115/6, 3/2, 12 \\ 81/2, 6, 181/8, 4 \\ 9/2, 9/2, 1/2, -26 \end{pmatrix}$
G_{2213D}	$\left(-3/2, -3/2, 15/2, -7\right)$	$\begin{pmatrix} 319/6, 6, 57/4, 12 \\ 6, 319/6, 57/4, 12 \\ 171/4, 171/4, 239/4, 4 \\ 9/2, 9/2, 1/2, -26 \end{pmatrix}$

Table B.1: One-loop and two-loop beta function coefficients for gauge coupling evolutions described in the text taking the second Higgs doublet mass at 1 TeV.

Appendix C

Renormalization Group Evolution

Each of the two $SO(10)$ models we have considered for type-II seesaw has two types of nonstandard gauge symmetries, G_{2213} or G_{2213D} and G_{2113}. Here we derive RGEs for running Yukawa and fermion mass matrices from which, following the earlier approach [304], we derive RGEs for the mass eigenvalues and mixing angles. We define the rescaled β-functions

$$16\pi^2\mu\frac{\partial F_i}{\partial\mu} = \beta_{F_i}. \tag{C.1}$$

With G_{2113} symmetry the scalar field $\Phi_d(2, 1/2, 0, 1)$ through its VEV v_d gives masses to down quarks and charged leptons while $\Phi_u(2, -1/2, 0, 1)$ through its VEV v_u gives Dirac masses to up quarks and neutrinos. These fields are embedded into separate bi-doublets in the presence of G_{2213} and their vacuum structure has been specified in Sec. 5. We have derived the beta functions for RG evolution of Yukawa matrices (Y_i), fermion mass matrices (M_i), and the vacuum expectation values ($v_{u,d}$). The rescaled beta functions are given below in both cases,

G_{2113} Symmetry:

$$\begin{aligned}
\beta_{Y_u} &= \left[\frac{3}{2}Y_uY_u^\dagger + \frac{1}{2}Y_dY_d^\dagger + T_u - \sum_i C_i^q g_i^2\right]Y_u, \\
\beta_{Y_d} &= \left[\frac{3}{2}Y_dY_d^\dagger + \frac{1}{2}Y_uY_u^\dagger + T_d - \sum_i C_i^q g_i^2\right]Y_d,
\end{aligned}$$

$$\begin{aligned}
\beta_{Y_\nu} &= \left[\frac{3}{2}Y_\nu Y_\nu^\dagger + \frac{1}{2}Y_e Y_e^\dagger + T_u - \sum_i C_i^l g_i^2\right] Y_\nu, \\
\beta_{Y_e} &= \left[\frac{3}{2}Y_e Y_e^\dagger + \frac{1}{2}Y_\nu Y_\nu^\dagger + T_d - \sum_i C_i^l g_i^2\right] Y_e,
\end{aligned}$$

$$\begin{aligned}
\beta_{M_u} &= \left[\frac{3}{2}Y_u Y_u^\dagger + \frac{1}{2}Y_d Y_d^\dagger - \sum_i \tilde{C}_i^q g_i^2\right] M_u, \\
\beta_{M_d} &= \left[\frac{3}{2}Y_d Y_d^\dagger + \frac{1}{2}Y_u Y_u^\dagger - \sum_i \tilde{C}_i^q g_i^2\right] M_d, \\
\beta_{M_D} &= \left[\frac{3}{2}Y_\nu u Y_\nu^\dagger + \frac{1}{2}Y_e Y_e^\dagger - \sum_i \tilde{C}_i^l g_i^2\right] M_D, \\
\beta_{M_e} &= \left[\frac{3}{2}Y_e u Y_e^\dagger + \frac{1}{2}Y_\nu Y_\nu^\dagger - \sum_i \tilde{C}_i^l g_i^2\right] M_e,
\end{aligned} \tag{C.2}$$

where the beta-functions for VEVs are

$$\begin{aligned}
\beta_{v_u} &= \left[\sum_i C_i^v g_i^2 - T_u\right] v_u, \\
\beta_{v_d} &= \left[\sum_i C_i^v g_i^2 - T_d\right] v_d,
\end{aligned} \tag{C.3}$$

with

$$T_u = \mathrm{Tr}(3Y_u^\dagger Y_u + Y_\nu^\dagger Y_\nu),\ T_d = \mathrm{Tr}(3Y_d^\dagger Y_d + Y_e^\dagger Y_e). \tag{C.4}$$

The parameters occurring in these equations, and also in eq. (C.9) and eq. (C.10) given below are

$$\begin{aligned}
&a = \frac{3}{2},\ b = \frac{1}{2},\ a' = b' = 0, \\
&C_i^q = (9/4, 3/4, 1/4, 8),\ C_i^l = (9/4, 3/4, 9/4, 0), \\
&\tilde{C}_i^q = (0, 0, 1/4, 8), \tilde{C}_i^l = (0, 0, 9/4, 0),\ C_i^v = (9/4, 3/4, 0, 0), \\
&i = 2L, 1R, BL, 3C.
\end{aligned} \tag{C.5}$$

G_{2213} Symmetry:

Following definitions of Sec. 5 in the presence of left-right symmetry. the rescaled beta functions for RGEs of the Yukawa and fermion mass matrices are

$$\begin{aligned}
\beta_{Y_u} &= (Y_uY_u^\dagger + Y_dY_d^\dagger)Y_u + Y_u(Y_u^\dagger Y_u + Y_d^\dagger Y_d) + T_uY_u + \hat{T}_1Y_d - \sum_i C_i^q g_i^2 Y_u, \\
\beta_{Y_d} &= (Y_dY_d^\dagger + Y_uY_u^\dagger)Y_d + Y_d(Y_d^\dagger Y_d + Y_u^\dagger Y_u) + T_dY_d + \hat{T}_2Y_u - \sum_i C_i^q g_i^2 Y_d, \\
\beta_{Y_\nu} &= (Y_\nu Y_\nu^\dagger + Y_eY_e^\dagger)Y_\nu + Y_\nu(Y_\nu^\dagger Y_\nu + Y_e^\dagger Y_e) + T_uY_\nu + \hat{T}_1Y_e - \sum_i C_i^l g_i^2 Y_\nu, \\
\beta_{Y_e} &= (Y_eY_e^\dagger + Y_\nu Y_\nu^\dagger)Y_e + Y_e(Y_e^\dagger Y_e + Y_\nu^\dagger Y_\nu) + T_dY_e + \hat{T}_2Y_\nu - \sum_i C_i^l g_i^2 Y_e,
\end{aligned}$$

$$\begin{aligned}
\beta_{M_u} &= (Y_uY_u^\dagger + Y_dY_d^\dagger)M_u + M_u(Y_u^\dagger Y_u + Y_d^\dagger Y_d) - \sum_i \tilde{C}_i^q g_i^2 M_u + \hat{T}_1 \tan\beta M_d, \\
\beta_{M_d} &= (Y_dY_d^\dagger + Y_uY_u^\dagger)M_d + M_d(Y_d^\dagger Y_d + Y_u^\dagger Y_u) - \sum_i \tilde{C}_i^q g_i^2]M_d + \frac{\hat{T}_2}{\tan\beta}M_u, \\
\beta_{M_D} &= (Y_\nu u Y_\nu^\dagger + Y_eY_e^\dagger)M_D + M_D(Y_\nu^\dagger Y_\nu + Y_e^\dagger Y_e) - \sum_i \tilde{C}_i^l g_i^2 M_D + \hat{T}_1 \tan\beta M_e, \\
\beta_{M_e} &= (Y_eY_e^\dagger + Y_\nu Y_\nu^\dagger)M_e + M_e(Y_e^\dagger Y_e + Y_\nu^\dagger Y_\nu) - \sum_i \tilde{C}_i^l g_i^2 M_e + \frac{\hat{T}_2}{\tan\beta}M_D, \quad \text{(C.6)}
\end{aligned}$$

where the rescaled beta functions for VEVs β_{v_u}, β_{v_d} are the same as in eq. (C.3) with different coefficients C_i^v defined below and functions T_u and T_d are the same as in eq. (C.4). Other two traces entering in this case are

$$\begin{aligned}
\hat{T}_1 &= \mathrm{Tr}(3Y_d^\dagger Y_u + Y_e^\dagger Y_\nu), \\
\hat{T}_2 &= \mathrm{Tr}(3Y_u^\dagger Y_d + Y_\nu^\dagger Y_e). \quad \text{(C.7)}
\end{aligned}$$

The parameters occurring in these equations and also in eq. (C.9) and eq. (C.10) given below are

$$\begin{aligned}
a &= b = 2,\ a' = b' = 1, \\
C_i^q &= (9/4, 9/4, 1/4, 8),\ C_i^l = (9/4, 9/4, 9/4, 0),\ \tilde{C}_i^q = (0, 0, 1/4, 8), \\
\tilde{C}_i^l &= (0, 0, 9/4, 0),\ C_i^v = (9/4, 9/4, 0, 0),\ (i = 2L, 2R, BL, 3C). \quad \text{(C.8)}
\end{aligned}$$

Then following the procedure described in [304], and using the definition of parameters in the two different mass ranges, given above we obtain RGEs for mass eigenvalues and elements of CKM mixing matrix $V_{\alpha\beta}$ which can be expressed in the generalized form for both cases,

Mass Eigenvalues:

$$
\begin{aligned}
\beta_{m_i} &= \left[-\sum_k \tilde{C}_k^{(q)} g_k^2 + a y_i^2 + 2b \sum_{j=d,s,b} |V_{uj}|^2 y_j^2 + a' \frac{\hat{T}_1 \tan\beta}{m_i} \sum_{j=d,s,b} |V_{uj}|^2 m_j \right] m_i, \\
&\quad \text{where } i = u, c, t \\
\beta_{m_i} &= \left[-\sum_k \tilde{C}_k^{(q)} g_k^2 + a y_i^2 + 2b \sum_{j=u,c,t} |V_{dj}|^2 y_j^2 + b' \frac{\hat{T}_2}{\tan\beta m_i} \sum_{j=u,c,t} |V_{dj}|^2 m_j \right] m_i, \\
&\quad \text{where } i = d, s, b \\
\beta_{m_i} &= \left[-\sum_k \tilde{C}_k^{(l)} g_k^2 + a y_i^2 + 2b \sum_{j=N_1,N_2,N_3} y_j^2 + b' \frac{\hat{T}_2}{\tan\beta m_i} \sum_{j=N_1,N_2,N_3} m_j \right] m_i, \\
&\quad \text{where } i = e, \mu, \tau \\
\beta_{m_i} &= \left[-\sum_k \tilde{C}_k^{(l)} g_k^2 + a y_i^2 + a' \frac{\hat{T}_1 \tan\beta}{m_i} \sum_{j=e,\mu,\tau} m_j \right] m_i, \\
&\quad \text{where } i = N_1, N_2, N_3 \, .
\end{aligned}
\tag{C.9}
$$

CKM Matrix Elements:

$$
\begin{aligned}
\beta_{V_{\alpha\beta}} &= \sum_{\gamma=u,c,t;\gamma\neq\alpha} \left[a' \frac{\hat{T}_1 \tan\beta}{m_\alpha - m_\gamma} (V \hat{M}_d V^\dagger)_{\alpha\gamma} + \frac{b}{v_d^2} \frac{m_\alpha^2 + m_\gamma^2}{m_\alpha^2 - m_\gamma^2} (V \hat{M}_d^2 V^\dagger)_{\alpha\gamma} \right] V_{\gamma\beta} \\
&- \sum_{\gamma=d,s,b;\gamma\neq\beta} V_{\alpha\gamma} \left[b' \frac{\hat{T}_2}{\tan\beta (m_\gamma - m_\alpha)} (V^\dagger \hat{M}_u V)_{\gamma\beta} \right. \\
&+ \left. \frac{b}{v_u^2} \frac{m_\gamma^2 + m_\beta^2}{m_\gamma^2 - m_\beta^2} (V^\dagger \hat{M}_u^2 V)_{\gamma\beta} \right] .
\end{aligned}
\tag{C.10}
$$

Then using third generation dominance, the beta functions for all the 9 elements are easily obtained for respective mass ranges where in addition to the parameters in the respective cases in eq. (C.5) and eq. (C.8), $a' = b' = 0$ in the mass range $M_{R^0} \to M_{R^+}$ with G_{2113} symmetry, but $a' = b' = 1$ in the mass range $M_{R^+} \to M_{GUT}$ with G_{2213} or G_{2213D} symmetry and, in the latter case, the nonvanishing traces $\hat{T}_{1,2}$ are easily evaluated in the mass basis.

Appendix D

Block Diagonalisation and Determination of $\mathcal{M}_\nu$

In this section we discuss the various steps of block diagonalisation in order to calculate the light neutrino mass, sterile neutrino mass and right-handed neutrino mass and their mixings. The complete 9×9 mass matrix in the flavor basis $\{\nu_L, S_L, N_R^C\}$ is

$$\mathcal{M} = \begin{pmatrix} m_\nu^{II} & M_L & M_D \\ M_L^T & 0 & M \\ M_D^T & M^T & M_N \end{pmatrix}, \tag{D.1}$$

where $M_L = y_\chi v_{\chi_L}$, $M = y_\chi v_{\chi_R}$, $M_N = f v_R$
and M_D is the Dirac neutrino mass matrix as discussed in Sec. 5.
Assuming a generalized unitary transformation from mass basis to flavor basis, gives

$$|\psi\rangle_{flavor} = \mathcal{V}\,|\psi\rangle_{mass} \tag{D.2}$$

or

$$\begin{pmatrix} \nu_\alpha \\ S_\beta \\ N_\gamma^C \end{pmatrix} = \begin{pmatrix} \mathcal{V}_{\alpha i}^{\nu\nu} & \mathcal{V}_{\alpha j}^{\nu S} & \mathcal{V}_{\alpha k}^{\nu N} \\ \mathcal{V}_{\beta i}^{S\nu} & \mathcal{V}_{\beta j}^{SS} & \mathcal{V}_{\beta k}^{SN} \\ \mathcal{V}_{\gamma i}^{N\nu} & \mathcal{V}_{\gamma j}^{NS} & \mathcal{V}_{\gamma k}^{NN} \end{pmatrix} \begin{pmatrix} \hat{\nu}_i \\ \hat{S}_j \\ \hat{N}_k \end{pmatrix} \tag{D.3}$$

with

$$\mathcal{V}^\dagger \mathcal{M} \mathcal{V}^* = \hat{\mathcal{M}} = \text{diag}\left(\hat{\mathcal{M}}_{\nu_i}; \hat{\mathcal{M}}_{\mathcal{S}_j}; \hat{\mathcal{M}}_{\mathcal{N}_k}\right) \tag{D.4}$$

Here $\mathcal{M}_\nu$ is the 9×9 neutral fermion mass matrix in flavor basis with α, β, γ running over three generations of light-neutrinos, sterile-neutrinos and right handed heavy-neutrinos in their respective flavor states and $\hat{\mathcal{M}}_\nu$ is the diagonal mass matrix with $(i, j, k = 1, 2, 3)$ running over corresponding mass states .
In the first step of block diagonalisation, the full neutrino mass matrix is reduced to a block diagonal form $\hat{\mathcal{M}}_{\rm BD}$ and in the second step we further block diagonalize to obtain the three matrices as three different block diagonal elements, $\mathcal{M}_{\rm BD}$= $diag(\mathcal{M}_\nu, m_S, m_N)$ whose each diagonal element is a 3×3 matrix.In our estimation, we have used the mass hierarchy $M_N > M \gg M_D, M_L, f v_L$. Finally in the third step we discuss complete diagonalization to arrive at the physical masses and their mixings.

D.0.2.1 Determination of $\mathcal{M}_{\rm BD}$

With two unitary matrix transformations $\mathcal{Q}_1$ and $\mathcal{Q}_2$,

$$\mathcal{Q}^\dagger \mathcal{M}_\nu \mathcal{Q}^* = \hat{\mathcal{M}}_{\rm BD}, \tag{D.5}$$

where

$$\mathcal{Q} = \mathcal{Q}_1\, \mathcal{Q}_2 \tag{D.6}$$

i.e the product matrix $\mathcal{Q} = \mathcal{Q}_1\, \mathcal{Q}_2$ directly give $\mathcal{M}_{\rm BD}$ from $\mathcal{M}_\nu$ Here $\hat{\mathcal{M}}_{\rm BD}$, and $\mathcal{M}_{\rm BD}$ are the intermediate block-diagonal, and full block-diagonal mass matrices, respectively,

$$\hat{\mathcal{M}}_{\rm BD} = \begin{pmatrix} \mathcal{M}_{eff} & 0 \\ 0 & m_N \end{pmatrix} \tag{D.7}$$

and

$$\mathcal{M}_{\rm BD} = \begin{pmatrix} \mathcal{M}_\nu & 0 & 0 \\ 0 & m_S & 0 \\ 0 & 0 & m_N \end{pmatrix} \tag{D.8}$$

D.0.2.2 Determination of Q_1

In the leading order parametrization the standard form of $\mathcal{Q}_1$ is

$$\mathcal{Q}_1 = \begin{pmatrix} 1-\frac{1}{2}R^*R^T & R^* \\ -R^T & 1-\frac{1}{2}R^TR^* \end{pmatrix}, \tag{D.9}$$

where R is a 6×3 dimensional matrix.

$$R^\dagger = M_N^{-1}\left(M_D^T, M^T\right) = \left(K^T, J^T\right) \tag{D.10}$$

$$J = M{M_N}^{-1}K = M_D M_N^{-1} I = KJ^{-1} = M_D M^{-1} \tag{D.11}$$

Therefore, the transformation matrix $\mathcal{Q}_1$ can be written purely in terms of dimensionless parameters J and K

$$\mathcal{Q}_1 = \begin{pmatrix} 1-\frac{1}{2}KK^\dagger & -\frac{1}{2}KJ^\dagger & K \\ -\frac{1}{2}JK^\dagger & 1-\frac{1}{2}JJ^\dagger & J \\ -K^\dagger & -J^\dagger & 1-\frac{1}{2}(K^\dagger K + J^\dagger J) \end{pmatrix} \tag{D.12}$$

while the light and heavy mass matrices are

$$\mathcal{M}_{eff} = \begin{pmatrix} fv_L & M_L \\ M_L^T & 0 \end{pmatrix} - \begin{pmatrix} M_D M_N^{-1} M_D^T & M_D M_N^{-1} M \\ M^T M_N^{-1} M_D^T & M^T M_N^{-1} M \end{pmatrix} \tag{D.13}$$

$$m_N = M_N + .. \tag{D.14}$$

Denoting

$$\mathcal{M}_{eff} = \begin{pmatrix} Z & B \\ C & D, \end{pmatrix} \tag{D.15}$$

$$Z = fv_L - M_D M_N^{-1} M_D^T, \tag{D.16}$$

$$B = M_L - M_D M_N^{-1} M, \tag{D.17}$$

$$C = M_L^T - M^T M_N^{-1} M_D^T, \tag{D.18}$$

$$D = M^T M_N^{-1} M, \tag{D.19}$$

D.0.2.3 Determination of $\mathcal{Q}_2$

The remaining mass matrix $\mathcal{M}_{eff}$ can be further block diagonalized using another transformation matrix

$$\mathcal{S}^\dagger \mathcal{M}_{\rm eff} \mathcal{S}^* = \begin{pmatrix} \mathcal{M}_\nu & 0 \\ 0 & m_S \end{pmatrix} \tag{D.20}$$

such that in eq.(D.0.2.1)

$$\mathcal{Q}_2 = \begin{pmatrix} \mathcal{S} & 0 \\ 0 & 1 \end{pmatrix} \tag{D.21}$$

$$S = \begin{pmatrix} 1 - \frac{1}{2} P^* P^T & P^* \\ -P^T & 1 - \frac{1}{2} P^T P^* \end{pmatrix} \tag{D.22}$$

Using eq.(D.22) in eq.(D.20) ,we get through eq.(D.15)-eq.(D.19),

$$\begin{aligned} P^\dagger &= (M^T M_N^{-1} M)^{-1} \left(M^T M_N^{-1} M_D^T - M_L^T \right) \\ &= M^{-1} M_D^T - M^{-1} M_N M^{-1} M_L \end{aligned} \tag{D.23}$$

where we have used y_χ to be symmetric. leading to

$$\begin{aligned} \mathcal{M}_\nu = m_\nu^{II} + \left(M_D M_N^{-1} M_D^T \right) \\ -(M_D M_N^{-1} M_D^T) + M_L (M^T M_N^{-1} M)^{-1} M_L^T \\ -M_L (M^T M_N^{-1} M)^{-1} (M^T M_N^{-1} M_D^T) \\ -(M_D M_N^{-1} M)(M^T M_N^{-1} M)^{-1} M_L^T, \\ m_S = -M M_N^{-1} M^T + ..., \end{aligned} \tag{D.24}$$

The 3×3 block diagonal mixing matrix $\mathcal{Q}_2$ has the following form

$$\mathcal{Q}_2 = \begin{pmatrix} S & \mathbf{0} \\ \mathbf{0} & \mathbf{1} \end{pmatrix} = \begin{pmatrix} 1 - \frac{1}{2} I I^\dagger & I & 0 \\ -I^\dagger & 1 - \frac{1}{2} I^\dagger I & 0 \\ 0 & 0 & 1 \end{pmatrix} \tag{D.25}$$

where we have used eq.(D.11) to define $I = KJ^{-1} = M_D M^{-1}$.

Complete diagonalization and physical neutrino masses

The 3×3 block diagonal matrices $\mathcal{M}_\nu$, m_S and m_N can further be diagonalized to give physical masses for all neutral leptons by a 9×9 unitary matrix $\mathcal{U}$ as

$$\mathcal{U} = \begin{pmatrix} U_\nu & 0 & 0 \\ 0 & U_S & 0 \\ 0 & 0 & U_N \end{pmatrix} . \tag{D.26}$$

where the 3×3 unitary matrices U_ν, U_S and U_N satisfy

$$\begin{aligned} U_\nu^\dagger \, \mathcal{M}_\nu \, U_\nu^* &= \hat{\mathcal{M}_\nu} = \text{diag}\left(\mathcal{M}_{\nu 1}, \mathcal{M}_{\nu 2}, \mathcal{M}_{\nu 3}\right) , \\ U_S^\dagger \, m_S \, U_S^* &= \hat{m_S} = \text{diag}\left(m_{S1}, m_{S2}, m_{S3}\right) , \\ U_N^\dagger \, m_N \, U_N^* &= \hat{m_N} = \text{diag}\left(m_{N1}, m_{N2}, m_{N3}\right) \end{aligned} \tag{D.27}$$

With this discussion, the complete mixing matrix is

$$\begin{aligned} \mathcal{V} = \mathcal{Q} \cdot \mathcal{U} &= \mathcal{Q}_1 \cdot \mathcal{Q}_2 \cdot \mathcal{U} \\ &= \begin{pmatrix} 1 - \frac{1}{2} K K^\dagger & -\frac{1}{2} K J^\dagger & K \\ -\frac{1}{2} J K^\dagger & 1 - \frac{1}{2} J J^\dagger & J \\ -K^\dagger & -J^\dagger & 1 - \frac{1}{2}(K^\dagger K + J^\dagger J) \end{pmatrix} . \\ & \quad \begin{pmatrix} 1 - \frac{1}{2} I I^\dagger & I & 0 \\ -I^\dagger & 1 - \frac{1}{2} I^\dagger I & 0 \\ 0 & 0 & 1 \end{pmatrix} \begin{pmatrix} U_\nu & 0 & 0 \\ 0 & U_S & 0 \\ 0 & 0 & U_N \end{pmatrix} \\ &= \begin{pmatrix} 1 - \frac{1}{2} I I^\dagger & I - \frac{1}{2} K J^\dagger & K \\ -I^\dagger & 1 - \frac{1}{2}(I^\dagger I + J J^\dagger) & J - \frac{1}{2} I^\dagger K \\ 0 & -J^\dagger & 1 - \frac{1}{2} J^\dagger J \end{pmatrix} \cdot \begin{pmatrix} U_\nu & 0 & 0 \\ 0 & U_S & 0 \\ 0 & 0 & U_N \end{pmatrix} \end{aligned} \tag{D.28}$$

Appendix E

SO(10) Representation

E.1 Decomposition of $SO(10)$ irreducible representations

Since we have been extensively using the decomposition of various $SO(10)$ representations in to it subgroups, and very often we required various scalar sub-multiplets at various scalars following extended survival hypothesis and residing in the symmetry at the corresponding scale, we would often require the decomposition table. We have borrowed the tables for various representations from a very good review on $SO(10)$ group theory by Fukuyama *et al* [153].

$(4_C, 2_L, 2_R)$	$(3_C, 2_L, 2_R, 1_{B-L})$	$(3_C, 2_L, 1_R, 1_{B-L})$	$(3_C, 2_L, 1_Y)$	$(5, 1_X)$
$(\mathbf{6}, \mathbf{1}, \mathbf{1})$	$\left(\mathbf{3}, \mathbf{1}, \mathbf{1}; -\frac{1}{3}\right)$ $\left(\overline{\mathbf{3}}, \mathbf{1}, \mathbf{1}; \frac{1}{3}\right)$	$\left(\mathbf{3}, \mathbf{1}; 0, -\frac{1}{3}\right)$ $\left(\overline{\mathbf{3}}, \mathbf{1}; 0, \frac{1}{3}\right)$	$\left(\mathbf{3}, \mathbf{1}; -\frac{1}{3}\right)$ $\left(\overline{\mathbf{3}}, \mathbf{1}; \frac{1}{3}\right)$	$(\mathbf{5}, 2)$ $(\overline{\mathbf{5}}, -2)$
$(\mathbf{1}, \mathbf{2}, \mathbf{2})$	$(\mathbf{1}, \mathbf{2}, \mathbf{2}; 0)$	$\left(\mathbf{1}, \mathbf{2}; \frac{1}{2}, 0\right)$ $\left(\mathbf{1}, \mathbf{2}; -\frac{1}{2}, 0\right)$	$\left(\mathbf{1}, \mathbf{2}; \frac{1}{2}\right)$ $\left(\mathbf{1}, \mathbf{2}; -\frac{1}{2}\right)$	$(\mathbf{5}, 2)$ $(\overline{\mathbf{5}}, -2)$

Table E.1: Decomposition of the representation **10**

$(4_C,2_L,2_R)$	$(3_C,2_L,2_R,1_{B-L})$	$(3_C,2_L,1_R,1_{B-L})$	$(3_C,2_L,1_Y)$	$(5,1_X)$
$(\mathbf{4},\mathbf{2},\mathbf{1})$	$(\mathbf{3},\mathbf{2},\mathbf{1};\frac{1}{6})$ $(\mathbf{1},\mathbf{2},\mathbf{1};-\frac{1}{2})$	$(\mathbf{3},\mathbf{2};0,\frac{1}{6})$ $(\mathbf{1},\mathbf{2};0,-\frac{1}{2})$	$(\mathbf{3},\mathbf{2};\frac{1}{6})$ $(\mathbf{1},\mathbf{2};-\frac{1}{2})$	$(\mathbf{10},-1)$ $(\overline{\mathbf{5}},3)$
$(\overline{\mathbf{4}},\mathbf{1},\mathbf{2})$	$(\overline{\mathbf{3}},\mathbf{1},\mathbf{2};-\frac{1}{6})$ $(\mathbf{1},\mathbf{1},\mathbf{2};\frac{1}{2})$	$(\overline{\mathbf{3}},\mathbf{1};\frac{1}{2},-\frac{1}{6})$ $(\overline{\mathbf{3}},\mathbf{1};-\frac{1}{2},-\frac{1}{6})$ $(\mathbf{1},\mathbf{1};\frac{1}{2},\frac{1}{2})$ $(\mathbf{1},\mathbf{1};-\frac{1}{2},\frac{1}{2})$	$(\overline{\mathbf{3}},\mathbf{1};\frac{1}{3})$ $(\overline{\mathbf{3}},\mathbf{1};-\frac{2}{3})$ $(\mathbf{1},\mathbf{1};1)$ $(\mathbf{1},\mathbf{1};0)$	$(\overline{\mathbf{5}},3)$ $(\mathbf{10},-1)$ $(\mathbf{10},-1)$ $(\mathbf{1},-5)$

Table E.2: Decomposition of the representation **16**

$(4_C,2_L,2_R)$	$(3_C,2_L,2_R,1_{B-L})$	$(3_C,2_L,1_R,1_{B-L})$	$(3_C,2_L,1_Y)$	$(5,1_X)$
$(\mathbf{1},\mathbf{1},\mathbf{3})$	$(\mathbf{1},\mathbf{1},\mathbf{3};0)$	$(\mathbf{1},\mathbf{1};1,0)$ $(\mathbf{1},\mathbf{1};0,0)$ $(\mathbf{1},\mathbf{1};-1,0)$	$(\mathbf{1},\mathbf{1};1)$ $(\mathbf{1},\mathbf{1};0)$ $(\mathbf{1},\mathbf{1};-1)$	$(\mathbf{10},4)$ $(\mathbf{1},0)$ $(\overline{\mathbf{10}},-4)$
$(\mathbf{1},\mathbf{3},\mathbf{1})$	$(\mathbf{1},\mathbf{3},\mathbf{1};0)$	$(\mathbf{1},\mathbf{3};0,0)$	$(\mathbf{1},\mathbf{3};0)$	$(\mathbf{24},0)$
$(\mathbf{6},\mathbf{2},\mathbf{2})$	$(\mathbf{3},\mathbf{2},\mathbf{2};-\frac{1}{3})$ $(\overline{\mathbf{3}},\mathbf{2},\mathbf{2};\frac{1}{3})$	$(\mathbf{3},\mathbf{2};\frac{1}{2},-\frac{1}{3})$ $(\mathbf{3},\mathbf{2};-\frac{1}{2},-\frac{1}{3})$ $(\overline{\mathbf{3}},\mathbf{2};\frac{1}{2},\frac{1}{3})$ $(\overline{\mathbf{3}},\mathbf{2};-\frac{1}{2},\frac{1}{3})$	$(\mathbf{3},\mathbf{2};\frac{1}{6})$ $(\mathbf{3},\mathbf{2};-\frac{5}{6})$ $(\overline{\mathbf{3}},\mathbf{2};\frac{5}{6})$ $(\overline{\mathbf{3}},\mathbf{2};-\frac{1}{6})$	$(\mathbf{10},4)$ $(\mathbf{24},0)$ $(\mathbf{24},0)$ $(\overline{\mathbf{10}},-4)$
$(\mathbf{15},\mathbf{1},\mathbf{1})$	$(\mathbf{1},\mathbf{1},\mathbf{1};0)$ $(\mathbf{3},\mathbf{1},\mathbf{1};\frac{2}{3})$ $(\overline{\mathbf{3}},\mathbf{1},\mathbf{1};-\frac{2}{3})$ $(\mathbf{8},\mathbf{1},\mathbf{1};0)$	$(\mathbf{1},\mathbf{1};0,0)$ $(\mathbf{3},\mathbf{1};0,\frac{2}{3})$ $(\overline{\mathbf{3}},\mathbf{1};0,-\frac{2}{3})$ $(\mathbf{8},\mathbf{1};0,0)$	$(\mathbf{1},\mathbf{1};0)$ $(\mathbf{3},\mathbf{1};\frac{2}{3})$ $(\overline{\mathbf{3}},\mathbf{1};-\frac{2}{3})$ $(\mathbf{8},\mathbf{1};0)$	$(\mathbf{24},0)$ $(\overline{\mathbf{10}},-4)$ $(\mathbf{10},4)$ $(\mathbf{24},0)$

Table E.3: Decomposition of the representation **45**

$(4_C,2_L,2_R)$	$(3_C,2_L,2_R,1_{B-L})$	$(3_C,2_L,1_R,1_{B-L})$	$(3_C,2_L,1_Y)$	$(5,1_X)$
$(\mathbf{1},\mathbf{1},\mathbf{1})$	$(\mathbf{1},\mathbf{1},\mathbf{1};0)$	$(\mathbf{1},\mathbf{1};0,0)$	$(\mathbf{1},\mathbf{1};0)$	$(\mathbf{24},0)$
$(\mathbf{1},\mathbf{3},\mathbf{3})$	$(\mathbf{1},\mathbf{3},\mathbf{3};0)$	$(\mathbf{1},\mathbf{3};1,0)$ $(\mathbf{1},\mathbf{3};0,0)$ $(\mathbf{1},\mathbf{3};-1,0)$	$(\mathbf{1},\mathbf{3};1)$ $(\mathbf{1},\mathbf{3};0)$ $(\mathbf{1},\mathbf{3};-1)$	$(\mathbf{15},4)$ $(\mathbf{24},0)$ $(\overline{\mathbf{15}},-4)$
$(\mathbf{20'},\mathbf{1},\mathbf{1})$	$(\overline{\mathbf{6}},\mathbf{1},\mathbf{1};\frac{2}{3})$ $(\mathbf{6},\mathbf{1},\mathbf{1};-\frac{2}{3})$ $(\mathbf{8},\mathbf{1},\mathbf{1};0)$	$(\overline{\mathbf{6}},\mathbf{1};0,\frac{2}{3})$ $(\mathbf{6},\mathbf{1};0,-\frac{2}{3})$ $(\mathbf{8},\mathbf{1};0,0)$	$(\overline{\mathbf{6}},\mathbf{1};\frac{2}{3})$ $(\mathbf{6},\mathbf{1};-\frac{2}{3})$ $(\mathbf{8},\mathbf{1};0)$	$(\overline{\mathbf{15}},-4)$ $(\mathbf{15},4)$ $(\mathbf{24},0)$
$(\mathbf{6},\mathbf{2},\mathbf{2})$	$(\mathbf{3},\mathbf{2},\mathbf{2};-\frac{1}{3})$ $(\overline{\mathbf{3}},\mathbf{2},\mathbf{2};\frac{1}{3})$	$(\mathbf{3},\mathbf{2};\frac{1}{2},-\frac{1}{3})$ $(\mathbf{3},\mathbf{2};-\frac{1}{2},-\frac{1}{3})$ $(\overline{\mathbf{3}},\mathbf{2};\frac{1}{2},\frac{1}{3})$ $(\overline{\mathbf{3}},\mathbf{2};-\frac{1}{2},\frac{1}{3})$	$(\mathbf{3},\mathbf{2};\frac{1}{6})$ $(\mathbf{3},\mathbf{2};-\frac{5}{6})$ $(\overline{\mathbf{3}},\mathbf{2};\frac{5}{6})$ $(\overline{\mathbf{3}},\mathbf{2};-\frac{1}{6})$	$(\mathbf{15},4)$ $(\mathbf{24},0)$ $(\mathbf{24},0)$ $(\overline{\mathbf{15}},-4)$

Table E.4: Decomposition of the representation **54**

$(4_C, 2_L, 2_R)$	$(3_C, 2_L, 2_R, 1_{B-L})$	$(3_C, 2_L, 1_R, 1_{B-L})$	$(3_C, 2_L, 1_Y)$	$(5, 1_X)$
$(\mathbf{1}, \mathbf{2}, \mathbf{2})$	$(\mathbf{1}, \mathbf{2}, \mathbf{2}; 0)$	$\left(\mathbf{1}, \mathbf{2}; \frac{1}{2}, 0\right)$	$\left(\mathbf{1}, \mathbf{2}; \frac{1}{2}\right)$	$(\mathbf{5}, 2)$
		$\left(\mathbf{1}, \mathbf{2}; -\frac{1}{2}, 0\right)$	$\left(\mathbf{1}, \mathbf{2}; -\frac{1}{2}\right)$	$(\overline{\mathbf{5}}, -2)$
$(\mathbf{10}, \mathbf{1}, \mathbf{1})$	$(\mathbf{1}, \mathbf{1}, \mathbf{1}; -1)$	$(\mathbf{1}, \mathbf{1}; 0, -1)$	$(\mathbf{1}, \mathbf{1}; -1)$	$(\overline{\mathbf{10}}, 6)$
	$\left(\mathbf{3}, \mathbf{1}, \mathbf{1}; -\frac{1}{3}\right)$	$\left(\mathbf{3}, \mathbf{1}; 0, -\frac{1}{3}\right)$	$\left(\mathbf{3}, \mathbf{1}; -\frac{1}{3}\right)$	$(\mathbf{5}, 2)$
	$\left(\mathbf{6}, \mathbf{1}, \mathbf{1}; \frac{1}{3}\right)$	$\left(\mathbf{6}, \mathbf{1}; 0, \frac{1}{3}\right)$	$\left(\mathbf{6}, \mathbf{1}; \frac{1}{3}\right)$	$(\overline{\mathbf{45}}, -2)$
$(\overline{\mathbf{10}}, \mathbf{1}, \mathbf{1})$	$(\mathbf{1}, \mathbf{1}, \mathbf{1}; 1)$	$(\mathbf{1}, \mathbf{1}; 0, 1)$	$(\mathbf{1}, \mathbf{1}; 1)$	$(\mathbf{10}, -6)$
	$\left(\overline{\mathbf{3}}, \mathbf{1}, \mathbf{1}; \frac{1}{3}\right)$	$\left(\overline{\mathbf{3}}, \mathbf{1}; 0, \frac{1}{3}\right)$	$\left(\overline{\mathbf{3}}, \mathbf{1}; \frac{1}{3}\right)$	$(\overline{\mathbf{5}}, -2)$
	$\left(\overline{\mathbf{6}}, \mathbf{1}, \mathbf{1}; -\frac{1}{3}\right)$	$\left(\overline{\mathbf{6}}, \mathbf{1}; 0, -\frac{1}{3}\right)$	$\left(\overline{\mathbf{6}}, \mathbf{1}; -\frac{1}{3}\right)$	$(\mathbf{45}, 2)$
$(\mathbf{6}, \mathbf{3}, \mathbf{1})$	$\left(\mathbf{3}, \mathbf{3}, \mathbf{1}; -\frac{1}{3}\right)$	$\left(\mathbf{3}, \mathbf{3}; 0, -\frac{1}{3}\right)$	$\left(\mathbf{3}, \mathbf{3}; -\frac{1}{3}\right)$	$(\mathbf{45}, 2)$
	$\left(\overline{\mathbf{3}}, \mathbf{3}, \mathbf{1}; \frac{1}{3}\right)$	$\left(\overline{\mathbf{3}}, \mathbf{3}; 0, \frac{1}{3}\right)$	$\left(\overline{\mathbf{3}}, \mathbf{3}; \frac{1}{3}\right)$	$(\overline{\mathbf{45}}, -2)$
$(\mathbf{6}, \mathbf{1}, \mathbf{3})$	$\left(\mathbf{3}, \mathbf{1}, \mathbf{3}; -\frac{1}{3}\right)$	$\left(\mathbf{3}, \mathbf{1}; 1, -\frac{1}{3}\right)$	$\left(\mathbf{3}, \mathbf{1}; \frac{2}{3}\right)$	$(\overline{\mathbf{10}}, 6)$
		$\left(\mathbf{3}, \mathbf{1}; 0, -\frac{1}{3}\right)$	$\left(\mathbf{3}, \mathbf{1}; -\frac{1}{3}\right)$	$(\mathbf{45}, 2)$
		$\left(\mathbf{3}, \mathbf{1}; -1, -\frac{1}{3}\right)$	$\left(\mathbf{3}, \mathbf{1}; -\frac{4}{3}\right)$	$(\overline{\mathbf{45}}, -2)$
	$\left(\overline{\mathbf{3}}, \mathbf{1}, \mathbf{3}; \frac{1}{3}\right)$	$\left(\overline{\mathbf{3}}, \mathbf{1}; 1, \frac{1}{3}\right)$	$\left(\overline{\mathbf{3}}, \mathbf{1}; \frac{4}{3}\right)$	$(\mathbf{45}, 2)$
		$\left(\overline{\mathbf{3}}, \mathbf{1}; 0, \frac{1}{3}\right)$	$\left(\overline{\mathbf{3}}, \mathbf{1}; \frac{1}{3}\right)$	$(\overline{\mathbf{45}}, -2)$
		$\left(\overline{\mathbf{3}}, \mathbf{1}; -1, \frac{1}{3}\right)$	$\left(\overline{\mathbf{3}}, \mathbf{1}; -\frac{2}{3}\right)$	$(\mathbf{10}, -6)$
$(\mathbf{15}, \mathbf{2}, \mathbf{2})$	$(\mathbf{1}, \mathbf{2}, \mathbf{2}; 0)$	$\left(\mathbf{1}, \mathbf{2}; \frac{1}{2}, 0\right)$	$\left(\mathbf{1}, \mathbf{2}; \frac{1}{2}\right)$	$(\mathbf{45}, 2)$
		$\left(\mathbf{1}, \mathbf{2}; -\frac{1}{2}, 0\right)$	$\left(\mathbf{1}, \mathbf{2}; -\frac{1}{2}\right)$	$(\overline{\mathbf{45}}, -2)$
	$\left(\mathbf{3}, \mathbf{2}, \mathbf{2}; \frac{2}{3}\right)$	$\left(\mathbf{3}, \mathbf{2}; \frac{1}{2}, \frac{2}{3}\right)$	$\left(\mathbf{3}, \mathbf{2}; \frac{7}{6}\right)$	$(\overline{\mathbf{45}}, -2)$
		$\left(\mathbf{3}, \mathbf{2}; -\frac{1}{2}, \frac{2}{3}\right)$	$\left(\mathbf{3}, \mathbf{2}; \frac{1}{6}\right)$	$(\mathbf{10}, -6)$
	$\left(\overline{\mathbf{3}}, \mathbf{2}, \mathbf{2}; -\frac{2}{3}\right)$	$\left(\overline{\mathbf{3}}, \mathbf{2}; -\frac{1}{2}, -\frac{2}{3}\right)$	$\left(\overline{\mathbf{3}}, \mathbf{2}; -\frac{7}{6}\right)$	$(\mathbf{45}, 2)$
		$\left(\overline{\mathbf{3}}, \mathbf{2}; \frac{1}{2}, -\frac{2}{3}\right)$	$\left(\overline{\mathbf{3}}, \mathbf{2}; -\frac{1}{6}\right)$	$(\overline{\mathbf{10}}, 6)$
	$(\mathbf{8}, \mathbf{2}, \mathbf{2}; 0)$	$\left(\mathbf{8}, \mathbf{2}; \frac{1}{2}, 0\right)$	$\left(\mathbf{8}, \mathbf{2}; \frac{1}{2}\right)$	$(\mathbf{45}, 2)$
		$\left(\mathbf{8}, \mathbf{2}; -\frac{1}{2}, 0\right)$	$\left(\mathbf{8}, \mathbf{2}; -\frac{1}{2}\right)$	$(\overline{\mathbf{45}}, -2)$

Table E.5: Decomposition of the representation **120**

$(4_C, 2_L, 2_R)$	$(3_C, 2_L, 2_R, 1_{B-L})$	$(3_C, 2_L, 1_R, 1_{B-L})$	$(3_C, 2_L, 1_Y)$	$(5, 1_X)$
$(\mathbf{6}, \mathbf{1}, \mathbf{1})$	$\left(\mathbf{3}, \mathbf{1}, \mathbf{1}; -\frac{1}{3}\right)$	$\left(\mathbf{3}, \mathbf{1}; 0, -\frac{1}{3}\right)$	$\left(\mathbf{3}, \mathbf{1}; -\frac{1}{3}\right)$	$(\mathbf{5}, 2)$
	$\left(\overline{\mathbf{3}}, \mathbf{1}, \mathbf{1}; \frac{1}{3}\right)$	$\left(\overline{\mathbf{3}}, \mathbf{1}; 0, \frac{1}{3}\right)$	$\left(\overline{\mathbf{3}}, \mathbf{1}; \frac{1}{3}\right)$	$(\overline{\mathbf{45}}, -2)$
$(\overline{\mathbf{10}}, \mathbf{3}, \mathbf{1})$	$(\mathbf{1}, \mathbf{3}, \mathbf{1}; 1)$	$(\mathbf{1}, \mathbf{3}; 0, 1)$	$(\mathbf{1}, \mathbf{3}; 1)$	$(\mathbf{15}, -6)$
	$\left(\overline{\mathbf{3}}, \mathbf{1}, \mathbf{3}; \frac{1}{3}\right)$	$\left(\overline{\mathbf{3}}, \mathbf{3}; 0, \frac{1}{3}\right)$	$\left(\overline{\mathbf{3}}, \mathbf{3}; \frac{1}{3}\right)$	$(\overline{\mathbf{45}}, -2)$
	$\left(\overline{\mathbf{6}}, \mathbf{1}, \mathbf{3}; -\frac{1}{3}\right)$	$\left(\overline{\mathbf{6}}, \mathbf{3}; 0, -\frac{1}{3}\right)$	$\left(\overline{\mathbf{6}}, \mathbf{3}; -\frac{1}{3}\right)$	$(\mathbf{50}, 2)$
$(\mathbf{10}, \mathbf{1}, \mathbf{3})$	$(\mathbf{1}, \mathbf{1}, \mathbf{3}; -1)$	$(\mathbf{1}, \mathbf{1}; 1, -1)$	$(\mathbf{1}, \mathbf{1}; 0)$	$(\mathbf{1}, 10)$
		$(\mathbf{1}, \mathbf{1}; 0, -1)$	$(\mathbf{1}, \mathbf{1}; -1)$	$(\overline{\mathbf{10}}, 6)$
		$(\mathbf{1}, \mathbf{1}; -1, -1)$	$(\mathbf{1}, \mathbf{1}; -2)$	$(\mathbf{50}, 2)$
	$\left(\mathbf{3}, \mathbf{1}, \mathbf{3}; -\frac{1}{3}\right)$	$\left(\mathbf{3}, \mathbf{1}; 1, -\frac{1}{3}\right)$	$\left(\mathbf{3}, \mathbf{1}; \frac{2}{3}\right)$	$(\overline{\mathbf{10}}, 6)$
		$\left(\mathbf{3}, \mathbf{1}; 0, -\frac{1}{3}\right)$	$\left(\mathbf{3}, \mathbf{1}; -\frac{1}{3}\right)$	$(\mathbf{50}, 2)$
		$\left(\mathbf{3}, \mathbf{1}; -1, -\frac{1}{3}\right)$	$\left(\mathbf{3}, \mathbf{1}; -\frac{4}{3}\right)$	$(\overline{\mathbf{45}}, -2)$
	$\left(\mathbf{6}, \mathbf{1}, \mathbf{3}; \frac{1}{3}\right)$	$\left(\mathbf{6}, \mathbf{1}; 1, \frac{1}{3}\right)$	$\left(\mathbf{6}, \mathbf{1}; \frac{4}{3}\right)$	$(\mathbf{50}, 2)$
		$\left(\mathbf{6}, \mathbf{1}; 0, \frac{1}{3}\right)$	$\left(\mathbf{6}, \mathbf{1}; \frac{1}{3}\right)$	$(\overline{\mathbf{45}}, -2)$
		$\left(\mathbf{6}, \mathbf{1}; -1, \frac{1}{3}\right)$	$\left(\mathbf{6}, \mathbf{1}; -\frac{2}{3}\right)$	$(\mathbf{15}, -6)$
$(\mathbf{15}, \mathbf{2}, \mathbf{2})$	$(\mathbf{1}, \mathbf{2}, \mathbf{2}; 0)$	$\left(\mathbf{1}, \mathbf{2}; \frac{1}{2}, 0\right)$	$\left(\mathbf{1}, \mathbf{2}; \frac{1}{2}\right)$	$(\mathbf{5}, 2)$
		$\left(\mathbf{1}, \mathbf{2}; -\frac{1}{2}, 0\right)$	$\left(\mathbf{1}, \mathbf{2}; -\frac{1}{2}\right)$	$(\overline{\mathbf{45}}, -2)$
	$\left(\mathbf{3}, \mathbf{2}, \mathbf{2}; \frac{2}{3}\right)$	$\left(\mathbf{3}, \mathbf{2}; \frac{1}{2}, \frac{2}{3}\right)$	$\left(\mathbf{3}, \mathbf{2}; \frac{7}{6}\right)$	$(\overline{\mathbf{45}}, -2)$
		$\left(\mathbf{3}, \mathbf{2}; -\frac{1}{2}, \frac{2}{3}\right)$	$\left(\mathbf{3}, \mathbf{2}; \frac{1}{6}\right)$	$(\mathbf{15}, -6)$
	$\left(\overline{\mathbf{3}}, \mathbf{2}, \mathbf{2}; -\frac{2}{3}\right)$	$\left(\overline{\mathbf{3}}, \mathbf{2}; -\frac{1}{2}, -\frac{2}{3}\right)$	$\left(\overline{\mathbf{3}}, \mathbf{2}; -\frac{7}{6}\right)$	$(\mathbf{50}, 2)$
		$\left(\overline{\mathbf{3}}, \mathbf{2}; \frac{1}{2}, -\frac{2}{3}\right)$	$\left(\overline{\mathbf{3}}, \mathbf{2}; -\frac{1}{6}\right)$	$(\overline{\mathbf{10}}, 6)$
	$(\mathbf{8}, \mathbf{2}, \mathbf{2}; 0)$	$\left(\mathbf{8}, \mathbf{2}; \frac{1}{2}, 0\right)$	$\left(\mathbf{8}, \mathbf{2}; \frac{1}{2}\right)$	$(\mathbf{50}, 2)$
		$\left(\mathbf{8}, \mathbf{2}; -\frac{1}{2}, 0\right)$	$\left(\mathbf{8}, \mathbf{2}; -\frac{1}{2}\right)$	$(\overline{\mathbf{45}}, -2)$

Table E.6: Decomposition of the representation $\overline{\mathbf{126}}$

$(4_C, 2_L, 2_R)$	$(3_C, 2_L, 2_R, 1_{B-L})$	$(3_C, 2_L, 1_R, 1_{B-L})$	$(3_C, 2_L, 1_Y)$	$(5, 1_X)$
$(\mathbf{1},\mathbf{1},\mathbf{1})$	$(\mathbf{1},\mathbf{1},\mathbf{1};0)$	$(\mathbf{1},\mathbf{1};0,0)$	$(\mathbf{1},\mathbf{1};0)$	$(\mathbf{1},0)$
$(\mathbf{15},\mathbf{1},\mathbf{1})$	$(\mathbf{1},\mathbf{1},\mathbf{1};0)$	$(\mathbf{1},\mathbf{1};0,0)$	$(\mathbf{1},\mathbf{1};0)$	$(\mathbf{24},0)$
	$(\mathbf{3},\mathbf{1},\mathbf{1};\frac{2}{3})$	$(\mathbf{3},\mathbf{1};0,\frac{2}{3})$	$(\mathbf{3},\mathbf{1};\frac{2}{3})$	$(\overline{\mathbf{10}},-4)$
	$(\overline{\mathbf{3}},\mathbf{1},\mathbf{1};-\frac{2}{3})$	$(\overline{\mathbf{3}},\mathbf{1};0,-\frac{2}{3})$	$(\overline{\mathbf{3}},\mathbf{1};-\frac{2}{3})$	$(\mathbf{10},4)$
	$(\mathbf{8},\mathbf{1},\mathbf{1};0)$	$(\mathbf{8},\mathbf{1};0,0)$	$(\mathbf{8},\mathbf{1};0)$	$(\mathbf{24},0)$
$(\mathbf{6},\mathbf{2},\mathbf{2})$	$(\mathbf{3},\mathbf{2},\mathbf{2};-\frac{1}{3})$	$(\mathbf{3},\mathbf{2};\frac{1}{2},-\frac{1}{3})$	$(\mathbf{3},\mathbf{2};\frac{1}{6})$	$(\mathbf{10},4)$
		$(\mathbf{3},\mathbf{2};-\frac{1}{2},-\frac{1}{3})$	$(\mathbf{3},\mathbf{2};-\frac{5}{6})$	$(\mathbf{24},0)$
	$(\overline{\mathbf{3}},\mathbf{2},\mathbf{2};\frac{1}{3})$	$(\overline{\mathbf{3}},\mathbf{2};\frac{1}{2},\frac{1}{3})$	$(\overline{\mathbf{3}},\mathbf{2};\frac{5}{6})$	$(\mathbf{24},0)$
		$(\overline{\mathbf{3}},\mathbf{2};-\frac{1}{2},\frac{1}{3})$	$(\overline{\mathbf{3}},\mathbf{2};-\frac{1}{6})$	$(\overline{\mathbf{10}},-4)$
$(\mathbf{10},\mathbf{2},\mathbf{2})$	$(\mathbf{1},\mathbf{2},\mathbf{2};-1)$	$(\mathbf{1},\mathbf{2};\frac{1}{2},-1)$	$(\mathbf{1},\mathbf{2};-\frac{1}{2})$	$(\overline{\mathbf{5}},8)$
		$(\mathbf{1},\mathbf{2};-\frac{1}{2},-1)$	$(\mathbf{1},\mathbf{2};-\frac{3}{2})$	$(\overline{\mathbf{40}},4)$
	$(\mathbf{3},\mathbf{2},\mathbf{2};-\frac{1}{3})$	$(\mathbf{3},\mathbf{2};\frac{1}{2},\frac{1}{3})$	$(\mathbf{3},\mathbf{2};\frac{1}{6})$	$(\overline{\mathbf{40}},4)$
		$(\mathbf{3},\mathbf{2};-\frac{1}{2},-\frac{1}{3})$	$(\mathbf{3},\mathbf{2};-\frac{5}{6})$	$(\mathbf{75},0)$
	$(\mathbf{6},\mathbf{2},\mathbf{2};\frac{1}{3})$	$(\mathbf{6},\mathbf{2};\frac{1}{2},\frac{1}{3})$	$(\mathbf{6},\mathbf{2};\frac{5}{6})$	$(\mathbf{75},0)$
		$(\mathbf{6},\mathbf{2};-\frac{1}{2},\frac{1}{3})$	$(\mathbf{6},\mathbf{2};-\frac{1}{6})$	$(\mathbf{40},-4)$
$(\overline{\mathbf{10}},\mathbf{2},\mathbf{2})$	$(\mathbf{1},\mathbf{2},\mathbf{2};1)$	$(\mathbf{1},\mathbf{2};\frac{1}{2},1)$	$(\mathbf{1},\mathbf{2};\frac{3}{2})$	$(\mathbf{40},-4)$
		$(\mathbf{1},\mathbf{2};-\frac{1}{2},1)$	$(\mathbf{1},\mathbf{2};\frac{1}{2})$	$(\mathbf{5},-8)$
	$(\overline{\mathbf{3}},\mathbf{2},\mathbf{2};\frac{1}{3})$	$(\overline{\mathbf{3}},\mathbf{2};\frac{1}{2},\frac{1}{3})$	$(\overline{\mathbf{3}},\mathbf{2};\frac{5}{6})$	$(\mathbf{75},0)$
		$(\overline{\mathbf{3}},\mathbf{2};-\frac{1}{2},\frac{1}{3})$	$(\overline{\mathbf{3}},\mathbf{2};-\frac{1}{6})$	$(\mathbf{40},-4)$
	$(\overline{\mathbf{6}},\mathbf{2},\mathbf{2};-\frac{1}{3})$	$(\overline{\mathbf{6}},\mathbf{2};\frac{1}{2},-\frac{1}{3})$	$(\overline{\mathbf{6}},\mathbf{2};\frac{1}{6})$	$(\overline{\mathbf{40}},4)$
		$(\overline{\mathbf{6}},\mathbf{2};-\frac{1}{2},-\frac{1}{3})$	$(\overline{\mathbf{6}},\mathbf{2};-\frac{5}{6})$	$(\mathbf{75},0)$
$(\mathbf{15},\mathbf{3},\mathbf{1})$	$(\mathbf{1},\mathbf{3},\mathbf{1};0)$	$(\mathbf{1},\mathbf{3};0,0)$	$(\mathbf{1},\mathbf{3};0)$	$(\mathbf{24},0)$
	$(\mathbf{3},\mathbf{3},\mathbf{1};\frac{2}{3})$	$(\mathbf{3},\mathbf{3};0,\frac{2}{3})$	$(\mathbf{3},\mathbf{3};\frac{2}{3})$	$(\mathbf{40},-4)$
	$(\overline{\mathbf{3}},\mathbf{3},\mathbf{1};-\frac{2}{3})$	$(\overline{\mathbf{3}},\mathbf{3};0,-\frac{2}{3})$	$(\overline{\mathbf{3}},\mathbf{3};-\frac{2}{3})$	$(\overline{\mathbf{40}},4)$
	$(\mathbf{8},\mathbf{3},\mathbf{1};0)$	$(\mathbf{8},\mathbf{3};0,0)$	$(\mathbf{8},\mathbf{3};0)$	$(\mathbf{75},0)$
$(\mathbf{15},\mathbf{1},\mathbf{3})$	$(\mathbf{1},\mathbf{1},\mathbf{3};0)$	$(\mathbf{1},\mathbf{1};1,0)$	$(\mathbf{1},\mathbf{1};1)$	$(\mathbf{10},4)$
		$(\mathbf{1},\mathbf{1};0,0)$	$(\mathbf{1},\mathbf{1};0)$	$(\mathbf{75},0)$
		$(\mathbf{1},\mathbf{1};-1,0)$	$(\mathbf{1},\mathbf{1};-1)$	$(\overline{\mathbf{10}},-4)$
	$(\mathbf{3},\mathbf{1},\mathbf{3};\frac{2}{3})$	$(\mathbf{3},\mathbf{1};1,\frac{2}{3})$	$(\mathbf{3},\mathbf{1};\frac{5}{3})$	$(\mathbf{75},0)$
		$(\mathbf{3},\mathbf{1};0,\frac{2}{3})$	$(\mathbf{3},\mathbf{1};\frac{2}{3})$	$(\mathbf{40},-4)$
		$(\mathbf{3},\mathbf{1};-1,\frac{2}{3})$	$(\mathbf{3},\mathbf{1};-\frac{1}{3})$	$(\mathbf{5},-8)$
	$(\overline{\mathbf{3}},\mathbf{1},\mathbf{3};-\frac{2}{3})$	$(\overline{\mathbf{3}},\mathbf{1};1,-\frac{2}{3})$	$(\overline{\mathbf{3}},\mathbf{1};\frac{1}{3})$	$(\overline{\mathbf{5}},8)$
		$(\overline{\mathbf{3}},\mathbf{1};0,-\frac{2}{3})$	$(\overline{\mathbf{3}},\mathbf{1};-\frac{2}{3})$	$(\overline{\mathbf{40}},4)$
		$(\overline{\mathbf{3}},\mathbf{1};-1,-\frac{2}{3})$	$(\overline{\mathbf{3}},\mathbf{1};-\frac{5}{3})$	$(\mathbf{75},0)$
	$(\mathbf{8},\mathbf{1},\mathbf{3};0)$	$(\mathbf{8},\mathbf{1};1,0)$	$(\mathbf{8},\mathbf{1};1)$	$(\overline{\mathbf{40}},4)$
		$(\mathbf{8},\mathbf{1};0,0)$	$(\mathbf{8},\mathbf{1};0)$	$(\mathbf{75},0)$
		$(\mathbf{8},\mathbf{1};-1,0)$	$(\mathbf{8},\mathbf{1};-1)$	$(\mathbf{40},-4)$

Table E.7: Decomposition of the representation **210**

List of Publications

1. **New mechaism for type-II seesaw dominance in SO(10) with low mass Z', RH neutrinos, and verifiable LFV, LNV, and proton decay.**
   Bidyut Prava Nayak and M. K. Parida, Eur. Phys. J **C** 75 (2015) 183 [arXiv:1312.3185][hep-ph].

2. **Singlet fermion assisted dominant seesaw with lepton flavor, and number violation, and leptogenesis.**
   M. K. Parida and Bidyut Prava Nayak, Adv. High Energy Phys. 2017 (2017) 4023493 [arXiv:1607.07236][hep-ph].

3. **Dilepton events with displaced vertices, double beta decay, and resonant leptogenesis with type-II seesaw dominance, TeV scale Z' and heavy neutrinos.**
   Bidyut Prava Nayak and M. K. Parida [arXiv:1509.06192][hep-ph] (Communicated).